AD_____

Award Number: DAMD17-00-1-0454

TITLE: Assessment of the Activation State of Rho Family GTP-Binding Proteins in Breast Cancer Cells and Specimens

PRINCIPAL INVESTIGATOR: Yi Zheng, Ph.D.

CONTRACTING ORGANIZATION: Cincinnati Children's Hospital
Medical Center
Cincinnati, Ohio 45229-3039

REPORT DATE: August 2004

TYPE OF REPORT: Final

PREPARED FOR: U.S. Army Medical Research and Materiel Command
Fort Detrick, Maryland 21702-5012

DISTRIBUTION STATEMENT: Approved for Public Release;
Distribution Unlimited

The views, opinions and/or findings contained in this report are those of the author(s) and should not be construed as an official Department of the Army position, policy or decision unless so designated by other documentation.

REPORT DOCUMENTATION PAGE

Form Approved
OMB No. 074-0188

Public reporting burden for this collection of information is estimated to average 1 hour per response, including the time for reviewing instructions, searching existing data sources, gathering and maintaining the data needed, and completing and reviewing this collection of information. Send comments regarding this burden estimate or any other aspect of this collection of information, including suggestions for reducing this burden to Washington Headquarters Services, Directorate for Information Operations and Reports, 1215 Jefferson Davis Highway, Suite 1204, Arlington, VA 22202-4302, and to the Office of Management and Budget, Paperwork Reduction Project (0704-0188), Washington, DC 20503

1. AGENCY USE ONLY (Leave blank)	2. REPORT DATE	3. REPORT TYPE AND DATES COVERED
	August 2004	Final (3 July 2000 - 2 July 2004)

4. TITLE AND SUBTITLE
Assessment of the Activation State of Rho Family GTP-Binding Proteins in Breast Cancer Cells and Specimens

5. FUNDING NUMBERS
DAMD17-00-1-0454

6. AUTHOR(S)
Yi Zheng, Ph.D.

7. PERFORMING ORGANIZATION NAME(S) AND ADDRESS(ES)
Cincinnati Children's Hospital Medical Center
Cincinnati, Ohio 45229-3039

E-Mail: yi.zheng@chmcc.org

8. PERFORMING ORGANIZATION REPORT NUMBER

9. SPONSORING / MONITORING AGENCY NAME(S) AND ADDRESS(ES)
U.S. Army Medical Research and Materiel Command
Fort Detrick, Maryland 21702-5012

10. SPONSORING / MONITORING AGENCY REPORT NUMBER

11. SUPPLEMENTARY NOTES
Original contains color plates: ALL DTIC reproductions will be in black and white

12a. DISTRIBUTION / AVAILABILITY STATEMENT
Approved for Public Release; Distribution Unlimited

12b. DISTRIBUTION CODE

13. Abstract ***(Maximum 200 Words)*** *(abstract should contain no proprietary or confidential information)*

Rho GTPases are known to play roles in various aspects of cancer development. To establish a causal link between activation of individual Rho GTPases and certain aspects of breast cancer, we have started to search for a functional association of Rho GTPases with mitogenic conditions and various physiological or pathological situations that may be connected to mammary cell transformation. As stated in this final report, we have established a method using the Rho GTPase-interactive effector domains of WASP, PAK1, and Rhotekin to semi-quantitatively define the activation states of Rho family members Cdc42, Rac1, and RhoA in cancer cells, and have applied this method to a number of cellular conditions which are related to mammary tumorigenesis. These studies are significant since the findings further confirmed the involvement of Rho GTPases in diverse physiological and pathological situations that may contribute to mammary carcinogenesis. The results obtained strongly support our long term goal to implicate specific Rho GTPases in breast cancer development and to devise novel anti-cancer therapeutics targeting individual Rho signaling pathways.

14. SUBJECT TERMS
cancer biology, cell signaling, GTP-binding proteins, Rho/Rac/Cdc42, effector targets

15. NUMBER OF PAGES
116

16. PRICE CODE

17. SECURITY CLASSIFICATION OF REPORT	18. SECURITY CLASSIFICATION OF THIS PAGE	19. SECURITY CLASSIFICATION OF ABSTRACT	20. LIMITATION OF ABSTRACT
Unclassified	Unclassified	Unclassified	Unlimited

Table of Contents

Cover	1
SF 298	2
Table of Contents	3
Introduction	4
Body	5-10
Key Research Accomplishments	11
Reportable Outcomes	12
Conclusions	13
References	14
Appendices	16

Introduction

The Rho family small GTPases function as molecular switches that control the signal flows from a variety of cell surface receptors and cellular tumor suppressors. Among the panel of receptors and tumor suppressors that require Rho family GTPases to relay signals leading to mammary cell transformation and metastasis, the epidermal growth factor receptor, the erbB-2 gene product, the colony stimulating factor-1 receptor, the cell adhesion receptor integrins, and the PTEN and p53 tumor suppressors are the prominent ones. Overexpression or mutation of these receptors and many signal transducers downstream of these receptors, as well as genetic defects in PTEN or p53 tumor suppressor, are known to correlate with breast carcinogenesis. We hypothesized that in breast cancer cells overexpressing or bearing mutations of one of the oncogenic receptors, Ras proteins, Rho-specific activators (guanine nucleotide exchange factors) or the PTEN or p53 tumor suppressors, a higher percentage of Rho family members, Rho, Rac or Cdc42, would be in the active state. Determination of the activation states of these GTPases in breast tumors and defining which tumor types show increased Rho, Rac, or Cdc42 activation may lead the way in the search for a direct connection between Rho pathways and breast cancer genesis, and may provide novel treatment strategies targeted at the Rho signaling components. We have utilized the Rho GTPase effector pulldown method to measure the activation state of endogenous Rho family GTPases in the oncogenic and mitogenic pathways of model cell systems and have succeeded in implicating multiple gain of oncogenic function or loss of tumor suppressor function in activating Rho GTPases under pathologically relevant situations.

In the initial proposal we planed to further screen a panel of breast cancer specimens for RhoA, Rac1 and Cdc42 activities to tie the cellular studies with primary tumor situations. During a lengthy transfer period from my former institution (University of Tennessee) to my current institution (Cincinnati Children's), however, we have lost both precious time and sample specimens in addition to expert manpower (it took us over one year to obtain authorization to transfer this grant during which time all related work had to be suspended). Nonetheless, we have made significant progress in achieving the major goals of the original proposal as described below.

Body

The first two aims (Task 1 and Task 2) were proposed for months 1-10 and months 6-24 of the funding period. Specifically, we have proposed to determine which p21-binding domains (PBDs) of effectors are most suitable for the detection of activated RhoA and Rac1 (Task 1) and to begin to apply the efector PBD-binding assay to the examination of endogenous Rho family GTPases in mitogen-stimulated or oncogene-transformed cells (Task 2). Such studies are necessary for later investigation of the potential involvement of Rho pathways in transducing mitogenic/oncogenic signals in mammary cells and in breast cancer specimens. To this end, we have mostly completed the tasks as we proposed. In the proposal we planned to further screen a panel of breast cancer specimens for RhoA, Rac1 and Cdc42 activities to tie the cellular studies with primary tumor situations (Task 3). During a lengthy grant transfer period from my former institution (University of Tennessee) to my current institution (Cincinnati Children's), however, we have lost both precious time and sample specimens in addition to expert manpower (it took us over one year to obtain authorization to transfer this grant during which time all related work had to be suspended). As a result Task 3 has not been completed on time as planned.

1. Activation and translocation of Cdc42 and Rac1 by mitogenic and adhesion signals.

The Rho family GTPases Cdc42 and Rac1 are important signal transducers of many receptor-initiated pathways (1, 2) and are regulated by mitogenic signals such as bradykinin and PDGF as well as by adhesion (3, 4, 5). We have investigated the relationship between membrane translocation and activation of endogenous Cdc42 and Rac1 in response to mitogenic and integrin stimulation. The mitogen bradykinin induced translocation of Cdc42 and Rac1 to a membrane fraction of Swiss 3T3 cells within two minutes, which correlated with the activation kinetics of the GTPases. PDGF treatment of the cells induced rapid translocation and activation of Rac1 but not Cdc42 within 30 seconds. The activation of Cdc42 and Rac1 appeared to precede actin microspike formation or membrane ruffle induction of the cells. However, the translocated GTPases were found to remain membrane bound for a much longer time course than their activation status, suggesting that a deactivation event occurs at the membrane level. Cell adhesion on fibronectin matrix resulted in transient activation of both Cdc42 and Rac1, and caused a partial inhibition of bradykinin or PDGF effect on the small G-proteins. Pretreatment of the cells with genistein or wortmannin significantly reduced the bradykinin, PDGF, or fibronectin stimulated Cdc42 or Rac1 activity,

indicating that both tyrosine kinase and PI3 kinase are required elements of the small G-protein pathways. Finally, Cdc42 and Rac1 activation by bradykinin were abolished by pertussis toxin treatment, whereas the outcome by the PDGF or integrin treatment was unaffected. These results suggest that mitogenic agonist and integrin mediated signals are integrated at the small G-protein level, and tyrosine kinase, PI3 kinase, and/or heterotrimeric G-proteins are intimately involved in the Cdc42 and Rac1 activation process.

2. Examination of proto-Dbl guanine nucleotide exchange activity in cells.

The *dbl* oncogene encodes a prototype member of the Rho GTPase guanine nucleotide exchange factor (GEF) family (9). Oncogenic activation of proto-Dbl occurs through the truncation of N-terminal 497 residues (10). The C-terminal half of proto-Dbl includes residues 498-680 and 710-815 that fold into the Dbl homology (DH) domain and the pleckstrin homology (PH) domain, respectively, both of which are essential for cell transformation via the Rho GEF activity or cytoskeletal targeting function (11). We have investigated the mechanism of the apparent negative regulation of proto-Dbl imposed by the N-terminal sequences, employing the GST-effector pull down assays to detect the effect of various proto-Dbl constructs on the endogenous Rho GTPase activities (12). Deletion of the N-terminal 285 or C-terminal 100 residues of proto-Dbl did not significantly effect on either its transforming activity or GEF activity, while removal of the N-terminal 348 amino acids resulted in a significant increase in both transformation and GEF potential. Together with other cell biology evidence, our findings unveiled an autoinhibitory mode of regulation of proto-Dbl that is mediated by the intramolecular interaction between its N-terminal sequences and PH domain, directly impacting on both the GEF function and intracellular distribution (reprint enclosed in Appendix).

3. Modulation of RhoA activity in epithelial cells by Na,K-ATPase.

The mechanism by which the formation of tight junctions and desmosomes are regulated in polarized epithelial cells are not well understood (13-14). Such mechanism may be tightly associated with mammary epithelial transformation (15). In collaboration with Dr. A. K. Rajasekaran's laboratory (UCLA), we have investigated the involvement of RhoA GTPase in Na,K-ATPase mediated assembly of tight junctions and desmosomes in MDCK cells (16). We found that an increased sodium level caused by the inhibition of Na,K-ATPase prevents the formation of tight junctions and desmosomes and this effect is negatively correlated with the endogenous RhoA

activity. Furthermore, we showed that the Na,K-ATPase ion transport function and suppression of cell motility are separate events that require PI3 kinase and Rac1 activities (17). The results indicate that the intracellular sodium level maintained by the Na,K-ATPase is an upstream regulator of PI3 kinase and Rac1/RhoA function in epithelial cells and might play a crucial role in the biogenesis of polarized epithelia, cell motility regulation and ion transport (see attached reprint/preprint).

4. Genetic deletion of the Pten tumor suppresor gene promotes cell motility by activation of Rac1 and Cdc42 GTPases.

Aside from examining the cellular functions of Rho proteins in the oncogene/mitogen stimulated clonal cell systems, we were interested in determining the contribution of Rho GTPases to cell behaviors in primary cells with a defined genetic background that might better represent tumor cells. We reasoned that since no constitutively active mutations of Rho GTPases were found in human tumors, Rho might play a role as transducer of mitogenic "second hit" in tumor induction to mediate or cooperate with an established "first hit" that are frequently associated with cancer. One likely "first hit" could be the defect of tumor suppressors such as PTEN, p53 or pRb, loss of function of which are known to be associated with a wide variety of human tumors.

Pten is a recently identified tumor suppressor gene which is deleted or mutated in a variety of primary human cancers including breast cancer (6). Pten has been implicated in controlling cell migration, among other functions, but the exact mechanism is not very clear (7). In collaboration with Dr. Hong Wu's laboratory (UCLA), we have shown that *Pten* deficiency led to increased cell motility (8). Significant increases in the endogenous activities of Rac1 and cdc42, two small GTPases involved in regulating the actin cytoskeleton, were observed in Pten-/- cells. Overexpression of dominant negative mutant forms of Rac1 and cdc42 reversed the cell migration phenotype of Pten-/- cells. These studies suggest that Pten negatively controls cell motility by down-regulating Rac1 and Cdc42 (reprint enclosed in Appendix).

5. The p19Arf-p53 tumor suppressor pathway suppresses cell migration by downregulating PI3K and Rho/Rac activities

The $p19^{Arf}$-p53 and $p27^{Kip1}$-Rb tumor suppressor pathways play a critical role in cell-cycle checkpoint control and/or apoptosis (18). By using primary MEFs that lack *Arf*, *p53*, *Kip1* or *Rb*, we have studied the involvement of the p19Arf-p53 pathway in the regulation of cell motility and its relationship with Rho GTPases (19). In subconfluent culture and serum free conditions, a significant

percentage of the $p19^{Arf}$ or p53 deficient cells appeared to be in a round shape and displayed intense cortical actin staining, while the $p27^{Kip1}$- or pRb-deficient cells were similar to wild type MEFs in morphology and actin structure. Both $p19^{Arf}$- and p53-deficient cells produced long trails, while the *Kip1* and *Rb* knock out cells were similar to the wild type cells, showing no sign of movement in the experimental conditions. In a wound healing assay the $Arf^{-/-}$ and $p53^{-/-}$ cells migrated about two folds faster than the wild type, $Kip1^{-/-}$ or $Rb^{-/-}$ cells under the low serum conditions at which the difference in cell growth was less than 10%. When $p19^{Arf}$ and p53 were reintroduced into $Arf^{-/-}$ and $p53^{-/-}$ cells, respectively, by retroviral induction, the migration phenotype of these cells were fully reversed. Moreover, the Gln22/Ser23 mutant of p53 was able to rescue the migration phenotype of $p53^{-/-}$ cells similarly as wild type p53, but the His175 mutant which is defective in DNA binding was inactive. Thus, deletion of *Arf* and/or *p53,* but not *Kip1* or *Rb,* led to actin cytoskeleton reorganization and a significant increase in cell motility, and a transcriptional event of p53 is involved in this process.

To begin to understand the molecular mechanism underlying this observation, we have made a discovery that the endogenous PI3-kinase and RhoA/Rac1 activities were significantly elevated in the *Arf*-/- and *p53*-/- cells, and these activities are required for $p19^{Arf}$- and p53-regulated migration. Reintroduction of the wild type *Arf* or *p53* gene into the *Arf*-/- or *p53*-/- cells reversed the PI3K and Rac1/RhoA activities as well as the migration phenotype (19). These results suggest a functional relationship between the p53 tumor suppressor pathway and the PI3 kinase-Rho GTPase signaling module that controls actin structure and cell motility and show that $p19^{Arf}$ and p53 negatively regulate cell migration by suppression of PI3K and Rac1/RhoA activities (reprint in the Appendix).

6. Rho GTPases contribute to the cell growth regulation by p53 and cooperate with p53-deficiency to promote primary MEF transformation

Since deletion of the $p19^{Arf}$ or p53 gene resulted in a significant increase in RhoA and Rac1 activities in primary MEFs, we sought to dissect the contribution of the Rho GTPases to the cell growth and gene transcription phenotypes of the $p19^{Arf}$ and p53 deficient cells (20). We found that (1) $p19^{Arf}$ or p53 deficiency led to a significant increase in PI3 kinase activity which in turn upregulated Rac1 and RhoA activities; (2) deletion of *p19Arf* or *p53* led to an increase in cell growth rate that was in part dependent on RhoA as well as Rac and Cdc42 activities; (3) $p19^{Arf}$ or p53 deficiency caused an enhancement of the growth related transcription factor NF-kB and cyclin D1 activities which appeared to be partly dependent on RhoA and Cdc42 but not Rac1; (4) forced expression of a fast cycling or constitutively active mutant of RhoA, as well as Rac1 and Cdc42,

could further promote the *p53*$^{-/-}$ and *Arf*$^{-/-}$ cell proliferation and caused transformation of both cells; (5) multiple pathways regulated by RhoA including that of ROCK might be required for RhoA to fully promote the transformation of *p53*$^{-/-}$ cells; and (6) RhoA may contribute to the p53-regulated cell proliferation by modulating cell cycle machinery while hyperactivation of RhoA further suppressed a p53-independent apoptotic signal. These results provide strong evidence indicating that signals through the Rho family GTPases contribute to the cell growth regulation by *p19Arf* and *p53*. Furthermore, the fact that RhoA can synergize with p19^{Arf} or p53 defect to promote primary cell transformation suggests that mitogenic/oncogenic signals stimulating Rho pathways may serve as potentail "second hits" to cooperate with p53-pathway defect in inducing tumorgenesis (reprint in the Appendix).

7. Development of a novel strategy targeting Rho GTPase activity in tumor cells

Given the implication of the signaling pathways mediated by Rho GTPases in many aspects of tumor cell biology (21), we have begun to design novel approaches targeting at Rho that might be applicable to tumor cells. Recently we have developed a strategy to specifically target individual Rho GTPase by utilizing the negative regulatory role of Rho GAPs (22). Because unlike Ras, upregulation or overexpression of Rho GTPases, but not constitutively activative mutations, has been associated with human cancer, we reasoned that the GTPase-activating function of Rho GAP domain could be explored to downregulate Rho GTPase activity if it is properly targeted to the intracellular locations where individual active Rho GTPase resides. As a demonstration of principle, we have shown that a set of chimeric molecules could be generated by fusing the RhoGAP domain of p190, a GTPase-activating protein that accelerates the intrinsic GTPase activity of the three closely related Rho GTPases, RhoA, RhoB and RhoC, with the C-terminal hypervariable sequences of the Rho GTPases, to specifically target RhoA, RhoB or RhoC function. The p190-Rho chimeras were active as GAPs toward the Rho proteins *in vitro*, colocalized with the respective Rho proteins and specifically downregulated Rho protein activities in cells depending on which Rho GTPase sequences were included in the chimeras. In particular, the p190-RhoA chimera was able to specifically inhibit the RhoA activity in cells and block the RhoA-induced cell transformation whereas the p190-RhoC chimera specifically reversed the migration phenotype induced by RhoC activation and was effective in reversing the anchorage-independent growth and invasion phenotypes caused by RhoC overexpression in HME-RhoC breast cancer cells, and in inhibiting the migration and invasion phenotypes attributed to RhoC upregulation in the highly metastatic A375-M

human melanoma cells (22). Thus, we have developed a novel strategy utilizing RhoGAP-Rho chimeras to specifically downregulate individual Rho protein activity and have shown that this approach could be applied to multiple human tumor cells to reverse the growth and/or invasion phenotypes associated with deregulation of a distinct subtype of Rho GTPase (reprint in the Appendix).

Key Research Accomplishments

- Established that the Rho GTPase-interactive effector domains of WASP, PAK1, and Rhotekin constitute the activation-state specific probes for Cdc42, Rac, and Rho that can be utilized to detect endogenous Cdc42-GTP, Rac1-GTP, and RhoA-GTP species, respectively.

- Applied GST-WASP, GST-PAK1 and GST-Rhotekin probes to NIH 3T3 cells transfected with various proto-Dbl oncogene products to reveal the activation states of Cdc42 and RhoA that were regulated by proto-Dbl derivatives, suggesting that residues 286 to 482 of proto-Dbl are involved in an autoinhibition mechanism.

- Applied GST-WASP, GST-PAK1, and GST-Rhotekin to the tumor-suppressor, PTEN, p19Arf or p53, knock-out mouse embryonic fibroblasts to determine that the three major Rho GTPase activities become upregulated in the respective systems, which correlate with increased motility and/or proliferation of the cells, suggesting that PTEN, p19Arf and p53 negatively control cell motility and growth by suppressing PI3 kinase activity and down-regulating RhoA, Rac1 and Cdc42. These studies implicate the Rho GTPases in the loss of tumor suppressor phenotypes for the first time and may have important potential in putting Rho GTPases on the novel anti-cancer target list.

- Applied GST-Rhotekin and GST-PAK1 to an epithelial cell system to determine that inhibition of Na,K-ATPase negatively regulates RhoA and positively regulates Rac1, which may in turn affect the formation of tight junctions and desmosomes as well as ion transport function.

- Development of a RhoGAP-based targeting strategy toward individual Rho GTPases in tumor cells.

- Part of the support from this grant allowed me to write two review articles published in TiBS and Trends Cell Biol.

Reportable Outcomes

1. Liliental, J., Moon, S. Y., Lesche, R., Mamillapalli, R., Gavrilova, N., **Zheng, Y.**, Sun, H., and Wu, H. (2000) Genetic deletion of the PTEN tumor suppresor gene promotes cell motility by activation of Rac1 and Cdc42 GTPases. *Curr. Biol.* 10, 401-404.

2. Bi, F., Debreceni, B., Zhu, K., Salani, B., Eva, A, and **Zheng, Y**. (2001) Autoinhibition mechanism of proto-Dbl. *Mol. Cell. Biol.* 21, 1463-1474.

3. Rajasekaran, S. A., Palmer, L. G., Moon, S. Y., Soler, A. P., Apodaca, G. L., Harper, J. F., **Zheng, Y**., and Rajasekaran, A. K. (2001) Na,K-ATPase Activity Is Required for Formation of Tight Junctions, Desmosomes, and Induction of Polarity in Epithelial Cells. *Mol. Biol. Cell* 12, 3717-3732.

4. **Zheng, Y.** (2001) Dbl family guanine nucleotide exchange factors. *Trends Biochem. Sci.* 26, 724-732.

5. Moon, S. Y. and **Zheng, Y.** (2003) Rho GTPase-activating proteins in cell regulation. *Trends Cell Biol.* 13, 14-23.

6. Guo, F., Gao, Y., Wang, L., and **Zheng, Y**. (2003) p19Arf-p53 tumor suppressor pathway regulates cell motility by suppression of PI3 kinase and Rac activities. *J. Biol. Chem.* 278, 14414-14419.

7. Wang, L., Yang, L., Luo, Y., and **Zheng, Y**. (2003) A novel strategy for donwregulating individual Rho GTPase activities in tumor cells. *J. Biol. Chem.* 278, 44617-44625.

8. Guo, F., and **Zheng, Y**. (2004) Involvement of Rho family GTPases in p19Arf or p53 mediated proliferation of primary mouse embryonic fibroblasts. *Mol. Cell Biol.* 24, 1426-1428.

9. Barwe, S. P., Anilkumar, G., Moon, S. Y., **Zheng, Y.**, Whitelegge, J., Rajasekaran, S. A., and Rajasekaran, A. K. (2004) Multiple functions of NaK-ATPase: role in PI3 kinase signaling and suppression of cell motility. *Submitted*

Conclusions

Rho GTPase signaling pathways have begun to be appreciated to play roles in breast carcinogenesis. To establish a causal link between activation of individual Rho GTPase activities and certain aspects of breast cancer development, we have started to search for an effect on Rho GTPase activities in mitogenic conditions, and in various potential pathological situations that may be connected to mammary cell transformation and metastasis. As stated in this final report, we have established a method using the Rho GTPase-interactive effector domains of WASP, PAK1, and Rhotekin to quantitatively define the activation-states of Rho family members Cdc42, Rac, and Rho in cells, and have applied this method to a number of cellular conditions which are potentially related to mammary tumorigenesis: (1) in a Swiss 3T3 model cell system to determine the activation kinetics of endogenous Cdc42 and Rac1 in response to the mitogen, bradykinin or PDGF, stimulation; (2) in NIH 3T3 cells transfected with various proto-Dbl oncogene products to reveal the activation states of Cdc42 and RhoA that were regulated by proto-Dbl derivatives, suggesting that residues 286 to 482 of proto-Dbl are involved in an autoinhibition mechanism; (3) in the tumor-suppressors, PTEN, p19Arf and p53, knock-out mouse embryonic fibroblasts to determine that all three major Rho GTPases activities become upregulated in the systems due to elevated PI3 kinase activity, that correlate with increased motility, proliferation, transformation and/or invasion of the cells. Our results suggest that the commonly mutated tumor suppressors such as PTEN, p19Arf and p53 negatively control cell motility and proliferation by down-regulating Rho GTPase activities and genetic defects of these critical tumor suppressors may cause mammary cancer in part through increased Rho GTPase signaling; (4) in an epithelial cell system to determine that inhibition of Na,K-ATPase negatively regulates PI3 kinase and subsequently Rac1 activity, which may in turn affect the formation of tight junctions and desmosomes as well as ion transport function; (5) we have begun to design new strategies targeting at individual Rho GTPases to reverse breast tumor cell phenotypes. One particular effort has been by utilizing the RhoGAP-Rho GTPase fusion chimeras that could specifically downregulate specific submembers of Rho GTPases. These studies are significant since the findings have further confirmed the involvement of Rho GTPases in diverse physiological and pathological situations that may contribute to oncogenesis. The results obtained also strengthened our long term goal to implicate specific Rho GTPases in breast cancer development, and to devise novel anti-cancer therapeutics targeting individual Rho pathways.

References

1. Hall, A. (1998) Rho GTPases and the actin cytoskeleton. *Science* 279, 509-514.

2. van Aelst, L., and D'Souza-Schorey, C. (1997) Rho GTPases and signaling networks. *Genes & Dev.* 11, 2295-2322.

3. Zohn, I. M., Campbell, S. L., Khosravi-Far, R., Rossman, K. L., and Der, C. J. (1998) Rho family proteins and Ras transformation: the RHOad less traveled gets congested. *Oncogene* 13, 1415-1438.

4. Ridley, A. J. (1996) Rho: theme and variations. *Curr. Biol.* 6, 1256-1264.

5. Schwartz, M. A., and Shattil, S. J. (2000) Signaling networks linking integrins and Rho family GTPases. *Trends Biochem. Sci.* 25, 388-341.

6. Eng, C., Peacocke, M. (1998) Genetics of Cowden syndrome: through the looking glass of oncology. Int. J. Oncology 12, 701-710.

7. Tamura, M., Gu, J., Matsumoto, K., Aota, S., Parsons, R., Yamada, K. M. (1998) Inhibition of cell migration, spreading, and focal adhesions by tumor suppressor PTEN. *Science* 280, 1614-1617.

8. Liliental, J., Moon, S. Y., Lesche, R., Mamillapalli, R., Gavrilova, N., Zheng, Y., Sun, H., and Wu, H. (2000) Genetic deletion of the PTEN tumor suppresor gene promotes cell motility by activation of Rac1 and Cdc42 GTPases. *Curr. Biol.* 10, 401-404.

9. Zheng, Y. (2001) Dbl family guanine nucleotide exchange factors for Rho GTPases. *Trends Biochem. Sci.* in press.

10. Ron, D., Tronick, S. R., Aaronson, S. A., and Eva, A. (1998) Molecular cloning and characterization of the human dbl proto-oncogene: evidence that its overexppresion is sufficient to transform NIH3T3 cells. EMBO J. 7, 2465-2473.

11. Zheng, Y., Zangrilli, D., Cerione, R. A., and Eva, A. (1996) The pleckstrin homology domain mediates transformation by oncogenic Dbl through specific intracellular targeting. J. Biol. Chem. 271, 19017-19020.

12. Bi, F., Debreceni, B., Zhu, K., Salani, B., Eva, A, and Zheng, Y. (2001) Autoinhibition mechanism of proto-Dbl. *Mol. Cell. Biol.* 21, 1463-1474.

13. Yap, A. S., Brieher, W. M., and Gumbiner, B. M. (1997) Molecular and functional analysis of cadherin-based adherens junctions. Ann. Rev. Cell Dev. Biol. 13, 119-146.

14. Garrod, D., Chidgey, M., and North, A. (1996) Desmosomes: differentiation, development, dynamics, and disease. Curr. Opin. Cell Biol. 5, 670-678.

15. Keely, P., Parise, L., and Juliano, R. (1998) Integrins and GTPases in tumour cell growth, motility and invasion. *Trends Cell Biol.* 8, 101-106.

16. Rajasekaran, S. A., Palmer, L. G., Moon, S. Y., Soler, A. P., Apodaca, G. L., Harper, J. F., Zheng, Y., and Rajasekaran, A. K. (2001) Na,K-ATPase regulates the formation of tight junctions and desmosomes through RhoA GTPase. *Mol. Biol. Cell* 12, 3717-3732.

17. Barwe, S. P., Anilkumar, G., Moon, S. Y., Zheng, Y., Whitelegge, J., Rajasekaran, S. A., and Rajasekaran, A. K. (2004) Multiple functions of NaK-ATPase: role in PI3 kinase signaling and suppression of cell motility. *Submitted*

18. Sherr, C. J. (2001). The Ink4a/ARF network in tumor suppression. Nature Reviews Mol. Cell Biol. 2, 731-737.

19. Guo, F., Gao, Y., Wang, L., and Zheng, Y. (2003) p19Arf-p53 tumor suppressor pathway regulates cell motility by suppression of PI3 kinase and Rac activities. *J. Biol. Chem.* 278, 14414-14419.

20. Guo, F., and Zheng, Y. (2004) Involvement of Rho family GTPases in p19Arf or p53 mediated proliferation of primary mouse embryonic fibroblasts. *Mol. Cell Biol.* 24, 1426-1428.

21. Sahai, E., and Marshall, C. J. (2002) Rho-GTPases and Cancer. Nature Reviews Cancer 2, 133-142.

22. Wang, L., Yang, L., Luo, Y., and Zheng, Y. (2003) A novel strategy for donwregulating individual Rho GTPase activities in tumor cells. *J. Biol. Chem.* 278, 44617-44625.

Appendices

Reprints and preprints of research work supported by the grant are enclosed. Nine manuscripts described in Reportable Outcomes are included.

MOLECULAR AND CELLULAR BIOLOGY, Mar. 2001, p. 1463–1474 Vol. 21, No. 5
0270-7306/01/$04.00+0 DOI: 10.1128/MCB.21.5.1463–1474.2001
Copyright © 2001, American Society for Microbiology. All Rights Reserved.

Autoinhibition Mechanism of Proto-Dbl

FENG BI,[1] BALAZS DEBRECENI,[1] KEJIN ZHU,[1] BARBARA SALANI,[2] ALESSANDRA EVA,[2] AND YI ZHENG[1]*

Department of Molecular Sciences, University of Tennessee Health Science Center, Memphis, Tennessee 38163,[1] and Laboratorio di Bioligia Molecolare, Istituto G. Gaslini, 16148 Genoa, Italy[2]

Received 29 September 2000/Returned for modification 9 November 2000/Accepted 30 November 2000

The *dbl* oncogene encodes a prototype member of the Rho GTPase guanine nucleotide exchange factor (GEF) family. Oncogenic activation of proto-Dbl occurs through truncation of the N-terminal 497 residues. The C-terminal half of proto-Dbl includes residues 498 to 680 and 710 to 815, which fold into the Dbl homology (DH) domain and the pleckstrin homology (PH) domain, respectively, both of which are essential for cell transformation via the Rho GEF activity or cytoskeletal targeting function. Here we have investigated the mechanism of the apparent negative regulation of proto-Dbl imposed by the N-terminal sequences. Deletion of the N-terminal 285 or C-terminal 100 residues of proto-Dbl did not significantly affect either its transforming activity or GEF activity, while removal of the N-terminal 348 amino acids resulted in a significant increase in both transformation and GEF potential. Proto-Dbl displayed a mostly perinuclear distribution pattern, similar to a polypeptide derived from its N-terminal sequences, whereas onco-Dbl colocalized with actin stress fibers, like the PH domain. Coexpression of the N-terminal 482 residues with onco-Dbl resulted in disruption of its cytoskeletal localization and led to inhibition of onco-Dbl transforming activity. The apparent interference with the DH and PH functions by the N-terminal sequences can be rationalized by the observation that the N-terminal 482 residues or a fragment containing residues 286 to 482 binds specifically to the PH domain, limiting the access of Rho GTPases to the catalytic DH domain and masking the intracellular targeting function of the PH domain. Taken together, our findings unveiled an autoinhibitory mode of regulation of proto-Dbl that is mediated by the intramolecular interaction between its N-terminal sequences and PH domain, directly impacting both the GEF function and intracellular distribution.

The proto-Dbl protein is the prototype member of a large family of guanine nucleotide exchange factors (GEFs) for Rho GTPases (8, 50). Oncogenic activation of proto-Dbl occurs by truncation of the amino-terminal 497 residues (41), resulting in constitutively active carboxyl-terminal sequences that include a Dbl homology (DH) domain in tandem with a pleckstrin homology (PH) domain, the conserved motifs of the Dbl family. Many members of this family, including Vav, Ect2, Tim, Ost, Dbs, Lbc, Lfc, Lsc, and Net, possess transformation or invasion ability, similar to onco-Dbl upon activation. In many cases, the DH-PH module represents the minimum structural unit that is required for cell transformation (8, 50).

A large body of evidence has helped establish that the biological functions of Dbl family members are intimately dependent upon their ability to interact with and activate Rho GTPases and that the cellular effects of Dbl-like proteins, including actin cytoskeletal reorganization, cell growth stimulation, and transformation, are likely the consequences of coordinated action of their immediate downstream substrates, the Rho family GTPases (8, 47, 50). The evidence includes the findings that Dbl family oncoprotein-induced foci are morphologically similar to those transformed by constitutively activated Rho GTPases but distinct from that seen when cells are transformed by Ras, Raf, or Src (23); coexpression of Dbl family members with dominant negative mutants of Rho family GTPases blocks their transforming activity (20, 23, 32, 52); mutants of the GEFs that are no longer able to interact or activate Rho protein substrates behave dominant-negatively in cells (46, 54); and many cellular activities induced by Dbl family proteins, such as actin cytoskeleton reorganization, c-Jun kinase (JNK) activation, SRF transcriptional activation, and NF-κB activation, are associated with the activation of signaling pathways known to be mediated by the Rho GTPase effector targets (24, 30, 36, 48). Therefore, the ability to interact and activate Rho proteins is essential for Dbl family functions.

Current biochemical and structural data have pointed to the conserved structural motif of the Dbl family, the DH domain, as the primary interactive site with Rho GTPases (2, 20, 31, 44, 54). The DH domain does not have significant sequence homology with other subtypes of small GTPase activators such as the Cdc25 domain and Sec7 domain, which are specific to Ras and ARF, respectively (6, 14), indicating that the DH-Rho protein interaction employs a distinct mechanism (9). Deletions or mutations within the DH domain have been reported to result in loss of GEF activity and cellular functions by the GEFs (20, 40, 43, 54, 55), suggesting that an intact DH domain, likely its Rho GTPase-interactive ability, is critical for the cellular effects of Dbl family members.

The invariable location of a PH domain immediately C-terminal to the DH domain of the Dbl family GEFs suggests a functional interdependence between the two domains. Indeed, a regulatory role of the PH domain in the function of Dbl family members has been recognized. Derivatives of the Dbl family members onco-Dbl, Lbc, Lfc, and Dbs that are trun-

* Corresponding author. Mailing address: Department of Molecular Sciences, University of Tennessee, 858 Madison Avenue, Memphis, TN 38163. Phone: (901) 448-5138. Fax: (901) 448-7360. E-mail: yzheng@utmem.edu.

cated within the PH domain are impaired in their transforming activity (38, 48, 49, 53). In these cases, the PH domain was found to promote the translocation of the Dbl family proteins to the plasma membrane or cytoskeleton, where the Rho GTPase substrates reside. It is therefore likely that the PH domain of the Dbl proteins, acting similarly to the SH2/SH3 domains in the Ras pathway (10, 39), serves to bring the catalytic DH domain to specific intracellular locations to effectively activate the Rho GTPases.

Many members of the Dbl family appear to exist in an inactive, basal state prior to full activation. The incoming upstream signals, such as the heterotrimeric G-protein Gα and Gβγ subunits, protein tyrosine or serine/threonine kinases, adaptor or scaffolding proteins, and phosphoinositol lipids, may contribute in varying degrees to GEF activation processes (12, 13, 18, 19, 26, 34, 46). The best-understood example of self-regulation among the family members is the proto-Vav protein. The N-terminal autoinhibitory extension of proto-Vav forms an α-helix that binds in the DH domain active site through direct contact with the Rho GTPase binding pocket, blocking access to GTPases (3). Phosphorylation of Tyr174, which is an integral part of the autoinhibition interface, by Syk or Src-like kinases causes the N-terminal peptide to become unstructured and released from the DH domain, resulting in proto-Vav activation (3). The yeast Dbl family member Cdc24, which is a Cdc42-specific GEF, forms a protein complex with the scaffolding molecule Far1 and the Gβγ subunits to mediate the mating response of *Saccharomyces cerevisiae* (34). Mammalian p115RhoGEF becomes activated as a Rho GEF upon $G\alpha_{13}$ binding to its N-terminal RGS domain, suggesting that the coupling between a Gα and p115Rho GEF may relieve the intrinsic constraint of the DH domain (19). Moreover, phosphorylation of the Rac1-specific GEF Tiam1 by Ca^{2+}/calmodulin-dependent protein kinase II has been shown to lead to its translocation to the plasma membrane and activation (13), possibly by interference of the PH domain function of Tiam1, which has previously been demonstrated to determine its subcellular location (45). These cases suggest that the Dbl family GEFs employ a diverse range of self-regulatory mechanisms to maintain themselves in the basal state.

Proto-Dbl activation occurs through truncation of N-terminal 497 amino acids (42), suggesting that the N-terminal half of the molecule contains a negative regulatory element(s) for the C-terminal DH-PH functional module. A previous database search found limited similarities between the N terminus of proto-Dbl and the intermediate filament protein vimentin, spanning a 300-amino-acid region which was predicted to consist of an extended α-helical coiled-coil structure (41). However, where the inhibitory function resides upstream of the DH domain (residues 498 to 690) and how the N terminus exerts the inhibitory function remain unclear. In the present article, we report the finding that proto-Dbl protein involves an intramolecular interaction between the N terminus and the PH domain to maintain an autoinhibited, inactive state. The N- and C-terminal domain interaction effectively limits the access of the Rho GTPase substrates RhoA and Cdc42 to the catalytic site of the DH domain and masks the intracellular targeting function of the PH domain, resulting in suppression of its GEF function and a unique perinuclear localization pattern in cells. Such an autoinhibition state prevents proto-Dbl from transforming cells, and presents a basal mode that could be subject to modulation by a variety of upstream signals.

MATERIALS AND METHODS

Construction of mutant proto-Dbl cDNAs. Constructs pZipneo-onco-Dbl, pZipneoGST-DH-PH, pKH3-DH-PH, pKH3-Cdc42, and KH3-RhoA were generated as described before (54). Various proto-Dbl truncation mutants, including T1-T7, N1-N4, and the DH and PH domains (Fig. 1A), were generated by PCR cloning using the high-fidelity *Pfu* DNA polymerase (Stratagene) as described (28). The resulting constructs in the pZipneo vector were subsequently sequence proofed by automated fluorescence sequencing. The cDNAs encoding T1-T7, DH-PH, DH, or PH were subcloned into the pKH3 vector for expression as the trihemagglutinin (HA_3)-tagged proteins in Cos-7 cells. The Myc-tagged N2 and Flag-tagged N1 constructs were generated by subcloning the corresponding cDNA sequences to the pCMV6 and pCMV2B vectors, respectively. The *Bam*HI fragments encoding T1, N1, and the DH-PH module were also subcloned into the *Bgl*II and *Bam*HI sites of pVL1392 vector together with the cDNAs encoding the glutathione *S*-transferase (GST) or His_6 sequences for insect cell expression (51). The N2, N3, and N4 cDNAs were subcloned into the *Bam*HI and *Eco*RI sites of the pGEX-2T vector for expression in *Escherichia coli* as GST fusions. The pSR-lbc and pSR-v-ras plasmids used for the transformation assays were described before (52).

Expression of recombinant proteins in *E. coli* and insect cells. Expression and purification of GST fusion small GTP-binding proteins (GST-Cdc42, GST-RhoA, GST-N17Cdc42, and GST-N19RhoA) from pGEX vector-transformed *E. coli* were carried out as described previously (20). Production of GST-N2, -N3, and -N4 and the GST-PH domain of Dbl in *E. coli* was carried out similarly. Production and purification of the Sf9 insect cell expressed His_6-tagged T1, DH-PH module, or N1 polypeptide were performed as described (51). The concentration and integrity of purified proteins were estimated by Coomassie blue staining after sodium dodecyl sulfate-polyacrylamide gel electrophoresis (SDS-PAGE).

Cell culture and transfection. Cells were maintained in Dulbecco's modified Eagle's medium (DMEM) supplemented with 10% calf serum (NIH 3T3) or 10% fetal bovine serum (Cos-7). Transfections were carried out using the Lipofectamine reagent (Gibco Life Sciences, Inc.). To generate stable cell lines, NIH 3T3 cells were transfected with pZipneoGST constructs or a combination of the pKH3 construct with pCMV2B vector (Stratagene), which contains a neomycin resistance selection marker and were selected in DMEM supplemented with 5% calf serum and G418 (350 μg/ml). The drug-resistant colonies were cloned and subcultured in the same medium after 18 days.

To assay transforming activity, NIH 3T3 cells were transfected with the pZipneo-proto-Dbl constructs onco-Dbl and *lbc* or v-*ras* cDNA by the calcium phosphate method as described (53). For inhibition assays, different doses of the cDNAs encoding the N-terminal polypeptide N1 or N2 in the pCEFL vector or the pCEFL vector alone were cotransfected with onco-Dbl, *lbc*, or v-*ras* cDNAs into the cells. The transfected NIH 3T3 cells were fed every 2 days with fresh DMEM supplemented with 10% calf serum. At 12 to 14 days posttransfection, the cell culture dishes were either visualized directly under the microscope for focus formation or stained with a 2% solution of Giemsa for focus scoring (53).

In vitro GDP/GTP exchange assay. The time courses for [^{3}H]GDP/GTP exchange of Rho family GTPases in the presence and absence of purified His_6-tagged or HA_3-tagged proto-Dbl mutants were determined as previously described using the nitrocellulose filtration method (51). The GEF reaction buffer contains [^{3}H]GDP-loaded Cdc42 with 20 mM Tris-HCl (pH 7.6), 100 mM NaCl, 10 mM $MgCl_2$, 0.5 mM GTP, and 1 mM dithiothreitol (DTT) supplemented with various proto-Dbl mutants.

Complex formation and immunoprecipitation. Cos-7 cells were transfected with various proto-Dbl constructs or the N-terminal polypeptide N1 by the Lipofectamine method (54). At 48 h posttransfection, complex formation between the HA_3-tagged proto-Dbl mutants and GST-fused dominant negative Cdc42 (N17Cdc42) were carried out by incubation of the mutant proto-Dbl-expressing cell lysates with the immobilized GST fusion proteins (54). Complex formation between GST-N1, GST-N2, GST-N3, or GST-N4 and the DH-PH, DH, or PH protein or between the GST-PH domain and the HA_3-N1 polypeptide were carried out similarly. The coprecipitation complexes were probed with anti-HA monoclonal antibody and visualized with chemiluminiscence reagents (Amersham Pharmacia). To detect coimmunoprecipitation between the N2 polypeptide and various Dbl mutants, the Myc-N2-encoding cDNAs in vector pCMV6 were cotransfected with the DH-PH, DH, or PH construct in the pKH3 vector into Cos-7 cells, and the cell lysates were subjected to anti-HA immuno-

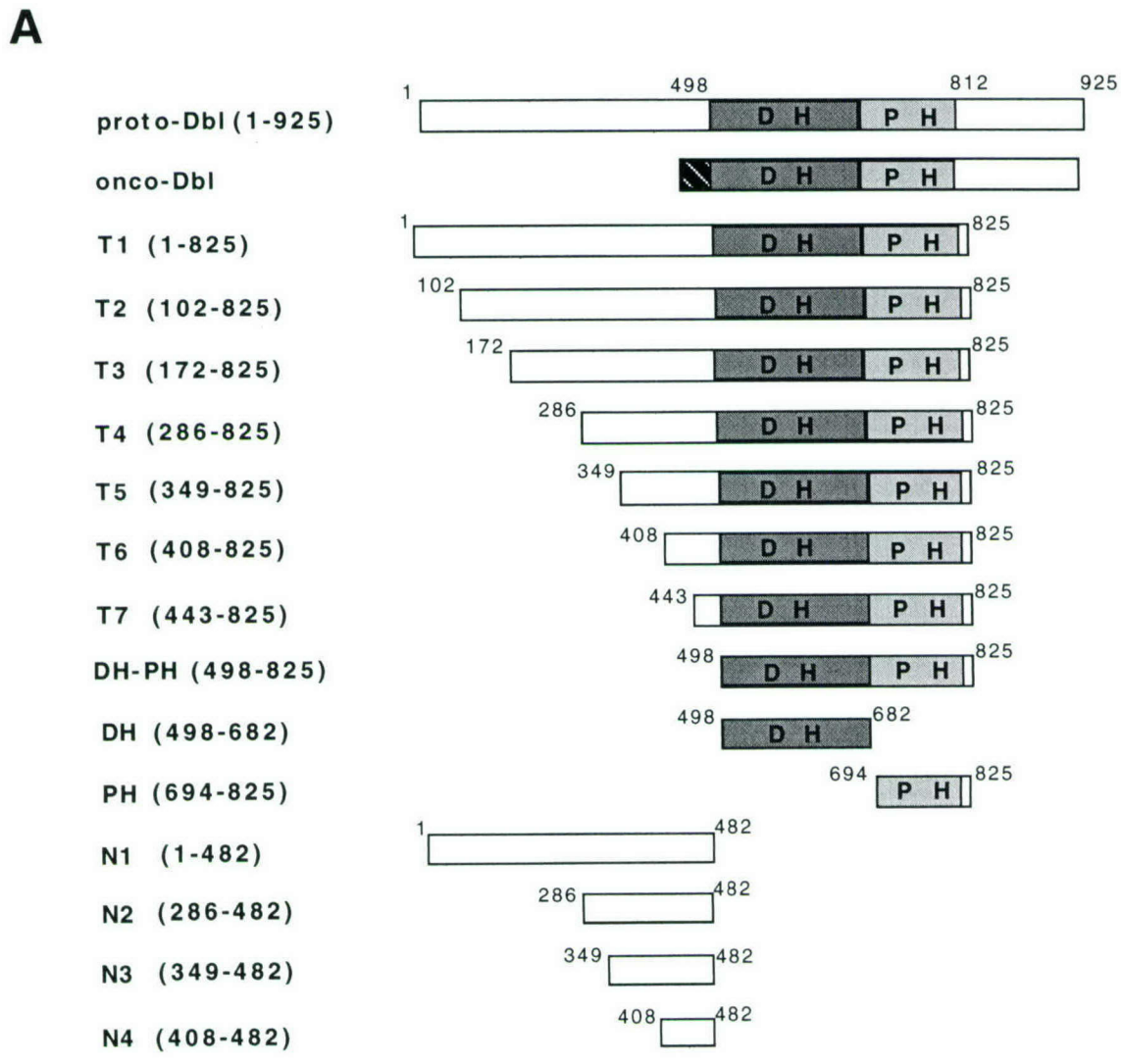

FIG. 1. N terminus of proto-Dbl contains an inhibitory motif for transforming activity. (A) Schematic representation of the structures of proto-Dbl, onco-Dbl, and various deletion mutants. Numbering refers to proto-Dbl sequences. (B) Focus-forming activities of various proto-Dbl constructs in NIH 3T3 cells. The cDNAs encoding various proto-Dbl mutants were cloned into plasmid pZipneo-GST and transfected into NIH 3T3 cells (0.1 μg/60-mm dish). At 14 days posttransfection, the number of foci was quantified visually after crystal violet staining.

precipitation with an anti-HA monoclonal antibody immobilized on agarose beads (Roche Biochemicals). The coprecipitates were washed three times before being probed with anti-HA or anti-Myc in Western blots.

In vivo Rho GTPase activation assay. The glutathione-agarose-immobilized GST-PAK1, which contains the p21-binding domain (PBD) of human PAK1 (residues 51 to 135), and GST-PKN, which contains the site required for RhoA-GTP recognition of protein kinase N (residues 1 to 128), were expressed and purified in *E. coli* by using the pGEX-KG vector as previously described (29). The active, GTP-bound form of Cdc42 or RhoA in fresh Cos-7 cell lysates coexpressing the small GTPase and various proto-Dbl constructs was captured by incubation with the GST-fused effector domains for 40 min at 4°C (54).

Fluorescence microscopy. Log-phase growing fibroblasts were seeded at a density of 3×10^4 cells per 12-mm round coverslip (Fisher Scientific) overnight before fixation in phosphate-buffered saline containing 4% paraformaldehyde for 10 min at room temperature. The cells were permeabilized in Tris-buffered saline containing 0.2% Triton X-100 for 5 min and double stained for HA-tagged protein and F-actin using anti-HA monoclonal antibody and rhodamine-phalloidin (Molecular Probes). Coverslips were mounted onto slides in 50% glycerol–Tris-buffered saline. Stained cells were analyzed with a conventional fluorescence microscope and a Zeiss confocal microscope (54).

RESULTS

Effect of deletion mutations on proto-Dbl transforming activity. To delineate a possible structural motif embedded within the N-terminal sequences that confers an inhibitory function, we generated a series of deletion mutants of proto-Dbl in which the N-terminal 101, 171, 285, 348, 407, 442, or 497 residues and/or the C-terminal 100 amino acids (T1 to T7 and DH-PH) were removed while leaving the DH-PH module intact (Fig. 1A). To evaluate the transforming potential of these proto-Dbl constructs, the respective cDNAs were cloned into the mammalian pZipneo vector and transfected into NIH 3T3 cells. As positive and negative controls, pZipneo-proto-Dbl, pZipneo-onco-Dbl, and the pZipneo vector alone were tested in parallel.

As shown in Fig. 1B, under assay conditions in which proto-Dbl displayed 1 to 2% of the transforming activity of onco-Dbl, the vector alone consistently yielded null foci. Deletion of the C-terminal 100 residues from proto-Dbl (T1) yielded a similar number of foci as proto-Dbl itself, indicating that the C-terminal sequences after the PH domain do not contribute directly to proto-Dbl regulation. Sequential removal of the N-terminal sequences, however, apparently unleashed the transforming activity in a two-step manner: the T2, T3, and T4 constructs, which lack the N-terminal 101, 171, and 285 residues, respectively, displayed a minor increase in transforming activity, with 7 to 9% of the transforming activity of onco-Dbl, whereas further truncation to residue 348, 407, or 442 (T5, T6, and T7, respectively) resulted in significant activation of transforming activity indistinguishable from that of onco-Dbl. Since the deletion mutants were expressed equally well in NIH 3T3 cells and Cos-7 cells, giving rise to polypeptides of the expected molecular weights (data not shown; see Western blots described below), the differences between the mutants in transformation are likely to reflect the true biological activities in cells rather than their differences in stability. Consistent with a previous observation (20), the DH-PH module (residues 498 to 825) behaved like onco-Dbl (Fig. 1B), implying that the DH and PH domains together constitute the structural module sufficient for maximum transforming activity. These results suggest that the extreme N terminus (residues 1 to 101) of proto-Dbl contains a minor negative regulatory element and that sequences between residues 286 and 348 contain an additional element(s) that is involved in imposing a major constraining effect on the oncogenic activity of the subsequent DH-PH module.

Effect of deletion mutations on the GEF activity of proto-Dbl protein. The transforming activity of onco-Dbl was found to correlate closely with its Rho GEF activity (54). We pondered whether proto-Dbl, under the constraint of the N-terminal sequences, is defective in functioning as a GEF for Cdc42 and RhoA, resulting in the apparent suppression of transforming activity. To this end, the T1 mutant, which bears the C-terminal 100-amino-acid truncation and functions like proto-Dbl in transformation assays, and the DH-PH module, which mimics onco-Dbl in both GEF catalysis and transformation ability (20), were expressed in Sf9 insect cells as His_6-tagged fusion proteins and purified by Ni^{2+}-agarose affinity chromatography. When equal molar amounts of His_6-T1 and His_6-DH-PH were assayed for the ability to stimulate [^{3}H]GDP/GTP exchange of Cdc42, we observed that while DH-PH was very efficient in accelerating the GEF reaction, such that over 90% of bound [^{3}H]GDP was dissociated from Cdc42 within 5 min under its stimulation, T1 was only marginally active in stimulating the GEF reaction, such that only ~10% of Cdc42-bound [^{3}H]GDP was replaced by GTP within the same time period compared with that in the absence of T1 (Fig. 2A). Thus, the N-terminal sequences of proto-Dbl negatively regulate the GEF activity of the DH-PH module.

Next, we examined the catalytic GEF activity of a panel of proto-Dbl mutants on Cdc42 in vitro. The T1, T4, T5, T6, and DH-PH cDNAs in the pKH3 vector, which provides an HA_3 tag at the N terminus, were transiently expressed in Cos-7 cells, and the proteins were purified by immunoprecipitation from the cell lysates by using anti-HA agarose beads. Upon elution by HA peptides, the purified deletion mutants were analyzed by anti-HA Western blot, and the amount of each protein was visualized by chemiluminiscence imaging of the blot (Fig. 2B). While the T5 and T6 mutants, which lacked the N-terminal 348 and 407 residues, respectively, showed activities in stimulating [^{3}H]GDP dissociation from Cdc42 similar to that of the DH-PH module, T1 and T4, which contain an intact N terminus or residues 286 to 825, respectively, were comparable in displaying a significantly weaker GEF activity at equal molar quantities (Fig. 2C). These results indicate that the N-terminal sequences directly impose an inhibitory effect on the GEF activity of the DH-PH module. To test if the N terminus interacts with the catalytic DH domain, resulting in inhibition, the N1 polypeptide encoding residues 1 to 482 was generated in Sf9 insect cells as a GST fusion and included in the GEF activity assays with the DH-PH module. As shown in Fig. 2D, no detectable effect was observed when a fourfold molar excess of GST-N1 was present together with the DH-PH module in stimulating [^{3}H]GDP dissociation from Cdc42 compared with DH-PH alone. We conclude that the N terminus of proto-Dbl interferes with the GEF function through a mechanism other than direct blockage of substrate binding to the DH domain as is the case with Vav (3).

To determine the Rho GTP ase exchange potential of the mutants in cells, the HA-tagged proto-Dbl mutants were transiently cotransfected with HA-tagged, wild-type Cdc42 or RhoA in Cos-7 cells. The expression level of the mutants and Cdc42 or RhoA could be directly compared (Fig. 3). The relative amounts of activated GTPases in the cell lysates were measured by GST-PAK1 or GST-PKN pull-down, which specifically recognizes and stabilizes the GTP-bound form of Cdc42 or RhoA (29). As shown in Fig. 3, both the T1 and T4 mutants demonstrated significantly lower Cdc42 activating potential, while T5 and T6 were similar to the DH-PH module in their ability to generate Cdc42-GTP. Similar observations were also made when RhoA was examined as an in vivo substrate (data not shown). These results indicate that the cellular Rho GTPase-activating potential of the proto-Dbl mutants correlates with their in vitro GEF activity. This pattern of GEF activity and the Rho protein-activating potential of the mutants are reminiscent of the above-described transforming abilities of the mutants (Fig. 1B). We deduce from these results that the sequences between residues 286 and 348 contain the critical structural element(s) that appears to hinder the GEF function of the DH-PH module and that the lack of transforming ac-

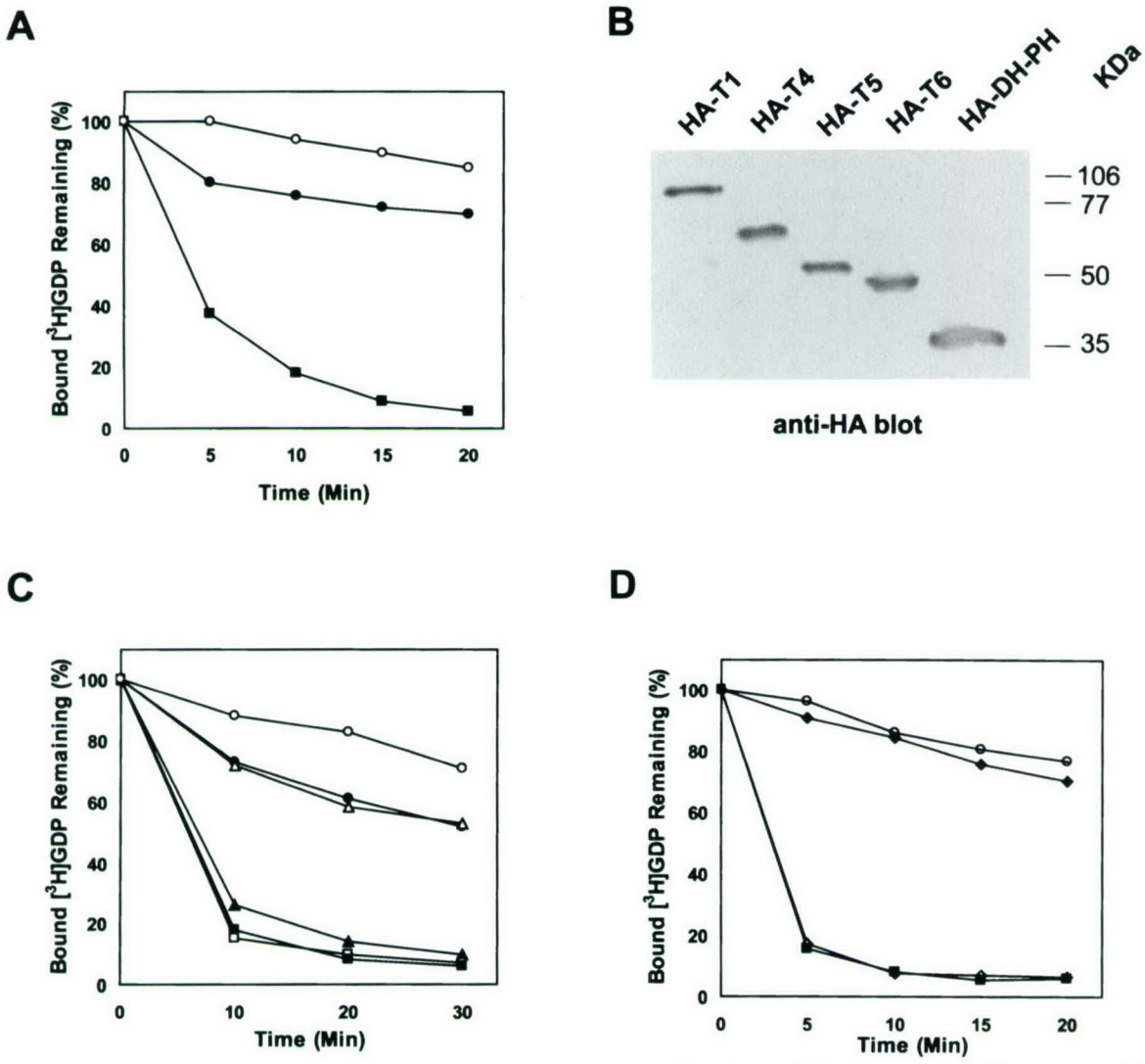

FIG. 2. GEF activity of proto-Dbl is negatively regulated by the presence of the N-terminal sequences. (A) Time courses of [^{3}H]GDP dissociation from Cdc42 catalyzed by T1 and the DH-PH module. The insect cell-expressed His_6-T1 and His_6-DH-PH were purified to homogeneity by Ni^{2+}-agarose affinity chromatography. Approximately 10 pmol of each (T1, solid circles; DH-PH, solid squares; buffer, open circles) was used to assay GEF activity on ~1 μg of Cdc42-[^{3}H]GDP in a buffer containing 20 mM Tris-HCl (pH 7.6), 100 mM NaCl, 10 mM $MgCl_2$, 0.5 mM GTP, and 1 mM DTT. The GEF reactions were terminated at the indicated time points by nitrocellulose filtration. (B) HA_3-tagged deletion mutants were purified from Cos-7 cell lysates by using the immobilized anti-HA antibody. After elution with 0.2 mM HA peptides, the mutants were analyzed by Western blot with anti-HA antibody. (C) Effect of deletion mutations on GEF activity. Approximately equal molar amounts of the mutants purified from Cos-7 cell lysates (20 μl) were assayed for the ability to stimulate [^{3}H]GDP dissociation from Cdc42 at various times. Open circles, buffer; solid circles, T1; open triangles, T4; solid triangles, T5; open squares, T6; solid squares, DH-PH. (D) Effect of isolated N-terminal peptide N1 on GEF activity of DH-PH. [^{3}H]GDP dissociation from Cdc42 was assayed in the presence (solid squares and open diamonds) or absence of His_6-DH-PH (open circles and solid diamonds) and an approximately fourfold molar excess of purified GST-N1 (diamonds) at various time points.

tivity of proto-Dbl reflects the suppressive effect on the catalytic GEF activity by the N-terminal negative regulatory constraint(s).

Rho GTPase-binding activities of deletion mutants of proto-Dbl. To further investigate the functional properties of the various deletion mutants of proto-Dbl, we next compared their abilities to directly bind to the Rho GTPase substrate Cdc42. Cos-7 cell lysates expressing similar amounts of HA-tagged T1, T4, T5, T6, and the DH-PH module (Fig. 4) were incubated with the glutathione-agarose-immobilized, GST-fused, dominant negative form of Cdc42, N17Cdc42, that is known to bind to the DH domain of onco-Dbl with high affinity (20). After extensive washing the coprecipitates of GST-N17Cdc42 were subjected to anti-HA Western blotting. Among the five HA-tagged polypeptides, T5, T6, and the DH-PH module displayed a similarly strong binding pattern to N17Cdc42. T4 bound significantly more weakly, and T1 binding was barely detectable (Fig. 4). These results are consistent with the relative effectiveness of the mutants in activating the guanine nucleotide exchange of Cdc42 in vitro and in vivo (Fig. 2 and 3) and coincide with the mutants' transformation abilities (Fig. 1B). They suggest that the N-terminal residues, particularly residues 285

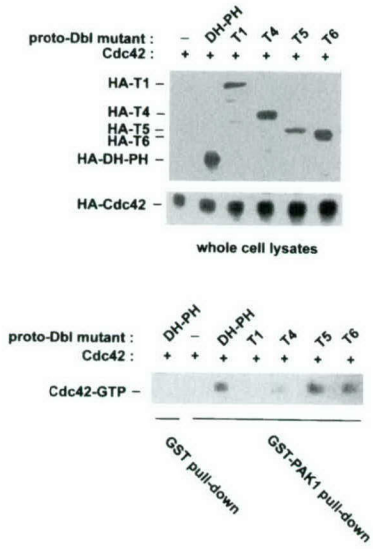

FIG. 3. Cdc42 exchange potential of proto-Dbl mutants in cells. HA_3-Cdc42 was expressed alone or together with HA-DH-PH, HA-T1, HA-T4, HA-T5, or HA-T6 in Cos-7 cells. The cell lysates were probed with anti-HA antibody in a Western blot. The cell lysates were subjected to a GST or GST-PAK1 pull-down assay, and the glutathione-agarose coprecipitates were detected by anti-HA Western blotting to reveal the relative amount of Cdc42-GTP in cells.

to 348, are involved in negative allosteric control of proto-Dbl activity by limiting the access of Rho GTPase to the catalytic site on the DH domain.

N-terminal sequences dictate the intracellular localization pattern of proto-Dbl. Onco-Dbl and the PH domain of Dbl were colocalized with Triton X-100-insoluble particulates in previous cell fractionation studies (53). Whether the N-terminal constraining sequences of proto-Dbl would interfere with the PH domain intracellular targeting function, thereby causing an alteration in the intracellular distribution pattern of

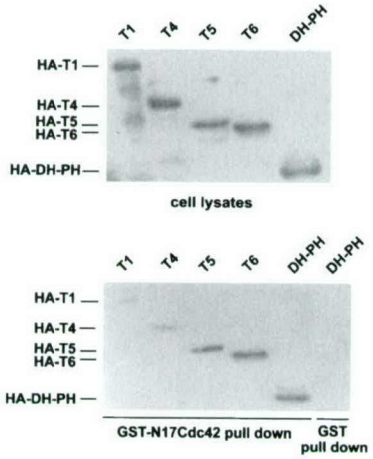

FIG. 4. In vitro binding activity of proto-Dbl mutants to GST-N17Cdc42. Various proto-Dbl constructs were expressed in Cos-7 cells by transient transfection. A portion of cell lysates was analyzed by anti-HA Western blotting. The cell lysates were incubated with 2 μg of GST or GST-Cdc42N17 immobilized on glutathione beads for 1 h at 4°C under constant agitation. After three washes, bound proteins were detected by immunoblotting with anti-HA antibody.

FIG. 5. Intracellular distribution patterns of proto-Dbl and various deletion mutants. (A) Stable transfectants of HA-tagged T1 (proto-Dbl), DH-PH module, DH domain, PH domain, N-terminal N1 polypeptide, or DH-PH module coexpressed with the N1 polypeptide were generated in NIH 3T3 cells by G418 selection. Cell lysates ($\sim 5 \times 10^5$ cells) of the G418-resistant clones were subjected to anti-HA immunoprecipitation followed by Western blotting with anti-HA antibody. (B) Fluorescence microscopy of the cellular localization patterns of the proto-Dbl mutants. Stably transfected cells were maintained in low serum (2%) overnight before being fixed and double stained as described in the text. The cells were analyzed by confocal microscopy with double filters for fluorescein and rhodamine. The overlap of fluorescein and rhodamine images is shown in yellow.

proto-Dbl from that of onco-Dbl, has not been assessed. To examine the effect of the N-terminal sequences on proto-Dbl cellular localization and to determine the contribution of individual structural motifs to the proto-Dbl localization pattern, we have generated stable transfectants of NIH 3T3 cells expressing the HA-tagged proto-Dbl (T1), DH-PH module, DH domain, PH domain, or the N1 polypeptide (residues 1 to 482), as well as a cell clone coexpressing Flag-tagged N1 together with HA-DH-PH (DH-PH+N1). Western blot analysis of the anti-HA immunoprecipitates from the respective cell lysates confirmed that HA-tagged polypeptides of the expected molecular sizes were expressed in the cell lines (Fig. 5A). In addition, an anti-Flag Western blot further confirmed that Flag-N1 was coexpressed with HA-DH-PH in the DH-PH+N1 cells (data not shown). After fixation, the cells were double stained with anti-HA monoclonal antibody plus fluorescein-labeled anti-mouse immunoglobulin antibody and rhodamine-labeled phalloidin to visualize HA-tagged polypeptide distribution and cellular actin structures. Under a confocal microscope, we found that proto-Dbl displayed a mostly perinuclear distribution pattern similar to that of the N1 polypeptide (Fig. 5B). The DH-PH module, on the other hand, was found to colocalize with actin stress fibers, like the PH domain alone, whereas the DH domain was mostly diffused throughout cells, with some degree of concentration around the nucleus (Fig. 5B). These results are consistent with the previous cell fractionation data showing a significant portion of the DH-PH module and the PH domain in the Triton X-100-insoluble fraction and the DH domain mostly in the cytosol (53) and suggest that the N-terminal sequences in proto-Dbl affect the cellular distribution pattern of proto-Dbl. In the N1 polypeptide-coexpressing cells, the actin-stress fiber colocalization pattern of DH-PH was disrupted and changed to the mostly perinuclear localization, similar to that of the N1 polypeptide alone (Fig. 5B). Thus, the N-terminal sequences of proto-Dbl contain the structural element(s) that dictates the intracellular distribution of proto-Dbl. This is likely due to the interference of the PH domain targeting function that de-

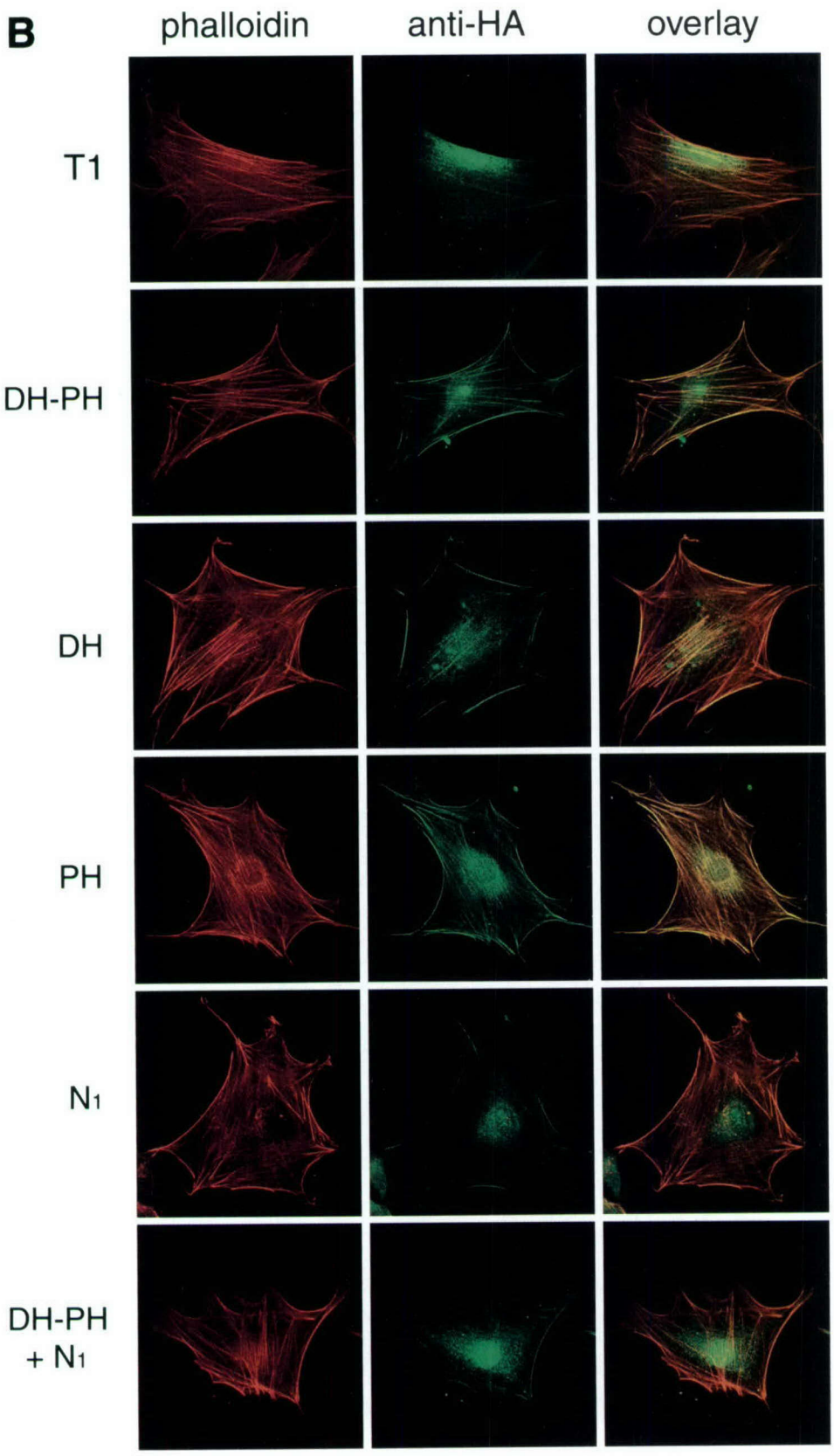

FIG. 5—*Continued.*

termines the localization pattern of onco-Dbl by the N-terminal sequences.

Isolated N-terminal fragment of proto-Dbl inhibits onco-Dbl transforming activity. The negative regulatory function of the N-terminal sequences raised the possibility that the isolated N terminus of proto-Dbl might interfere with the biological activity of oncogenic Dbl. To test this hypothesis, the cDNAs encoding the N1 (residues 1 to 482) and N2 (residues 286 to 482) polypeptides were cloned into the mammalian expression vector pCEFL and cotransfected with onco-Dbl into NIH 3T3 cells. Compared with the empty vector, N1 reduced onco-Dbl transforming activity by ~90% at a dose of 2 μg/100-mm dish, while N2 consistently caused ~25% inhibition under similar conditions (Fig. 6). At a lower dose (0.2 μg/100-mm dish), however, only N1 showed significant inhibition of onco-Dbl activity. Neither N1 nor N2 had a detectable effect on proto-Dbl transforming activity when the foci were induced by proto-Dbl overexpression (2 μg of cDNA/100-mm dish; data not shown). To confirm that the N-terminal sequence-caused inhibition was specific for onco-Dbl, we examined the ability of N1 and N2 to affect the transforming functions of a *dbl*-related oncogene, *lbc*, and oncogenic v-*ras*. Distinct from their effects on onco-Dbl, neither peptide showed any sign of inhibiting oncogene-induced focus formation at 2 μg of cDNA/dish (Fig. 6). These results indicate that the N terminus of proto-Dbl can specifically act on onco-Dbl or the onco-Dbl pathway and negatively influence its biological activity.

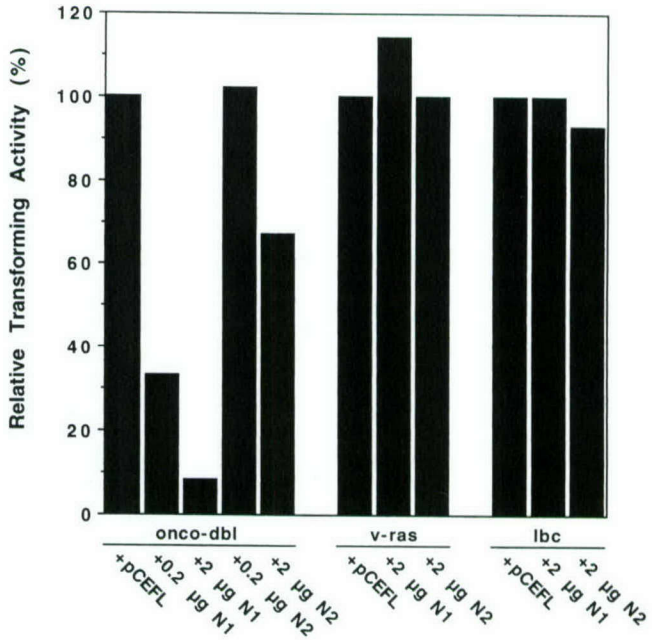

FIG. 6. N-terminal sequences of proto-Dbl specifically inhibit onco-Dbl transforming activity. NIH 3T3 cells were transfected with pZipneo-onco-Dbl (4 ng/100-mm dish) together with pCEFL vector or cDNAs encoding the N1 or N2 sequences in pCEFL vector at the indicated doses (micrograms per 100-mm dish). The *lbc* oncogene (0.1 μg/100-mm dish) together with the pCEFL vector or the N1 or N2 cDNA in the pCEFL vector (2 μg/dish) or oncogenic v-*ras* cDNA (0.1 μg/dish) together with vector or the N1 or N2 cDNA (2 μg/dish) in pCEFL were cotransfected in parallel. The focus-forming activity of each oncogene cotransfected with the empty pCEFL vector was set at 100%. The relative focus-forming activities represent results from four independent experiments.

Interaction of N-terminal sequences with the PH domain of proto-Dbl. The above-characterized negative regulatory function of the N terminus of proto-Dbl could be rationalized by an intramolecular interaction involving the N-terminal regulatory sequences and the C-terminal functional module, thereby affecting the GEF activity of the DH domain and the intracellular targeting function of the PH domain. To test this hypothesis, we first employed a glutathione-agarose pull-down assay using the insect cell-expressed GST-N1 peptide as a probe to detect possible interaction with the C-terminal functional motifs, i.e., the DH-PH module, DH domain, or PH domain. The DH-PH module, DH domain, and PH domain were transiently expressed in Cos-7 cells as HA-tagged proteins, and the cell lysates were incubated with immobilized GST or GST-N1. As shown in Fig. 7A, GST-N1 was able to stably associate with the DH-PH module and the PH domain but not with the DH domain, whereas the GST control did not bind to any of the three proteins. When the N1 polypeptide was expressed in Cos-7 cells and subjected to the pull-down assay with the immobilized GST-PH domain, we found that GST-PH was able to tightly bind to HA-N1 in the glutathione-agarose coprecipitates under conditions in which GST alone did not interact with N1 (Fig. 7B). Therefore, the N-terminal 482 residues of proto-Dbl can form a physical complex with the C-terminal DH-PH functional module via the PH domain.

To further delineate the region of amino acids in the N terminus that may contribute to direct interaction with the PH domain, the sequentially deleted N2, N3, and N4 polypeptides, encoding residues 286 to 482, 349 to 482, and 408 to 482, respectively, were employed as GST-tagged probes to detect possible binding to the PH domain. Figure 7C shows that while none of the three N-terminal peptides bound to the DH domain at a detectable level, N2, but not N3 or N4, was capable of binding directly to the PH domain. These results imply that the region between amino acids 286 and 348 contains an important element(s) that is involved in interaction with the PH domain.

To test whether stable association between the N terminus and the PH domain could occur in cells, a Myc-tagged N2 peptide was coexpressed with the HA-tagged DH-PH module, DH domain, or PH domain in Cos-7 cells, and the coimmunoprecipitation pattern of Myc-N2 with the HA-tagged proteins was determined. In contrast to the lack of detectable association by HA-DH, both HA-DH-PH and HA-PH formed a stable complex with Myc-N2, as revealed by the anti-Myc Western blot of the anti-HA immunoprecipitates (Fig. 7D). Thus, the N-terminal sequences of proto-Dbl can bind tightly to the C-terminal PH domain in cells and are likely to do so intramolecularly. Such an interaction may have a direct impact on both the GEF activity and intracellular localization of proto-Dbl, which are essential for its transforming activity, causing the observed autoinhibitory behaviors.

DISCUSSION

Although most Dbl family members contain diverse multifunctional motifs, they all have the structural array of a central DH domain in tandem at the carboxyl terminus with a PH

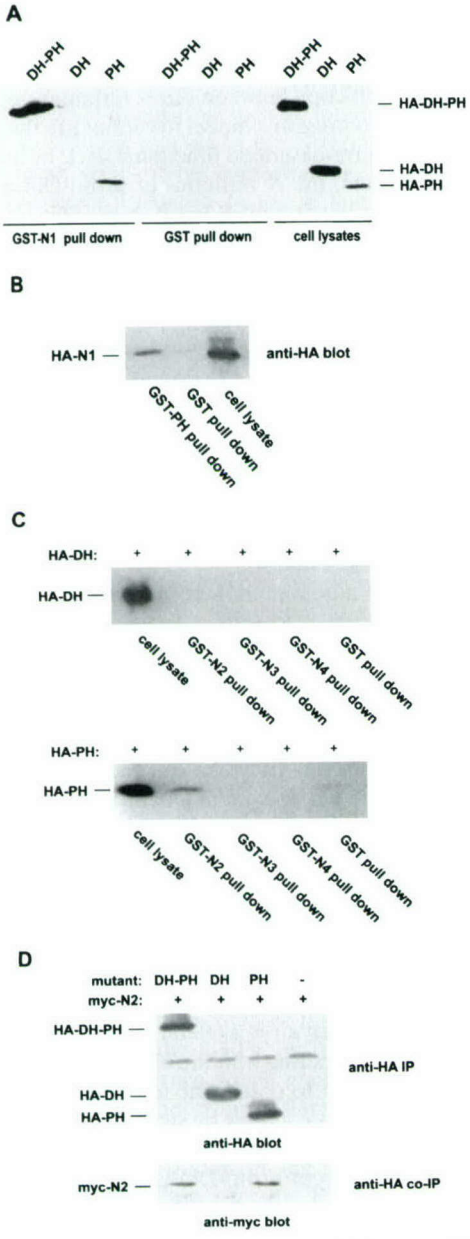

FIG. 7. N-terminal sequences of proto-Dbl interact directly with the PH domain. (A) GST-N1 polypeptide forms a stable complex with the DH-PH module or the PH domain of proto-Dbl. The DH-PH module, DH domain, or PH domain was transiently expressed in Cos-7 cells as an HA-tagged protein. About 2 μg of GST or GST-N1 immobilized on glutathione-agarose beads was incubated with the cell lysates for 1 h at 4°C. After three washes, the agarose bead coprecipitates were subjected to anti-HA Western blotting analysis. (B) PH domain complexes with N1 polypeptide of proto-Dbl in vitro. Immobilized GST or GST-PH (~2 μg/sample) was incubated with Cos-7 lysates expressing HA-N1, and the coprecipitates were detected by anti-HA immunoblotting. (C) Immobilized GST-N2 (residues 286 to 482), GST-N3 (349 to 482), or GST-N4 (408 to 482) was incubated with cell lysates expressing HA-DH or HA-PH. The association of the HA-tagged DH or PH domain with the GST fusion coprecipitates was detected by anti-HA Western blot. (D) DH-PH module and the PH domain but not the DH domain associate with the N2 polypeptide in cells. The Myc-tagged N2 polypeptide was coexpressed in Cos-7 cells with the HA-tagged DH-PH, DH, or PH construct. Cell lysates were subjected to anti-HA immunoprecipitation (IP) followed by anti-HA or anti-Myc Western blotting.

domain. Previous studies of onco-Dbl have established that the DH domain is primarily responsible for Rho GTPase binding and GEF activity, while the PH domain is involved in intracellular targeting and is necessary for the transforming activity of onco-Dbl (8, 50). Truncation of the N-terminal 497 residues of proto-Dbl results in oncogenic activation (42), suggesting that the N-terminal sequences contain negative regulatory elements imposing a constraint on the C-terminal DH-PH module. To date, the mechanism which the N terminus employs in the negative regulation of proto-Dbl activity and the regions of the molecule contributing to the regulation remain unclear. In this study, we provide direct evidence that proto-Dbl adopts an autoinhibitory mechanism for controlling its biochemical and biological activities. We identified the region between amino acids 275 and 349 as a critical inhibitory motif that impairs GEF catalytic activity and the intracellular targeting activity of the DH-PH module. The autoinhibitory effects are likely to arise through direct intramolecular interaction of this region with the PH domain, limiting the access of Rho GTPases to the DH domain and masking the intracellular targeting function of the PH domain. Such an autoinhibitory mode may be optimal for proto-Dbl regulation, since incoming upstream signals could exert their effects by modulation of either the N-terminal motif or the C-terminal PH domain.

Inhibitory effects of N-terminal sequences of proto-Dbl on the DH-PH module. Our previous structural mapping studies indicate that the DH-PH module of Dbl represents the minimum constitutively active structural unit that confers Rho GTPase exchange activity and cell-transforming potential (20). We show here that the presence or absence of the C-terminal 100 amino acids just outside the PH domain did not cause any change in transforming activity for either proto-Dbl or onco-Dbl, indicating that these sequences are not involved in regulation of the DH-PH module. A series of deletion mutations into the N terminus resulted in an apparent two-step activation of the proto-Dbl transforming activity: removal of the N-terminal 100 or 274 residues caused minor but significant enhancement, while further truncation to residue 348 led to full-blown activation of the focus-forming activity that is similar to the capacity of the DH-PH module (Fig. 1). These results prompted us to speculate that the N-terminal sequences impose a two-layer regulatory mechanism on the DH-PH module. The N-terminal 100 residues and sequences between residues 275 and 349 either act independently in negatively controlling the DH-PH activity or act coordinately so that the N-terminal 100 residues may further reinforce the negative constraint imposed by the following sequences. This is analogous to the situation of the *vav* proto-oncogene product, in which removal of the N-terminal 66 or 127 residues led to only partial activation of the transforming activity, while full activation was achieved by truncation of the N-terminal 186 residues (1).

The cellular transforming activity of Dbl is intimately dependent upon its catalytic GEF activity on Rho GTPases (54). The inhibitory effects of deletions of proto-Dbl on transformation indeed reflect their relative GEF activities on Cdc42 and RhoA when the purified mutants were tested in vitro (Fig. 2). The N terminus appears to potently inhibit the GEF ability of the DH-PH module, implying that an intramolecular interaction is at work in the regulatory mechanism. Residues 275 to

a multistage activation switch. Cell **102:**387–397.
28. **Li, R., and Y. Zheng.** 1997. Residues of the Rho family GTPases Rho and Cdc42Hs that specify sensitivity to Dbl-like guanine nucleotide exchange factors. J. Biol. Chem. **272:**4671–4681.
29. **Li, R., B. Debreceni, B. Jia, Y. Gao, G. Tigyi, and Y. Zheng.** 1999. Localization of the PAK1-, WASP-, and IQGAP1-specifying regions of the small GTPase Cdc42. J. Biol. Chem. **274:**29648–29654.
30. **Lin, R., R. A. Cerione, and D. Manor.** 1999. Specific contributions of the small GTPases Rho, Rac, and Cdc42 to Dbl transformation. J. Biol. Chem. **274:**23633–23641.
31. **Liu, X., H. Wang, M. Eberstadt, A. Schnuchel, E. T. Olejniczak, R. P. Meadows, J. M. Schkeryantz, D. A. Janowick, J. E. Harlan, E. A. S. Harris, D. E. Staunton, and S. W. Fesik.** 1998. NMR structure and mutagenesis of the N-terminal Dbl homology domain of the nucleotide exchange factor Trio. Cell **95:**269–277.
32. **Michiels, F., G. G. M. Habets, J. C. Stam, R. A. van der Kammen, and J. G. Collard.** 1995. A role for Rac in Tiam1-induced membrane ruffling and invasion. Nature **375:**338–340.
33. **Miki, T., C. L. Smith, J. E. Long, A. Eva, and T. P. Fleming.** 1993. Oncogene ect2 is related to regulators of small GTP-binding proteins. Nature **362:**462–465.
34. **Nern, A., and R. A. Arkowitz.** 1999. A Cdc24p-Far1p-Gbg protein complex required for yeast orientation during mating. J. Cell Biol. **144:**1187–1202.
35. **Nishida, K., Y. Kaziro, and T. Satoh.** 1999. Association of the proto-oncogene product Dbl with G protein βγ subunits. FEBS Lett. **459:**186–190.
36. **Olivo, C., C. Vanni, P. Mancini, L. Silengo, M. R. Torris, G. Tarone, P. Defilippi, and A. Eva.** 2000. Distinct involvment of Cdc42 and RhoA GTPases in actin organization and cell shape in untransformed and Dbl oncogene transformed NIH 3T3 cells. Oncogene **19:**1428–1436.
37. **Olson, M. F., N. G. Pasteris, J. L. Gorski, and A. Hall.** 1996. Faciogenital dysplasia protein (FGD1) and Vav, two related proteins required for normal embryonic development, are upstream regulators of Rho GTPases. Curr. Biol. **6:**1628–1633.
38. **Olson, M. F., P. Sterpetti, K. Nagata, D. Toksoz, and A. Hall.** 1997. Distinct roles for the DH and PH domains in the Lbc oncogene. Oncogene **15:**2827–2831.
39. **Pawson, T.** 1995. Protein modules and signaling networks. Nature **373:**573–580.
40. **Qian, X., W. C. Vass, A. G. Papageorge, P. H. Anborgh, and D. R. Lowy.** 1998. N terminus of Sos1 Ras exchange factor: critical roles for the Dbl and pleckstrin homology domains. Mol. Cell. Biol. **18:**771–778.
41. **Ron, D., S. R. Tronick, S. A. Aaronson, and A. Eva.** 1988. Molecular cloning and characterization of the human dbl proto-oncogene: evidence that its overexpression is sufficient to transform NIH3T3 cells. EMBO J. **7:**2465–2473.
42. **Ron, D., G. Graziani, S. A. Aaronson, and A. Eva.** 1989. The N-terminal region of proto-dbl down regulates its transforming activity. Oncogene **4:** 1067–1072.
43. **Ron, D., M. Zannini, M. Lewis, R. B. Wickner, L. T. Hunt, G. Graziani, S. R. Trinick, S. A. Aaronson, and A. Eva.** 1991. A region of proto-Dbl essential for its transforming activity shows sequence similarity to a yeast cell-cycle gene, Cdc24, and the human break point cluster gene, bcr. New Biol. **3:**372–379.
44. **Soisson, S. M., A. S. Nimnual, M. Uy, D. Bar-Sagi, and J. Kuriyan.** 1998. Crystal structure of the Dbl and Pleckstrin homology domains from the human son of sevenless protein. Cell **95:**259–268.
45. **Stam, J. C., E. E. Sander, F. Michiels, F. N. van Leeuwen, H. E. T. Kain, R A. van der Kammen, and J. G. Collard.** 1997. Targeting of Tiam1 to the plasma membrane requires the cooperative function of the N-terminal pleckstrin homology domain and an adjacent protein interaction domain. J. Biol. Chem. **272:**28447–28454.
46. **Tatsumoto, T., X. Xie, R. Blumenthal, I. Okamoto, and T. Miki.** 1999. Human Ect2 is an exchange factor for Rho GTPases, phosphorylated in G2/M phases, and involved in cytokinesis. J. Cell Biol. **147:**921–927.
47. **Van Aelst, L., and C. D'Souza-Schorey.** 1997. Rho GTPases and signaling networks. Genes Dev. **11:**2295–2322.
48. **Whitehead, I. P., Q. T. Lambert, J. A. Glaven, K. Abe, K. L. Rossman, G. M. Mahon, J. M. Trzaskos, R. Kay, S. L. Campbell, and C. J. Der.** 1999. Dependence of Dbl and Dbs transformation on MEK and NF-κB activation. Mol. Cell. Biol. **19:**7759–7770.
49. **Whitehead, I., H. Kirk, C. Tognon, G. Trigo-Gonzalez, and R. Kay.** 1995. Expression cloning of Lfc, a novel oncogene with structural similarities to guanine nucleotide exchange factors and to the regulatory region of protein kinase C. J. Biol. Chem. **270:**18388–18395.
50. **Whitehead, I. P., S. Campbell, K. L. Rossman, and C. J. Der.** 1997. Dbl family proteins. Biochim. Biophys. Acta **1332:**F1–F23.
51. **Zheng, Y., M. Hart, and R. A. Cerione.** 1995. Guanine nucleotide exchange catalyzed by *dbl* oncogene product. Methods Enzymol. **256:**77–84.
52. **Zheng, Y., M. Olson, A. Hall, R. A. Cerione, and D. Toksoz.** 1995. Direct involvement of the small GTP-binding protein Rho in *lbc* oncogene function. J. Biol. Chem. **270:**9031–9034.
53. **Zheng, Y., D. Zangrilli, R. A. Cerione, and A. Eva.** 1996. The pleckstrin homology domain mediates transformation by oncogenic Dbl through specific intracellular targeting. J. Biol. Chem. **271:**19017–19020.
54. **Zhu, K., B. Debreceni, R. Li, and Y. Zheng.** 2000. Identification of Rho GTPase-dependent sites in the DH domain of oncogenic Dbl that are required for transformation. J. Biol. Chem. **275:**25993–26001.
55. **Zhu, K., B. Debreceni, F. Bi, and Y. Zheng.** 2001. Oligomerization of DH domain is essential for Dbl-induced transformation. Mol. Cell. Biol. **21:**425–437.

reprints from

TRENDS in
Biochemical Sciences TiBS

Elsevier Science London
84 Theobald's Road
London
UK WC1X 8RR
Tel +44 (0)20 7611 4000
Fax +44 (0)20 7611 4001

Dbl family guanine nucleotide exchange factors

Yi Zheng

The Dbl family of guanine nucleotide exchange factors are multifunctional molecules that transduce diverse intracellular signals leading to the activation of Rho GTPases. The tandem Dbl-homology and pleckstrin-homology domains shared by all members of this family represent the structural module responsible for catalyzing the GDP–GTP exchange reaction of Rho proteins. Recent progress in genomic, genetic, structural and biochemical studies has implicated Dbl family members in diverse biological processes, including growth and development, skeletal muscle formation, neuronal axon guidance and tissue organization. The detailed pictures of their autoregulation, agonist-controlled activation and mechanism of interaction with Rho GTPase substrates, have begun to emerge.

Yi Zheng
Dept of Molecular Sciences, University of Tennessee Health Science Center, Memphis, TN 38163, USA.
e-mail: yzheng@utmem.edu

The *dbl* oncogene product was originally isolated from a diffuse B-cell lymphoma. Subsequent amino acid sequence analysis found that a region in the central portion of the Dbl protein, now known as the Dbl homology (DH) domain, shares significant similarity with the yeast cell division cycle protein Cdc24 and the human break point cluster region protein Bcr. Suspicion that Cdc24 might act upstream of the GTPase Cdc42 in yeast led to the finding that both Dbl and Cdc24 function as guanine nucleotide exchange factors (GEFs), stimulating the replacement of GDP bound to specific Rho family GTPases with GTP [1,2]. Over the past decade, many proteins have been placed in the Dbl family because they contain a DH domain and a tandem pleckstrin homology (PH) domain that is invariably located immediately C-terminal to the DH domain.

The current biochemical model depicts that Dbl family GEFs function immediately upstream of Rho GTPases (Fig. 1). Stimulation of growth factor receptors, cytokine receptors, cell-to-cell or extracellular matrix-to-cell adhesion receptors, or the G-protein-coupled serpentine receptors, can all initiate intracellular signals that lead to Rho GTPase activation, a process that probably involves Dbl family members. Concomitantly, the incoming signals might also modulate Rho GTPase-activating proteins (RhoGAPs) and Rho GDP-dissociation inhibitors (RhoGDIs), both of which serve to negatively regulate Rho functions, resulting in elevated levels of Rho-GTP. The active Rho species interact, in turn, with a large array of effector targets that further relay the signals to downstream signaling components, resulting in diverse biological responses (Fig. 1; reviewed in Refs [3,4]).

This review focuses on recent progress in our understanding of the biological functions and molecular mechanisms underlying the biochemical activities of Dbl family GEFs. The mode of regulation of Dbl family members and the mechanistic interactions between the GEFs and Rho GTPase substrates are discussed in depth.

Evolution and biological functions

The DH domain does not share significant sequence homology with other subtypes of small G-protein GEF motifs such as the Cdc25 domain and the Sec7 domain, which specifically interact with Ras and ARF family small GTPases, respectively, nor with other Rho protein interactive motifs, indicating that the Dbl family proteins are evolutionarily unique. Recently completed genome sequencing projects have revealed that there are at least three Dbl family GEFs in *Saccharomyces cerevisiae*, 18 in *Caenorhabditis elegans*, 23 in *Drosophila melanogaster* and 46 in *Homo sapiens* [5]. This number might increase further when detailed annotations of the genomic sequences become available; indeed, there are at least 20 additional partial sequences in the human genome that appear to encode DH domain-containing proteins. The number of GEF substrates (i.e. Rho family GTPases) also increases with evolution, from six in *S. cerevisiae* to 18 in human, but they are far outnumbered by the positive regulators in higher eukaryotes, suggesting that the function of individual GEFs is more specialized in mammals. Indeed, many mammalian Dbl family members are tissue- and cell-type specific, and their biochemical GEF activities range from being highly selective for one Rho GTPase substrate to more promiscuous towards multiple Rho proteins (Table 1).

The first genetic evidence of Dbl family functions came from studies of Cdc24, a bud site assembly molecule in *S. cerevisiae* whose function is closely associated with that of Cdc42 [3]. Disruption of *CDC24* led to cell death, indicating that Cdc24 had an essential role in cell growth. Various Cdc24 mutant phenotypes also imply that Cdc24 is an essential component regulating vegetative growth, cell mating, polarity establishment and cell orientation [6]. Rom2, another Dbl family member of budding yeast that can suppress mutations of the phosphatidylinositol kinase (PI3K) homolog *tor2*, appears to be the physiological activator of Rho1 and Rho2 GTPases, and acts in the Tor2–Rho1/Rho2 pathway controlling the actin cytoskeleton and cell shape [7].

http://tibs.trends.com 0968-0004/01/$ – see front matter © 2001 Elsevier Science Ltd. All rights reserved. PII: S0968-0004(01)01973-9

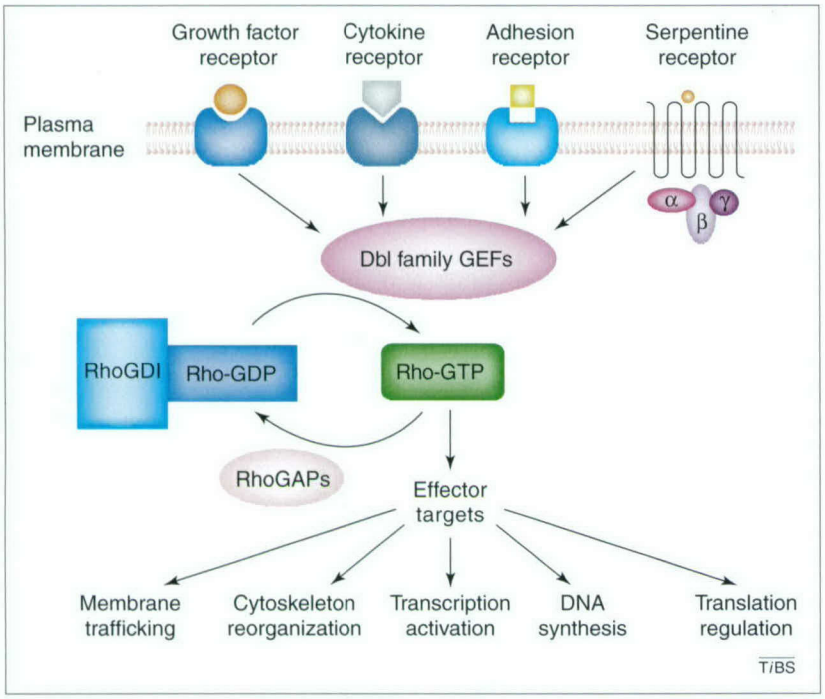

Fig. 1. Signaling role of Dbl family GEFs in the regulation of Rho GTPase functions. In mammalian cells, stimulation of a variety of cell surface receptors, including growth factor receptors, cytokine receptors, cell–cell or cell–extracellular matrix adhesion receptors, and G-protein-coupled serpentine receptors, might all lead to the activation of specific Dbl family GEFs. The activated GEFs, in turn, catalyze the exchange of bound GDP for GTP on specific Rho GTPases, resulting in their activation. The receptor-mediated signals might also affect the biochemical activity of two classes of negative regulators of Rho GTPases; that is, RhoGAPs and RhoGDIs. Suppression of the negative regulators, together with the activating potential of GEFs, might synergistically drive Rho GTPases to the active conformation. The GTP-bound Rho proteins can then interact with multiple effector targets, leading to diverse cellular responses such as actin cytoskeleton reorganization, endocytosis and exocytosis, transcription activation, stimulation of DNA synthesis, and/or translational regulation. Abbreviations: GAP, GTPase-activating protein; GDI, GDP-dissociation inhibitor; GEF, guanine nucleotide exchange factor.

The functional link between Dbl family GEFs and Rho GTPases was further strengthened when UNC-73, a large multifunctional protein in *C. elegans* containing two separate DH–PH motifs, was found to regulate actin structure and movement by activating the Rho GTPase Rac, and a loss of DH domain function resulted in multiple defects in axon guidance and neuronal cell migration [8]. In *Drosophila*, the Dbl protein SIF was suggested to be involved in regulation of synaptic differentiation because it is associated with the plasma membrane of synaptic terminals, and mutations in SIF led to defects in neuronal morphology [9]. Recently, a set of genetic studies presented strong evidence that Trio, a homolog of UNC-73, mediates the effects of axon guidance factors on actin dynamics [10–12]. The genetic phenotypes of Trio mutations suggest a biochemical pathway linking the transmembrane tyrosine phosphatase Dlar and the Abl tyrosine kinase to the Trio–Rac–Pak signaling complex. In mice, Trio deficiency causes skeletal muscle deformation and neuronal disorder [13], and elimination of the *vav* gene, which encodes a hematopoietic cell specific Dbl family GEF, results in impaired lymphoid development, and defective immune responses of B- and T-lymphocytes [14], suggesting more complex roles of the GEFs in mammals. Interestingly, Dbl knockout mice do not display major abnormalities (A. Eva, pers. commun.), raising the possibility that multiple Dbl family genes could play redundant roles.

The compelling evidence that Dbl family GEFs are involved in human genetic disorders came from the studies of the FGD1 GEF [15]. A mutation in the DH domain of FGD1 that results in a loss of FGD1 function, cosegregates with faciogenital dysplasia, a developmental disorder. More recently, a mutation in the Dbl member ARHGEF6 (also known as αPIX) was found to be associated with X-linked nonsyndromic mental retardation [16]. Whether the DH domain in Bcr, which is present in the p210 isoform of Bcr–Abl fusions in chronic myelogenous and acute lymphocytic leukemias [17], or the Rho-specific GEF activity of LARG [18,19], which is retained in an MLL–LARG fusion in acute myeloid leukemia [20], play a role in these diseases, remains to be seen.

Biochemical functions

Dbl family GEFs contain diverse structural motifs in addition to the conserved DH–PH domains (Fig. 2). Early biochemical studies using oncogenic Dbl as a model system established that, whereas the DH domain is responsible for GEF catalytic activity, the adjacent PH domain is involved in intracellular targeting of the DH domain [1,2]. Although the PH-directed localization of the DH–PH module to the plasma membrane and the actin cytoskeleton conform to the generalized view that PH domains function as regulated membrane-binding modules [21], it also suggests a unique capability of the PH domain to associate with actin or actin-binding components. The DH domain, together with the PH domain, constitutes the minimum structural unit bearing transforming function [1,2]. This appears to be a generalized principle among Dbl family GEFs as similar conclusions have been drawn in the cases of, for example, Lbc, Lfc and Dbs. Demonstration of substrate-binding and catalytic activities in reconstituted GEF reactions, and examination of Rho GTPase activation states induced by overexpression of GEFs, have provided the bulk of the data on the biochemical functions of Dbl members, although much of this is currently limited to the three most prominent Rho GTPases: RhoA, Rac1 and Cdc42 ([1,2]; Table 1). Some of the GEFs, for example Cdc24, FGD1, Tiam1 and Lbc, are specific for a single Rho protein, whereas others, including Dbl, Ost, Ect2 and Bcr, are more promiscuous, targeting multiple Rho GTPases. The early view that certain members of the Dbl family might function by binding to Rho GTPases without GEF activity (e.g. Ect2) [2] does not seem to hold up, as recent studies have revealed that the lack of GEF activity of certain GEFs might have been caused by the requirement of missed regulatory signals

Table 1. A selected list of novel mammalian Dbl family members[a]

Dbl family member	GTPase substrates	Biological activities/unique distributions	Accession No.
FGD2	GEF for Cdc42	Embryonic development	NM013710
Lbc/Brx	GEF for Rho	Proto-oncogene product; binds to nuclear hormone receptor	NM006738
p115RhoGEF/Lsc	GEF for Rho	Proto-oncogene product; binds to Gα13 and Gα12	U64105
Net1	GEF for Rho	Proto-oncogene product	U02081
Ost/Dbs	GEF for Cdc42 and Rho; binds to Rac	Proto-oncogene product; at least three isoforms	Z35654
p190RhoGEF	GEF for Rho	Inhibits neurite outgrowth; binds to microtubules	U73199
Kalirin/Duo	GEF for Rac and Rho	Two DH–PH modules; multiple isoforms as a result of alternative splicing	AF232669
Asef	GEF for Rac	Enriched in brain; binding to tumor suppressor APC leads to activation	AB042199
Pix/Cool	GEF for Rac	At least two isoforms; binds to Rac effector PAK	AF044673
Frabin	GEF for Cdc42	Binds to actin	AF038388
Vav3	GEF for Rho and Rac	Proto-oncogene product	NM020505
hPEM-2	GEF for Cdc42	Predominantly expressed in brain	AB007884
GEF-H1	GEF for Rac and Rho	Associates with microtubules	U72206
GTRAP48/KIAA0380/ PDZ-RhoGEF	GEF for Rho	Predominantly expressed in brain cerebellum; associates with neuronal glutamate transporter; binds to Gα13	AF225961
LARG	GEF for RhoA	Fuses to MLL gene in acute myeloid leukemia; interacts with Gα12 and Gα13	AF180681
Tiam2	GEF for Rac	Two isoforms; cerebellum and testis specific	NM012454
Stef	GEF for Rac1	To be determined	AB022915
p114RhoGEF	GEF for RhoA	To be determined	AB011093
Ngef/ephexin	GEF for RhoA, Rac1, Cdc42	Proto-oncogene product; predominantly expressed in brain; mediates Eph regulation of growth cone	NM019867
Collybistin	To be determined	Two splice variants; predominantly expressed in brain	AJ250425
Intersectin	GEF for Cdc42	Two splice variants; one is brain-specific	NM003024

[a]Abbreviations: APC, adenomatous polyposis coli; DH, Dbl homolgy; GEF, guanine nucleotide exchange factor; PAK, p21-associated kinase; PH, pleckstrin homology.

(e.g. phosphorylation) [22]. Furthermore, DH domain mutants that retain substrate-binding activity but are catalytically compromised act as dominant-negatives in cells [23], suggesting that a threshold of GEF activity, in addition to the Rho-binding activity, is required for function. It remains to be seen whether all Rho GTPases use Dbl members as activators as some of them, for example RhoE, seem to exist in a constitutively active form [24].

A few additional lines of evidence also help establish that Dbl family GEFs function by activation of Rho GTPases in cells: (1) the foci induced by Dbl family oncoproteins are morphologically similar to those transformed by constitutively active Rho GTPases, but distinct from those seen when cells are transformed by other types of oncogenes such as Ras, Raf or Src [1]; (2) coexpression of Dbl family members with dominant-negative mutants of Rho family GTPases blocks their transforming activity [3]; (3) mutants of GEFs that are no longer able to interact or activate Rho protein substrates behave as dominant negatives in cells [22,23]; and (4) many cellular activities induced by Dbl family proteins, such as actin cytoskeleton reorganization, cytokinesis, stimulation of G1 to S phase transition, c-Jun N-terminal kinase activation, cyclin D1 induction, and activation of the serum response factor and nuclear factor-κB transcription factors, are associated with the activation of signaling pathways known to be mediated by active Rho GTPases or by Rho GTPase effector targets [1,3,25].

It is therefore not surprising that many Dbl family members display transforming activity in fibroblast transfection assays and some, through activation of Rac1 or a related pathway, regulate cell migration and tumor metastasis. The issues currently attracting much attention are which GEF-regulated pathways are essential for cell transformation or metastasis, and whether interference with selected pathways can be explored for anti-cancer drug design. However, it is important to note that given the multifunctional nature of these proteins (Fig. 2), it is possible that many of the GEF molecules bear GEF-independent functions [26,27]. Determining what these other functions might be and whether they affect the GEF-elicited pathways, should also provide leads to a more comprehensive understanding of GEF functions.

Mechanisms of regulation

Many members of the Dbl family seem to exist in an inactive or partially active state before stimulation. Current literature suggests that their basal states can be maintained by one or multiple forms of four possible regulatory modes involving intra- or inter-molecular interactions (Fig. 3). The first is through the intramolecular interaction between DH and PH domains. Examples of such an interaction include the Dbl family members Vav and Sos1 in which binding to the PI3K product phosphoinositol (3,4,5) trisphosphate [PtdIns(3,4,5)P_3] by the PH domain seems to alleviate an inhibitory effect on the DH domain [28,29].

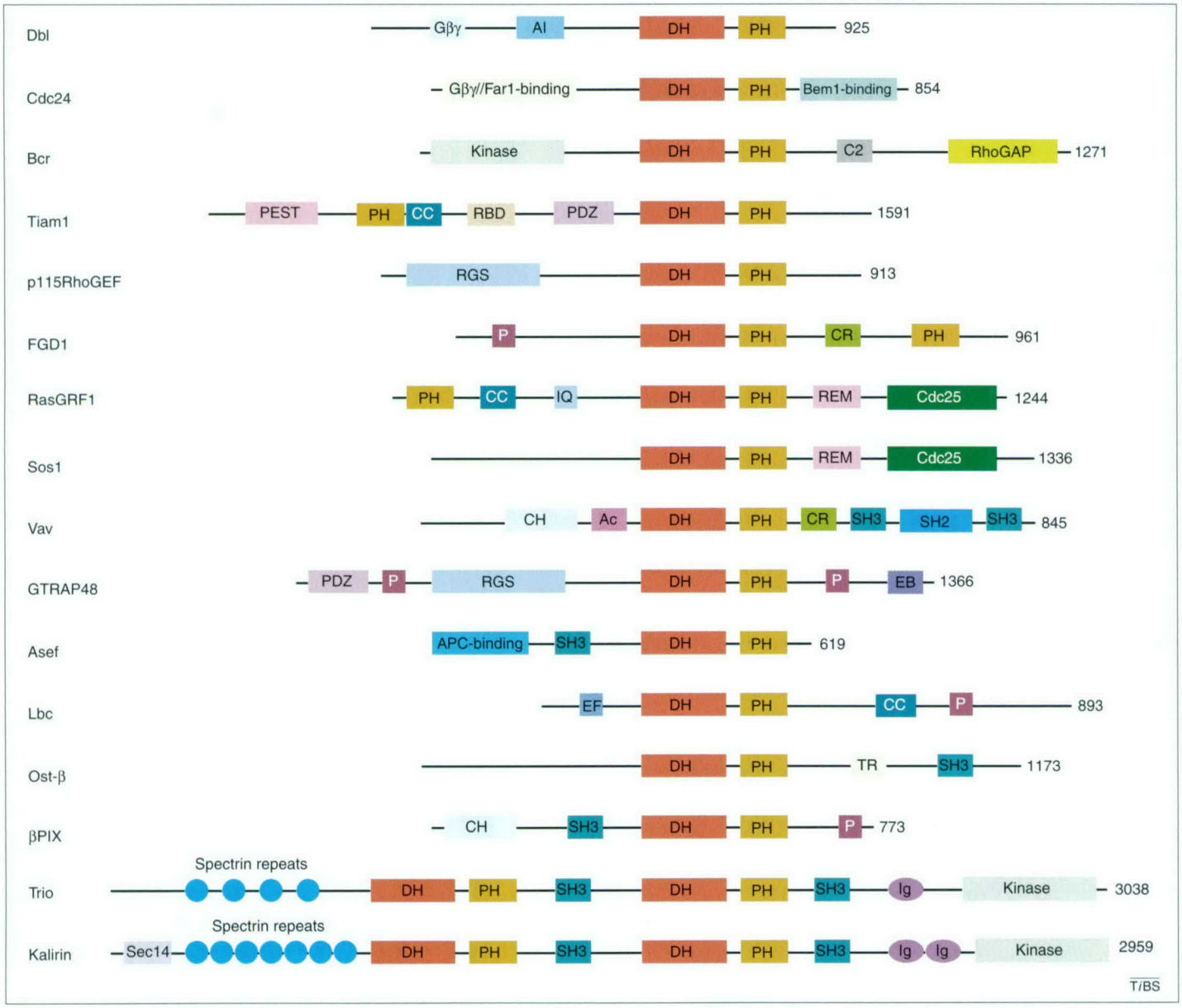

Fig. 2. Domain structures of representative Dbl family members. Abbreviations: Ac, acidic amino acid rich motif; AI, autoinhibitory domain; C2, calcium-dependent lipid binding; CC, coiled coil; Cdc25, RasGEF motif; CH, calponin homology; CR, cysteine-rich zinc butterfly motif; DH, Dbl homology; EB, EAAT4 binding; EF, EF hand calcium-binding motif; Gβγ, Gβγ binding domain; Ig, immunoglobulin-like; IQ, calmodulin binding motif; Kinase, serine/threonine kinase motif; P, proline-rich SH3-binding motif; PDZ, DHR or GLGF domain; PEST, amino acids P, E, S and T rich, degradation motif; PH, pleckstrin homology; RBD, Ras-binding domain; REM, Ras exchanger motif; RGS, regulator of G-protein signaling motif; RhoGAP, Rho GTPase-activating protein motif; Sec14, sec14-like; SH2, Src homology 2; SH3, Src homology 3; TR, Tat/RAG8-related.

The second possible mode of regulation is through the intramolecular interaction of a regulatory domain with the DH or PH domain of the GEF protein. Such interactions are expected to impose a constraint on the normal DH and/or PH domain function by masking the access of the Rho GTPase substrate and/or altering intracellular targeting mediated by the PH domain. Examples of such regulation include Vav and Dbl [30,31], and maybe also Asef, Lbc and p115RhoGEF. The third possible mode involves oligomerization through an intermolecular interaction between DH domains. This mode of regulation has been suggested recently in the cases of RasGRF1, RasGRF2 and onco-Dbl [32,33], and is postulated to play a role in the efficient execution of GEF function. Finally, additional cellular factors could interfere with specific Dbl member function through direct protein–protein interactions, helping maintain the GEF at a basal state. Examples in this category include the recently discovered interaction of tumor metastasis suppressor nm23H1 with Tiam1, which results in a decrease in GEF activity of Tiam1 towards Rac1 [34], and the potential recruitment of an inhibitory factor through the C terminus of p115RhoGEF [35]. Incoming upstream signals, via heterotrimeric G proteins, protein kinases, adaptor molecules and/or phosphoinositol lipids, could contribute to the alteration of these regulatory modes, resulting in intracellular translocation of GEF and stimulation of GEF catalytic activity. A few representative cases of GEF regulation are illustrated in Fig. 4.

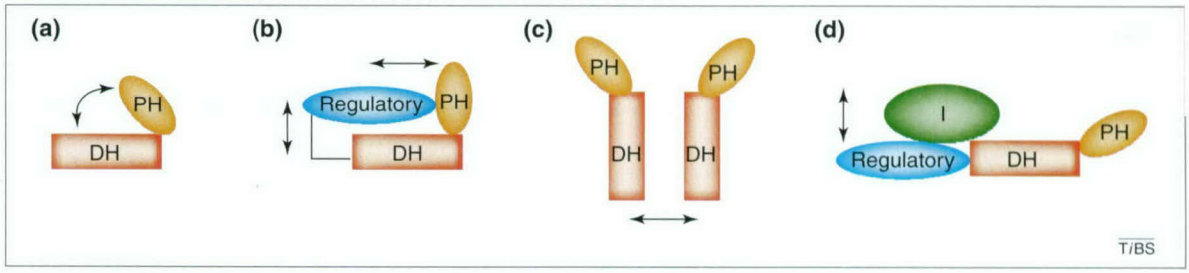

Fig. 3. Intra- and inter-molecular interactions implicated in regulation of Dbl family GEFs. (a) Potential DH and/or PH interaction within a DH–PH functional module might block the access of Rho GTPase substrates. (b) Interaction between an intramolecular regulatory domain and the DH or PH domain could mask the DH domain and/or affect the targeting function of the PH domain. (c) Oligomerization through DH domains might allow the recruitment of multiple Rho substrates into one signaling complex. (d) Recruitment of an inhibitory cellular factor (I) by the regulatory sequences of GEF could suppress the GEF activity and help maintain the basal state. Abbreviations: DH, Dbl homology; GEF, guanine nucleotide exchange factor; PH, pleckstrin homology.

Activation by GTP-binding proteins

Bradykinin, LPA, bombesin and other G-protein-coupled receptor stimuli are known to activate Rho GTPase pathways [3,4]. Both Gα and Gβγ subunits have been suggested to have roles in inducing Rho-mediated actin stress fiber formation and/or focal adhesion assembly. Gβγ in *S. cerevisiae* was first found to directly interact with a RhoGEF, Cdc24, in response to pheromone-receptor activation [2,3] (Fig. 4d). Rsr1, a Ras-related GTPase, also directly interacts with Cdc24 to target it to the budding site of the cell [1,2] (Fig. 4d). Subsequent biochemical studies identified p115RhoGEF, LARG and GTRAP48/PDZ-RhoGEF, as a subset of GEFs containing a regulator of G-protein signaling (RGS)-like domain that binds to, and might be activated by, Gα13 [20,36,37] (Fig. 4b). Dbl protein was also suggested to be able to bind Gβγ and Gα13 through its N-terminal regulatory sequences [38,39], although it remains to be seen whether such interactions are physiologically relevant. Early experiments in Swiss 3T3 fibroblasts suggested that Cdc42, Rac1 and RhoA act in a linear cascade to mediate signals causing cytoskeleton changes [4], and that they are all involved in Ras-induced transformation [3,4]. The GEFs between these small G-protein hierarchy chains remain to be identified. One possible scenario pictures the link as a single GEF molecule such as Tiam1, which was recently found to contain a Ras-binding domain [40] and therefore might activate Rac1 promptly in response to Ras (J. Sondek, pers. commun.; Fig. 4a). Alternatively, a class of GEFs containing both a DH domain and a Ras-activating Cdc25 domain, such as Sos and RasGRF, could serve to activate Ras and Rac1 simultaneously or sequentially in response to stimuli, as both these motifs have recently been found to confer GEF activity towards Rac1 and Ras, respectively [29,41]. However, activation of the DH domain in these two-headed GEFs might require additional modulators such as E3b1 and Eps8 in the case of Sos1 [42], where a macromolecular complex seems to be needed to unmask the GEF activity for Rac1.

Activation by protein kinases

In response to extracellular stimuli, many Dbl family GEFs become phosphorylated by protein kinases, which could contribute to their activation. The best-understood case is Vav, which is phosphorylated by Src family tyrosine kinases after cytokine or adhesion receptor activation [14]. In the basal state, a stretch of N-terminal sequences folds into an α-helical structure and binds to the active site of the DH domain, masking the access of Rac1 [30]. Upon phosphorylation at residue Tyr174, these amino acid sequences become unstructured and the constraint on the DH domain is relieved. Another example of activation by phosphorylation is Ect2, a regulator of cytokinesis whose GEF activity towards Rho is induced by Cdk-related kinases during cell-cycle progression [22]. The physiologically meaningful phosphorylation events that regulate many GEF functions remain to be clarified.

Regulation by phosphoinositol kinases

The PI3K homolog Tor2 was shown to be involved in activation of the GEF Rom2 and the GTPase Rho1 cascade in yeast [7], suggesting that the lipid product of the kinase, PtdIns(3,4,5)P_3, might play a role in GEF activation. In mammalian cells, early studies have shown that treatment with the PI3K inhibitor wortmannin inhibited the activation of Rac downstream of growth factor receptor activation [3,4]. In addition, the invariable presence of a PH domain in Dbl family GEFs makes it a valid hypothesis that phosphoinositol phosphates might affect GEF activity and/or location by binding to the PH domain. Indeed, many PH domains derived from Dbl family members were shown to be capable of interaction with phosphatidylinositol phospholipids. The more convincing evidence that such interaction could contribute to the modulation of GEF function came from studies of Vav and Sos1, both of which displayed enhanced GEF activity towards Rac1 upon PtdIns(3,4,5)P_3 binding to the PH domain [28,29]. Interestingly, PtdIns(4,5)P_2, the substrate of PI3K, was found to inhibit substrate binding and GEF activity of the DH domain of Vav and Sos1 [43], suggesting that phosphatidylinositol phospholipids regulate the intramolecular interaction between DH and PH domains. Moreover, phosphorylation of Vav also seems to contribute to its activation by PtdIns(3,4,5)P_3. By contrast, the GEF activity of Dbl towards Cdc42 was found to be inhibited by either PtdIns(4,5)P_2 or PtdIns(3,4,5)P_3 binding to the PH domain [44]. Although lipid binding is important for plasma membrane targeting, it apparently is not essential for cytoskeleton localization of onco-Dbl, nor for cell transformation.

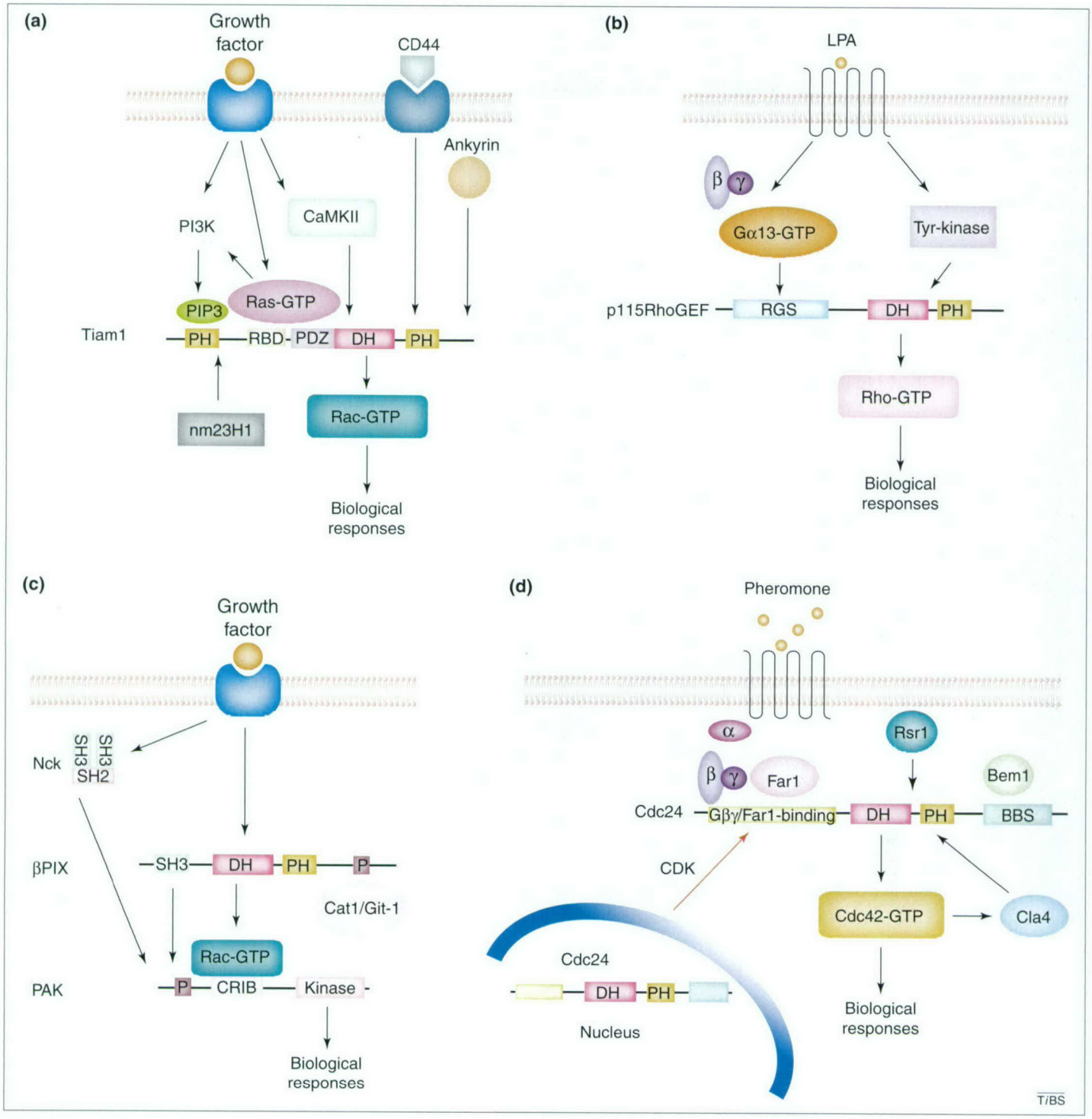

Fig. 4. Regulation of four Dbl family GEFs in intracellular signaling networks. (a) The Dbl family member Tiam1 is regulated by diverse mechanisms including phosphorylation by Ca^{2+}/calmodulin-dependent kinase II (CaMKII) or related kinases, interaction with phosphatidylinositol-3-kinase (PI3K) product PtdIns(3,4,5)P_3, binding to cell surface molecule CD44 or cytoskeleton protein ankyrin, as well as direct binding to activated Ras. By contrast, interaction with the tumor metastasis suppressor nm23H1 negatively regulates Tiam1 GEF activity. (b) G-protein-coupled receptors could use the heterotrimeric G-protein Gα13 and an as yet to be identified tyrosine kinase, to regulate intracellular localization and GEF activity of p115RhoGEF. Binding of p115RhoGEF through the N-terminal RGS domain to activated Gα13 could stimulate GTP-hydrolysis of Gα13 and return it to the GDP-bound state, meanwhile causing an activation of the GEF activity of p115RhoGEF and translocating it to the plasma membranes, where it activates the Rho-mediated pathways. (c) βPIX might serve as a scaffold in activation of Rac1–PAK pathway. βPIX effectively forms a stable complex with Rac through the DH domain, with PAK through the SH3 domain, and with other molecules such as Cat1/Git-1 through the C-terminal proline-rich region; and can exert both GEF/Rac-dependent and GEF-independent functions in the signaling pathway of growth factors. (d) Heterotrimeric G-protein βγ subunits, small G-protein Rsr1, multiple adaptor molecules (Far1 and Bem1), Cdc42-effector Cla4 kinase, and cell cycle-dependent kinase, together contribute to the effective onset and offset of the GEF activity towards Cdc42 and the intracellular localization of Cdc24. Far1 binds to the N terminus of Cdc24 and in response to cell-cycle progression translocates it to the plasma membrane where it could meet with Gβγ and Bem1 through direct interaction mediated by the unique N-terminal or C-terminal sequences of Cdc24 and activate Cdc42. One of the Cdc42 effectors, Cla4, could in turn phosphorylate Cdc24 and mediate its dissociation from the signaling complex. Abbreviations: BBS, Bem1 binding site; CDK, cyclin-dependent kinase; CRIB, Cdc42/Racl-interactive binding; DH, Dbl homology; GEF, guanine nucleotide exchange factor; P, proline-rich sequences; PAK, p21-associated kinase; PH, pleckstrin homology; RBD, Ras-binding domain; RGS, regulator of G-protein signaling; SH, Src homology.

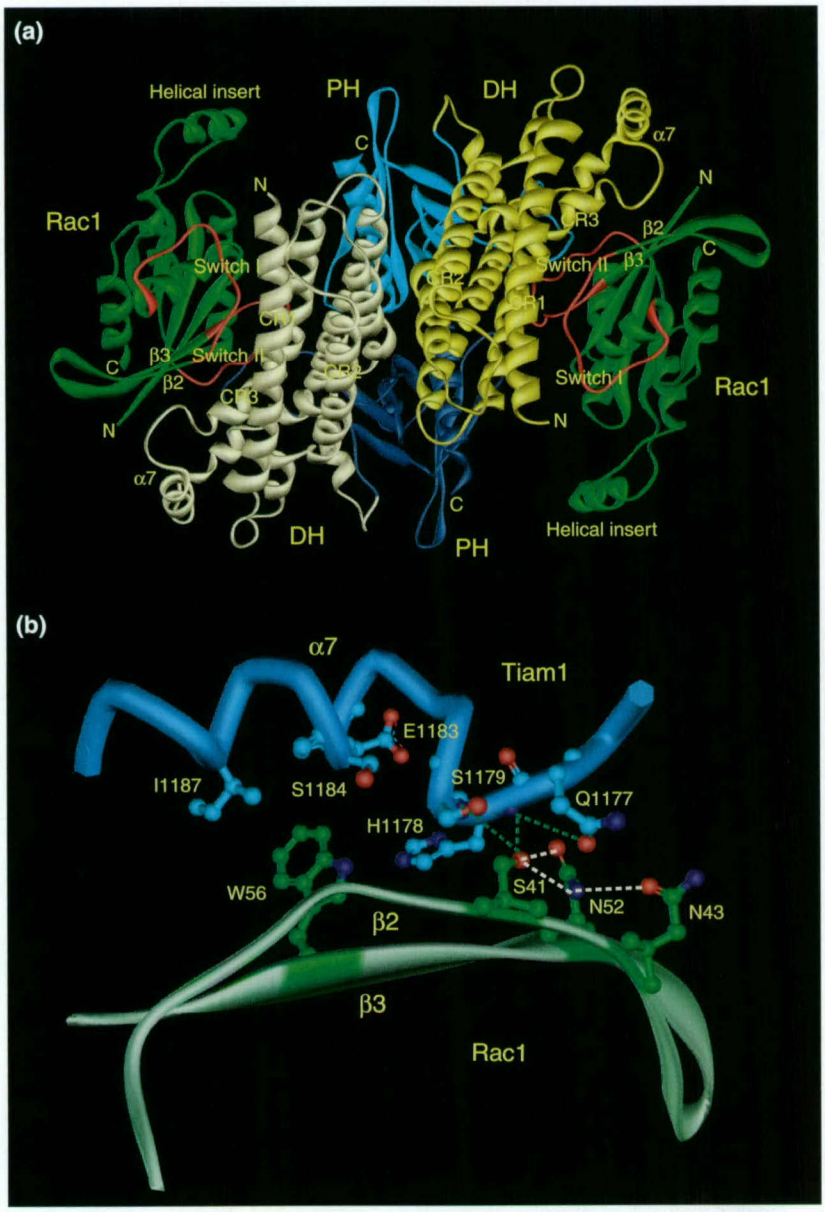

Fig. 5. Mechanism of Rac1 activation by the DH–PH module of Tiam1. (a) The three-dimensional view of Tiam1–Rac1 tetramer complex. Two identical units of Tiam1–Rac1 complex are in a back-to-back dimer configuration through interaction of extensive hydrophobic surface areas in DH domains. Switch regions of Rac1 are shown in red, and the rest of Rac1 are shown in green. One set of DH–PH module is in light gold and light blue, and the other unit is in darker colors. (b) Expanded view of the regions of Tiam1–Rac1 complex that specify GEF–Rac interaction. The β2/β3 residues S41, N43, N52, and W56 of Rac1 form both hydrogen bonds and van der Waal's contacts with the α7/α7b residues Q1177, S1179, H1178, E1183, S1184 and I1187 of Tiam1. Abbreviations: DH, Dbl homology; GEF, guanine nucleotide exchange factor; PH, pleckstrin homology.

Regulation by other intermolecular interactions

In *S. cerevisiae*, the GEF activity of Cdc24 is subjected to regulation by two adaptor/scaffolding molecules, Bem1 and Far1 (Fig. 4d). The formation of a Cdc24–Far1–Gβγ complex signals a landmark for orientation of the cytoskeleton during growth [45]. In mammalian cells, Far1-like large scaffolding molecules are still to be identified. Filamin, an actin crosslinker, was shown to be a potential target of the PH domain of Trio [46], whereas Frabin, a FGD1-related GEF, was found to contain intrinsic actin cross-linking activity [47].

The membrane-associated molecule radixin interacts with Dbl and might also recruit RhoGDI to the complex [48]. Other regulatory interactions of GEFs reported recently include Asef interaction with, and subsequent activation by, the tumor suppressor APC [49]; p115RhoGEF interaction with HIV gp41, which leads to a negative effect on GEF function [50]; Tiam1 binding to the hyaluronic acid-binding receptor CD44 and the cytoskeletal protein ankyrin, both of which positively regulate the Rac1-specific GEF activity [51,52]; and Tiam1 interaction with tumor metastasis suppressor nm23H1, which results in a decrease in GEF activity towards Rac1 [34] (Fig. 4a). Most recently, two novel Dbl family GEFs, ephexin and GTRAP48, have been shown to form a signaling complex at the receptor level with EphA and EAAT4, respectively [37,53], mediating neuronal growth cone dynamics or glutamate transporter functions. It is foreseeable that future studies of GEFs converging from diverse biological areas could uncover more unique, physiological meaningful interactions that have regulatory effect on GEF functions.

Overall, the biochemical mechanisms of the spatial and temporal regulation of GEFs remain poorly understood. In addition to GEF activation, concomitant upstream signals are probably required to suppress the negative regulations imposed upon Rho GTPase substrates by RhoGAPs and RhoGDIs [3,4]. To this end, the regulatory networks employed by PIX [54] and Cdc24 [45,55] (Fig. 4c,d) provide some clues that a large signaling complex could function to enhance the counter-reactive ability of a GEF for negative regulations and to ensure signaling specificity.

Mechanism of guanine nucleotide exchange on Rho GTPases

Similar to the mechanisms of Ras and heterotrimeric Gα activation by their respective GEFs, the Dbl family GEFs are thought to involve sequential GDP-dissociation and GTP-binding steps to facilitate GDP–GTP exchange on Rho GTPase substrates [56]. The exchange reactions are initiated when GEFs recognize the GDP-bound Rho proteins, followed by stimulation of GDP dissociation to achieve a binary GEF–Rho complex in which the small G protein exists in a nucleotide-free state. This transient reaction intermediate is then dissociated by GTP binding to the Rho protein. The highlights of the biochemical function of Dbl family GEFs in such a scheme are that they serve dual roles in the reaction: to destabilize GDP–Rho interactions and to stabilize the nucleotide-depleted, transition state of the substrate. The ~10-fold higher concentration of GTP over that of GDP in cells is also an important factor in driving the exchange reaction towards production of the GTP-bound state.

The three-dimensional structures of three distinct DH domains of Dbl family members TrioN,

Sos1 and βPIX, depict that they fold into highly homologous α-helical bundles and are unrelated to other proteins that interact with Rho family GTPases and other GEF families [57–59]. Systematic mutagenesis of DH domains of Dbl and TrioN mapped conserved region (CR) 1, CR3 and a part of α6 of the DH domain, as well as the DH–PH junction site that is exposed near the center of one side of the molecule, as the important sites involved in the formation of a Rho GTPase interactive pocket [23,57]. Recent determination of the structure of the DH–PH module of Tiam1 bound to Rac1 provides a framework for interpreting these and other biochemical studies aimed at delineating the structural determinants of the Rho proteins involved in GEF coupling [60] (Fig. 5a). First, Rac1 makes direct contact with the CR1, CR3 and the C terminus of α9 close to the PH junction site, confirming that residues of these DH regions are involved in GEF interaction. Second, the interaction with Tiam1 has altered the conformation of the sequences in, and immediately flanking, the switch 1 and switch 2 regions of Rac1, two stretches of amino acid residues that display most conformational changes in response to nucleotide binding. Not unlike the cases of other GEF–G complexes, Tiam1 disturbed the native coordination of Rac1 for a Mg^{2+} cofactor. This, in part, explains the previously observed lowered Mg^{2+}-binding affinity to Rho proteins when a GEF is present [61]. Third, a large portion of the β2/β3 and switch 2 regions of Rac1 engages in extensive surface contact with Tiam1 residues, providing docking sites for GEF recognition and stabilizing the complex. One residue in the β2/β3 region, W56, appears to be the key structural element dictating the specificity by interacting with the α7 region of Tiam1 that represents the most variable part of the molecule in this 'lock and fit' model [62] (Fig. 5b). A unique feature of the Tiam1–Rac1 interaction is that the GEF might not be involved in direct interference with the binding of either α- or β-phosphate of the guanine nucleotide, raising the possibility that the Dbl family GEF reaction mechanism might be different from that of Cdc25 or Sec7 GEF domains.

Interestingly, the Tiam1–Rac1 complex dimerizes through a largely hydrophobic surface area of the DH domain, including the CR2 region (Fig. 5a), shedding further support for a self-regulatory role of the DH domain in a subset of Dbl family proteins. Moreover, conformationally different from the isolated Sos1 DH–PH module [58], the PH domain of Tiam1 does not seem to contribute to Rac1 binding in the complex. It is likely that the PH domain plays a predominantly structural role in maintaining the integrity of the adjacent DH domain in this case, or alternatively, the snap shot of the crystals might have failed to capture a more dynamic interaction between the PH domain and the DH domain or the small G protein. Indeed, the PH domain of Dbs, a Dbl member closely related to Dbl, appears to be involved in the exchange mechanism on Cdc42 based upon data obtained by X-ray crystallography and mutagenesis studies (J. Sondek, pers. commun.). In addition, ancillary regions of Dbl proteins might be involved directly in Rho protein binding and/or catalysis [63].

It should be noted that although Dbl family GEFs appear to be the major class of molecules that positively regulate Rho GTPase activities, exceptional cases involving non-DH domain motifs or phosphoinositol lipids have been reported to stimulate guanine nucleotide exchange or GDP dissociation of Rho GTPases. For example, Salmonella SopE protein can effectively activate Rac1 and Cdc42 to facilitate bacteria entry into the host cells [64], and the Rap1-specific GEF, C3G, is an active GEF towards the Rho protein TC10 in insulin-stimulated GLUT4 translocation [65]. The biochemical and structural basis of these GEF reactions requires further investigation.

Conclusions

Recent genetic, biological, structural and biochemical studies have implicated Dbl family GEFs as the major positive regulators of Rho GTPases in diverse biological settings. *In vitro* biochemical studies have established the role of the conserved DH domain in Rho GTPase interaction and activation, and the role of the tandem PH domain in intracellular targeting and/or regulation of DH domain function. More systematic characterizations of the biochemical functions, modes of regulation and signaling mechanisms of Dbl family members in various physiologically relevant systems will probably assign each to specific intracellular pathways and will be an important step towards understanding the mechanism of control of signal flows through these GEFs and their specific Rho GTPase substrates. With increasing appreciation of a close relationship between the activation status of Dbl family members, their Rho GTPase substrates and pathological conditions such as cancer, drug discovery efforts aimed at interfering with the GEF functions of Dbl proteins could prove to be worthy endeavors.

Acknowledgements

The number of papers cited have been limited by space constraints. I thank Yuan Gao for database searches, and Feng Bi and Yuan Gao for help with graphics. I am grateful to David Worthylake for Tiam1–Rac1 coordinates. Work in my laboratory is supported by the National Institutes of Health, the American Cancer Society and the Dept of Defense Breast Cancer Program.

References

1 Whitehead, I.P. *et al.* (1997) Dbl family proteins. *Biochim. Biophys. Acta* 1332, F1–F23
2 Cerione, R.A. and Zheng, Y. (1996) The Dbl family of oncogenes. *Curr. Opin. Cell Biol.* 8, 216–222
3 Van Aelst, L. and D'Souza-Schorey, C. (1997) Rho GTPases and signaling networks. *Genes Dev.* 11, 2295–2322
4 Hall, A. (1998) Rho GTPases and the actin cytoskeleton. *Science* 279, 509–514
5 Venter, J.C. *et al.* (2001) The sequence of the human genome. *Science* 291, 1304–1351
6 Butty, A-C. *et al.* (1998) The role of Far1p in linking the heterotrimeric G protein to polarity establishment proteins during yeast mating. *Science* 282, 1511–1516
7 Schmidt, A. *et al.* (1997) The yeast phosphatidylinositol kinase homolog TOR2 activates RHO1 and RHO2 via the exchange factor ROM2. *Cell* 88, 531–542
8 Steven, R. *et al.* (1998) Unc-73 activates the Rac GTPase and is required for cell and growth cone migrations in *C. elegans*. *Cell* 92, 785–795

9 Sone, M. *et al.* (1997) Still life, a protein in synaptic terminals of *Drosophila* homologous to GDP–GTP exchangers. *Science* 275, 543–547

10 Newsome, T.P. *et al.* (2000) Trio combines with Dock to regulate Pak activity during photoreceptor axon pathfinding in *Drosophila*. *Cell* 101, 283–294

11 Liebl, E.C. *et al.* (2000) Dosage-sensitive, reciprocal genetic interactions between the Abl tyrosine kinase and the putative GEF trio reveal trio's role in axon pathfinding. *Neuron* 26, 107–118

12 Awasaki, T. *et al.* (2000) The *Drosophila* trio plays an essential role in patterning of axons by regulating their directional extension. *Neuron* 26, 119–131

13 O'Brien, S.P. *et al.* (2000) Skeletal muscle deformity and neuronal disorder in Trio exchange factor-deficient mouse embryos. *Proc. Natl. Acad. Sci. U. S. A.* 97, 12074–12078

14 Bustelo, X.R. (2000) Regulatory and signaling properties of the Vav family. *Mol. Cell. Biol.* 20, 1461–1477

15 Pasteris, N.G. *et al.* (1994) Isolation and characterization of the faciogenital dysplasia (Arskog–Scott syndrome) gene: a putative Rho/Rac guanine nucleotide exchange factor. *Cell* 79, 669–678

16 Kutsche, K. *et al.* (2000) Mutation in ARHGEF6, encoding a guanine nucleotide exchange factor for the Rho GTPases, in patients with X-linked mental retardation. *Nat. Genet.* 26, 247–250

17 Kin, Y. *et al.* (2001) The Dbl-homology domain of BCR is not a simple spacer in p210Bcr-Abl of the Philadelphia chromosome. *J. Biol. Chem.* 276, 39462–39468

18 Fukuhara, S. *et al.* (2000) Leukemia-associated Rho guanine nucleotide exchange factor (LARG) links heterotrimeric G proteins of the G12 family to Rho. *FEBS Lett.* 485, 183–188

19 Reuther, G.W. *et al.* (2001) Leukemia-associated Rho guanine nucleotide exchange factor, a Dbl family protein found mutated in leukemia, causes transformation by activation of RhoA. *J. Biol. Chem.* 276, 27145–27151

20 Kourlas, P.J. *et al.* (2000) Identification of a gene at 11q23 encoding a guanine nucleotide exchange factor: evidence for its fusion with MLL in acute myeloid leukemia. *Proc. Natl. Acad. Sci. U. S. A.* 97, 2145–2150

21 Blomberg, N. *et al.* (1999) The PH superfold: a structural scaffold for multiple functions. *Trends Biochem. Sci.* 24, 441–445

22 Tatsumoto, T. *et al.* (1999) Human Ect2 is an exchange factor for Rho GTPases, phosphorylated in G2/M phases, and involved in cytokinesis. *J. Cell Biol.* 147, 921–927

23 Zhu, K. *et al.* (2000) Identification of Rho GTPase-dependent sites in the DH domain of oncogenic Dbl that are required for transformation. *J. Biol. Chem.* 275, 25993–26001

24 Foster, R. *et al.* (1996) Identification of a novel human Rho protein with unusual properties: GTPase deficiency and *in vivo* farnesylation. *Mol. Cell. Biol.* 16, 2689–2699

25 Whitehead, I.P. *et al.* (1999) Dependence of Dbl and Dbs transformation on MEK and NF-κB activation. *Mol. Cell. Biol.* 19, 7759–7770

26 Nagata, K. *et al.* (1998) Activation of G1 progression, JNK mitogen-activated protein kinase, and actin filament assembly by the exchange factor FGD1. *J. Biol. Chem.* 273, 15453–15457

27 Daniels, R.H. *et al.* (1999) αPix stimulates p21-activated kinase activity through exchange factor-dependent and -independent mechanisms. *J. Biol. Chem.* 274, 6047–6050

28 Han, J. *et al.* (1998) Role of substrates and products of PI 3-kinase in regulating activation of Rac-related guanosine triphosphatases by Vav. *Science* 279, 558–560

29 Nimnual, A.S. *et al.* (1998) Coupling of Ras and Rac guanosine triphosphatases through the Ras exchanger Sos. *Science* 279, 560–563

30 Aghazadeh, B. *et al.* (2000) Structural basis for relief of autoinhibition of the Dbl homology domain of proto-oncogene Vav by tyrosine phosphorylation. *Cell* 102, 625–633

31 Bi, F. *et al.* (2001) Autoinhibition mechanism of proto-Dbl. *Mol. Cell. Biol.* 21, 1463–1474

32 Anborgh, P.H. *et al.* (1999) Ras-specific exchange factor GRF: oligomerization through its Dbl homology domain and calcium-dependent activation of Raf. *Mol. Cell. Biol.* 19, 4611–4622

33 Zhu, K. *et al.* (2001) Oligomerization of DH domain is essential for Dbl-induced transformation. *Mol. Cell. Biol.* 21, 425–437

34 Otsuki, Y. *et al.* (2001) Tumor metastasis suppressor nm23H1 regulates Rac1 GTPase by interaction with Tiam1. *Proc. Natl. Acad. Sci. U. S. A.* 98, 4385–4390

35 Wells, C.D. *et al.* (2001) Identification of potential mechanisms for regulation of p115RhoGEF through analysis of endogenous and mutant forms of the exchange factor. *J. Biol. Chem.* 276, 28897–28905

36 Hart, M.J. *et al.* (1998) Direct stimulation of the guanine nucleotide exchange activity of p115RhoGEF by Gα13. *Science* 280, 2112–2114

37 Jackson, M. *et al.* (2001) Modulation of the neuronal glutamate transporter EAAT4 by two interacting proteins. *Nature* 410, 89–93

38 Nishida, K. *et al.* (1999) Association of the proto-oncogene product Dbl with G protein βγ subunits. *FEBS Lett.* 459, 186–190

39 Jin, S. and Exton, J.H. (2000) Activation of RhoA by association of Gα(13) with Dbl. *Biochem. Biophys. Res. Commun.* 277, 718–721

40 Ponting, C.P. (1999) Raf-like Ras/Rap-binding domains in RGS12- and still-life-like signaling proteins. *J. Mol. Med.* 77, 695–698

41 Fan, W-T. *et al.* (1998) The exchange factor Ras-GRF2 activates Ras-dependent and Rac-dependent mitogen-activated protein kinase pathways. *Curr. Biol.* 8, 935–938

42 Scita, G. *et al.* (1999) EPS8 and E3B1 transduce signals from Ras to Rac. *Nature* 401, 290–293

43 Das, B. *et al.* (2000) Control of intramolecular interactions between the pleckstrin homology and Dbl homology domains of Vav and Sos1 regulates Rac binding. *J. Biol. Chem.* 275, 15074–15081

44 Russo, C. *et al.* (2001) Modulation of oncogenic Dbl activity by phosphoinositol phosphate binding to PH domain. *J. Biol. Chem.* 276, 19524–19531

45 Gulli, M-P. *et al.* (2000) Phosphorylation of the Cdc42 exchange factor Cdc24 by the PAK-like kinase Cla4 may regulate polarized growth in yeast. *Mol. Cell* 6, 1155–1167

46 Bellanger, J-M. *et al.* (2000) The Rac1- and RhoG-specific GEF domain of Trio targets filamin to remodel cytoskeletal actin. *Nat. Cell Biol.* 2, 888–892

47 Obaishi, H. *et al.* (1998) Frabin, a novel FGD1-related actin filament-binding protein capable of changing cell shape and activating c-Jun N-terminal kinase. *J. Biol. Chem.* 273, 18697–18700

48 Takahashi, K. *et al.* (1998) Interaction of radixin with Rho small G protein GDP/GTP exchange protein Dbl. *Oncogene* 16, 3279–3284

49 Kawasaki, Y. *et al.* (2000) Asef, a link between the tumor suppressor APC and G-protein signaling. *Science* 289, 1194–1197

50 Zhang, H. *et al.* (1999) Functional interaction between the cytoplasmic leucine-zpper domain of HIV-1 gp41 and p115RhoGEF. *Curr. Biol.* 9, 1271–1274

51 Bourguignon, L.Y. *et al.* (2000) CD44 interaction with Tiam1 promotes Rac1 signaling and hyaluronic acid-mediated breast tumor cell migration. *J. Biol. Chem.* 275, 1829–1838

52 Bourguignon, L.Y. *et al.* (2000) Ankyrin–Tiam1 interaction promotes Rac1 signaling and metastatic breast tumor cell invasion and migration. *J. Cell Biol.* 150, 177–191

53 Shamah, S. *et al.* (2001) EphA receptors regulate growth cone dynamics through the novel guanine nucleotide exchange factor ephexin. *Cell* 105, 233–244

54 Manser, E. *et al.* (1998) PAK kinases are directly coupled to the PIX family of nucleotide exchange factors. *Mol. Cell* 1, 183–192

55 Bose, I. *et al.* (2001) Assembly of scaffold-mediated complexes containing Cdc42p, the exchange factor Cdc4p, and the effector Cla4p required for cell cycle-regulated phosphorylation of Cdc42p. *J. Biol. Chem.* 276, 7176–7186

56 Cherfils, J. and Chardin, P. (1999) GEFs: structural basis for their activation of small GTP-binding proteins. *Trends Biochem. Sci.* 24, 306–311

57 Liu, X. *et al.* (1998) NMR structure and mutagenesis of the N-terminal Dbl homology domain of the nucleotide exchange factor Trio. *Cell* 95, 269–277

58 Soisson, S.M. *et al.* (1998) Crystal structure of the Dbl and pleckstrin homology domains from the human son of sevenless protein. *Cell* 95, 259–268

59 Aghazadeh, B. *et al.* (1998) Structure and mutagenesis of the Dbl homology domain. *Nat. Struct. Biol.* 5, 1098–1107

60 Worthylake, D.K. *et al.* (2000) Crystal structure of Rac1 in complex with the guanine nucleotide exchange region of Tiam1. *Nature* 408, 682–688

61 Zhang, B. *et al.* (2000) The role of Mg^{2+} cofactor in guanine nucleotide exchange and GTP hydrolysis reactions of Rho family GTPases. *J. Biol. Chem.* 275, 25299–25307

62 Gao, Y. *et al.* Trp56 of Rac1 specifies interaction with a subset of guanine nucleotide exchange factors. *J. Biol. Chem.* (in press)

63 Movilla, N. and Bustelo, X.R. (1999) Biological and regulatory properties of Vav-3, a new member of the Vav family of oncoproteins. *Mol. Cell. Biol.* 19, 7870–7885

64 Hardt, W-D. *et al.* (1998) *S. typhimurium* encodes an activator of Rho GTPases that induces membrane ruffling and nuclear responses in host cells. *Cell* 93, 815–826

65 Chiang, S-H. *et al.* (2001) Insulin-stimulated GLUT4 translocation requires the CAP-dependent activation of TC10. *Nature* 410, 944–948

Trends Cell Biol. January 2003 Vol.13 No. 1, pp. 1–58 ISSN 0962-8924

TRENDS in Cell Biology

Listeria: using functional mimicry to aid infection

Interdisciplinary biology – computational modeling

PHD domains and E3 ubiquitin ligases

Protein palmitoylation

Tubes series: the ECM in vascular morphogenesis

BioMedNet bmn.com

Visit http://bmn.com/cellbiology for access to all the news, reviews and informed opinion on the latest scientific advances in cell biology

Rho GTPase-activating proteins in cell regulation

Sun Young Moon and Yi Zheng

Division of Experimental Hematology, Children's Hospital Research Foundation, Cincinnati, OH 45229, USA

Rho family small GTPases serve as molecular switches involved in the regulation of diverse cellular functions including various cytoskeleton-related events and gene transcription. The Rho GTPase-activating proteins (RhoGAPs) are one of the major classes of regulators of Rho GTPases found in all eukaryotes that are crucial in cell cytoskeletal organization, growth, differentiation, neuronal development and synaptic functions. Recent studies have implicated them as specific negative regulators of Rho protein signalling pathways and provided insight into how the RhoGAP-catalysed GTPase-activating reaction might proceed. Progress has also been made in understanding how various intracellular signals might converge on or diverge from RhoGAPs leading to their tight regulation or GAP-independent function.

Rho family GTPases act as binary molecular switches that are turned on and off in response to a variety of extracellular stimuli. Rho proteins in the GTP-bound active state can interact with a number of effectors to transduce signals leading to diverse biological responses including actin cytoskeletal rearrangements, regulation of gene transcriptions, cell cycle regulation, control of apoptosis and membrane trafficking [1–3]. When the bound GTP is hydrolysed to GDP, Rho proteins return to the inactive basal state. Three classes of regulatory proteins are involved in balancing Rho GTPases between the on and off states: the guanine nucleotide exchange factors (GEFs), which promote the release of bound GDP and facilitate GTP binding [4]; the GTPase-activating proteins (GAPs), which increase the intrinsic GTPase activity of Rho GTPases to accelerate the return of the proteins to the inactive state [5]; and the guanine nucleotide dissociation inhibitors (GDIs), which sequester the GDP-bound form of Rho GTPases and may also regulate their intracellular localization [6]. One emerging theme from recent studies of Rho GTPase regulation is that a balanced act between the activation and the deactivation signals – that is, the cycling of Rho proteins between the GTP- and GDP-bound states – might be required for effective signal flow through Rho GTPases to elicit downstream biological functions, and this could involve the concerted action of all classes of the regulatory proteins (Fig. 1) [7].

The RhoGAP family is defined by the presence of a conserved RhoGAP domain in the primary sequences that consists of about 150 amino acids and shares at least 20% sequence identity with other family members. The RhoGAP domain is distinct from the GAP modules that are responsible for turning off other classes of GTPases (e.g. Ras, Ran or ARF), and it is sufficient for the binding to GTP-bound Rho proteins and accelerating their GTPase

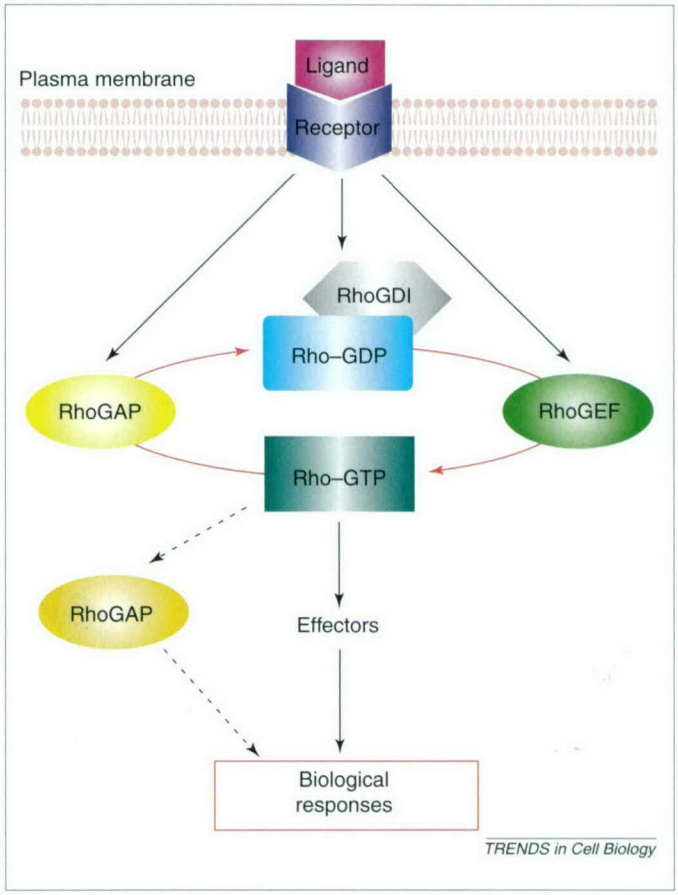

Fig. 1. A biochemical model of Rho GTPase-activating protein (RhoGAP) function in the signalling scheme of Rho GTPases. The cycle between the active, GTP-bound, and the inactive, GDP-bound, Rho GTPases is regulated by three classes of regulators: guanine nucleotide exchange factors (GEFs); GTPase-activating proteins (GAPs); and guanine nucleotide dissociation inhibitors (GDIs). Extracellular signals conveyed through specific cell surface receptors modulate the activities of these regulators, which in turn regulate the activation state of individual Rho GTPases. The active Rho GTPases are capable of interacting with multiple effectors, including certain RhoGAPs, leading to diverse biological responses. In general, a RhoGAP can act as a negative regulator that catalyses the intrinsic GTPase activity of Rho proteins to return them to the inactive state, or as an effector that mediates the Rho protein-elicited responses.

Corresponding author: Yi Zheng (yi.zheng@chmcc.org).

http://ticb.trends.com 0962-8924/02/$ - see front matter © 2002 Elsevier Science Ltd. All rights reserved. PII: S0962-8924(02)00004-1

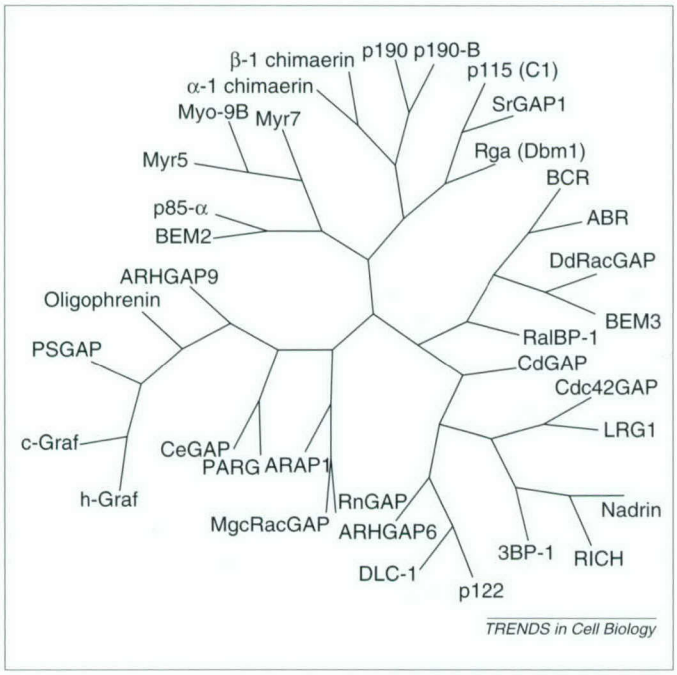

Fig. 2. A Rho GTPase-activating protein (RhoGAP) family tree based on the sequence homology of the conserved RhoGAP domain. The known RhoGAP domain sequences from yeast to human were aligned by using the Clustal-W program. The evolutionary tree was drawn with the Phylip program.

activity. Since the initial identification of Breakpoint cluster region protein (Bcr) as a RhoGAP in 1991 [8], over 30 RhoGAPs have been reported in eukaryotes, ranging from yeast to human (Fig. 2). Recent human genome analysis has put a limit of around 80 on the number of RhoGAPs in *Homo sapiens*, far outnumbering their cellular substrates, the Rho family GTPases, which comprise 20 members. The overabundance of RhoGAPs evidently suggests that each RhoGAP might play a specialized role in regulating individual Rho GTPase activity and in influencing their specific functions. The biochemical GAP activity of each RhoGAP must therefore be fine-tuned in cells by tight regulation in a spatial and temporal manner such that Rho GTPases would not be in the off state all the time. This review focuses on recent progress in studies of the function and mechanism of regulation of RhoGAPs. For a summary of the early history of RhoGAP studies or for a broader discussion of Rho GTPase regulation, a few excellent reviews should be referred to Refs [2,3,5].

RhoGAPs as negative regulators of Rho GTPase function

Biochemically the RhoGAP domain binds to the GTP-bound Rho proteins and stimulates their intrinsic GTPase activity. The mechanism of how RhoGAPs help Rho GTPase hydrolyse bound GTP has been derived from recent structural studies. *In vivo*, much of the available data of RhoGAP function strongly support their role as negative regulators of Rho protein pathways.

Rho GTPase-activating reaction

The essence of the RhoGAP reaction is to catalyse the intrinsic GTPase activity of Rho proteins. Recent mechanistic studies from the structural angle have provided insight on how the RhoGAP-catalysed GTPase-activating reaction might proceed. Although the sequences of RhoGAP domains are different from those of other classes of GAPs such as Ras GTPase-activating proteins (RasGAPs), the tertiary folding pattern as well as the basic GTPase-activating mechanism of the RhoGAP domain appears to be similar to that of RasGAP [9,10]. The RhoGAP domain consists of nine α helices and a highly conserved arginine residue is presented in a loop structure [11]. The RhoGAP domain interacts with both the switch I and II regions and the P-loop of Rho GTPases that constitute the GTP-binding core (Fig. 3). The comparison of the ground state of the Cdc42GAP reaction in which the

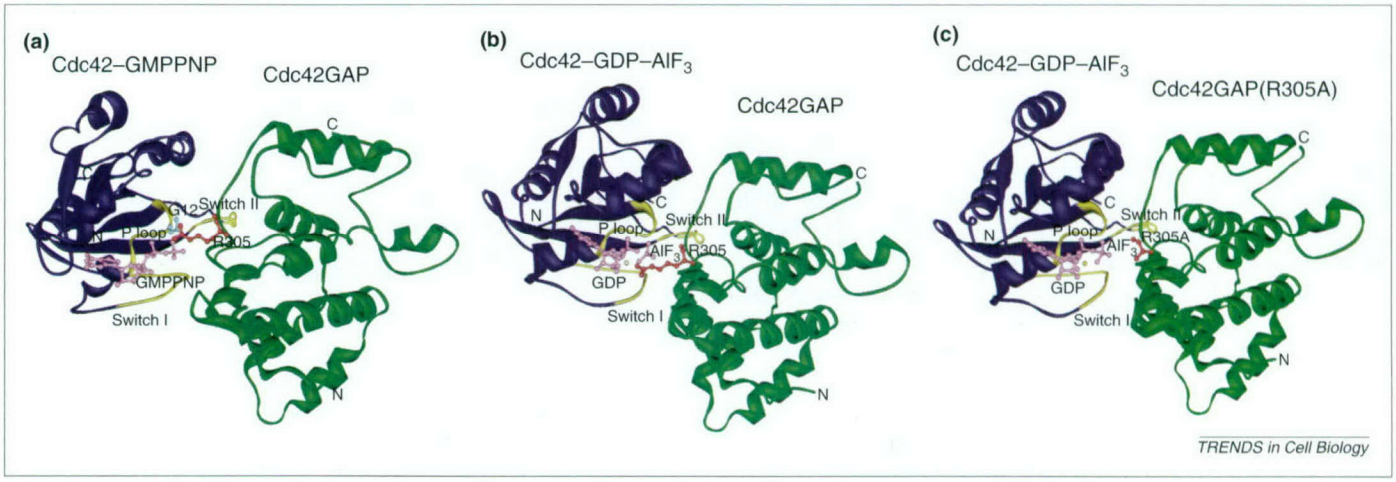

Fig. 3. The GTPase-activating mechanism of Rho GTPase-activating protein (RhoGAP). (a) Crystal structure of the ground state of Cdc42GAP reaction with Cdc42 bound to GMP–PNP. (b) Structure of Cdc42–GDP/AlF3–Cdc42GAP complex, a GAP-reaction transition state mimic. (c) Structure of the transition state mimic of Cdc42GAP reaction bearing an Arg305 to Ala mutation in the GAP domain. Compared with the ground state conformation (a), formation of the transition state complex (b) caused a 20° rigid body rotation of Cdc42 with respect to the GAP domain. Although the catalytic arginine (Arg305) plays a substantial role for executing GAP catalytic activity, mutation of this arginine to alanine (c) does not abolish the complex formation between Cdc42GAP and Cdc42 in the transitional state. In the complex of Cdc42GAP and Cdc42–GDP in the presence of AlF3, which is thought to mimic the γ-phosphate group of GTP (b), the two switch regions of Cdc42 are stabilized by Cdc42GAP. Mutation of the Arg305 of Cdc42GAP leads to an increased mobility of the A-A1 loop of the GAP domain and a weakening or loss of hydrogen bonds between the loop and the switch II region of Cdc42 (c). Concomitantly, Gln61 of Cdc42 is disordered and cannot position the hydrolytic water molecule for the catalytic attack in the complex with the mutant GAP.

small G protein is bound to GMPPNP, a non-hydrolysable GTP analog, with a transition state mimic in which the G protein is bound to GDP and AlF3, reveals a 20° rigid body rotation of the G protein with respect to the GAP. Such a conformational change would place the catalytic arginine residue of RhoGAP into the active site of Rho GTPase and stabilize charges developed during the formation of the transitional state. The arginine would interact with Gln61 of the GTPase, which is responsible for positioning a hydrolytic water molecule for catalysis. Stabilization of this glutamine residue restricts the freedom of the water molecule and may reduce the energy barrier for GTP hydrolysis [12]. The significance of the catalytic arginine of RhoGAP in accelerating Rho GTP hydrolysis has been further confirmed by mutational approaches [12,13]. One of the issues remaining to be addressed by the structural studies, however, is how substrate specificity of RhoGAPs is achieved in RhoGAP–Rho GTPase pairwise interactions, because mutagenesis studies have also shown that residues outside the switch regions and the P-loop of Rho GTPases are clearly involved in directing RhoGAP specificity [13,14].

Neuronal morphogenesis

One of the established physiological roles of Rho GTPases is the regulation of the actin cytoskeleton during neuronal migration, axonal growth and guidance, and formation of synapses [15]. Consequently, regulators and effectors of Rho GTPases are found to play key roles in neuronal morphogenesis. Oligophrenin-1, a RhoGAP family member that is highly expressed in human fetal brain and acts on multiple Rho GTPases as a GAP, was found to be associated with X-linked mental retardation [16]. This finding strongly implicates the involvement of RhoGAP in the nervous system.

Recent studies of p190 RhoGAP, one of the first Rho-specific GAPs identified, in gene targeted mice show that the RhoGAP is required for axon outgrowth, guidance and fasciculation, and neuronal morphogenesis [17,18]. In cells of the neural tube floor plate of p190 knockout mice, excessive accumulations of polymerized actin were found, suggesting a negative role of p190 in the regulation of Rho-mediated actin assembly within the neuroepithelium [17]. p190 was co-enriched with F-actin at the distal end of the axon and its oversynthesis induced neurite formation in a neuronal cell line [18], indicating that p190 could be an important regulator of Rho-mediated actin reorganization in neuronal growth cones. Furthermore, deletion of neuronal adhesion molecules in mice causes defects similar to those seen in p190-null mice, and p190 appears to be one of the major Src kinase substrates in the neuron [18]. These studies implicate p190 in neuronal development and neuritogenesis by mediating Src-dependent adhesion through balancing the Rho GTPase activity. Such a role is further strengthened by an RNA interference study of p190 RhoGAP in *Drosophila*, where blockage of p190 leads to the retraction of axonal branches by upregulating RhoA activity and affecting a signalling pathway from RhoA to effector Drok to the actin/myosin contractility component myosin regulatory light chain [19].

The growing neurites possess growth cones at the tip where both positive and negative molecular guidance cues are detected. Target cells can find a path to the growth tip in response to the guidance cues during neural development. Recently, Wong *et al.* [20] have obtained compelling evidence showing the involvement of a RhoGAP in the intracellular signalling pathway connecting the extracellular guidance cue to the actin cytoskeleton in neuronal cells. The Slit proteins, by binding to the Robo receptor, control the migration of neurons by repelling axons and migrating neurons. One set of the Robo cytoplasmic domain interacting proteins are Slit–Robo GAPs (srGAPs), which are Cdc42-specific GAPs. Binding of Slit to Robo leads to the activation of srGAP, which in turn inactivates the Rho GTPase Cdc42. The differential cellular localization of srGAP induced by recruitment to the Slit-activated Robo receptor could generate a gradient of Cdc42 activity that controls local actin polymerization. The resulting polarized actin structure could thus provide a mechanism of Slit-initiated repulsive effects in neuronal migration [20].

RhoGAP also appears to play essential roles in neuronal synaptic transmission. Nadrin, a neuron-specific RhoGAP, is involved in the regulation of Ca^{2+}-dependent exocytosis [21]. The cortical filament network under the presynaptic membrane is thought to be a barrier for the secretory vesicles to fuse with the membrane, and Nadrin is co-localized in the neurite termini with cortical actin filaments [21] and is part of a molecular complex – with EBP50 (an Ezrin binding protein) and EPI64 (a rabGAP domain-containing protein) – that associates with Ezrin at the cell membrane [22]. Nadrin could therefore inhibit Rho GTPase activities to disassemble cortical actin filaments, which in turn would affect exocytosis.

Cell growth and differentiation

Rho family GTPases, their GEFs and effectors regulate cell growth and differentiation [1,2,4]. A few recent studies also put RhoGAPs among the regulators of cell growth and differentiation, possibly through their ability to suppress Rho GTPase function. Mice lacking the Rho-specific GAP, p190-B, exhibit a severe reduction in thymus size [23] and axon defects in the brain including a severe reduction in the major midline forebrain crossing tracts as well as a thinner cortex [23]. These defects are associated with a failure in cell differentiation. Strikingly, the animals display a uniform 30% reduction in size, resembling that observed in mice lacking CRE-binding factor (CREB). At the cellular level, the p190-B knockout exhibits smaller cell size, like the $CREB^{-/-}$ cells, and this effect can be attributed to the enhanced Rho activity and a hyperactive Rho–Rho kinase–insulin receptor substrate–CREB signalling chain due to p190-B deletion. Thus, the p190-B function is associated with cell differentiation in the thymus and brain, and cell size and animal size determination.

One line of evidence suggests that RhoGAP might be involved in the cytokinesis step of cell division by affecting central spindle formation. The RhoGAP member MgcRacGAP and its *Caenorhabditis elegans* orthologue CYK-4 localize to the central spindle during cytokinesis [24,25],

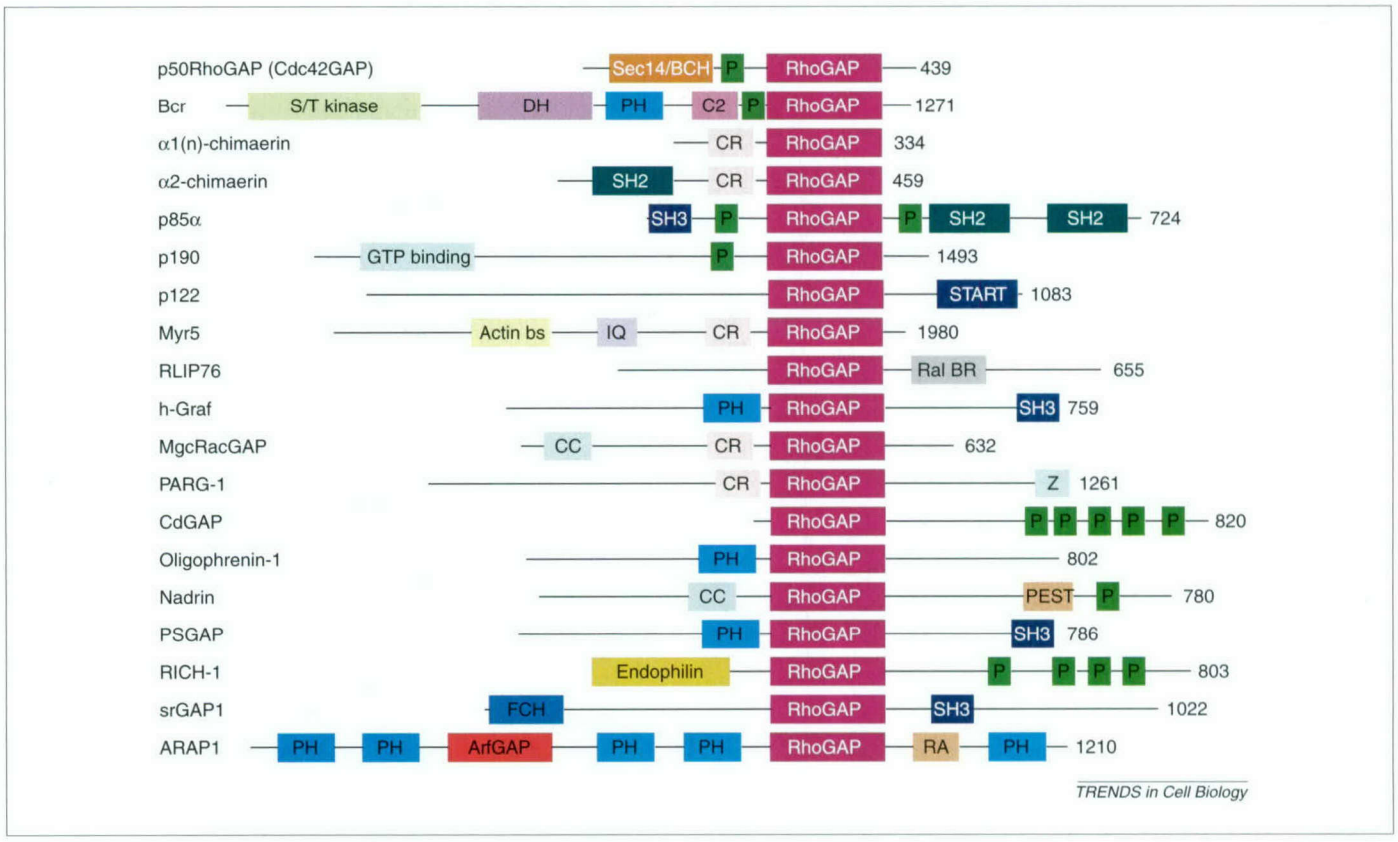

Fig. 4. Multifunctional domain features of Rho GTPase-activating protein (RhoGAP) family members. Abbreviations: Actin bs, actin filament binding site; C2, calcium-dependent lipid binding; CC, coiled coil; CR, cysteine rich, zinc butterfly motif, binds diacylglycerol and phorbol ester; DH, Dbl homology; Endophilin, Endophilin homology domain; FCH, Fes/CIP4 homology domain; IQ, calmodulin binding; PH, pleckstrin homology; P, proline-rich SH3 binding motif; PEST, amino acids P-, E-, S- and T-rich degradation motif; RA, Ras-associating (also known as ralGDS/AF-6) domain; Ral BR, Ral GTPase binding region; Rho GAP, Rho GTPase-activating protein motif; Sec14/BCH, Sec14 homology/BNIP2 and Cdc42 GAP homology; SH2, Src homology 2; SH3, Src homology 3; S/T kinase, serine and threonine kinase; START; Star-related lipid transport domain; Z, PDZ binding region.

and MgcRacGAP can be co-precipitated with microtubules through its N-terminal region [24]. In *C. elegans*, a CYK-4 mutant initiates but does not complete the formation of a central spindle. Moreover, the localization of CYK-4 to microtubules of the central spindle is dependent upon the kinesin-like protein ZEN-4/CeMKLP1, suggesting that CYK-4 and ZEN-4/CeMKLP1 cooperate in central spindle assembly [26]. Consistent with these observations in worms, mammalian CYK-4 and MKLP1 form a hetero-tetramer, named centraspindlin, that is involved in microtubule bundling [25]. In these cases it is not clear whether the RhoGAP activity in MgcRacGAP or CYK-4 is necessary for the function; however, it is likely that central spindle localization of CYK-4 could accelerate GTP hydrolysis by RhoA, a known cytokinesis regulator [27], thereby allowing contractile ring disassembly and completion of cytokinesis.

Endocytosis

Rho GTPases have emerged as important regulators of endocytosis [28], and there is evidence that RhoGAP could play a role in this process. RalBP1, also termed RIP1 or RLIP76, serves as an effector of Ral GTPase and contains a RhoGAP domain that is active towards Cdc42 and Rac1 [29–31]. Two EH (Eps15 homology) domain-containing proteins, POB (Partner of RalBP1) and Rel (RalBPa-associated Eps-homology domain), were found to associate with the C-terminus of RalBP1 [32,33], whereas the N-terminal region of RalBP1 interacts with the plasma membrane clathrin adaptor AP2 complex [34]. EH domain-containing molecules are often involved in endocytosis. In fact POB has been shown to bind Epsin and Eps15, both of which regulate endocytosis of epidermal growth factor (EGF) and insulin receptors [35]. Thus, RalBP1 is expected to have a role in the endocytosis process, although how its RhoGAP activity or the relationship with Rho GTPases fits in functionally remains to be seen.

Tumour suppression

Rho family GTPases have been implicated in many aspects of tumorigenesis [36]. Upregulation of Rho GTPase expression or activity has been associated with multiple human tumour types. It is therefore logical to expect that certain RhoGAPs might be negatively involved in tumour cell growth or progression by downregulating Rho GTPase activity. Indeed, a few RhoGAPs have been suggested to have potential tumour suppressor roles. The RhoGAP member *DLC1* (deleted in liver cancer) gene is deleted in 44% of primary hepatocellular carcinomas (HCC) and 90% of HCC cell lines [37]. *GRAF*, the focal adhesion kinase associated RhoGAP, was identified as a fusion partner of the mixed-lineage leukaemia gene by a unique chromosome translocation in juvenile myelomonocytic leukaemia

Table 1. Selected mammalian Rho GTPase-activating proteins

Name	*In vitro* specificity	Tissue distribution	Notes	Refs
Bcr	Rac and Cdc42	Predominantly brain	Bcr–Abl oncoprotein in leukemias	[8,31]
Abr	Rac1, Rac2 and Cdc42	Predominantly brain	Deleted in seven of eight informative cases of medulloblastoma	[32,70]
n(α1)/α2-Chimaerin	Rac > Cdc42/Rac > Cdc42	Brain/brain and testis	Full-length acts as an effector of Cdc42 and Rac1/involved in neuritogenesis in N1E-115	[40,71]
β1/β2-Chimaerin	Rac/Rac	Testis/brain	Expressed in late stage of spermatogenesis/interact with Tmp-21 protein	[60,61,63]
p85α, p85β?	No activity	Ubiquitous	An adaptor subunit of PI 3-kinase; interacts with Cdc42Hs and Rac	[37,38]
p190	RhoA > Rac, Cdc42,	Ubiquitous	A substrate of Src; regulates axonal growth and guidance and is required for normal neural development	[10,11]
p190-B	RhoA, Rac1 and Cdc42	Ubiquitous	A regulatory molecule of cell and organism size by regulating RhoGTPase, which modulates CREB activity	[15]
p122/DLC1	RhoA/ND	ND/ubiquitous	Interact with and activate PLC-δ1/A candidate tumor- suppressor gene	[29,51]
Myr5/Myr7	RhoA	Ubiquitous/brain	Unconventional class IX myosin	[49,50]
RalBP1 (RLIP76, RIP1)	Rac and Cdc42	Ubiquitous	Interacts with Ral GTPase, POB, Rel and AP2	[21–23]
MgcRacGAP/CYK4 (*C. elegans*)	Rac, Cdc42 > RhoA	Highly expressed in testis (in human), and in embryonic brain and testis (in mouse).	Control of growth and differentiation of hematopoietic cells; involved in cytokinesis; associated with mitotic spindle and midbody/ cooperates with a kinesin-like protein to assemble central spindle for cytokinesis	[16–18]
PARG1	RhoA > Rac, Cdc42	Ubiquitous	Interacts with PTPL1, a protein-tyrosine phosphatase	[72]
CdGAP	Rac and Cdc42	Ubiquitous	Interacts with, and negatively regulated by, intersectin	[64]
Oligophrenin-1	RhoA, Rac and Cdc42	Brain	Involved in X-linked mental retardation	[9]
Nadrin	RhoA, Rac and Cdc42	Brain	Regulates Ca^2-dependent exocytosis	[14]
PSGAP	RhoA and Cdc42	Ubiquitous	Interacts with both PYK2 and FAK, but only PYK2 inhibits PSGAP activity towards Cdc42	[73]
RICH1 and 2	Rac1 and Cdc42	Ubiquitous	Interact with CIP4, an effector of Cdc42	[74]
SrGAP1–3	Cdc42	Highly expressed in brain and spleen	Interact with Robo receptor; implicated in neuronal migration	[13]
ARAP1/ARAP3	Cdc42/RhoA, Rac1 and Cdc42	Ubiquitous/highly expressed in leukocytes and spleen	PIP_3 dependent Arf GAP activity	[46,47]
Graf	Cdc42 > RhoA	Highly in brain and liver	Interacts with FAK; phosphorylated by MAP kinase/human Graf fused to MLL	[30,75]

Abbreviations: *C. elegans*, *Caenorhabditis elegans*; FAK, focal-adhesion kinase; GAP, GTPase-activating protein; MAP, mitogen-activated protein; ND, not determined; PIP_3, phosphatidylinositol (3,4,5)-trisphosphate; PI 3-kinase, phosphoinositide 3-kinase.

[38]. Deletion, point mutation and insertion of this gene have been found in patients. *BCR* is well known for its fusion with *ABL* oncogene in a leukaemia-associated chromosomal translocation [39]. In Bcr-Abl fusion proteins, p190 and p210, the RhoGAP domain of Bcr is deleted, but the mechanistic consequence of the loss of the RhoGAP domain remains unclear. The homologous gene of *BCR*, the *ABR* locus, is deleted in seven of eight informative cases of medulloblastoma [40]. Finally, p190 RhoGAP has been proposed as a tumour suppressor based on overexpression studies in NIH3T3 fibroblasts. Either the N-terminal GTP-binding domain or the C-terminal RhoGAP domain of p190 repressed Ras-induced transformation, whereas blocking of the expression of endogenous p190 or application of a mutant of the GTP-binding domain induced transformation [41].

Mechanism of regulation of RhoGAPs

The activity spectrum of RhoGAPs with Rho GTPases varies widely *in vitro*. Certain RhoGAPs preferentially recognize a single Rho protein and catalyse its GTPase activity, whereas others display a broader range of specificity by interacting with all three commonly tested Rho substrates – RhoA, Rac1 and Cdc42 (Table 1). In cells, the specificity of the RhoGAP domain could be further enhanced, because microinjection of the RhoGAP domain of p122RhoGAP or Graf blocked the lysophosphatidic acid-induced actin stress fibre formation in fibroblasts that is mediated by RhoA in spite of their indiscriminate activity towards Rac1 or Cdc42 *in vitro* [42,43]. These observations suggest that there might be another layer of unappreciated regulation of RhoGAP specificity in cells that can affect substrate selection. More intriguingly, given the multidomain nature of many RhoGAPs (Fig. 4), various pathways might converge on them by interaction with the regulatory motifs, contributing to the tight regulation of the GAP activity.

Regulation by phosphorylation: p190 RhoGAP

Accumulating evidence indicates that RhoGAP activities may be modulated by protein kinases. One prominent example is p190 RhoGAP regulation by Src family tyrosine

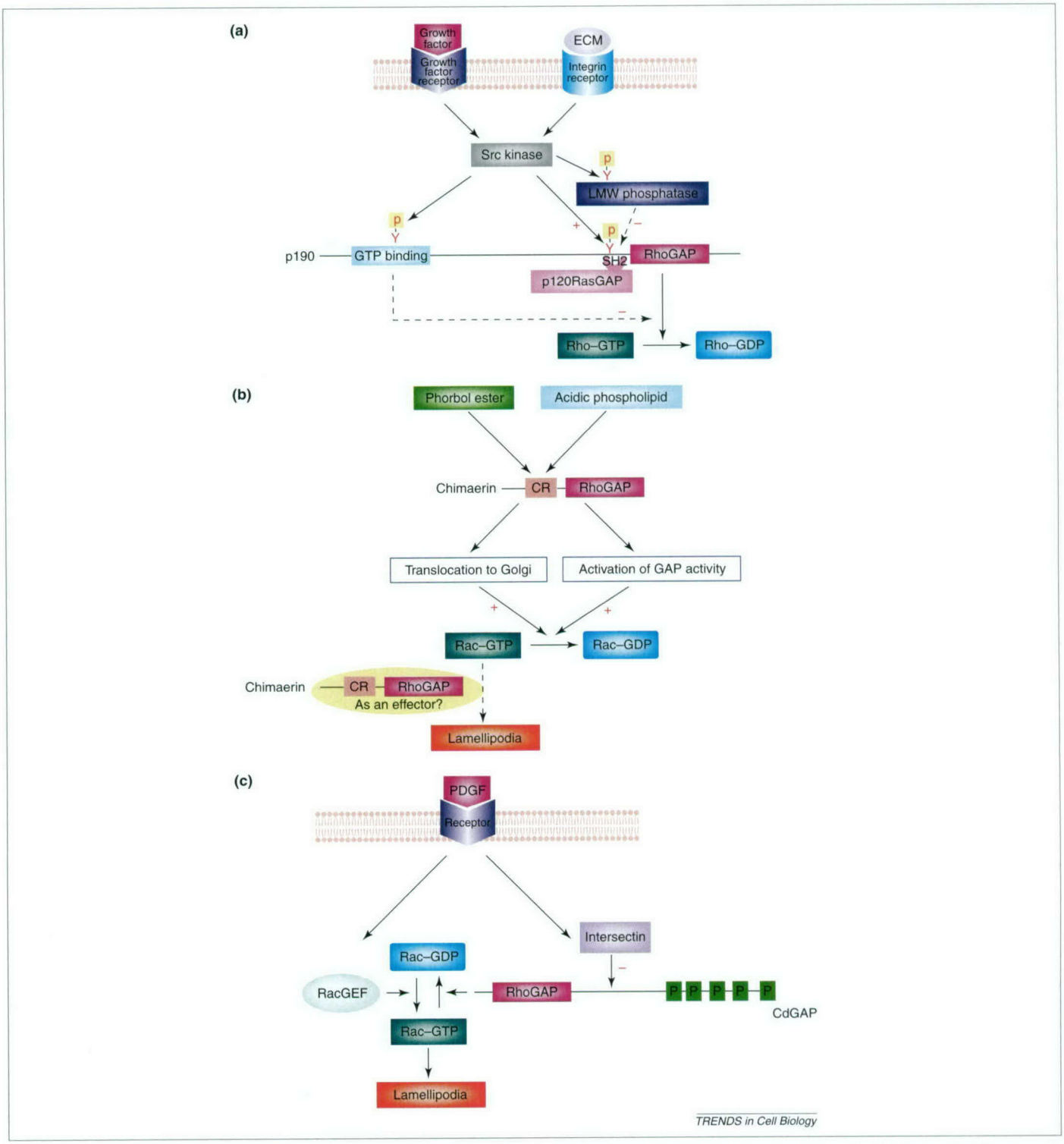

Fig. 5. Models for regulation of Rho GTPase-activating proteins (RhoGAPs). (a) Regulation of p190 RhoGAP by phosphorylation. Src family tyrosine kinases, activated by growth factor receptors such as the PDGF (platelet-derived growth factor) receptor or integrin adhesion receptor, are among the major regulators of p190. Tyrosine phosphorylation of p190 by Src initiates its association with p120 Ras GTPase-activating protein (RasGAP), translocation to plasma membrane and activation of catalytic GAP activity. The deactivation of p190 could be achieved in part by dephosphorylation by low molecular weight (LMW) tyrosine phosphatase, which itself is an Src substrate. Although the exact mechanism has yet to be elucidated, an intact N-terminal GTP-binding domain of p190 appears to be required for the normal function of the C-terminal RhoGAP domain. (b) Regulation of n-chimaerin by lipid binding. n-Chimaerin contains a cysteine-rich domain (CR domain) that might function as a phorbol ester/diacylglycerol (DAG) receptor site or protein–protein interactive site. *In vitro*, phosphatidylserine (PE) and phosphoric acid binding to n-chimaerin increases the catalytic GAP activity toward Rac1, whereas lysophosphatidic acid, phosphatidylinositols and arachidonic acids appear to inhibit the GAP activity. The binding of PE also translocates chimaerin to the perinuclear region and Golgi apparatus in the cell. There is evidence that full-length n-chimaerin can mediate, rather than downregulate, Rac1-induced lamellipodia formation. (c) Regulation of CdGAP by interaction with intersectin. CdGAP interacts with the SH3 domains of intersectin, an endocytic protein that contains five SH3 domains in addition to a Cdc42-specific GEF motif. This interaction might cause a conformational change in CdGAP that allows its proline-rich C-terminus to interfere with the RhoGAP domain, resulting in an inhibition of the GAP activity towards Rac1.

kinases. Activation of Src in cells leads to phosphorylation of two tyrosine residues of p190 that are located close to the RhoGAP domain (Fig. 5a) [44,45]. Upon phosphorylation, p190 recruits p120RasGAP through an SH2 domain–phosphotyrosine interaction. This effectively activates the Rho-specific GAP activity of p190, causing disruption of actin stress fibres, reduction of focal contacts and impairing the ability of the cell to adhere to fibronectin, the cellular effects consistent with decreased active Rho GTPase species in cells. An Src-independent signal emanating from growth factor receptors might also be required for full activation of p190 [46].

Countering the Src phosphorylation effect, a recent study showed that low molecular weight protein-tyrosine phosphatase (LMW-PTP), a key mediator of PDGF (platelet-derived growth factor) receptor signalling, could function as a negative regulator of p190RhoGAP. PDGF stimulation of cells could cause c-Src-dependent tyrosine phosphorylation on both LMW-PTP and p190 and lead to a direct interaction of these two proteins [47,48]. The phosphorylation of LMW-PTP by Src significantly increased the phosphatase activity of LMW-PTP and reduced Src-dependent phosphorylation of p190. One possible model subsequently is that c-Src activates p190 by direct phosphorylation, and this positive input to p190 could be kept in check by a LMW-PTP or other phosphatase-dependent mechanism to achieve a reversible, tight regulation (Fig. 5a).

The N-terminus of p190RhoGAP contains a unique GTP-binding domain. A mutant of the GTP-binding domain that fails to bind to guanine nucleotide inhibits the GAP activity of p190, suggesting that more complex intra- or intermolecular interaction might contribute to the regulation of the C-terminal RhoGAP domain [49]. Consistent with a regulatory role of the N-terminus, one report suggests that GTP binding to p190 is abolished by c-Src dependent phosphorylation *in vitro* [50]. This observation further raises the possibility that Src might act on p190 partly through modulation of the GTP-binding domain (Fig. 5a).

In addition to tyrosine phosphorylation by Src, p190 is phosphorylated on Ser/Thr residues in Src-transformed cells, which could be mediated by protein kinase C (PKC) [17]. Activation of PKC correlates with the phosphorylation and translocalization of p190 from the cytosol to membrane ruffles. This mechanism could provide another layer of p190 regulation.

Regulation by lipid binding: chimaerins

The Rac-specific GAP activity of chimaerin can be regulated *in vitro* by phospholipids through the CR cysteine-rich domain, which might also act as a phorbol ester/diacylglycerol (DAG) receptor site [51–53]. Full-length chimaerin expressed in mammalian cell lysates failed to stimulate Rac1 intrinsic GTPase activity, whereas GAP activity was detected when the CR domain of chimaerin was deleted. These observations suggest that an autoinhibitory mechanism might be involved, presumably through N-terminus interference with the C-terminal GAP domain function. Interestingly, the Rac GAP activity of n-chimaerin was increased by phosphatidylserine (PS) and phosphatidic acid (PA), and the stimulation by these phospholipids was further synergized by phorbol ester binding. Conversely, lysophosphatidic acid, phosphatidylinositol lipids and arachidonic acid inhibited the GAP activity. In fact, the binding of phorbol ester to the chimaerins appears to depend upon the presence of phospholipids as cofactors, suggesting the involvement of membrane organelles in regulating GAP activity and in targeting [51]. The latter function is supported by the observation that phorbol ester or DAG binding to the CR domain not only altered the catalytic GAP activity of β2-chimaerin, but also translocated chimaerin from cytosol to the perinuclear region and Golgi [52,53]. These studies of chimaerin illustrate the point that lipid interaction with a RhoGAP through noncatalytic motifs might have regulatory effects on both its intracellular location and biochemical GAP activity (Fig. 5b). There is additional evidence indicating that the CR domain of chimaerin could also interact with a protein localized in the *cis*-Golgi network, Tmp21-I, which might be involved in sorting and trafficking in the early secretory pathway [54], suggesting that chimaerins are subject to another level of regulation and might play a role in this aspect of Rac function.

Regulation by protein–protein interaction: CdGAP

CdGAP has a RhoGAP domain at the N-terminal end and multiple proline-rich motifs at the C-terminal end. The RhoGAP domain contains a biochemical GAP activity toward Cdc42 and Rac1, but not RhoA. CdGAP directly interacts through the middle region of the molecule with the SH3 domains of intersectin, an endocytic scaffolding protein that contains five consecutive SH3 domains in addition to a Cdc42-specific GEF module [55]. The binding of intersectin caused inhibition of the GAP activity of CdGAP *in vitro* and in cells. The effect appears to involve the proline-rich motifs of CdGAP [55]. This suggests that the interaction with intersectin might induce a conformational change in CdGAP, resulting in the interference of the GAP domain function (Fig. 5c). The regulatory mode of CdGAP presents an example of the involvement of protein–protein interaction in GAP activity regulation. The complex formed by intersectin recruitment of additional factors, including mSos1, Cdc42 and WASP [56], in addition to CdGAP, might constitute a highly sophisticated small G-protein signalling network in the regulation of cell actin structure.

RhoGAPs as signal convergent or divergent points

Aside from the RhoGAP domain, RhoGAP family members typically contain other functional motifs including catalytic domains such as protein kinase, Rho GEF and Arf GAP domains as well as protein–protein and protein–lipid adaptor modules such as SH2, SH3, PH and CR domains (Fig. 4). RhoGAPs might thus catalyse enzymatic reactions other than the stimulation of GTP hydrolysis of Rho proteins, and sometimes seemingly facilitate Rho protein signalling.

As Rho guanine nucleotide exchange factors

Both BCR and ABR contain a DH and a PH module – a combination that might activate Rho proteins as a GEF – as

well as a Rac-specific RhoGAP domain. Therefore potentially they can activate and inactivate Rho GTPases simultaneously [57], although the GEF activity of these molecules has yet to be demonstrated in cells. In *BCR*-deleted mice, neutrophil reactive oxidant generation was markedly elevated and the amount of membrane-associated Rac2 increased, strongly suggesting that BCR acts as a Rac-specific negative regulator *in vivo* [58].

Further insights about the role of proteins with both RhoGEF and RhoGAP domains have been gained from studies of *Dictyostelium discoideum* DRG (DdRacGAP) [59,60]. *DRG*-null cells have impaired motility towards chemoattractant stimuli and are defective in the contractile vacuole system that normally pumps water out of cells in a hypotonic environment. When either the RhoGEF or RhoGAP domain was introduced into *DRG*-null cells, the RhoGEF activity was able to restore chemoattraction, whereas the RhoGAP activity rescued the contractile vacuole system. In addition, overexpression of the RhoGAP domain of DRG caused defects in cytokinesis. Further *in vitro* analysis showed that the RhoGEF domain preferably interacts with Rac1 whereas the RhoGAP domain interacts with RhoE and Rab GTPases [60]. Because all three small GTPases are involved in the distinct cellular processes affected by *DRG* deficiency – that is, Rac1 in cell motility, RhoE in cytokinesis and Rab in the contractile vacuole system – DRG might regulate multiple signalling pathways via individual GTPases through each specialized domain structure. Future studies might reveal mammalian counterparts of DRG that have a similar ability to regulate diverse signalling pathways.

As Arf GTPase-activating proteins (GAPs)

Another example of RhoGAPs that shows cooperative interplay of multifunctional domains is the ARAP subfamily of RhoGAPs, members of which contain an ArfGAP domain that is active towards the Arf GTPases, an RA domain that might interact with Ras, five PH domains that serve as the binding elements for the PI 3-kinase product, $PI(3,4,5)P_3$ (phosphatidylinositol 3,4,5-trisphosphate), as well as a RhoGAP domain [61,62]. The ArfGAP activity of ARAPs can be activated by $PI(3,4,5)P_3$ binding, and the RhoGAP and ArfGAP domains appear to cooperate in mediating cytoskeleton rearrangement and cell morphological changes in response to PI 3-kinase. Thus, ARAPs are potential targets for multiple signals and might affect the activities of three different classes of small GTPases.

As positive signal transducers of Rho proteins

The presence of a RhoGAP domain in the regulatory subunits of PI 3-kinase, p85α and p85β, allows them to interact specifically with Rac1 and Cdc42, but they do not have detectable GAP activity [63]. Although several attempts have been made to explain the lack of GAP activity of p85 based on the structural information, the question remains open whether the RhoGAP domain truly functions as a GAP or simply serves as a Rho GTPase interactive motif [64,65]. The fact that interaction of Rac or Cdc42 with p85 could stimulate PI 3-kinase activity *in vitro* supports the notion that p85 might be an effector, not a downregulator, of Rho protein signalling [63,66,67]. Recent identification of a small GTPase-responsive domain in p85 sequences further reinforces this possibility, although the RhoGAP domain is not involved [68]. Another piece of evidence that a RhoGAP domain-containing molecule might act as an effector to potentiate Rho GTPase function came from studies of n-chimaerin, a Rac-specific RhoGAP [69]. Microinjection experiments have clearly demonstrated that whereas the RhoGAP domain alone inhibited Rac-stimulated lamellipodia formation, full-length n-chimaerin cooperated with Rac1 to mediate lamellipodia and filopodia formation. For this activity, the binding to Rac1 is indispensable but the GAP catalytic activity is not required. One logical conclusion from these cases is that certain RhoGAPs might potentiate, rather than downregulate, Rho signalling events.

Concluding remarks

RhoGAP family proteins are established as the major class of molecules that negatively regulate the biological activity of Rho GTPases. The multifunctional features of many RhoGAPs make them logical candidates for signal convergent or divergent points of Rho GTPases and other classes of signalling molecules. Whereas most RhoGAPs appear to serve primarily to downregulate their cognate Rho GTPase substrates, some may facilitate the effective cycling of Rho GTPases between the GTP- and GDP-bound conformational states by accelerating GTP hydrolysis. With the completion of multiple higher eukaryotic genome analysis in sight, a systematic survey of the tissue distribution, the Rho GTPase substrate specificity, the subcellular localization patterns, and the organ- or organism-specific roles of RhoGAP family members is the next step towards a comprehensive understanding of their function. How each RhoGAP collaborates with its Rho protein partner in a tightly regulated manner to terminate or emanate signals in physiologically relevant pathways poses another major challenge in this field.

Acknowledgements

We thank Drs X. Huang, M. Jansen, H. Zang and D. Williams for critical reading of the manuscript. Work in the authors' laboratory was supported by National Institutes of Health and US Army breast cancer program.

References

1 Bishop, A.L. and Hall, A. (2000) Rho GTPases and their effector proteins. *Biochem. J.* 348, 241–255
2 Van Aelst, L. and D'Souza-Schorey, C. (1997) Rho GTPases and signaling networks. *Genes Dev.* 11, 2295–2322
3 Hall, A. (1998) Rho GTPases and the actin cytoskeleton. *Science* 279, 509–514
4 Zheng, Y. (2001) Dbl family guanine nucleotide exchange factors. *Trends Biochem. Sci.* 26, 724–732
5 Lamarche, N. and Hall, A. (1994) GAPs for rho-related GTPases. *Trends Genet.* 10, 436–440
6 Olofsson, B. (1999) Rho guanine dissociation inhibitors: pivotal molecules in cellular signalling. *Cell. Signal.* 11, 545–554
7 Symons, M. and Settleman, J. (2000) Rho family GTPases: more than simple switches. *Trends Cell Biol.* 10, 415–419

8 Diekmann, D. *et al.* (1991) Bcr encodes a GTPase-activating protein for p21rac. *Nature* 351, 400–40022
9 Bax, B. (1998) Domains of rasGAP and rhoGAP are related. *Nature* 392, 447–448
10 Rittinger, K. *et al.* (1998) Support for shared ancestry of GAPs. *Nature* 392, 448–449
11 Gamblin, S.J. and Smerdon, S.J. (1998) GTPase-activating proteins and their complexes. *Curr. Opin. Struct. Biol.* 8, 195–201
12 Nassar, N. *et al.* (1998) Structures of Cdc42 bound to the active and catalytically compromised forms of Cdc42GAP. *Nat. Struct. Biol.* 5, 1047–1052
13 Li, R. *et al.* (1997) Structural determinants required for the interaction between RhoA and the GTPase-activating domain of p190. *J. Biol. Chem.* 272, 32830–32835
14 Longenecker, K.L. *et al.* (2000) Structure of the BH domain from graf and its implications for Rho GTPase recognition. *J. Biol. Chem.* 275, 38605–38610
15 Luo, L. (2000) Rho GTPases in neuronal morphogenesis. *Nat. Rev. Neurosci.* 1, 173–180
16 Billuart, P. *et al.* (1998) Oligophrenin-1 encodes a rhoGAP protein involved in X-linked mental retardation. *Nature* 392, 923–926
17 Brouns, M.R. *et al.* (2000) The adhesion signaling molecule p190 RhoGAP is required for morphogenetic processes in neural development. *Development* 127, 4891–4903
18 Brouns, M.R. *et al.* (2001) p190 RhoGAP is the principal Src substrate in brain and regulates axon outgrowth, guidance and fasciculation. *Nat. Cell Biol.* 3, 361–367
19 Billuart, P. *et al.* (2002) Regulating axon branch stability: the role of p190 RhoGAP in repressing a retraction signaling pathway. *Cell* 107, 195–207
20 Wong, K. *et al.* (2001) Signal transduction in neuronal migration: roles of GTPase activating proteins and the small GTPase Cdc42 in the Slit-Robo pathway. *Cell* 107, 209–221
21 Harada, A. *et al.* (2000) Nadrin, a novel neuron-specific GTPase-activating protein involved in regulated exocytosis. *J. Biol. Chem.* 275, 36885–36891
22 Reczek, D. and Bretscher, A. (2001) Identification of EPI64, a TBC/rabGAP domain-containing microvillar protein that binds to the first PDZ domain of EBP50 and E3KARP. *J. Cell Biol.* 153, 191–206
23 Sordella, R. *et al.* (2002) Modulation of CREB activity by the Rho GTPase regulates cell and organism size during mouse embryonic development. *Dev. Cell* 2, 553–565
24 Hirose, K. *et al.* (2001) MgcRacGAP is involved in cytokinesis through associating with mitotic spindle and midbody. *J. Biol. Chem.* 276, 5821–5828
25 Mishima, M. *et al.* (2002) Central spindle assembly and cytokinesis require a kinesin-like protein/RhoGAP complex with microtubule bundling activity. *Dev. Cell* 2, 41–54
26 Jantsch-Plunger, V. *et al.* (2000) CYK-4: a Rho family gtpase activating protein (GAP) required for central spindle formation and cytokinesis. *J. Cell Biol.* 149, 1391–1404
27 Madaule, P. *et al.* (1998) Role of citron kinase as a target of the small GTPase Rho in cytokinesis. *Nature* 394, 491–494
28 Ellis, S. and Mellor, H. (2000) Regulation of endocytic traffic by rho family GTPases. *Trends Cell Biol.* 10, 85–88
29 Cantor, S.B. *et al.* (1995) Identification and characterization of Ral-binding protein 1, a potential downstream target of Ral GTPases. *Mol. Cell. Biol.* 15, 4578–4584
30 Park, S.H. and Weinberg, R.A. (1995) A putative effector of Ral has homology to Rho/Rac GTPase activating proteins. *Oncogene* 11, 2349–2355
31 Jullien-Flores, V. *et al.* (1995) Bridging Ral GTPase to Rho pathways. RLIP76, a Ral effector with CDC42/Rac GTPase-activating protein activity. *J. Biol. Chem.* 270, 22473–22477
32 Ikeda, M. *et al.* (1998) Identification and characterization of a novel protein interacting with Ral-binding protein 1, a putative effector protein of Ral. *J. Biol. Chem.* 273, 814–821
33 Yamaguchi, A. *et al.* (1997) An Eps homology (EH) domain protein that binds to the Ral-GTPase target, RalBP1. *J. Biol. Chem.* 272, 31230–31234
34 Jullien-Flores, V. *et al.* (2000) RLIP76, an effector of the GTPase Ral, interacts with the AP2 complex: involvement of the Ral pathway in receptor endocytosis. *J. Cell Sci.* 113, 2837–2844
35 Nakashima, S. *et al.* (1999) Small G protein Ral and its downstream molecules regulate endocytosis of EGF and insulin receptors. *EMBO J.* 18, 3629–3642
36 Sahai, E. and Marshall, C.J. (2002) Rho-GTPases and cancer. *Nat. Rev. Cancer* 2, 133–142
37 Yuan, B.Z. *et al.* (1998) Cloning, characterization, and chromosomal localization of a gene frequently deleted in human liver cancer (DLC-1) homologous to rat RhoGAP. *Cancer Res.* 58, 2196–2199
38 Borkhardt, A. *et al.* (2000) The human GRAF gene is fused to MLL in a unique t(5;11)(q31;q23) and both alleles are disrupted in three cases of myelodysplastic syndrome/acute myeloid leukemia with a deletion 5q. *Proc. Natl Acad. Sci. USA* 97, 9168–9173
39 Shtivelman, E. *et al.* (1985) Fused transcript of abl and bcr genes in chronic myelogenous leukaemia. *Nature* 315, 550–554
40 McDonald, J.D. *et al.* (1994) Physical mapping of chromosome 17p13.3 in the region of a putative tumor suppressor gene important in medulloblastoma. *Genomics* 23, 229–232
41 Wang, D.Z. *et al.* (1997) The GTPase and Rho GAP domains of p190, a tumor suppressor protein that binds the M_r 120,000 Ras GAP, independently function as anti-Ras tumor suppressors. *Cancer Res.* 57, 2478–2484
42 Sekimata, M. *et al.* (1999) Morphological changes and detachment of adherent cells induced by p122, a GTPase-activating protein for Rho. *J. Biol. Chem.* 274, 17757–17762
43 Taylor, J.M. *et al.* (1999) Cytoskeletal changes induced by GRAF, the GTPase regulator associated with focal adhesion kinase, are mediated by Rho. *J. Cell Sci.* 112, 231–242
44 Roof, R.W. *et al.* (1998) Phosphotyrosine (p-Tyr)-dependent and -independent mechanisms of p190 RhoGAP-p120 RasGAP interaction: Tyr 1105 of p190, a substrate for c-Src, is the sole p-Tyr mediator of complex formation. *Mol. Cell. Biol.* 18, 7052–7063
45 Hu, K.Q. and Settleman, J. (1997) Tandem SH2 binding sites mediate the RasGAP–RhoGAP interaction: a conformational mechanism for SH3 domain regulation. *EMBO J.* 16, 473–483
46 Haskell, M.D. *et al.* (2001) Phosphorylation of p190 on Tyr1105 by c-Src is necessary but not sufficient for EGF-induced actin disassembly in C3H10T1/2 fibroblasts. *J. Cell Sci.* 114, 1699–1708
47 Bucciantini, M. *et al.* (1999) The low Mr phosphotyrosine protein phosphatase behaves differently when phosphorylated at Tyr131 or Tyr132 by Src kinase. *FEBS Lett.* 456, 73–78
48 Chiarugi, P. *et al.* (2000) The low M(r) protein-tyrosine phosphatase is involved in Rho-mediated cytoskeleton rearrangement after integrin and platelet-derived growth factor stimulation. *J. Biol. Chem.* 275, 4640–4646
49 Tatsis, N. *et al.* (1998) The function of the p190 Rho GTPase-activating protein is controlled by its N-terminal GTP binding domain. *J. Biol. Chem.* 273, 34631–34638
50 Roof, R.W. *et al.* (2000) Phosphorylation of the p190 RhoGAP N-terminal domain by c-Src results in a loss of GTP binding activity. *FEBS Lett.* 472, 117–121
51 Caloca, M.J. *et al.* (1997) Beta2-chimaerin is a high affinity receptor for the phorbol ester tumor promoters. *J. Biol. Chem.* 272, 26488–26496
52 Caloca, M.J. *et al.* (2001) Phorbol esters and related analogs regulate the subcellular localization of beta 2-chimaerin, a non-protein kinase C phorbol ester receptor. *J. Biol. Chem.* 276, 18303–18312
53 Caloca, M.J. *et al.* (1999) Beta2-chimaerin is a novel target for diacylglycerol: binding properties and changes in subcellular localization mediated by ligand binding to its C1 domain. *Proc. Natl Acad. Sci. USA* 96, 11854–11859
54 Wang, H. and Kazanietz, M.G. (2002) Chimaerins, novel non-protein kinase C phorbol ester receptors, associate with Tmp21-I (p23). Evidence for a novel anchoring mechanism involving the chimaerin C1 domain. *J. Biol. Chem.* 277, 4541–4550
55 Jenna, S. *et al.* (2002) The activity of the GTPase-activating protein CdGAP is regulated by the endocytic protein intersectin. *J. Biol. Chem* 277, 6366–6373
56 O'Bryan, J.P. *et al.* (2001) Mitogenesis and endocytosis: what's at the INTERSECTIoN? *Oncogene* 20, 6300–6308
57 Chuang, T.H. *et al.* (1995) Abr and Bcr are multifunctional regulators of the Rho GTP-binding protein family. *Proc. Natl Acad. Sci. USA* 92, 10282–10286

58 Voncken, J.W. *et al.* (1995) Increased neutrophil respiratory burst in bcr-null mutants. *Cell* 80, 719–728
59 Ludbrook, S.B. *et al.* (1997) Cloning and characterization of a rhoGAP homolog from *Dictyostelium discoideum*. *J. Biol. Chem.* 272, 15682–15686
60 Knetsch, M.L. *et al.* (2001) The *Dictyostelium* Bcr/Abr-related protein DRG regulates both Rac- and Rab-dependent pathways. *EMBO J.* 20, 1620–1629
61 Krugmann, S. *et al.* (2002) Identification of ARAP3, a novel PI3K effector regulating both Arf and Rho GTPases, by selective capture on phosphoinositide affinity matrices. *Mol. Cell* 9, 95–108
62 Miura, K. *et al.* (2002) ARAP1: a point of convergence for Arf and Rho signaling. *Mol. Cell* 9, 109–119
63 Zheng, Y. *et al.* (1994) Activation of phosphoinositide 3-kinase activity by Cdc42Hs binding to p85. *J. Biol. Chem.* 269, 18727–18730
64 Musacchio, A. *et al.* (1996) Crystal structure of the breakpoint cluster region-homology domain from phosphoinositide 3-kinase p85 alpha subunit. *Proc. Natl Acad. Sci. USA* 93, 14373–14378
65 Barrett, T. *et al.* (1997) The structure of the GTPase-activating domain from p50rhoGAP. *Nature* 385, 458–461
66 Tolias, K.F. *et al.* (1995) Rho family GTPases bind to phosphoinositide kinases. *J. Biol. Chem.* 270, 17656–17659
67 Bokoch, G.M. *et al.* (1996) Rac GTPase interacts specifically with phosphatidylinositol 3-kinase. *Biochem. J.* 315, 775–779
68 Chan, T. *et al.* (2002) Small GTPases and tyrosine kinases coregulate a molecular switch in the phosphoinositide 3-kinase regulatory subunit. *Cancer Cell* 1, 181–191
69 Kozma, R. *et al.* (1996) The GTPase-activating protein n-chimaerin cooperates with Rac1 and Cdc42Hs to induce the formation of lamellipodia and filopodia. *Mol. Cell. Biol.* 16, 5069–5080
70 Heisterkamp, N. *et al.* (1993) Human ABR encodes a protein with GAPrac activity and homology to the DBL nucleotide exchange factor domain. *J. Biol. Chem.* 268, 16903–16906
71 Hall, C. *et al.* (2001) alpha2-chimaerin, a Cdc42/Rac1 regulator, is selectively expressed in the rat embryonic nervous system and is involved in neuritogenesis in N1E-115 neuroblastoma cells. *J. Neurosci.* 21, 5191–5202
72 Saras, J. *et al.* (1997) A novel GTPase-activating protein for Rho interacts with a PDZ domain of the protein-tyrosine phosphatase PTPL1. *J. Biol. Chem.* 272, 24333–24338
73 Ren, X.R. *et al.* (2001) Regulation of CDC42 GTPase by proline-rich tyrosine kinase 2 interacting with PSGAP, a novel pleckstrin homology and Src homology 3 domain containing rhoGAP protein. *J. Cell Biol.* 152, 971–984
74 Richnau, N. and Aspenstrom, P. (2001) Rich, a rho GTPase-activating protein domain-containing protein involved in signaling by Cdc42 and Rac1. *J. Biol. Chem.* 276, 35060–35070
75 Hildebrand, J.D. *et al.* (1996) An SH3 domain-containing GTPase-activating protein for Rho and Cdc42 associates with focal adhesion kinase. *Mol. Cell. Biol.* 16, 3169–3178

THE JOURNAL OF BIOLOGICAL CHEMISTRY
Vol. 278, No. 16, Issue of April 18, pp. 14414–14419, 2003
Printed in U.S.A.
© 2003 by The American Society for Biochemistry and Molecular Biology, Inc.

$p19^{Arf}$-p53 Tumor Suppressor Pathway Regulates Cell Motility by Suppression of Phosphoinositide 3-Kinase and Rac1 GTPase Activities*

Received for publication, January 13, 2003, and in revised form, February 4, 2003
Published, JBC Papers in Press, February 10, 2003, DOI 10.1074/jbc.M300341200

Fukun Guo, Yuan Gao, Lei Wang, and Yi Zheng‡

From the Division of Experimental Hematology, Children's Hospital Research Foundation, University of Cincinnati, Cincinnati, Ohio 45229

The $p19^{Arf}$-p53 tumor suppressor pathway plays a critical role in cell-cycle checkpoint control and apoptosis, whereas Rho family small GTPases are key regulators of actin structure and cell motility. By using primary mouse embryonic fibroblasts that lack *Arf*, *p53*, or both, we studied the involvement of the $p19^{Arf}$-p53 pathway in the regulation of cell motility and its relationship with Rho GTPases. Deletion of *Arf* and/or *p53* led to actin cytoskeleton reorganization and a significant increase in cell motility. The endogenous phosphoinositide (PI) 3-kinase and Rac1 activities were elevated in $Arf^{-/-}$ and $p53^{-/-}$ cells, and these activities are required for $p19^{Arf}$- and p53-regulated migration. Reintroduction of the wild type *Arf* or *p53* genes into $Arf^{-/-}$ or $p53^{-/-}$ cells reversed the PI 3-kinase and Rho GTPase activities as well as the migration phenotype. These results suggest a functional relationship between an established tumor suppressor pathway and a signaling module that controls actin structure and cell motility and show that $p19^{Arf}$ and p53 negatively regulate cell migration by suppression of PI 3-kinase and Rac1 activities.

The p53 and pRb cell cycle inhibitors and their regulators, including $p19^{Arf}$ and $p27^{Kip1}$, are well established tumor suppressors that are components of a complex signaling network central to tumor suppression (1). Deletion or mutation in these tumor suppressors or their regulators occurs in the majority of tumor cases and correlates with the onset of a wide spectrum of cancer (2). Specifically the $p19^{Arf}$-p53 tumor suppressor pathway is thought to be involved primarily in monitoring proliferation signals to prevent cells from uncontrolled growth (3). Rho family small GTPases, on the other hand, are molecular switches that transduce diverse intracellular signals leading to cell proliferation, gene induction, apoptosis, and in particular, cytoskeleton remodeling and migration (4). Accumulating evidence has implicated the Rho GTPases, RhoA, Rac1, and Cdc42, in many aspects of tumor development, including tumor cell migration and proliferation (5). Many mitogenic signals, including those from growth factor receptors and integrins, can promote the exchange of GDP for GTP on Rho GTPases, enabling them to interact with an array of effector targets to elicit cytoskeletal changes (6, 7).

Although much of the attention in tumor suppressor studies has been focused on their roles in cell cycle control and/or apoptosis, preliminary evidence has become available suggesting a potential functional linkage between p53 and cell morphological effect/cell motility. For example, p53 has been shown to regulate the transcription of a number of genes involved in cell morphology and/or movement, including that of smooth muscle α-actin (8), collagens IIα1 and VIα1 (9), vascular epidermal growth factor (10), metalloproteinase-1 (11), and fibronectin (12). Moreover, overexpression of p53 seems to cause a partial reversion of Ras-induced morphological transformation (13) and to inhibit cell migration (14). A recent study further suggests that p53 may have a role in Cdc42-mediated filopodia formation and cell polarization (15).

To investigate the functional connection between the tumor suppressors and Rho GTPase-regulated cytoskeleton events, we have examined the actin cytoskeletal structure and migration capability of $p19^{Arf}$-, p53-, $p27^{Kip1}$-, or pRb-deficient primary mouse embryonic fibroblast (MEF)[1] cells. We report that the $p19^{Arf}$-p53 tumor suppressor pathway, but not the related $p27^{Kip1}$-pRb pathway, negatively regulates cell motility through suppression of the PI 3-kinase-Rac1 signaling module.

EXPERIMENTAL PROCEDURES

DNA Constructs—Site-directed mutagenesis of Rac1, Cdc42, RhoA, and p53 was performed by the polymerase chain reaction-based, oligonucleotide-mediated method (16). The retroviral constructs expressing $p19^{Arf}$, p53 wild type or mutant, and dominant negative Rho GTPases (Rac1N17, Cdc42N17, and RhoAN19) were generated by ligating the corresponding cDNA fragments into the *Bam*HI and *Eco*RI sites of the retroviral GFP bicistronic vector, MIEG3 (17).

Cell Culture, Retroviral Infection, and Cell Imaging—Primary MEFs from $p19Arf^{-/-}$, $p53^{-/-}$, $p19Arf^{-/-}/p53^{-/-}$, $p27Kip1^{-/-}$, and $pRb^{-/-}$ mice (all of the C57BL/6 × 129/sv background) were generous gifts from Dr. Martine Roussel (St. Jude, Memphis, TN) and were generated as described previously (18). Recombinant retroviruses were produced using the ecotropic Phoenix packaging cell system (17). The primary MEFs were infected with the retroviruses and harvested 48–72 h after infection. GFP-positive cells were isolated by fluorescence-activated cell sorting.

Primary MEFs were seeded onto coverslips at 3×10^4 cells/slip density. The cells were serum-starved for 12 h prior to fixation. The F-actin structure of the cells was visualized by rhodamine-phalloidin staining, and the stained cells were analyzed by using a conventional fluorescence microscope (Zeiss).

Cell Motility and Migration Assays—Single cell motility assays using the colloidal gold particles were carried out as described (19). The wound healing assays to semi-quantitatively determine the migration

* This work was supported by grants from the National Institutes of Health (GM53943) and the Department of Defense Breast Cancer Program (BC990290) (both to Y. Z.). The costs of publication of this article were defrayed in part by the payment of page charges. This article must therefore be hereby marked "*advertisement*" in accordance with 18 U.S.C. Section 1734 solely to indicate this fact.

‡ To whom correspondence should be addressed. Tel.: 513-636-0595; Fax: 513-636-3768; E-mail: yi.zheng@chmcc.org.

[1] The abbreviations used are: MEF, mouse embryonic fibroblast; GST, glutathione *S*-transferase; PAK, p21-activated kinase; PI 3-kinase, phosphoinositide 3-kinase; GFP, green fluorescent protein; PIP_3, inositol 1,4,5-trisphosphate; PTEN, phosphatase and tensin homolog deleted on chromosome 10; WASP, Wiskott-Aldrich syndrome protein.

This paper is available on line at http://www.jbc.org

distance were performed following a scratch of the confluent monolayer of cells as described (20). The migration distances of cells were monitored at various times and were measured at 9 h after the introduction of the wound under low serum (0.5%) conditions.

PI 3-kinase Assay, Chemical Inhibitors, and Immunoblotting—The endogenous PI 3-kinase activities of $Arf^{-/-}$, $p53^{-/-}$, $Arf^{-/-}/p53^{-/-}$, and $Arf^{-/-}$ or $p53^{-/-}$ cells reconstituted with *Arf* or *p53* were assayed according to a described protocol (21). Briefly the cells were lysed in buffer A containing 20 mM Tris-HCl, pH 8.0, 100 mM NaCl, 1 mM EDTA, 0.3 mM dithiothreitol, 0.5 mM phenylmethylsulfonyl fluoride, 1% Triton X-100, 10 μg/ml aprotinin, 10 μg/ml leupeptin, 0.1 mM sodium orthovanadate and 25 mM NaF. After centrifugation at 4 °C for 30 min at 14,000 rpm, the protein contents in the supernatant of cell lysates were measured by the Bradford method. An equal amount of proteins was incubated with anti-p85 polyclonal antibody coupled to protein A-agarose (Upstate Biotechnology) overnight or subjected to anti-p85 or anti-p110 Western blot analysis. The immunoprecipitates were washed twice with buffer C containing 20 mM Tris-HCl, pH 8.0, 100 mM NaCl, and 10 mM $MgCl_2$ and washed once with a kinase assay buffer (20 mM Tris-HCl, pH 7.6, 10 mM $MgCl_2$). 5 μg of sonicated phosphatidylinositol together with [γ-^{32}P]ATP (200 μCi/ml) in 45 μl of the kinase assay buffer were incubated with the washed beads at 25 °C for 10 min. The reactions were terminated by the addition of 100 μl of 1 N HCl. The reaction products were extracted by 200 μl of $CHCl_3$/MeOH (1:1) and resolved on a TLC silica plate coated with potassium oxalate in a solvent containing $CHCl_3$/MeOH/NH_4OH, 4 M (9:7:2). The PI 3-kinase reactions were analyzed by autoradiography.

Prior to Western blotting, the protein contents of the cell lysates were normalized by the Bradford method. Anti-phospho-Akt(Ser^{473}) and anti-PTEN antibodies were obtained from Cell Signaling, Inc., anti-p85 and the anti-p110 of PI 3-kinase antibodies were obtained from Upstate Biotechnology, Inc., and the PI 3-kinase inhibitors wortmannin and LY294002 were obtained from Sigma.

Endogenous Rho GTPases Activity Assay—GST-PAK1, GST-Rhotekin, and GST-WASP, which contain Rac1, RhoA, and the Cdc42-interactive domains of PAK1, Rhotekin, and WASP, respectively, were used to probe the endogenous Rac1-GTP, RhoA-GTP, and Cdc42-GTP activities as described (20).

RESULTS AND DISCUSSION

$p19^{Arf}$, p53, $p27^{Kip1}$, and pRb are well recognized cell cycle regulators that are critical to checkpoint control. $p19^{Arf}$, in response to oncogenic signals, stabilizes p53 by sequestering Mdm2, a negative regulator of p53 (3), whereas $p27^{Kip1}$, on its way through pRb, regulates G_1 transition by modulating growth-essential E2F transcription factors (1). All four are important components of a complex tumor suppressor network. To examine their potential involvement in the regulation of cell actin structure and motility, we have generated the $p19^{Arf}$-, p53-, $p27^{Kip1}$-, or pRb-deficient primary MEFs from the respective tumor suppressor knock-out mice. To avoid possible alteration of cell properties under tissue culture conditions, only low passages (<6 passages) of the primary cells were used and at least two independent p53- or $p19^{Arf}$-deficient MEF preparations were examined.

In subconfluent culture and serum-free conditions, a significant percentage of the $p19^{Arf}$- or p53-deficient cells appeared to be in a round shape and displayed intense cortical actin staining, whereas the $p27^{Kip1}$- or pRb-deficient cells were similar to wild type MEFs in morphology and actin structure (Fig. 1*A*). To determine whether the altered actin structures might be associated with cell motility modulation, the cells were plated onto colloidal gold-coated plates, and the motility of single cells was traced by the trails left behind their movement paths. As shown in Fig. 1*B*, in the absence of serum stimulation, both $p19^{Arf}$- and p53-deficient cells produced long trails, whereas the *Kip1* and *Rb* knock-out cells were similar to the wild type cells, showing no sign of movement.

To further quantify cell migration rate, we measured the migration distance of these cells in a wound healing assay. The $Arf^{-/-}$ and $p53^{-/-}$ cells migrated about 2-fold faster than the wild type, $Kip1^{-/-}$, or $Rb^{-/-}$ cells at 9-h intervals under

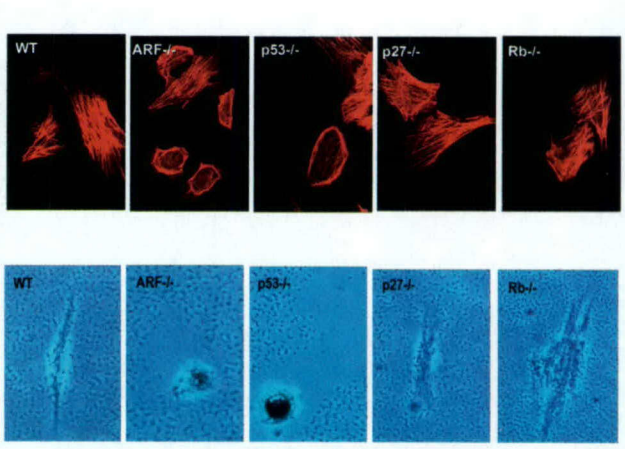

FIG. 1. **The effect of the deletion of p19Arf, p53, p27, or Rb on actin structure and cell motility of primary MEF cells.** 2×10^4 of wild type (*WT*) or knock-out MEF cells ($Arf^{-/-}$, $p53^{-/-}$, $p27^{-/-}$, $Rb^{-/-}$) were cultured overnight on coverglass. Subconfluent cells were starved in medium containing 0.5% serum for 12 h. After fixation in 3.7% formaldehyde, cells were permeabilized with 0.1% Triton X-100 and stained for F-actin by using rhodamine-conjugated phalloidin (*A*). Single cell-based motility was observed 9 h after the cells were plated on colloidal gold-coated culture dishes (*B*).

low serum (0.5% fetal bovine serum) conditions (Fig. 2, *A* and *B*), at which time the difference in cell growth was less than 10%. Similar results were also obtained when the cells were serum-starved over a 16-h period (data not shown). When $p19^{Arf}$ and p53 were reintroduced into $Arf^{-/-}$ and $p53^{-/-}$ cells, respectively, by retroviral induction, the migration phenotype of these cells was fully reversed (Fig. 2, *C* and *D*). The expression levels of p19Arf or p53 in the reconstituted cells were comparable with or slightly higher than that of the respective wild type cells (Fig. 2*E*). Thus, $p19^{Arf}$ and p53 negatively regulate cell migration.

$p19^{Arf}$ and p53 display both interdependent and independent activities in the regulation of cell cycle progression and in response to DNA damage (3). Deletion of both *Arf* and *p53* alleles led to an equally mobile cell phenotype as $p19Arf^{-/-}$ or $p53^{-/-}$ cells in the single cell-based motility assay and in the wound healing assay (Fig. 3*A*). Furthermore, introduction of $p19^{Arf}$ into the $Arf^{-/-}/p53^{-/-}$ cells did not affect cell migration (Fig. 3*A*). It appears that $p19^{Arf}$ acts upstream of p53 in the regulation of cell motility.

p53 functions as a DNA-binding dependent transcription factor in mediating multiple gene activation that is critical to its tumor suppressor activity (22). In addition, p53 is also known for a role in negatively regulating the transcription of an array of genes by repression of their transcription. To begin to address the issue of what function of p53 is required for the regulation of cell motility, we examined the ability of two p53 mutants, Gln^{22}/Ser^{23} and His^{175}, to suppress the migration phenotype of $p53^{-/-}$ cells. Although both mutants are defective in transcriptional regulation of p53-positive genes including that of $p21^{Waf1/Cip1}$ (23–25), the Gln^{22}/Ser^{23} mutation is located in the N-terminal transcription activation domain, which has also been shown to be critical for the binding of TATA-binding protein-associated factors (26, 27), whereas the His^{175} mutation resides in the central DNA binding domain of p53, which is the site of a majority of mutations seen in tumors (28). We observed that the Gln^{22}/Ser^{23} mutant was able to rescue the migration phenotype of $p53^{-/-}$ cells similar to wild type p53, but the His^{175} mutant was inactive (Fig. 3*B*). These results suggest that specific transcription activity controlled by p53 is responsible for the regulation of cell migration by the $p19^{Arf}$-p53 tumor suppressor pathway.

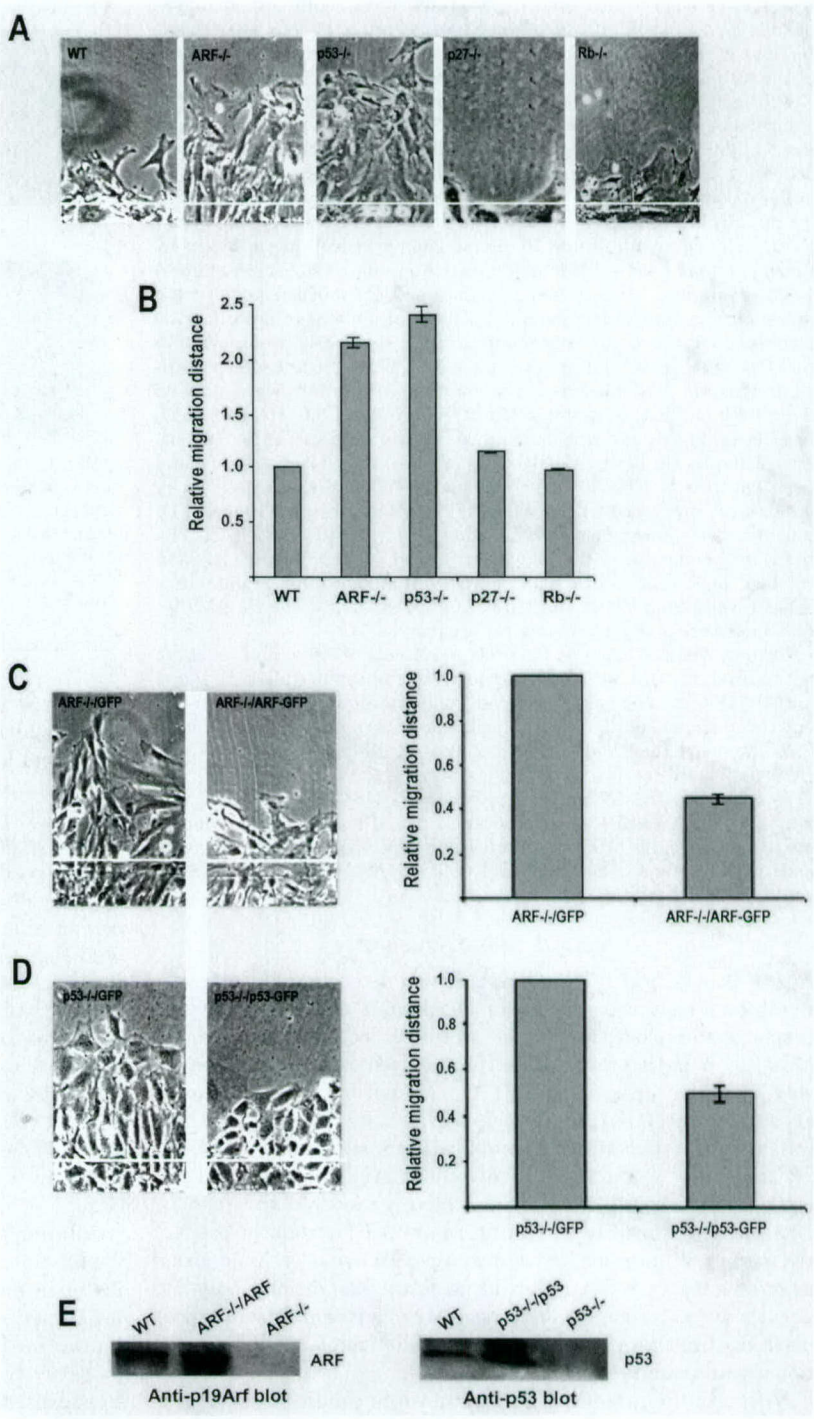

FIG. 2. **MEFs deficient in p19Arf or p53, but not p27 or Rb, display significantly enhanced migration.** *A*, equal numbers of wild type (*WT*) and knock-out cells were seeded on 35-mm dishes and cultured to confluency. Migration into the wound is shown 10 h after the wound was introduced under low serum conditions. *B*, migration distances were determined by taking three independent measurements from each dish. Each experiment was conducted in triplicate, and the mean ± S.D. was calculated. The relative migration distance is normalized to that of wild type. *C* and *D*, the effect of reintroducing $p19^{Arf}$ or p53 to $Arf^{-/-}$ or $p53^{-/-}$ cells on migration. $Arf^{-/-}$ or $p53^{-/-}$ cells were infected with retrovirus expressing GFP, Arf and GFP, or p53 and GFP as indicated. GFP-positive cells were isolated by fluorescence-activated cell sorting and assayed for their relative migration distances. *E*, the expression of p19Arf or p53 in the reconstituted $Arf^{-/-}/Arf$ or $p53^{-/-}/p53$ cells was probed by anti-p53 or anti-p19Arf Western blot.

PI 3-kinase has previously been implicated in the regulation of cell migration (29). To investigate whether PI 3-kinase contributes to $p19^{Arf}$- and p53-regulated cell motility, the endogenous PI 3-kinase activity and phospho-Akt(Ser^{473}) content, which is indicative of the endogenous PI 3-kinase activation status of $Arf^{-/-}$, $p53^{-/-}$, and $Arf^{-/-}/p53^{-/-}$ MEFs, were examined, and the requirement of PI 3-kinase in $p19^{Arf}$- and p53-mediated cell migration was assessed by using specific pharmacological inhibitors wortmannin or LY294002 at defined concentrations. As shown in Fig. 4, *A* and *B*, genetic deletion of *Arf*, *p53*, or *Arf* and *p53* led to 3–5-fold increases in PI 3-kinase activity and phospho-Akt(Ser^{473}), which were readily reversed by the reintroduction of *Arf* or *p53*. The expression levels of p85α and p110, as well as that of Akt, were not altered in these cells (Fig. 4*B*; data not shown). The enhanced PI 3-kinase activities are apparently required for the migration phenotype observed in these cells, because inhibitors of PI 3-kinase (wortmannin or LY294002) caused complete reversion of the migration phenotype without affecting the basal movement of the cells (Fig. 4*C*). Under these conditions, wortmannin or LY294002 potently inhibited PI 3-kinase activity (Fig. 4*C* and data not shown). On the other hand, the expression level of PTEN, a PIP_3 phosphatase that could be transiently regulated by p53 transcriptional activity (30), was not altered in the $Arf^{-/-}$, $p53^{-/-}$, or $Arf^{-/-}/p53^{-/-}$ cells nor in $Arf^{-/-}$ or $p53^{-/-}$ cells that were forced to express *Arf* or *p53* (Fig. 4*D*). We conclude that *Arf* and/or *p53* deletion up-regulates PI 3-kinase activity, resulting in increased cell motility.

Rho family members Rac1, RhoA, and Cdc42 are downstream signaling components of PI 3-kinase and have been

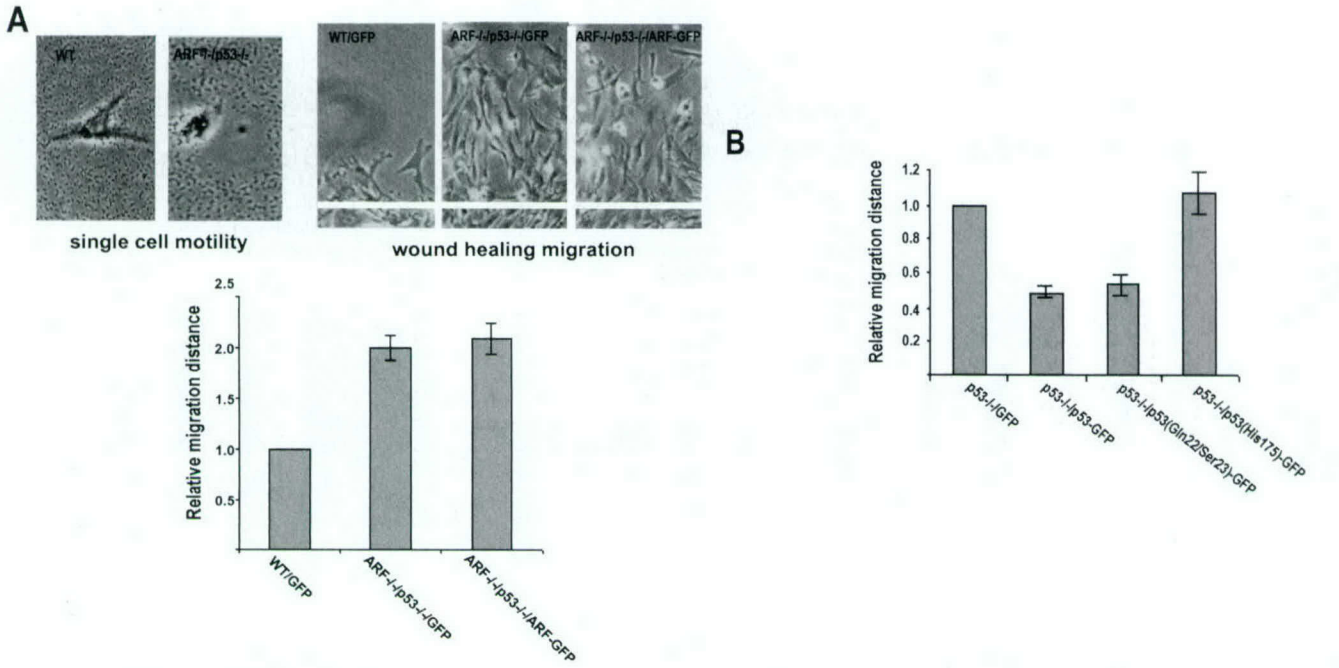

FIG. 3. *A*, $p19^{Arf}$ acts upstream of p53 in the regulation of cell migration. Single cell motility and wound healing migration of $p19Arf^{-/-}/p53^{-/-}$ cells transduced with GFP or GFP with $p19^{Arf}$ were compared with that of the wild type MEFs (*WT*). *B*, a specific transcriptional event(s) is required by p53 to modulate migration. Two mutant forms of p53, p53(Gln^{22}/Ser^{23}) and p53(His^{175}), were compared for their ability to rescue the migration phenotype of $p53^{-/-}$ cells with that of wild type p53.

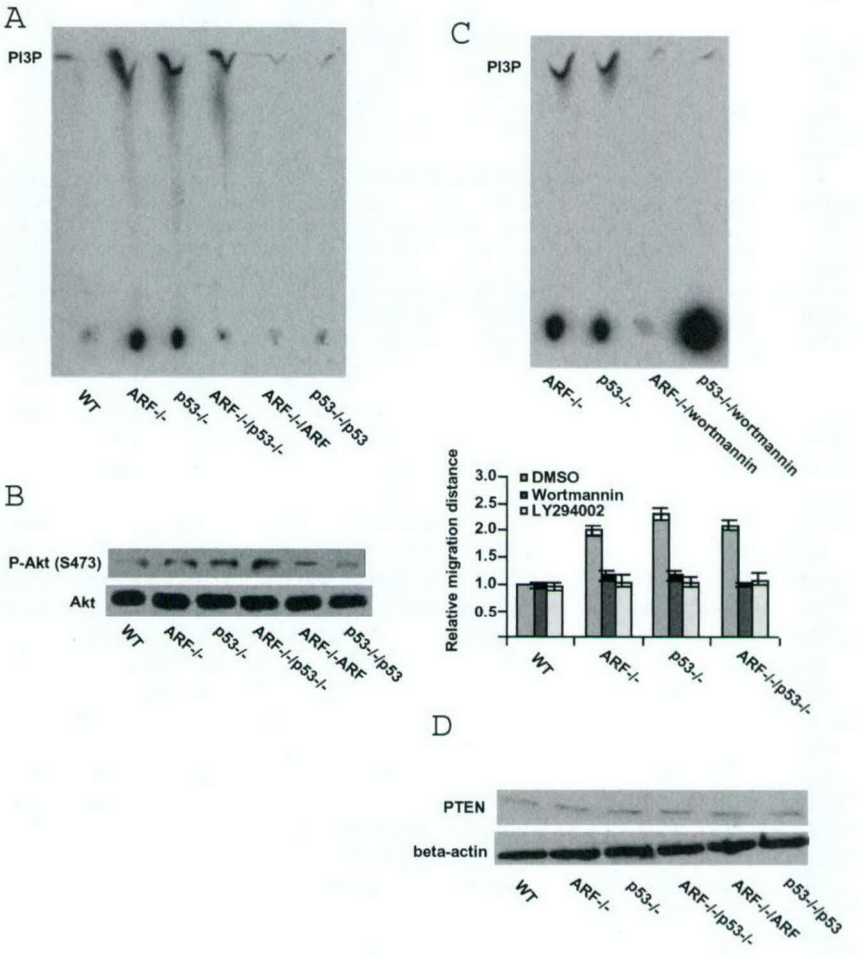

FIG. 4. **PI 3-kinase is required for the $p19^{Arf}$- and p53-regulated cell migration.** *A*, the PI 3-kinase activities of the knock-out or reconstituted cells were assayed. The cells were starved in a medium containing 0.5% serum for 12 h and harvested for anti-p85 immunoprecipitation. The PI 3-kinase activities in the immunoprecipitated fractions were measured by an *in vitro* lipid kinase assay using exogenous phosphatidylinositol as substrate. *WT*, wild type. *B*, log phase cells were starved in 0.5% serum for 12 h. The relative amounts of total Akt and phospho-Akt (*P-Akt* (*S473*)) in the cell lysates containing equal amount of proteins were measured by Western blotting. *C*, PI 3-kinase inhibitors reduced the PI 3-kinase activity and blocked the migration phenotype of $p19^{Arf}$- and/or p53-deficient cells. The cells were treated with 50 nM wortmannin, 20 μM LY294002, or Me_2SO alone for 10 h before the migration distances and the PI 3-kinase activities were measured. *D*, the amount of PTEN and β-actin in the cell lysates containing equal amount of proteins was determined by Western blotting.

implicated in the regulation of cell migration (31). To determine whether these Rho proteins might be involved in $p19^{Arf}$- and p53-regulated migration, we examined the activation status of these Rho proteins in $Arf^{-/-}$ and $p53^{-/-}$ cells by specific effector domain pull-down assays. As shown in Fig. 5*A*, in the absence of serum stimulation, the endogenous levels of GTP-

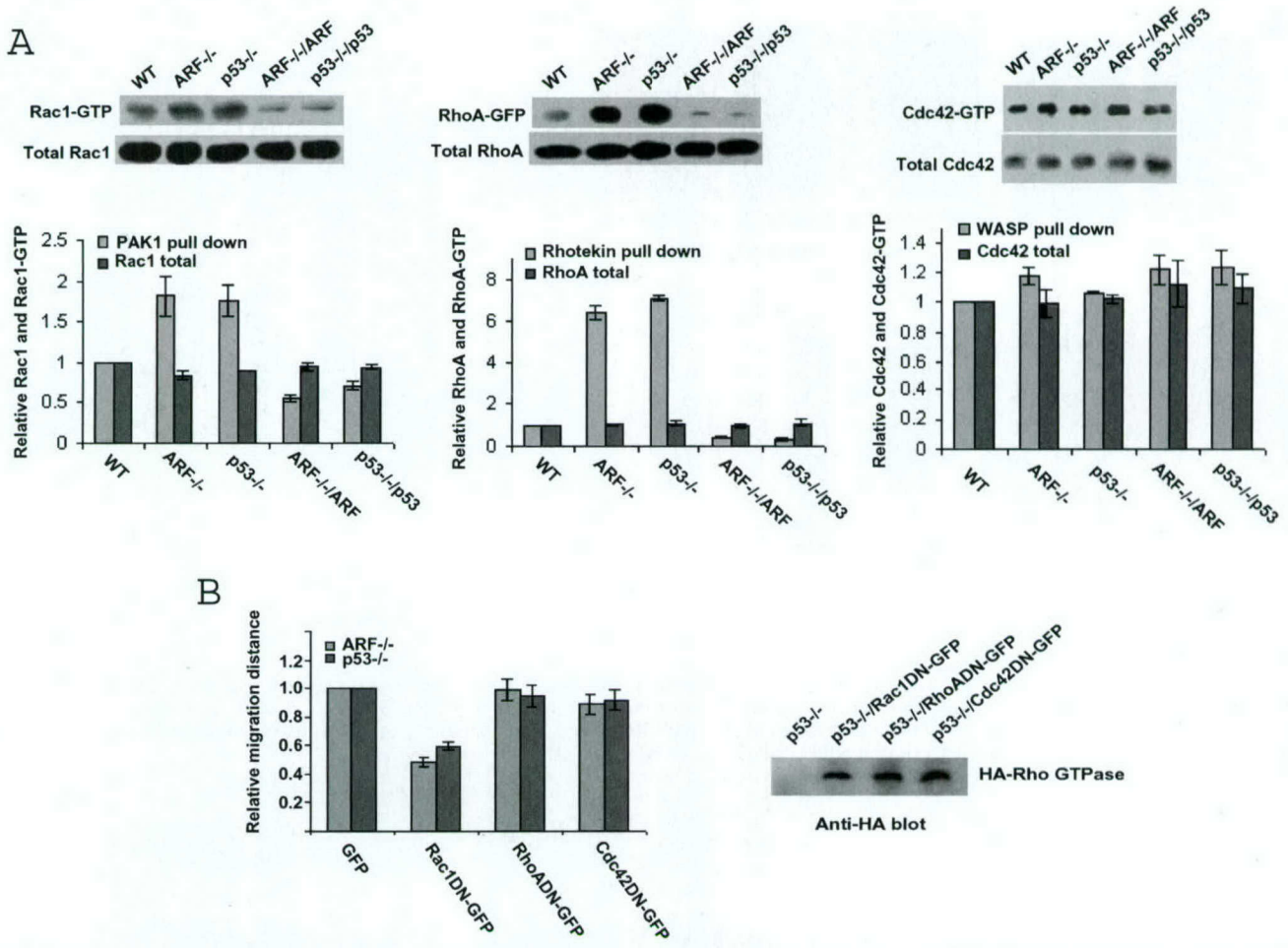

FIG. 5. **Rac1 is an essential mediator of p19^{Arf}- and p53-regulated cell migration.** *A*, endogenous Rac1, RhoA, or Cdc42 activities in the knock-out cells were assayed by using log phase cells that were serum-starved for 12 h prior to lysis and subject to GST-PAK1, GST-Rhotekin, or GST-WASP pull-down analysis. The amount of Rac1-GTP, RhoA-GTP, or Cdc42-GTP was detected by Western blotting of the respective co-precipitates with anti-Rac1, anti-RhoA, or anti-Cdc42 antibody and was normalized to that of the total amount of Rac1, RhoA, or Cdc42 in respect to that in wild type MEFs (*WT*). The results shown in the *lower panels* are means ± S.D. from three experiments. *B*, dominant negative Rac1, but not RhoA or Cdc42, inhibited the migration phenotype of the knock-out cells. GFP or GFP together with Rac1DN-, RhoADN-, or Cdc42DN-expressing primary MEFs was generated by retroviral induction. The amount of the three Rho GTPase mutants (N-terminal hemagglutinin (*HA*)-tagged) expressed in *p53*$^{-/-}$ cells was probed by anti-hemagglutinin Western blot.

bound active Rac1 and RhoA in *p19Arf* $^{-/-}$ or *p53*$^{-/-}$ cells increased by 2- and 6-fold, respectively, compared with those in wild type cells, whereas Cdc42-GTP increased by less than 20%. The Rac1, RhoA, or Cdc42 expression levels were not affected by *p19Arf* or *p53* deletion. When p19Arf or p53 was reintroduced into the knock-out cells, the active Rho protein contents were decreased to the level of wild type cells or lower (Fig. 5*A*), indicating that p19^{Arf} and p53 suppress the Rho protein activities. Furthermore, among the dominant negative mutants of Rac1 (Rac1N17), RhoA (RhoAN19), and Cdc42 (Cdc42N17), only Rac1N17 was able to completely reverse the migration phenotype in both *Arf*$^{-/-}$ and *p53*$^{-/-}$ cells, reducing their migration rates to that of the wild type MEFs, similar to the effect of reintroducing the *Arf* or *p53* gene (Fig. 5*B*). The three Rho GTPase mutants were expressed equally well in the cells (Fig. 5*B*). These results indicate that Rac1 is a specific mediator of p19^{Arf}- and p53-regulated cell migration.

The *p53* and *Rb* genes and their regulatory molecules are central to the growth malfunction of most tumor cells (1). The p19^{Arf}-p53 pathway, specifically, constitutes a checkpoint in cell cycle progression that is responsive to the proliferative signals normally required for cell proliferation (3). Mostly through its transcriptional activity, p53 can inhibit cell cycle progression or induce apoptosis in response to stress or DNA damage. Moreover, p53 is known to be a critical factor in maintaining genomic stability and in eliciting DNA repair reactions (22, 32). Some earlier evidence also pointed to a regulatory role of p53 in transcriptionally activating a number of genes that could be involved in modulating cell movement (8–12). Two recent studies have begun to address the possibility that p53 might contribute to the regulation of cell movement and polarity (14, 15). By genetic deletion of the tumor suppressors, we show that p19^{Arf} and p53, but not p27^{Kip1} or pRb, have a profound negative effect on cell motility and migration. p19^{Arf} likely depends on p53 for migration regulation, and specific transcriptional activity, or specific target genes controlled by p53, may serve as the link between the nuclear events and the cytoskeleton, focal adhesion contacts, or extracellular matrix components to promote the migration phenotype. We are currently examining the candidate gene products whose expression profiles are altered by the p19^{Arf} and p53 deficiencies in an effort to identify the molecule(s) responsible for the observed cellular effects.

The PI 3-kinase-Rac1 signaling module has been known to mediate growth factor-stimulated cell motility (31). Activation of PI 3-kinase (similar to deletion of the PTEN tumor suppressor, which is a PIP_3-specific phosphatase that counter-reacts with many PI 3-kinase effects) can cause activation of both

Rac1 and Akt and contributes to enhanced cell motility and invasion (20, 29). The cell morphological and actin structural changes we have observed in $Arf^{-/-}$ and $p53^{-/-}$ MEFs, *i.e.* a round appearance and intense cortical actin staining, are reminiscent of what was observed in the case of $PTEN^{-/-}$ cells (20), suggesting that elevation of the PIP_3 level in the cells may be significant to increased cell movement. Indeed, Rac1 and Akt appear to be important contributors to the migration phenotype in PTEN deficiency (20, 29). A few previous reports support the assumption that Rac may act independently of Akt in signaling to mammalian cell migration (33, 34), but a recent study employing constitutively active and dominant negative Akt in fibroblasts shows that Akt is an essential mediator of Rac-regulated cell motility stimulated through PI 3-kinase activation (29). In the context of our finding that PI 3-kinase and Rac1 of this module are required for $p19^{Arf}$- and p53-regulated migration, it seems logical that a hierarchical link among them may be at work to transduce signals resulting from the genetic defects of these tumor suppressors to cell activities related to migration, although the detailed relationship among them remains to be determined. The components that serve to further relay signals from Rac1 and/or Akt to cell motility might include PAK, phosphoinositide 5-kinase, and WAVE-like actin polymerization molecules (31, 35).

Gadea *et al.* (15) have recently shown that p53 function is necessary for the suppression of Cdc42-induced filopodia formation and may transcriptionally control the initiating components of filopodia. Although conceptually our observation draws a similar conclusion regarding the negative effect of the Cdc42-mediated cell response imposed by p53, the mechanistic details of our cell motility results may differ from the interpretation of Gadea *et al.* (15), drawn mostly from the Cdc42 and/or p53 overexpression experiments. In the present work, although Rac1 and RhoA activities are shown to be up-regulated by deletion of *Arf* or *p53*, Rac1, but not RhoA nor Cdc42, appears to provide the key functional linkage between the $p19^{Arf}$-p53 pathway and cell motility. However it remains likely that the contributions of Cdc42-mediated cell polarity and RhoA-mediated cell adhesion are an integral part of the $p19^{Arf}$- and p53-regulated cytoskeleton organization and related functional output.

A recent gene array study has identified heparin-binding epidermal growth factor-like growth factor (HB-EGF) as a p53-responsive gene product that could be up-regulated by DNA damage and p53 induction (36). HB-EGF may protect cells from H_2O_2-induced apoptosis through MAPK (mitogen-activated protein kinase) and PI 3-kinase activation, presenting a possible autocrine regulatory loop linking p53 induction with PI 3-kinase and Akt activation. Whether this p53-mediated regulatory pathway is functional in the $p53-/-$ background remains unknown. In light of our finding that *p53* deletion would cause an up-regulation rather than a down-regulation of PI 3-kinase activity, it is likely that the above proposed p53 to HB-EGF to PI 3-kinase pathway might be suppressed by another more dominant component unleashed by *p53* deletion, which preferably stimulates the PI 3-kinase-Rac1-Akt signaling module when the $p19^{Arf}$-p53 pathway is impaired. This possibility is currently under investigation.

In summary, we have demonstrated that the $p19^{Arf}$-p53 tumor suppressor pathway negatively regulates cell motility, revealing an interesting connection between the established tumor suppressor pathway and the PI 3-kinase-Rac1 signaling module that is known to modulate cell migration. The results provide insights into a previously under-appreciated cellular function of the tumor suppressor pathway and may have important implications in developing strategies that target Rho proteins in anti-cancer therapy.

Acknowledgments—We thank members of Zheng laboratory for help with retroviral production and cDNA constructs and Dr. Martine Roussel for the gift of MEFs and Arf cDNA.

REFERENCES

1. Sherr, C. J. (2001) *Nat. Rev. Mol. Cell. Biol.* **2,** 731–737
2. Hahn, W. C., and Weinberg, R. A. (2002) *Nat. Rev. Cancer* **2,** 331–341
3. Sherr, C. J. (1998) *Genes Dev.* **12,** 2984–2991
4. Hall, A. (1998) *Science* **279,** 509–514
5. Bishop, A. L., and A. Hall. (2000) *Biochem. J.* **348,** 241–255
6. Zheng, Y. (2001) *Trends Biochem. Sci.* **26,** 724–732
7. Sahai, E., and Marshall, C. J. (2002) *Nat. Rev. Cancer* **2,** 133–142
8. Comer, K. A., Dennis, P. A., Armstrong, l., Catino, J. J., Kastan, M. B., and Kumar, C. C. (1998) *Oncogene* **16,** 1299–1308
9. Zhao, R., Gish, K., Murphy, M., Yin, Y., Notterman, D., Hoffman, W. H., Tom, E., Mack, D. H., and Levine, A. J. (2000) *Genes Dev.* **14,** 981–993
10. Mukhopadhyay, D., Tsiokas, L., and Sukhatme, V. P. (1995) *Cancer Res.* **55,** 6161–6165
11. Sun, Y., Sun, Y., Wenger, L., Rutter, J. L., Brinckerhoff, C. E., and Cheung, H. S. (1999) *J. Biol. Chem.* **274,** 11535–11540
12. Iotsova, V., and Stehelin, D. (1996) *Cell Growth Differ.* **5,** 629–634
13. Gloushankova, N., Ossovskaya, V., Vasiliev, J., Chumakov, P., and Kopnin, B. (1997) *Oncogene* **15,** 2985–2989
14. Alexandrova, A., Ivanov, A., Chumakov, P., and Vasiliev, J. (2000) *Oncogene* **19,** 5826–5830
15. Gadea, G., Lapasset, L., Gauthier-Rouviere, C., and Roux, P. (2002) *EMBO J.* **21,** 2373–2382
16. Li, R., Debreceni, B., Jia, B., Gao, Y., Tigyi, G., and Zheng, Y. (1999) *J. Biol. Chem.* **274,** 29648–29654
17. Williams, D. A., Tao, W., Yang, F., Kim, C., Gu, Y., Mansfield, P., Levine, J., Petryniak, B., Derrow, C., Harris, C., Jia, B., Zheng, Y., Ambruso, D., Lowe, J., Atkinson, S., Dinauer, M. C., and Boxer, L. (2000) *Blood* **96,** 1646–1654
18. Zindy, F., Eischen, C. M., Randle, D. H., Kamijo, T., Cleveland, J. L., Sherr, C. J., and Roussel, M. F. (1998) *Genes Dev.* **12,** 2424–2433
19. Takaishi, K., Sasaki, T., and Takai, Y. (1995) *Methods Enzymol.* **256,** 336–347
20. Liliental, J., Moon, S. Y., Lesche, R., Mamillapalli, R., Gavrilova, N., Zheng, Y., Sun, H., and Wu, H. (2000) *Curr. Biol.* **10,** 401–404
21. Zheng, Y., Bagrodia, S., and Cerione, R. A. (1994) *J. Biol. Chem.* **269,** 18727–18730
22. Levine, A. J. (1997) *Cell* **88,** 323–331
23. Lin, J., Chen, J., Elenbaas, B., and Levine, A. (1994) *Genes Dev.* **8,** 1235–1246
24. Ryan, K. M., and Vousden, K. H. (1998) *Mol. Cell. Biol.* **18,** 3692–3698
25. Venot, C., Maratrat, M., Sierra, V., Conseiller, E., and Debussche, L. (1999) *Oncogene* **18,** 2405–2410
26. Murphy, M., Ahn, J., Walker, K. K., Hoffman, W. H., Evans, R. M., Levine, A. J., and George, D. L. (1999) *Genes Dev.* **13,** 2490–2501
27. Yun, J., Chae, H. D., Choy, H. E., Chung, J., Yoo, H. S., Han, M. H., and Shin, D. Y. (1999) *J. Biol. Chem.* **277,** 29677–29682
28. Ryan, K. M., Phillips, A. C., and Vousden, K. H. (2001) *Curr. Opin. Cell Biol.* **13,** 332–337
29. Higuchi, M., Masuyama, N., Fukui, Y., Suzuki, A., and Gotoh, Y. (2001) *Curr. Biol.* **11,** 1958–1962
30. Stambolic, V., MacPherson, D., Sas, D., Lin, Y., Snow, B., Jang, Y., Benchimol, S., and Mak, T. W. (2001) *Mol. Cell* **8,** 317–325
31. Ridley, A. J. (2001) *J. Cell Sci.* **114,** 2713–2722
32. Giaccia, A. J., and Kastan, M. B. (1998) *Genes Dev.* **12,** 2973–2983
33. Van Weering, D. H., de Rooij, J., Marte, B., Downward, J. Bos, J. L., and Burgering, B. M. (1998) *Mol. Cell. Biol.* **18,** 1802–1811
34. Welch, H., Eguinoa, A., Stephens, L. R., and Hawkins, P. T. (1998) *J. Biol. Chem.* **273,** 11248–11256
35. Tang, Y., Zhou, H., Chen, A., Pittman, R. N., and Field, J. (2000) *J. Biol. Chem.* **275,** 9106–9109
36. Fang, L., Li, G., Liu, G., Lee, S. W., and Aaronson, S. A. (2001) *EMBO J.* **20,** 1931–1939

MOLECULAR AND CELLULAR BIOLOGY, Feb. 2004, p. 1426–1438 Vol. 24, No. 3
0270-7306/04/$08.00+0 DOI: 10.1128/MCB.24.3.1426–1438.2004
Copyright © 2004, American Society for Microbiology. All Rights Reserved.

Involvement of Rho Family GTPases in p19Arf- and p53-Mediated Proliferation of Primary Mouse Embryonic Fibroblasts

Fukun Guo and Yi Zheng*

Division of Experimental Hematology, Children's Hospital Research Foundation, University of Cincinnati, Cincinnati, Ohio 45229

Received 1 October 2003/Returned for modification 29 October 2003/Accepted 30 October 2003

The Rho family GTPases Rac1, RhoA, and Cdc42 function as molecular switches that transduce intracellular signals regulating gene expression and cell proliferation as well as cell migration. $p19^{Arf}$ and p53, on the other hand, are tumor suppressors that act both independently and sequentially to regulate cell proliferation. To investigate the functional interaction and cooperativeness of Rho GTPases with the $p19^{Arf}$-p53 pathway, we examined the contribution of Rho GTPases to the gene transcription and cell proliferation unleashed by deletion of *p19Arf* or *p53* in primary mouse embryo fibroblasts. We found that (i) $p19^{Arf}$ or p53 deficiency led to a significant increase in PI 3-kinase activity, which in turn upregulated RhoA and Rac1 activities; (ii) deletion of *p19Arf* or *p53* led to an increase in cell growth rate that was in part dependent on RhoA, Rac1, and Cdc42 activities; (iii) $p19^{Arf}$ or p53 deficiency caused an enhancement of the growth-related transcription factor NF-κB and cyclin D1 activities that are partly dependent on RhoA or Cdc42 but not on Rac1; (iv) forced expression of the activating mutants of Rac1, RhoA, or Cdc42 caused a hyperproliferative phenotype of the $p19Arf^{-/-}$ and $p53^{-/-}$ cells and promoted transformation of both cells; (v) RhoA appeared to contribute to p53-regulated cell proliferation by modulating cell cycle machinery, while hyperactivation of RhoA further suppressed a p53-independent apoptotic signal; and (vi) multiple pathways regulated by RhoA, including that of Rho-kinase, were required for RhoA to fully promote the transformation of $p53^{-/-}$ cells. Taken together, these results provide strong evidence indicating that signals through the Rho family GTPases can both contribute to cell growth regulation by *p19Arf* and *p53* and cooperate with *p19Arf* or *p53* deficiency to promote primary cell transformation.

Rho family small GTPases are molecular switches that transduce diverse intracellular signals leading to cell proliferation, gene induction, and survival as well as cytoskeleton remodeling (7, 46). Many mitogenic signals, including those from growth factor receptors and integrins, can promote the exchange of GDP for GTP on Rho GTPases (56), enabling them to interact with an array of effector targets to elicit specific cellular effects (4). Accumulating evidence has implicated Rho GTPases in many aspects of tumor development (5, 37). RhoA, Rac1, and Cdc42 are proto-oncogene products themselves that when hyperactivated can transform fibroblast cells (31–33). Activation of these Rho proteins can stimulate transcriptional activation of some of the critical genes involved in cell growth regulation, such as nuclear factor κB and cyclin D1 and leads to cell cycle progression (49–52). These Rho family members are required for Ras transformation (3, 17, 23, 58), and their deregulation correlates with poor cancer prognosis in some cases (37). Moreover, the Rho GTPases appear to be intimately associated with morphological changes of tumor cells and have been linked to tumor cell migration and invasion through their ability to regulate actin cytoskeleton, cellular-extracellular matrix adhesion, and cell-cell communication (7, 15, 41).

The p53 cell cycle inhibitor and its regulators, including $p19^{ARF}$, are well-established tumor suppressors that are components of a complex signaling network central to tumor suppression (13, 18, 43). Deletion or mutation in p53 or its regulators occurs in many tumor cases and correlates with the onset of a wide spectrum of cancers. p53 is a key transcription factor essential for the response to cellular stress from DNA damage, hypoxia, and oncogene activation. When activated, p53 can trigger cell cycle arrest or apoptosis (2, 18), whereas $p19^{ARF}$ may serve as a sensor to oncogenic insult to stabilize p53 by sequestering Mdm2, a negative regulator of p53 activity (43). The $p19^{ARF}$-p53 tumor suppressor pathway therefore is thought to be primarily involved in monitoring proliferation signals to prevent cells from uncontrolled growth (43). For example, it has been well documented that excess of mitogenic signals can turn on Ras, which in turn transiently stimulates p53 activity to induce cell cycle arrest, apoptosis, or senescence (8, 22, 42).

With appreciation of a central role of the p53 pathway in tumor suppression and the critical involvement of Rho GTPases in cell cycle progression, it seems logical to envision a functional connection and/or cooperation between the p53 pathway and Rho GTPase-mediated signaling processes in tumorigenesis. In particular, we are interested in determining the contribution of Rho family members to cell behaviors in a genetic background bearing defects of p53 or its regulators that might better represent that of tumor cells. Previously, we have shown that the $p19^{Arf}$-p53 pathway negatively modulates PI 3-kinase and Rho GTPase activities and regulates actin cytoskeleton and cell migration through the PI 3-kinase–Rac GTPase signaling module (12). To investigate the potential contribution of Rho GTPases to $p19^{Arf}$- and p53-mediated cell growth control, in the present study we have further charac-

* Corresponding author. Mailing address: Children's Hospital Research Foundation, Experimental Hematology, 3333 Burnet Ave., Cincinnati, OH 55229. Phone: (513) 636-0595. Fax: (513) 636-3768. E-mail: yi.zheng@chmcc.org.

terized the relationship between the p19^{Arf}-p53 tumor suppressor pathway and Rho proteins in regulating cell proliferation and gene expression. The possible cooperative nature of the p19^{Arf}-p53 pathway defect with hyperactive Rho GTPases in inducing cell hyperproliferation and transformation was examined in *p19Arf*- or *p53*-null mouse embryo fibroblasts (MEFs). Moreover, we have examined the contribution of distinct effector pathways emanating from active RhoA to the transformation of p53$^{-/-}$ cells. Our findings strongly indicate that the Rho family GTPases, Rac1, RhoA, and Cdc42, contribute to cell growth regulation through *p19Arf* and *p53* and that mitogenic activation of the Rho proteins may further cooperate with *p19Arf* or *p53* deficiency to promote cell transformation.

MATERIALS AND METHODS

DNA constructs. The Rac1, RhoA, and Cdc42 dominant negative mutants (Rac1N17, RhoAN19, and Cdc42N17), fast-cycling mutants (Rac1L28, RhoAL30, and Cdc42L28), and constitutively active mutants (Rac1L61, RhoAL63, and Cdc42L61) and the effector domain mutants of RhoA in the constitutively active backbone (RhoAL63-V39, RhoAL63-T40, RhoAL63-L40, and RhoAL63-C42) were generated by site-directed mutagenesis based on oligonucleotide-mediated PCR (19). For retroviral expression, cDNAs encoding the dominant negative, fast-cycling, and constitutively active forms of Rac1, RhoA, and Cdc42, the effector domain mutants of RhoA, and ROCKI were ligated into the *Bam*HI and *Eco*RI sites in frame with the nucleotides encoding a three-hemagglutinin (HA_3) tag at the 5′ end of the retroviral vector MIEG3 that expresses enhanced green fluorescent protein bicistronically. The constructs expressing *p19Arf* and *p53* were described previously (57).

Cell culture and retroviral induction. Primary wild type, *p53*$^{-/-}$ and *p19Arf*$^{-/-}$ MEFs were kind gifts from Martine Roussel (St. Jude, Memphis, Tenn.) that were derived from mouse embryos of the C57BL/6 × 129/sv genetic background (57) and were cultured in Dulbecco's modified Eagle's medium with 10% fetal bovine serum, 2 mM glutamine, 0.1 mM nonessential amino acids, 55 μM β-mercaptoethanol, and 10 μg of gentamicin/ml. Recombinant retroviruses were produced using the Phoenix cell packaging system (11, 12). Primary MEFs were infected with the respective retroviruses and harvested 48 to 72 h postinfection. The enhanced green fluorescent protein-positive cells were isolated by fluorescence-activated cell sorting (FACS).

Immunoblotting. Whole-cell lysates were prepared by extraction of the MEF cells by the lysis buffer containing 20 mM Tris-HCl (pH 7.6), 100 mM NaCl, 10 mM $MgCl_2$, 1% Triton X-100, 0.2% sodium deoxycholate, 2 mM phenylmethylsulfonyl fluoride, 10 μg of leupeptin/ml, 10 μg of aprotinin/ml, and 0.5 mM dithiothreitol for 30 min. The nuclear proteins were purified by the method described before (14). Briefly, cells were washed in a hypotonic buffer (HB; 25 mM Tris-HCl [pH 7.6], 1 mM $MgCl_2$, 5 mM KCl) and lysed in HB containing 0.25% Nonidet P-40, 2 mM phenylmethylsulfonyl fluoride, 10 μg of leupeptin/ml, and 10 μg of aprotinin/ml for 30 min. The lysates were centrifuged at 500 × *g* for 5 min. The nuclear pellet was washed with HB containing 2 mM phenylmethylsulfonyl fluoride, 10 μg of leupeptin/ml, and 10 μg of aprotinin/ml, resuspended in a solution containing 20 mM Tris-HCl (pH 8.0), 0.42 M NaCl, 1.5 mM $MgCl_2$, and 25% glycerol, vortexed, and incubated at 4°C for 30 min. The extracts were centrifuged at 900 × *g* for 5 min, and the supernatants were taken as the nuclear protein lysates. Protein contents in the whole-cell lysates and nuclear lysates were normalized by the Bradford method. The lysates were separated by 10% sodium dodecyl sulfate (SDS)-polyacrylamide gel electrophoresis. The ectopic expression of the dominant negative, the fast-cycling, or the constitutively active forms of Rac1, RhoA, and Cdc42 were probed by using an anti-HA antibody (Boehringer Mannheim). NF-κB and cyclin D1 from the nuclear extracts were probed by using the anti-NF-κB p65 and anti-cyclin D1 antibodies (Santa Cruz Biotechnology), respectively.

Endogenous Rho GTPase activity assay. Glutathione *S*-transferase (GST)–PAK1, GST-Rhotekin, and GST-WASP, which contain Rac1, RhoA, and Cdc42 interactive domains of PAK1, Rhotekin, and WASP, respectively, were used to probe the endogenous Rac1-GTP, RhoA-GTP, and Cdc42-GTP activities by the affinity precipitation method as previously described (20).

PI 3-kinase assay. The endogenous PI 3-kinase activities of *Arf*$^{-/-}$, *p53*$^{-/-}$, and *Arf*$^{-/-}$ or *p53*$^{-/-}$ cells reconstituted with *Arf*, *p53*, or Rho protein mutants, respectively, were assayed according to a described protocol (12). Briefly, the cells were lysed in buffer A, containing 20 mM Tris-HCl (pH 8.0), 100 mM NaCl, 1 mM EDTA, 0.3 mM dithiothreitol, 0.5 mM phenylmethylsulfonyl fluoride, 1% Triton X-100, 10 μg of aprotinin/ml, 10 μg of leupeptin/ml, 0.1 mM sodium orthoranadate, and 25 mM NaF. After centrifugation at 4°C for 30 min at 14,000 rpm, the protein contents in the supernatant of cell lysates were measured by the Bradford method. Equal amounts of protein were incubated with anti-p85 polyclonal antibody coupled to protein A-agarose (Upstate Biotech., Inc.) overnight or subjected to anti-p85 Western blot analysis. The immunoprecipitates were washed twice with buffer C, containing 20 mM Tris-HCl (pH 8.0) 100 mM NaCl, and 10 mM $MgCl_2$ and washed once with a kinase assay buffer (20 mM Tris-HCl [pH 7.6], 10 mM $MgCl_2$). Five micrograms of sonicated phosphatidylinositol (PI) together with [γ-^{32}P]ATP (200 μCi/ml) in 45 μl of the kinase assay buffer was incubated with the washed beads at 25°C for 10 min. The reactions were terminated by the addition of 100 μl of 1 N HCl. The reaction products were extracted by 200 μl of $CHCl_3$–MeOH (1:1) and resolved on a thin-layer chromatographic silica plate coated with potassium oxalate in a solvent containing $CHCl_3$–MeOH–4 M NH_4OH (9:7:2). The PI kinase reactions were analyzed by autoradiography. The anti-p85 of PI 3-kinase antibody was obtained from Upstate Biotechnology, Inc., and the PI 3-kinase inhibitor wortmannin was obtained from Sigma.

Cell proliferation assay. Cell growth rates were measured by a [^{3}H]thymidine incorporation assay. Cells were cultured in a medium containing 2% serum for the assays. The cell cultures were assayed at 0, 1, 2, 3, and 4 days after the addition of 1 μCi of [^{3}H]-thymidine/ml to the medium followed by an incubation for 4 h at 37°C. The cells were harvested by trypsinization, and the [^{3}H]-thymidine incorporated into the cells was quantified by scintillation counting.

Luciferase reporter assay. To detect endogenous NF-κB and cyclin D1 gene expression, the luciferase reporter constructs fused with the promoter of NF-κB or cyclin D1 (Stratagene) that contain the promoter response elements of NF-κB and cyclin D1 were used to report transiently the relative activities of NF-κB and cyclin D1. Transient transfection of these reporter plasmids into primary MEFs was carried out using LipofectAMINE reagents (Invitrogen) according to the manufacturer's protocols. Twenty-four hours prior to harvesting, the cells were switched to a medium containing 0.5% serum. Analysis of luciferase and β-galactosidase activities of the transfected cells was performed by using a luciferase assay kit (Promega). Transfection efficiencies were routinely corrected by obtaining the ratio of the luciferase and the β-galactosidase activities observed in the same sample, as previously described (26).

Cell cycle progression and apoptosis analysis. Cell cycle progression of the p53$^{-/-}$ MEFs was monitored by cell cycle marker staining (propidium iodide labeling and Cytofix/Cytoperm fixation) followed by flow cytometry (phosphatidylethanolamine-conjugated anti-BrdU antibody) to examine whether dominant negative or constitutively active RhoA could affect the G_1/S phase and/or G_2/M phase transition in a p53-independent manner (11). The effects of RhoA mutants on p53-independent apoptotic response were tested by apoptosis staining of the p53$^{-/-}$ MEFs after DNA damage induction by gamma irradiation (20 Gy). The apoptotic cell population was revealed by 7AAD and allophycocyanin-conjugated Annexin V staining followed by flow cytometry analysis on a FACSCaliber machine (11).

Cell transformation assay. To determine the transforming activity of the *p53*$^{-/-}$ or *p19Arf*$^{-/-}$ MEF cells, 5,000 cells that stably express various fast-cycling or constitutively active mutants of Rac1, RhoA, or Cdc42 were combined with 5 × 10^4 parental *p53*$^{-/-}$ or *p19Arf*$^{-/-}$ cells. The cell cultures were fed every 2 days with fresh culture medium. Fourteen days postplating, foci were scored after fixation and staining of the cells on the plates.

RESULTS

p19Arf and p53 regulate PI 3-kinase, which in turn regulates Rho GTPase activities. Previously, we found that the endogenous PI 3-kinase, RhoA, and Rac1 activities were elevated in the *Arf*$^{-/-}$ and *p53*$^{-/-}$ primary MEF cells and that the PI 3-kinase and Rac1 activities were required for a fast-migration phenotype of the *Arf*$^{-/-}$ and *p53*$^{-/-}$ cells. Reintroduction of the wild-type *Arf* or *p53* gene into *Arf*$^{-/-}$ or *p53*$^{-/-}$ cells reversed the PI 3-kinase and Rho GTPase activities as well as the migration phenotype, indicating that p19^{Arf} and p53 negatively regulate cell migration by suppression of PI 3-kinase and Rac1 activities (12). To further dissect the relationship between PI 3-kinase and Rho GTPases in the *p19Arf*$^{-/-}$ and

p53$^{-/-}$ cells, we measured the Rac1, RhoA, and Cdc42 activities in the *Arf*$^{-/-}$ and *p53*$^{-/-}$ MEFs with or without the PI 3-kinase inhibitor (wortmannin) treatment. As shown in Fig. 1A, wortmannin (50 nM) treatment of the *Arf*$^{-/-}$ and *p53*$^{-/-}$ MEFs resulted in markedly decreased Rac1-GTP and RhoA-GTP species, to a level similar to that in the *Arf*- or *p53*-reconstituted cells or the wild-type cells (Fig. 1A). As we have observed previously, the Cdc42-GTP level was not significantly affected by the deletion of the *Arf* or *p53* gene, nor was it changed upon wortmannin treatment or *Arf* or *p53* reconstitution (Fig. 1A). On the other hand, the elevated endogenous PI 3-kinase activity in the *p53*$^{-/-}$ cells (compared with that of the wild-type MEFs) was not significantly altered by the expression of dominant negative Rac1N17, RhoAN19, or Cdc42N17 or by the fast-cycling Rac1L28, RhoAL30, or Cdc42L28 mutant, contrary to the effect of the reconstitution of wild-type p53 (Fig. 1B). Similarly, the dominant negative Rho protein mutants had no effect on the PI 3-kinase activity of the *Arf*$^{-/-}$ cells (data not shown). These results indicate that PI 3-kinase acts downstream of *p19Arf* or *p53* but upstream of Rho proteins to regulate cell behaviors.

Rho GTPases contribute to the growth phenotype of p19Arf$^{-/-}$ and p53$^{-/-}$ cells. p19^{Arf} and p53 are checkpoint molecules that upon overexpression can induce cell cycle arrest or apoptosis (43). Deletion of *Arf* or *p53* resulted in a significant increase in cell growth rate and saturation density (Fig. 2). Since the *Arf*$^{-/-}$ and *p53*$^{-/-}$ cells contained elevated levels of active Rho GTPase species (Fig. 1A), we examined whether Rac1, RhoA, or Cdc42 might contribute to the proliferative phenotype of these cells. As shown in Fig. 2, the increased cell growth rates due to *p19Arf* or *p53* deletion were partially inhibited by the dominant negative Rac1N17, RhoAN19, and Cdc42N17 mutants to various degrees under conditions at which the growth rate of wild-type MEFs was not significantly affected by these mutants. The expression levels of the dominant negative Rho mutants were comparable in these cells (12; data not shown), and the dominant negative inhibitory effects of Rac1N17, RhoAN19, and Cdc42N17 were specific toward the respective Rho proteins, as assayed by the effector domain pull-down assays (Fig. 2B). Although Cdc42 activity was not detectably upregulated by the *Arf* or *p53* deficiency (Fig. 1A), the fact that Cdc42N17 could partially inhibit the growth phenotype of the *Arf*$^{-/-}$ and *p53*$^{-/-}$ cells suggests either that the effector probe (the p21-binding domain of WASP) used in the activity assay was not sensitive enough or that basal Cdc42 activity is required for the *Arf* or *p53* defect-mediated growth. These results indicate that part of the growth stimulatory signals unleashed by *p53* or *p19Arf* deletion are mediated through the Rho family members.

Involvement of Rho GTPases in NF-κB and cyclin D1 activation induced by p19Arf or p53 deficiency. Transcription factor NF-κB has been shown to be functionally interconnected with p53 (36, 48). Since NF-κB is regulated by the Rho family GTPases and could mediate cell growth regulation by the Rho proteins (14, 29, 52), we determined the effect of *p19Arf* or *p53* deletion on the activity and expression of NF-κB and examined the contribution of Rac1, RhoA, and Cdc42 to its modulation in the *Arf*- or *p53*-null background. The *p19Arf*$^{-/-}$ and *p53*$^{-/-}$ cells were transiently transfected with the NF-κB-luciferase reporter plasmid that contains the promoter response elements of NF-κB, and the relative luciferase activities were compared with that of wild-type MEFs and that of *Arf*$^{-/-}$ or *p53*$^{-/-}$ cells reconstituted with the respective tumor suppressor genes. The NF-κB transcriptional activity was upregulated by *p19Arf* and *p53* deletions by ~3.5- and ~5.5-fold, respectively, and the observed activity changes were completely reversed when the *Arf* or *p53* gene was reintroduced into the knockout cells (Fig. 3A). These results demonstrate that p19^{Arf} and p53 negatively regulate NF-κB activity. To address whether the Rho proteins contribute to NF-κB regulation in *Arf*$^{-/-}$ and *p53*$^{-/-}$ cells, we transduced the dominant negative mutants of Rac1, RhoA, and Cdc42 (Rac1N17, RhoAN19, and Cdc42N17, respectively) as well as the GFP marker into the mutant cells and assayed the NF-κB reporter activities of these cells. Rac1N17 and Cdc42N17 had no detectable effect on the elevated reporter activities of NF-κB in *Arf*$^{-/-}$ and *p53*$^{-/-}$ cells (Fig. 3B), nor did they show significant inhibition of the increased nuclear expression level of NF-κB in these cells (Fig. 3C). In comparison, RhoAN19 attenuated the NF-κB activity and its nuclear expression level in *p53*-deficient cells but not in *p19Arf*-deficient cells (Fig. 3B and C). The dominant negative Rac1N17, RhoAN19, and Cdc42 N17 mutants were expressed similarly in these MEFs (12) and displayed various degrees of inhibition on the respective Rho protein activity and cell growth (Fig. 2). Moreover, Rac1N17 reversed the migration phenotype of these cells (14), indicating that these dominant negative Rho mutants were functionally expressed. These results suggest that RhoA participates in NF-κB regulation by p53 but that Rac1 and Cdc42 do not contribute to the upregulation of its activity, due to *p19Arf* or *p53* defects.

Cyclin D1 has been suggested as one of the key downstream effectors that mediate cell growth control by the Rho GTPases (49, 50, 51, 58). Deletion of *p19Arf* and *p53* resulted in significant upregulation of cyclin D1 activity (~3- and ~11-fold, respectively) and nuclear expression (Fig. 4A and C). Reconstitution of *p19Arf* and *p53* into the respective mutant cells readily reversed the cyclin D1 activity (Fig. 4A), indicating that both p19^{Arf} and p53 negatively regulate its activity. Since Rac1, RhoA, and Cdc42 can each stimulate cyclin D1 activation and deletions of *p19Arf* and *p53* result in activation of the Rho protein activities, we examined the possible involvement of the Rho GTPases in cyclin D1 regulation by *Arf* and *p53*. Transduction of dominant negative RhoA and Cdc42 in *Arf*$^{-/-}$ and *p53*$^{-/-}$ cells partially inhibited cyclin D1 at both the activity and the nuclear expression levels, whereas dominant negative Rac1 had no detectable effect (Fig. 4B and C). These results provide evidence that RhoA and Cdc42 but not Rac1 are involved in cyclin D1 regulation by p19^{Arf} and p53. It is therefore possible that RhoA and Cdc42 work through NF-κB and/or cyclin D1 modulation to contribute to the growth phenotype of the *p19Arf*$^{-/-}$ and *p53*$^{-/-}$ cells, while Rac1 adopts a distinct, NF-κB- and cyclin D1-independent pathway to influence *p19Arf*$^{-/-}$ and *p53*$^{-/-}$ cell growth.

Active Rho GTPases cooperate with p19Arf or p53 deletion to promote hyperproliferation and transformation. Since Rac1, RhoA, and Cdc42 appear to contribute to the growth regulation of *p19Arf*$^{-/-}$ and *p53*$^{-/-}$ cells, we next asked if hyperactive Rho proteins could further stimulate the proliferation of these cells. For this purpose, we introduced a set of

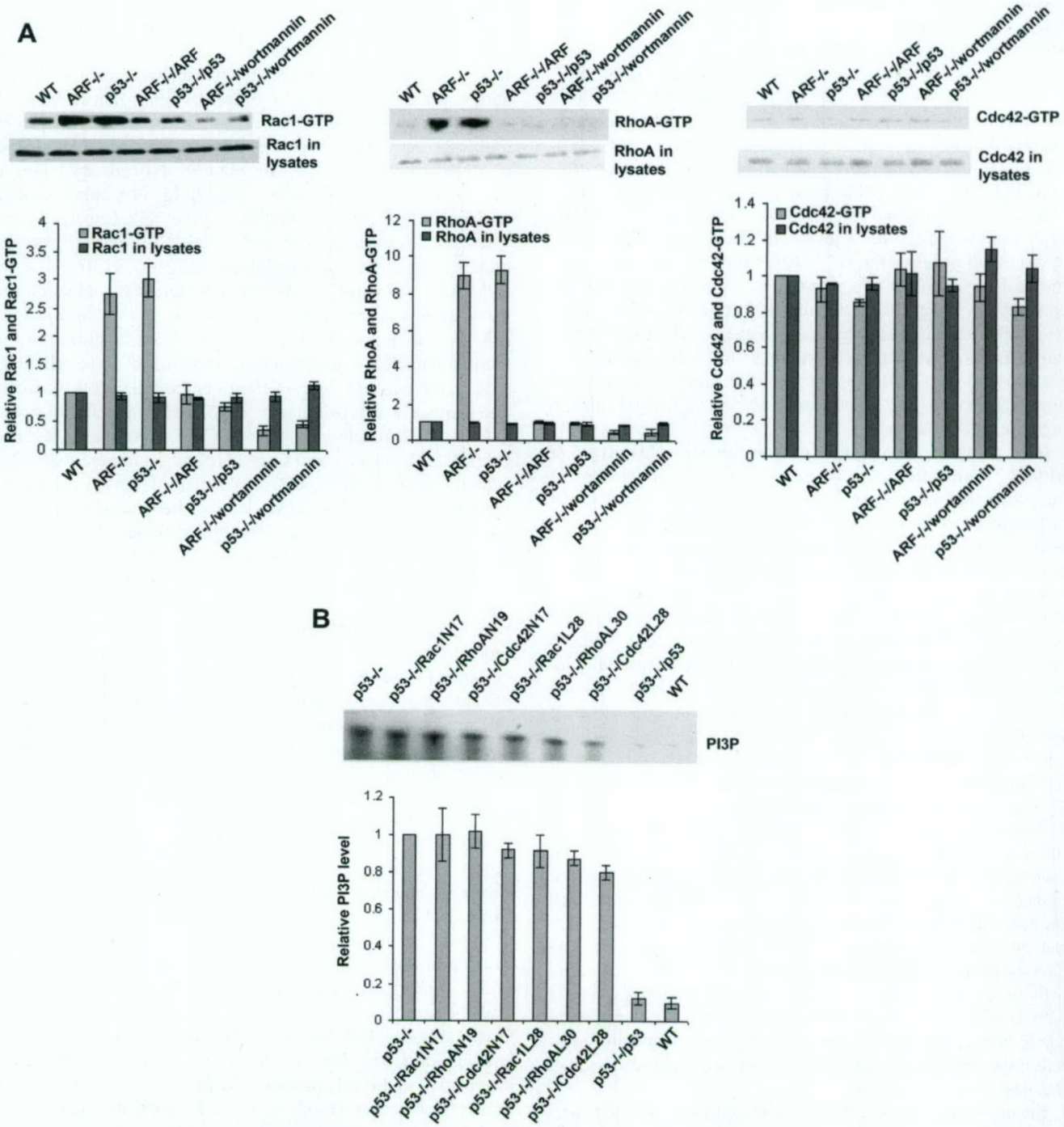

FIG. 1. Activation of Rac1 and RhoA by the p19^{Arf} or p53 defect is dependent on elevated PI 3-kinase activity. (A) The endogenous Rac1, RhoA, or Cdc42 activities in the *Arf* or *p53* knockout and reconstituted cells with or without wortmannin (50 nM) treatment were assayed by using log phase cells that were serum starved for 12 h. The lysates were subject to GST-PAK1, GST-Rhotekin, or GST-WASP pull-down analysis. The amount of Rac1-GTP, RhoA-GTP, or Cdc42-GTP was detected by Western blotting of the respective glutathione-agarose coprecipitates with anti-Rac1, anti-RhoA, or anti-Cdc42 antibody and was normalized to that of Rac1, RhoA, or Cdc42 in wild-type (WT) MEFs. The results are shown as the means ± the standard deviations of three experiments. (B) The PI 3-kinase activities of the *Arf* or *p53* knockout and reconstituted cells of the log phase cells were assayed. The cells were starved in a medium containing 0.5% serum for 12 h and harvested for anti-p85 immunoprecipitation. The PI 3-kinase activities in the immunoprecipitates were measured by an in vitro lipid kinase assay using exogenous PI as the substrate. The PI3P signals of various MEFs were normalized to those of the $p53^{-/-}$ MEFs in the quantification.

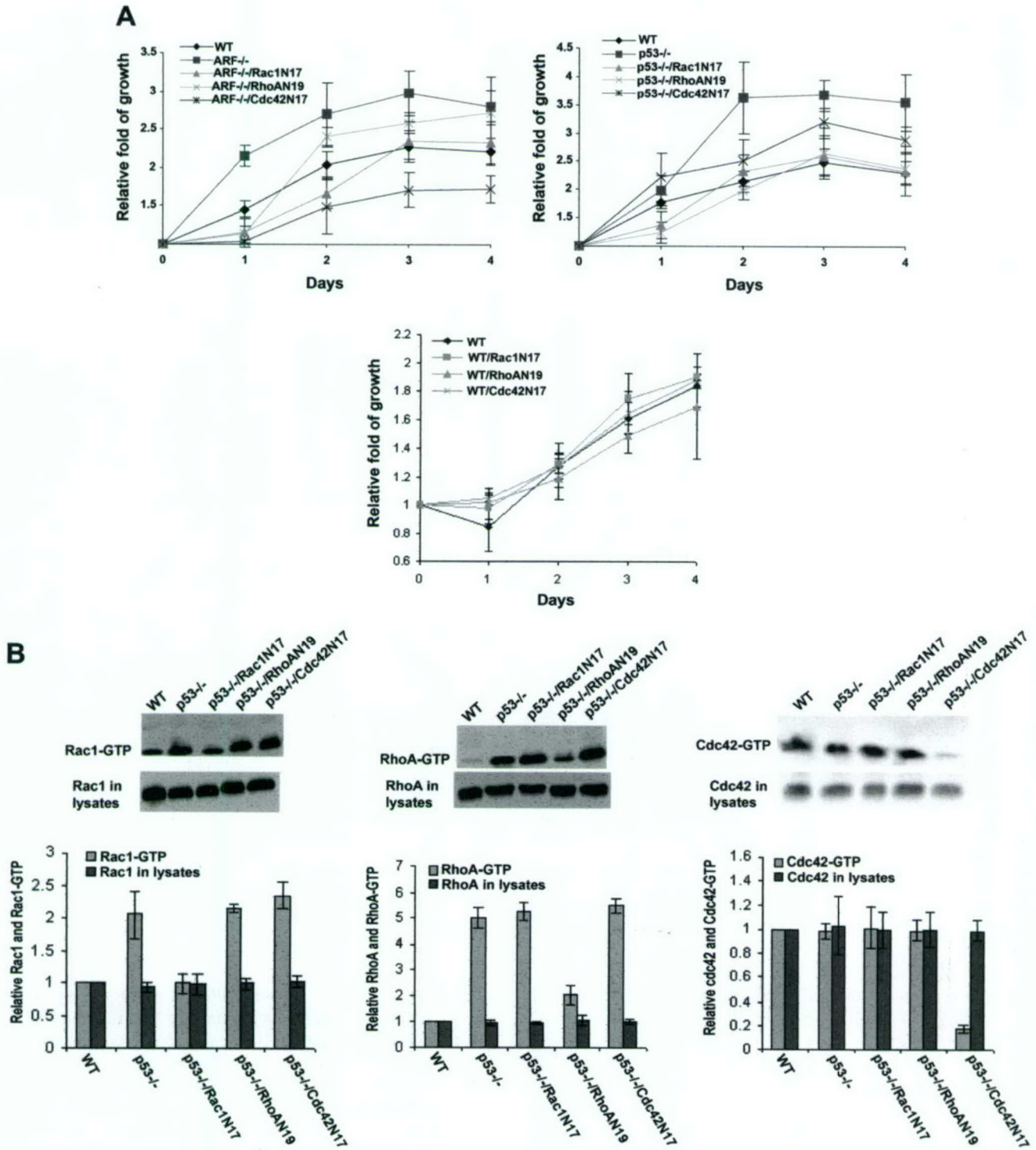

FIG. 2. Rac1, RhoA, and Cdc42 contribute to the growth regulation of *p19Arf*- or *p53*-null cells. The dominant negative mutants of Rho proteins were expressed in the $Arf^{-/-}$ or $p53^{-/-}$ MEFs by retroviral induction, and the Rho mutant-expressing cells were isolated by FACS. (A) Five thousand cells/well of the indicated cells were plated in 1-ml culture medium containing 5% fetal bovine serum on 24-well plates. At the time points of day 0, 1, 2, 3, and 4, incorporation of [^{3}H]thymidine into the cells was measured. Data are representative of three independent experiments and are expressed as the fold of growth relative to the respective value at day 0. Error bars represent the standard deviations of four repeats of one experiment. (B) Western blots of the endogenous Rac1, RhoA, and Cdc42 in the GTP-bound state were performed after the respective GST-effector domain pull-downs in the wild-type (WT) MEFs, p53-deficient MEFs, and p53-deficient MEFs expressing various dominant negative mutants of Rh proteins. The amounts of each Rho protein in the respective cell lysates and in the GTP-bound form were normalized to that of Rac1, RhoA, or Cdc42 in WT MEFs.

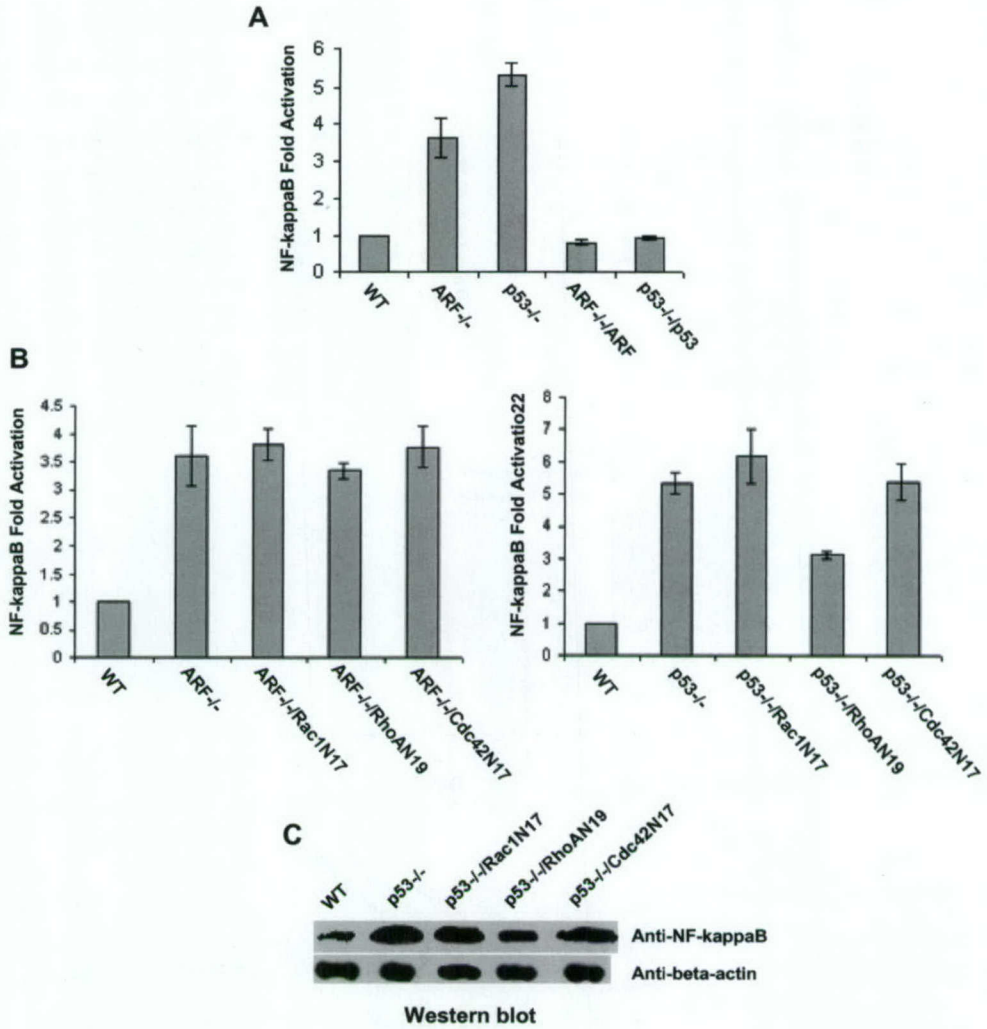

FIG. 3. Involvement of Rac1, RhoA, and Cdc42 in NF-κB activation induced by *p19Arf* or *p53* deletion. The NF-κB promoter-driven luciferase reporter was transiently expressed in the indicated MEF cells together with a vector expressing *Arf*, *p53*, or dominant negative mutants of Rho GTPases (A and B). After a 30-hour recovery followed by a 12-hour starvation, the luciferase activities in the cells were measured. The luciferase activities were expressed as the fold of activation relative to the activity induced by the empty vector alone in the wild-type (WT) cells and were normalized to an internal transfection control (β-galactosidase coexpressed with pCMV vector). To detect NF-κB protein levels (C), nuclear extracts containing 20 μg of proteins were separated by 10% SDS-polyacrylamide gel electrophoresis and the amount of NF-κB present was probed by anti-NF-κB p65 antibody. Anti-beta actin blotting was carried out in parallel as a loading control.

fast-cycling mutants of Rac1, RhoA, and Cdc42 (Rac1L28, RhoAL30, and Cdc42L28, respectively), which possess an increased intrinsic rate of exchange of GDP by GTP-mimicking mitogenic stimulation (21, 53), into the *p19Arf*$^{-/-}$ or *p53*$^{-/-}$ cells. The expression of Rac1L28, RhoAL30, and Cdc42L28 were confirmed by Western blot analysis (Fig. 5A). As shown in Fig. 5B, these fast-cycling Rho GTPase mutants were able to further enhance the growth rates of *p19Arf*$^{-/-}$ and *p53*$^{-/-}$ cells to various extents under conditions in which they had only minor effects on wild-type MEF growth, suggesting that active Rho proteins can cooperate with p19^{Arf} and p53 defects to promote hyperproliferation of the cells.

Oncogenic Ras was able to cooperate with *p19Arf* or *p53* deletion to promote MEF transformation in vitro and in vivo (16). Because Rac1, RhoA, and Cdc42 are all important downstream mediators of Ras signaling (17, 31–33), we wondered if the hyperactive Rho proteins could be sufficient to promote *Arf*$^{-/-}$ and *p53*$^{-/-}$ cell transformation. For this purpose, in addition to the fast-cycling Rho protein mutants, we generated *Arf*$^{-/-}$ and *p53*$^{-/-}$ primary MEFs expressing the constitutively active forms of Rac1, RhoA, and Cdc42 (Rac1L61, RhoAL63, and Cdc42L61, respectively). These mutants expressed equally well in the *p53*$^{-/-}$ cells (Fig. 6A) and in the *p19Arf*$^{-/-}$ cells (data not shown). Both forms of the activating Rac1, RhoA, and Cdc42 mutants, i.e., the fast-cycling and the constitutively active forms, displayed various foci-forming activity in *p53*$^{-/-}$ MEFs as well as in *p19Arf*$^{-/-}$ MEFs (Fig. 6B). Some of these mutants, e.g., RhoAL63, displayed activities as potent as that of oncogenic Ras, while others, such as Rac1L61, was only weakly transforming (Fig. 6B). Thus, like oncogenic Ras, active Rac1, RhoA, or Cdc42 can cooperate with *p53* or *p19Arf* deletion to promote primary cell transformation.

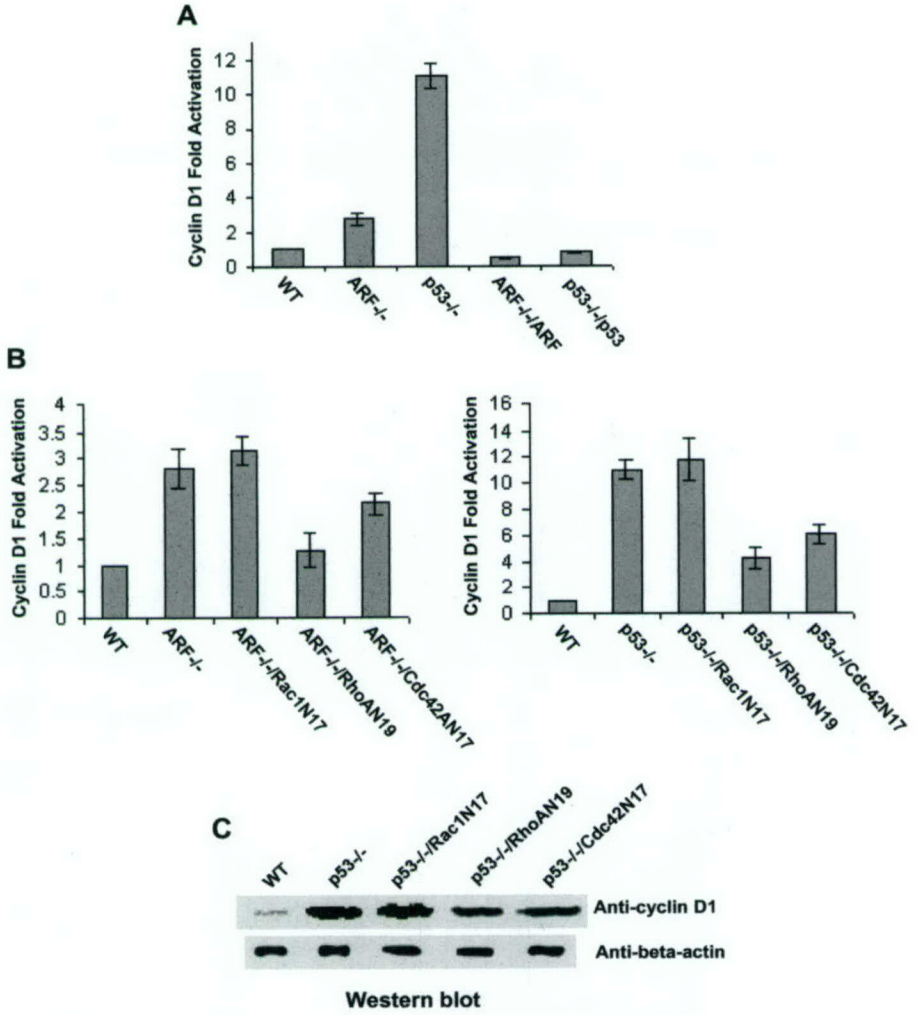

FIG. 4. Contribution of Rac1, RhoA, and Cdc42 to cyclin D1 regulation in *p19Arf*- or *p53*-deficient MEF cells. One microgram of cyclin D1-luciferase reporter plasmid was cotransfected with a vector expressing *Arf*, *p53*, or the dominant negative mutants of the Rho proteins into the indicated cells. The luciferase activities in the cell lysates were measured to determine the relative cyclin D1 transcriptional activities (A and B) and were normalized to those of a β-galactosidase transfection control. To directly compare the protein levels of cyclin D1, nuclear extracts containing 20 μg of proteins were separated by 10% SDS-polyacrylamide gel electrophoresis and the amount of cyclin D1 was probed with an anti-cyclin D1 antibody (C). Anti-beta actin blotting was done in parallel. WT, wild-type.

RhoA signaling modulates cell cycle progression and apoptotic response of p53-null cells. To further address the role of Rho in p53-mediated cell proliferation, we carried out a set of experiments comparing the cell cycle and apoptotic properties of $p53^{-/-}$ MEFs expressing the fast-cycling active mutant of RhoA or dominant negative mutant of RhoA. As shown in Fig. 7A, when the cell cycle progression of wild-type and p53−/− MEFs was analyzed by PI staining followed by FACS, the dominant negative RhoA mutant was found to effectively extend the G_1 phase and suppress the G_2/M phase of $p53^{-/-}$ MEFs that were altered due to a p53 defect, whereas the active RhoA mutant did not significantly alter the relative phases of the cell cycle. Moreover, p53 deficiency led to a decrease in the cellular apoptotic response to gamma irradiation compared with that of wild-type cells, which could be further suppressed by the expression of the active RhoA mutant (Fig. 7B). These results indicate that RhoA may contribute to p53-regulated cell proliferation by modulating cell cycle progression and that RhoA activation may cause hyperproliferation of $p53^{-/-}$ cells by further suppressing a p53-independent apoptotic signal.

Multiple pathways regulated by RhoA are involved in promoting transformation of $p53^{-/-}$ MEFs. To begin to unveil the molecular pathways regulated by Rho GTPases that are important for promoting transformation of $p53^{-/-}$ cells, we next examined the involvement of a key effector of RhoA, ROCK, in RhoA-mediated transformation. As shown in Fig. 8A, treatment of the RhoAL63-expressing $p53^{-/-}$ MEFs with a ROCK inhibitor, Y27632, led to a partial inhibition of the foci-forming activity elicited by RhoAL63, and ectopic expression of ROCKI in $p53^{-/-}$ cells was able to only partially recapitulate the transforming activity. To confirm the contribution of ROCK to RhoA-mediated transformation and to assess the involvement of additional effector pathways downstream of RhoA, we further tested a set of effector-domain mutants of

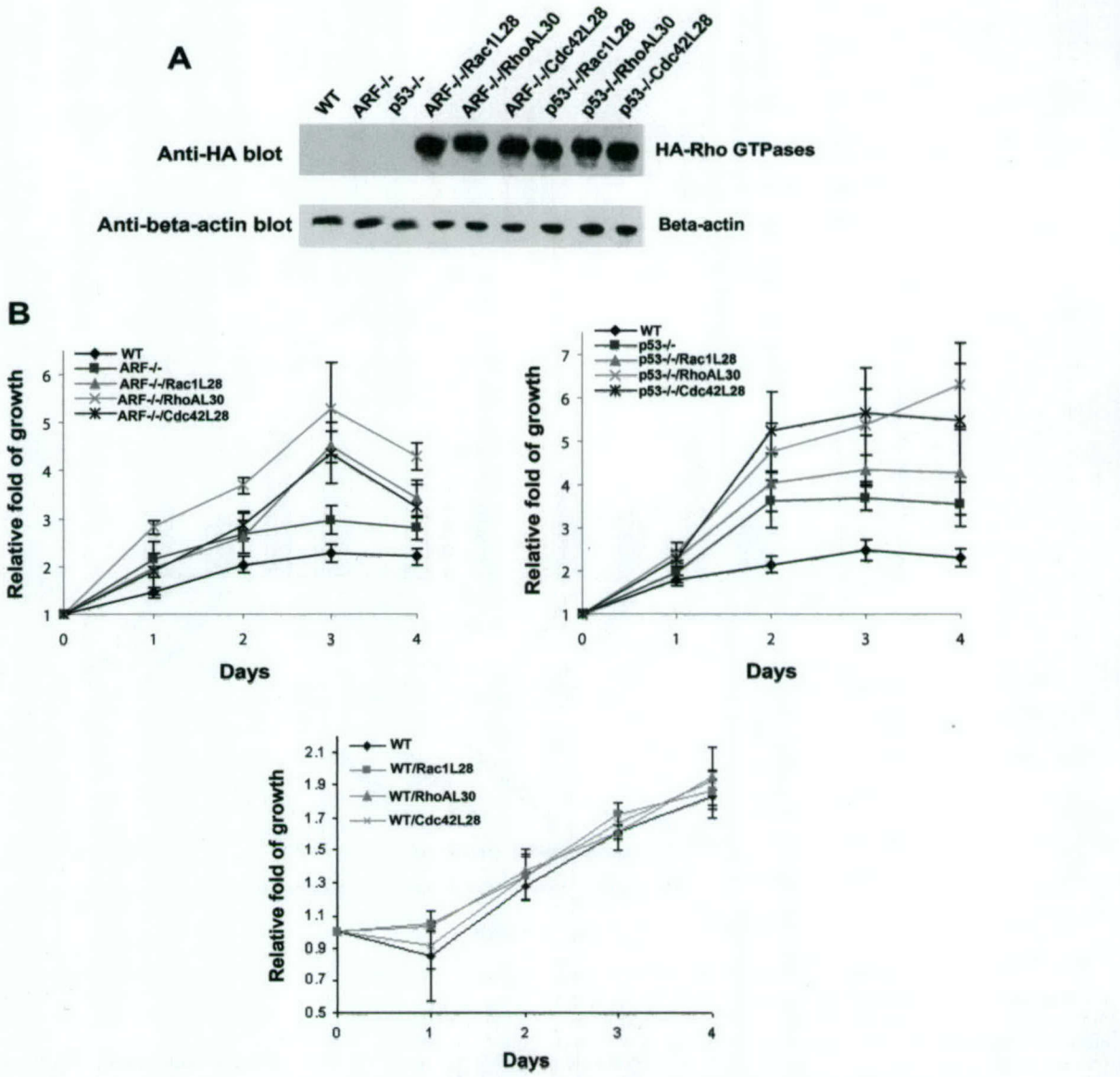

FIG. 5. The active Rac1, RhoA, and Cdc42 mutants can stimulate hyperproliferation of *p19Arf*- or *p53*-null cells. (A) Expression of the fast-cycling mutants of Rac1, RhoA, and Cdc42 that carry an N-terminal HA tag in *p19Arf*- or *p53*-null cells was probed by anti-HA Western blotting. (B) The indicated cells were plated in a culture medium containing 5% fetal bovine serum. At the indicated time points, the amount of incorporated [^{3}H]thymidine was quantified by scintillation counting. The data are representative of three independent experiments and are presented as the fold of growth relative to the respective cells at day 0. Error bars represent the standard deviations of four repeats. WT, wild type.

RhoA for their ability to induce transformation of $p53^{-/-}$ primary MEFs. As previously characterized in vitro (10, 38) and depicted in Fig. 8B, RhoA-F39V is defective in PKN binding but retains ROCK binding, RhoA-E40L is defective for ROCK recognition, RhoA-E40T retains ROCK and PKN binding but is defective in kinectin and mDia binding, and RhoA-Y42C is selectively defective in PKN binding. Consistent with the partial loss of transforming activity in the case of ROCK inhibitor-treated cells, RhoAL63-L40 that is defective in ROCK binding suffered partial loss of foci-forming activity (Fig. 8C). Since ROCK was found to be significantly upregulated in the mRNA level in the RhoA-transduced $p53^{-/-}$ cells in a gene array assay (unpublished data), these results strongly suggest that the RhoA-ROCK pathway is required for the RhoA-induced transformation of primary $p53^{-/-}$ MEFs, corroborating previous findings with NIH 3T3 cells (39). Interestingly, the RhoA mutant that retained ROCK and PKN binding but was defective for kinectin and mDia and possibly other effector pathways (RhoAL63-E40T) was partially active in transforming $p53^{-/-}$ cells, whereas the RhoA mutants that have lost PKN-binding ability (RhoA-F39V and RhoA-Y42C) remained partially or fully active (Fig. 8C). Therefore, additional effector pathways other than ROCK that emanated from active RhoA but not PKN appear to also be involved in the RhoA-mediated transformation of $p53^{-/-}$ cells. These results provide clues on the contribution of RhoA-regulated signaling

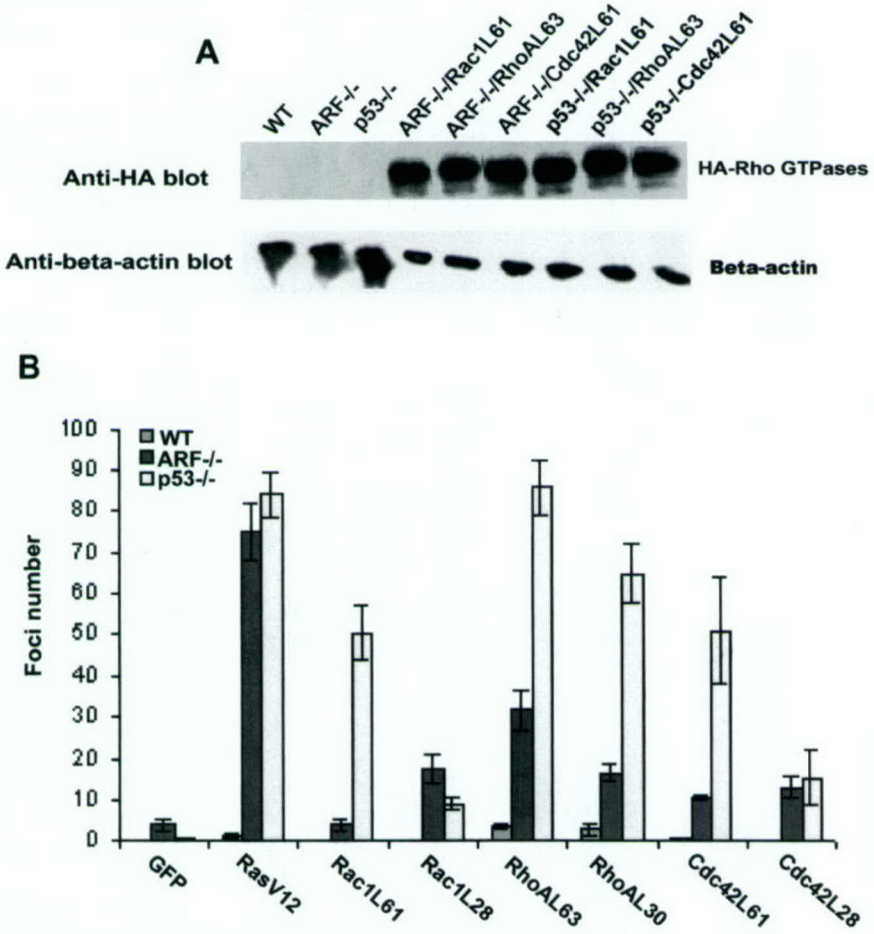

FIG. 6. The active Rac1, RhoA, and Cdc42 mutants cooperate with *p19Arf* or *p53* deletion to promote cell transformation. (A) Expression of the constitutively active mutants of Rac1, RhoA, and Cdc42 containing an N-terminal HA tag in *p19Arf*- or *p53*-null cells was probed by anti-HA Western blotting. (B) Five thousand MEF cells expressing the indicated proteins were mixed with 5×10^4 parental $p19Arf^{-/-}$ or $p53^{-/-}$ cells and cultured in 100-mm plates. The cell cultures were fed every 2 days with fresh culture medium. Fourteen days postplating, the foci were fixed, stained, and quantified under a microscope. The data are representative of two independent experiments. WT, wild type.

cascades to the transformation phenotype of a primary cell system.

DISCUSSION

In the present study, we demonstrate that Rho family GTPases Rac1, RhoA, and Cdc42 contribute to $p19^{Arf}$- and p53-regulated gene transcription and cell growth and that activation of these Rho GTPases can cooperate with p19Arf or p53 defects to promote hyperproliferation and transformation. The contributions of RhoA and Cdc42 to the growth phenotype of *p19Arf*- and *p53*-deficient cells may come in part through modulation of the transcriptional activities of a few key cell growth regulators, including the transcription factor NF-κB and the cell division kinase regulator cyclin D1, whereas Rac1 appears to be involved in p19Arf- p53 mediated cell growth independently of NF-κB and cyclin D1. Significantly, we show that RhoA is involved in p53-regulated cell proliferation by modulating the cell cycle and a p53-independent apoptotic signal and that multiple RhoA-regulated pathways, including that of ROCK, appear to be important for promoting transformation of $p53^{-/-}$ cells. Although more detailed mechanisms of the connection and cooperativeness between the Rho proteins and the $p19^{Arf}$-p53 tumor suppressor pathway remain to be explored, these results help establish an important functional relationship of Rho GTPases with the $p19^{Arf}$-p53 pathway, defects of which occur in many cases of human cancer (13, 43). The findings may have important implications for strategies that target Rho proteins in anticancer therapy.

Previous studies have shown by genetic disruption of the tumor suppressor genes that $p19^{ARF}$ and p53 but not $p27^{Kip1}$ or pRb have a profound negative effect on cell motility and migration (12). $p19^{ARF}$ likely depends on p53 for cell migration regulation, and a specific transcriptional activity or specific target genes controlled by p53 may serve as the link between p53 and actin cytoskeleton to promote the migration phenotype. In particular, we found that the endogenous PI 3-kinase and Rho GTPase activities were significantly elevated in $Arf^{-/-}$ and $p53^{-/-}$ cells and that both PI 3-kinase and Rac1 were required for the $p19^{Arf}$- and p53-regulated migration (12). In the present study, we further determined the relation-

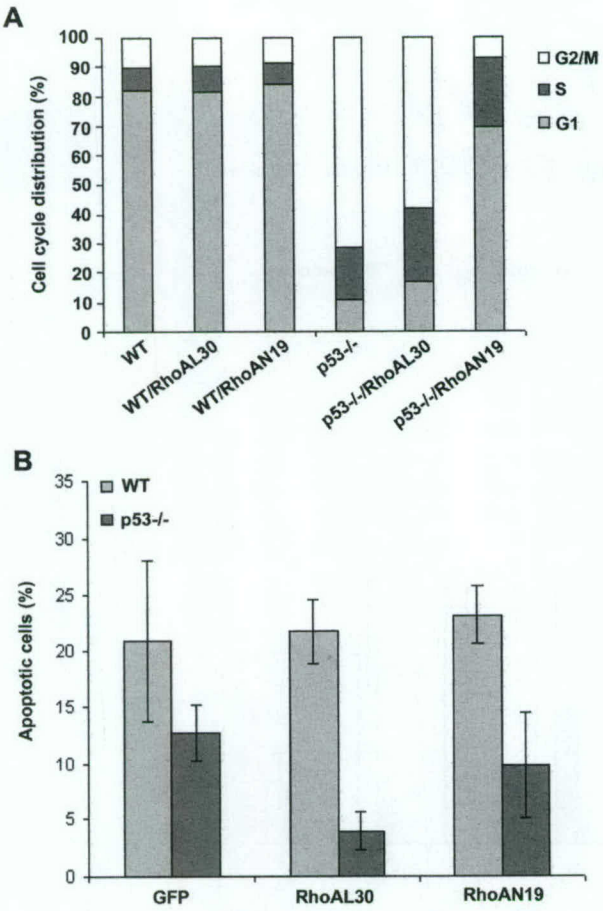

FIG. 7. Dominant negative RhoA affects cell cycle progression of $p53^{-/-}$ MEFs, while active RhoA suppresses gamma irradiation-induced apoptosis. (A) $p53^{-/-}$ cells transduced with GFP alone or with retrovirus expressing RhoAL30 or RhoAN19 were analyzed by FACS for cell cycle progression after PI staining in a culture medium containing 5% fetal bovine serum. The data are representative of the results of two independent experiments. (B) Various retroviral transduced MEF cells were analyzed by FACS for apoptotic cell population after gamma irradiation (20 Gy). Wild-type (WT) MEFs transduced with GFP alone were compared in parallel.

ship between PI 3-kinase and Rac1/RhoA activities in *p19Arf*- and *p53*-deficient MEFs and revealed that activation of Rac1/RhoA by a p19^{Arf} or p53 defect depended on the elevated PI 3-kinase activity and did not occur if PI 3-kinase activity was not elevated. Therefore, a pathway initiated from p19^{Arf} or p53 deficiency could lead to PI 3-kinase activation, which in turn activates Rac1 and RhoA (Fig. 9). We are currently examining the candidate genes whose expression profiles are altered by p19^{ARF} and p53 deficiencies in an effort to identify the molecule(s) responsible for PI 3-kinase and Rho GTPase activation. One possibility is that the gene(s) controlled by p53 (55) provides an autocrine mechanism that feeds back to stimulate the cells leading to PI 3-kinase activation and subsequently to Rho GTPase activation.

Aberrant activation of Rho GTPases can promote cell hyperproliferation and growth transformation (3, 5, 25, 58). The mechanism of Rho protein-stimulated cell growth leading to transformation appears to be at least twofold: activation of cell cycle promoting regulators such as cyclin D1 (49, 50) and inhibition of negative regulators of cell cycle progression such as p21^{Cip1} and p27^{Kip1} (28, 47). We found that *Arf* and *p53* deletion caused a markedly increased cyclin D1 activity which is in part dependent on RhoA and Cdc42, suggesting that these Rho proteins contribute to the growth phenotype of the $Arf^{-/-}$ and $p53^{-/-}$ cells by transducing signals to stimulate cyclin D1 activity. Surprisingly, Rac1 does not appear to be involved in the cyclin D1 regulation by p19^{Arf} or p53, but it must employ another mechanism to affect the proliferation of these cells, because Rac1 is required for the increased proliferation of the $Arf^{-/-}$ and $p53^{-/-}$ cells.

A number of mechanisms have been proposed for cyclin D1 activation and growth regulation by Rho GTPases. Rac1 and RhoA can activate NF-κB, which in turn activates cyclin D1 (14, 29). Rac1 and Cdc42 might promote extracellular signal-regulated kinase 1 and 2 activation by means of PAKs, which can directly phosphorylate and activate Raf and MEK (51). In addition, Rac1-mediated activation of c-Jun NH_2-terminal kinase and p38 mitogen-activated protein kinase cascades can lead to increased phosphorylation and activity of the AP-1 components Jun and ATF (58), and the recently identified Cdc42-Par6 atypical protein kinase C pathway may also stimulate NF-κB, causing cyclin D1 activation (7). We have observed that RhoA but not Rac1 or Cdc42 plays a role in NF-κB upregulation by *Arf* or *p53* deletion, raising the possibility that the contribution of RhoA to the growth phenotype of the cells may be due partly to activation of NF-κB, which in turn stimulates cyclin D1. The differential regulation of NF-κB and cyclin D1 activities by RhoA, Rac1, and Cdc42 in the $p19Arf^{-/-}$ and $p53^{-/-}$ cells suggests that each member of Rho family GTPases may utilize a distinct mechanism to contribute to the growth phenotype. The finding that Rac1 does not appear to contribute to the p19^{Arf}- or p53-mediated NF-κB or cyclin D1 regulation is somewhat surprising, since previous work by a number of laboratories using cloned fibroblast cell lines have implicated Rac1 as one important regulator of NF-κB and cyclin D1 activity (29, 50, 52). It is likely that the involvement of Rac1 in these transcription processes is cell context and pathway specific. Furthermore, our observations that individual Rho proteins may be involved differentially in p19Arf- and p53-regulated gene induction and cell proliferation add further evidence that p19^{Arf} and p53 have overlapping and interdependent as well as independent functions in the regulation of cell growth (24, 34, 43).

Whether the Rho proteins, Rac1 and Cdc42 in particular, can further regulate cell growth through suppression of cell cycle inhibitors such as p21^{Cip1} or p27^{Kip1} in the $Arf^{-/-}$ and $p53^{-/-}$ background remains to be examined further. It is clear, however, that RhoA could have an impact on cell proliferation in both a p53-dependent and a p53-independent manner through modulation of cell cycle and apoptotic machineries, given our observation that the dominant negative RhoA mutant could effectively extend the G_1 phase and suppress the G_2/M phase of $p53^{-/-}$ MEFs, while the active RhoA mutant could suppress the gamma irradiation-induced apoptosis independently of p53.

Constitutively active or fast-cycling Rho GTPase mutants, as well as many of their GEFs, can induce foci formation or

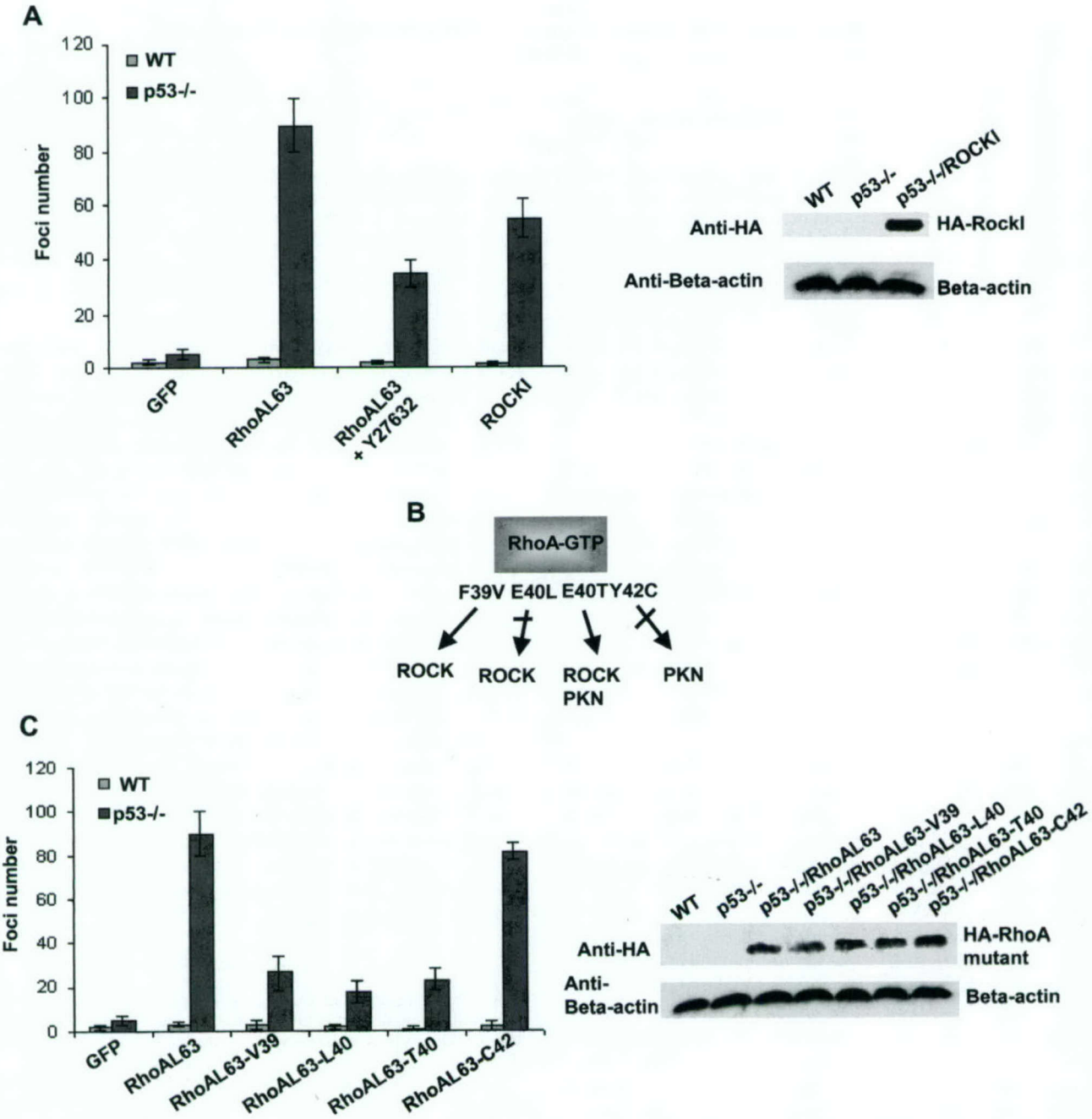

FIG. 8. Multiple effector pathways regulated by RhoA contribute to the transformation phenotype of $p53^{-/-}$ MEF cells. (A) Involvement of ROCK in the RhoAL63-elicited transformation of $p53^{-/-}$ MEFs. Colony-forming activities of $p53^{-/-}$ MEFs transduced with the RhoAL63 mutant or ROCK1 in the presence or absence of Y27632 (20 μM) were determined 14 days postplating. (B) Effector domain mutants of RhoA allow selective uncoupling of RhoA with ROCK, PKN, or other effectors. Single-point mutants made in the switch I domain of RhoA impair or retain specific effector binding as depicted. (C) The effect of effector domain mutations on active RhoA-induced transformation of $p53^{-/-}$ cells. Expression of the respective RhoAL63 mutants in the $p53^{-/-}$ cells was detected by anti-HA Western blot. The data shown are representative of two independent experiments. WT, wild type.

anchorage-independent growth of NIH 3T3 cells (21, 35, 52, 56, 58). We found that the activating mutants of Rac1, RhoA, and Cdc42 can induce a hyperproliferative and transforming phenotype in both the $Arf^{-/-}$ and $p53^{-/-}$ primary MEFs to an extent similar to that caused by oncogenic Ras in certain cases (e.g., active RhoA) (Fig. 6). Since a number of downstream effectors of Ras other than the Rho proteins, including PI 3-kinase and Raf, combine to contribute to the transforming phenotype of oncogenic Ras (3), the potency of some of the Rho members suggests that they may turn on distinct signaling components from Ras or may be more efficient in turning on the same set of growth-promoting factors as Ras in inducing

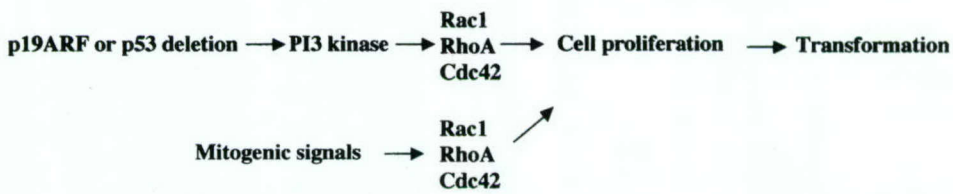

FIG. 9. A model depicting the relationship between the p19^{Arf}-p53 tumor suppressor pathway and the Rho GTPase signaling module in the regulation of cell proliferation and transformation. In addition to malfunction in checkpoint and apoptosis control, deficiency of p19^{Arf}and/or p53 may alter transcriptional balance and promote cell growth by upregulating PI 3-kinase and Rho GTPase activities. Mitogenic signals that cause activation of RhoA, Rac1, or Cdc42 could further modulate cell cycle and apoptotic machineries and cooperate with p53 deficiency to promote cell hyperproliferation and transformation.

cell transformation. In this regard, we have tested the latter possibility, that further enhancement of NF-κB and cyclin D1 activities by the active Rho mutants could be responsible for the efficient induction of transformation in the *Arf*$^{-/-}$ and *p53*$^{-/-}$ cells. We found that both the luciferase reporter activities and the nuclear expression levels of NF-κB and cyclin D1 remain unchanged with or without the expression of the active Rho protein mutants (data not shown). It is therefore possible that the active Rho GTPases stimulate additional factors that cooperate with the p53 pathway defects to promote cell transformation. It is also worth noting that the two different forms of active Rho GTPases, i.e., the fast-cycling and constitutively GTP-bound forms, may have distinct transcription profiles, as we have observed in a gene array study (unpublished data), which could help explain the quantitative differences of these mutants in promoting p19Arf$^{-/-}$ or p53$^{-/-}$ MEF transformation.

In an attempt to further dissect the requirement of RhoA downstream effectors for the transforming phenotype of active RhoA, we utilized ROCKI and the ROCK inhibitor, Y27632, as well as a set of the effector domain mutants of RhoA that impair or retain coupling with specific effectors in the transformation assay. Our results confirm an important role of the ROCK pathway in RhoA-mediated transformation of *p53*$^{-/-}$ cells, while also implying that multiple effectors downstream of RhoA may collaborate to allow the optimal effect of RhoA.

Our results present a seemingly paradoxical relationship between Rho GTPases and the p53 tumor suppressor pathway. On the one hand, basal activities of RhoA, Rac1, and Cdc42 are all part of the required proliferative signals of the p19Arf- or p53-regulated networks. On the other hand, hyperactive Rho proteins can cooperate with *p19Arf* or *p53* deletion or mutation to promote transformation, suggesting that events leading to the activation of Rho family GTPases may constitute second hits in tumor induction (Fig. 9). The later synergism between the Rho GTPases and the p53 pathway further indicates that signaling components of the Rho GTPases are capable of delivering quantitatively different and/or additional inputs to cell proliferation regulation by the p53 pathway. Given the intertwining, complex nature of cell growth regulatory mechanisms of the p53 pathway and Rho proteins, one remaining challenge would be to delineate which of the known or unknown pathways controlled by p19^{Arf}-p53 and each Rho GTPase might cooperate to promote cell hyperproliferation and transformation. Rho family GTPases have been implicated in many aspects of tumor development. Overexpression, upregulation, or rearrangement of RhoA, RhoC, Rac1, Rac2, Rac3, Cdc42, and RhoH have been detected in human tumors ranging from colon, breast, lung, and myeloma to head and neck squamous-cell carcinoma (6, 9, 26, 30, 40, 45). Due to their recognized roles in Ras transformation (58), growth factor and integrin signaling (41), cell cycle control (27), apoptosis (1, 44), and invasion and metastasis (54), Rho GTPases have been proposed as potential anticancer therapeutic targets (37). Interestingly, to date no activating mutations like those found in oncogenic *ras* have been discovered in Rho family members, suggesting that Rho proteins might primarily serve as signaling links from upstream mitogenic signals to play a modifier role in tumor induction. Our studies demonstrating a role of Rho proteins in p19^{Arf}- and p53-controlled cell growth and migration and a synergistic effect of active RhoA, Rac1, and Cdc42 with *p19Arf* or *p53* deletion on cell transformation further strengthen the view that these Rho GTPases may contribute to and/or cooperate with p53 deficiency in tumorigenesis and tumor progression. It remains to be seen if upregulation of Rho GTPase activities in the *p19Arf*$^{-/-}$ or *p53*$^{-/-}$ genetic background could result in a shortened latency in tumorigenesis in an animal model. Should that be the case, targeting individual Rho GTPases would be a worthy endeavor among future anticancer strategies.

ACKNOWLEDGMENTS

We thank members of the Zheng laboratory staff for help with retroviral production and cDNA constructs and Martine Roussel (St. Jude Children's Research Hospital) for the kind gifts of MEFs and Arf cDNA.

This work was supported in part by grants from the National Institutes of Health (grants GM60523 and GM53943) and the Department of Defense Breast Cancer Program (grant BC990290) (to Y.Z.).

REFERENCES

1. **Aznar, S., and J. C. Lacal.** 2001. Rho signals to cell growth and apoptosis. Cancer Lett. **165:**1–10.
2. **Balint, E., and K. H. Vousden.** 2001. Activation and activities of the p53 tumour suppressor protein. Br. J. Cancer **85:**1813–1823.
3. **Bar-Sagi, B., and A. Hall.** 2000. Ras and Rho GTPases: a family reunion. Cell **103:**227–238.
4. **Bishop, A. L., and A. Hall.** 2000. Rho GTPases and their effector proteins. Biochem. J. **348:**241–255.
5. **Boettner, B., and L. Van Aelst.** 2002. The role of Rho GTPases in disease development. Gene **286:**155–174.
6. **Clark, E. A., T. R. Golub, E. S. Lander, and R. O. Hynes.** 2000. Genomic analysis of metastasis reveals an essential role for RhoC. Nature **406:**532–535.
7. **Etienne-Manneville, S., and A. Hall.** 2002. Rho GTPases in cell biology. Nature **420:**629–635.
8. **Ferbeyre, G., E. de Stanchina, A. W. Lin, E. Querido, M. E. McCurrach, G. J.**

Hannon, and S. W. Lowe. 2002. Oncogenic *ras* and p53 cooperate to induce cellular senescence. Mol. Cell. Biol. **22:**3497–3508.
9. **Fritz, G., I. Just, and B. Kaina.** 1999. Rho GTPases are over-expressed in human tumors. Int. J. Cancer **81:**682–687.
10. **Fujisawa, K., P. Madaule, T. Ishizaki, G. Watanabe, H. Bito, Y. Saito, A. Hall, and S. Narumiya.** 1998. Different regions of Rho determine Rho-selective binding of different classes of Rho target molecules. J. Biol. Chem. **273:**18943–18949.
11. **Gu, Y., M-D. Filippi, J. E. Siefring, E. P. Williams, A. Jasti, R, Prabhakar, D. J. Kwiatkowski, and D. A. Williams.** The highly related Rho GTPases, Rac1 and Rac2, separately control hematopoietic cell survival and cycle progression, but together regulate adhesion and migration. Science, in press.
12. **Guo, F. K., Y. Gao, L. Wang, and Y. Zheng.** 2003. p19Arf-p53 tumor suppressor pathway regulates cell motility by suppression of phosphoinositide 3-kinase and Rac1 GTPase activities. J. Biol. Chem. **278:**14414–14419.
13. **Hahn, W. C., and R. A. Weinberg.** 2002. Modelling the molecular circuitry of cancer. Nat. Rev. Cancer **2:**331–341.
14. **Joyce, D., B. Bouzahzah, M. Fu, C. Albanese, M. D'Amico, J. Steer, J. U. Klein, R. J. Lee, J. E. Segall, J. K. Westwick, C. J. Der, and R. G. Pestell.** 1999. Integration of Rac-dependent regulation of cyclin D1 transcription through a nuclear factor-B-dependent pathway. J. Biol. Chem. **274:**25245–25249.
15. **Kaibuchi, K., S. Kuroda, M. Fukata, and M. Nakagawa.** 1999. Regulation of cadherin-mediated cell-cell adhesion by the Rho family GTPases. Curr. Opin. Cell Biol. **11:**591–596.
16. **Kamijo, T., F. Zindy, M. F. Roussel, D. E. Quelle, J. R. Downing, R. A. Ashmun, G. Grosveld, and C. J. Sherr.** 1997. Tumor suppression at the mouse INK4a locus mediated by the alternative reading frame product p19*ARF*. Cell **91:**649–659.
17. **Khosravi-Far, R., P. A. Solski, G. J. Clark, M. S. Kinch, and C. J. Der.** 1995. Activation of Rac1, RhoA, and mitogen-activated protein kinases is required for Ras transformation. Mol. Cell. Biol. **15:**6443–6453.
18. **Levine, A. J.** 1997. p53, the cellular gatekeeper for growth and division. Cell **88:**323–331.
19. **Li, R., B. Debreceni, B. Jia, Y. Gao, G. Tigyi, and Y. Zheng.** 1999. Localization of the PAK1-, WASP-, and IQGAP1-specifying regions of the small GTPase Cdc42. J. Biol. Chem. **274:**29648–29654.
20. **Liliental, J., S. Y. Moon, R. Lesche, R. Mamillapalli, N. Gavrilova, Y. Zheng, H. Sun, and H. Wu.** 2000. Genetic deletion of the PTEN tumor suppressor gene promotes cell motility by activation of Rac1 and Cdc42 GTPases. Curr. Biol. **10:**401–404.
21. **Lin, R., R. A. Cerione, and D. Manor.** 1999. Specific contributions of the small GTPases Rho, Rac, and Cdc42 to Dbl transformation. J. Biol. Chem. **274:**23633–23641.
22. **Ma, P., M. Magut, X. Chen, and C.-Y. Chen.** 2002. p53 is necessary for the apoptotic response mediated by a transient increase of Ras activity. Mol. Cell. Biol. **22:**2928–2938.
23. **Malliri, A., R. A. van der Kammen, K. Clark, M. van der Valk, F. Michiels, and J. G. Collard.** 2002. Mice deficient in the Rac activator Tiam1 are resistant to Ras-induced skin tumours. Nature **417:**867–871.
24. **McKeller, R. N., J. L. Fowler, J. J. Cunningham, N. Warner, R. J. Smeyne, F. Zindy, and S. X. Skapek.** 2002. The *Arf* tumor suppressor gene promotes hyaloid vascular regression during mouse eye development. Proc. Natl. Acad. Sci. USA **99:**3848–3853.
25. **Mira, J. P., V. Benard, J. Groffen, L. C. Sanders, and U. G. Knaus.** 2000. Endogenous, hyperactive Rac3 controls proliferation of breast cancer cells by p21-activated kinase-dependent pathway. Proc. Natl. Acad. Sci. USA **97:**185–189.
26. **Montaner, S., R. Perona, L. Saniger, and J. C. Lacal.** 1998. Multiple signaling pathways lead to the activation of the nuclear factor κB by the Rho family of GTPases. J. Biol. Chem. **273:**12779–12785.
27. **Olson, M. F., A. Ashworth, and A. Hall.** 1995. An essential role for rho, rac, and cdc42 GTPases in cell cycle progression through G1. Science **269:**1270–1272.
28. **Olson, M. J., H. F. Paterson, and C. J. Marshall.** 1998. Signals from Ras and Rho GTPases interact to regulate expression of p21Waf1/Cip1. Nature **394:**295–299.
29. **Perona, R., S. Montaner, L. Saniger, P. I. Sanchez, R. Bravo, and J. C. Lacal.** 1997. Activation of the nuclear factor-κB by Rho, Rac, and Cdc42 proteins. Genes Dev. **11:**463–475.
30. **Preudhomme, C., C. Roumier, M. P. Hildebrand, E. Dallery-Prudhomme, D. Lantoine, J. L. Lai, A. Daudignon, C. Adenis, F. Bauters, P. Fenaux, J. P. Kerckaert, and S. Galiegue-Zouitina.** 2000. Nonrandom 4p13 rearrangements of the RhoH/TTF gene, encoding a GTP-binding protein, in non-Hodgkin's lymphoma and multiple myeloma. Oncogene **19:**2023–2032.
31. **Qiu, R., J. Chen, D. Kirn, F. McCormick, and M. Symons.** 1995. An essential role for Rac in Ras transformation. Nature **374:**457–459.
32. **Qiu, R., J. Chen, F. McCormick, and M. Symons.** 1995. A role for Rho in Ras transformation. Proc. Natl. Acad. Sci. USA **92:**11781–11785.
33. **Qiu, R., A. Abo, F. McCormick, and M. Symons.** 1997. Cdc42 regulates anchorage-independent growth and is necessary for Ras transformation. Mol. Cell. Biol. **17:**3449–3458.
34. **Rocha, S., K. J. Campbell, and N. D. Perkins.** 2003. p53- and Mdm2-independent repression of NF-κB transactivation by the ARF tumor suppressor. Mol. Cell **12:**15–25.
35. **Roux, P., C. Gauthier-Rouviere, S. Doucet-Brutin, and P. Fort.** 1997. The small GTPases Cdc42Hs, Rac1 and RhoG delineate Raf-independent pathways that cooperate to transform NIH3T3 cells. Curr. Biol. **7:**629–637.
36. **Ryan, K. M., M. K. Ernst, N. R. Rice, and K. H. Vousden.** 2000. Role of NF-κB in p53-mediated programmed cell death. Nature **404:**892–897.
37. **Sahai, E., and C. J. Marshall.** 2002. Rho-GTPases and cancer. Nat. Rev. Cancer **2:**133–142.
38. **Sahai, E., A. S. Alberts, and R. Treisman.** 1998. RhoA effector mutants reveal distinct effector pathways for cytoskeletal reorganization, SRF activation and transformation. EMBO J. **17:**1350–1361.
39. **Sahia, E., T. Ishizaki, S. Narumiya, and R. Treisman.** 1999. Transformation mediated by RhoA requires activity of ROCK kinases. Curr. Biol. **9:**136–145.
40. **Schnelzer, A., D. Prechtel, U. Knaus, K. Dehne, M. Gerhard, H. Graeff, N. Harbeck, M. Schmitt, and E. Lengyel.** 2000. Rac1 in human breast cancer: overexpression, mutation analysis, and characterization of a new isoform. Oncogene **19:**3013–3020.
41. **Schwartz, M. A., and S. J. Shattil.** 2000. Signaling networks linking integrins and rho family GTPases. Trends Biochem. Sci. **25:**388–391.
42. **Serrano, M., A. W. Lin, M. E. McCurrach, D. Beach, and S. W. Lowe.** 1997. Oncogenic ras provokes premature cell senescence associated with accumulation of p53 and p16INK4a. Cell **88:**593–602.
43. **Sherr, C. J.** 2001. The Ink4a/ARF network in tumor suppression. Nat. Rev. Mol. Cell Biol. **2:**731–737.
44. **Subauste, M. C., M. Von Herrath, V. Benard, C. E. Chamberlain, T. S. Chuang, K. Chu, G. M. Bokoch, and K. M. Hahn.** 2000. Rho family proteins modulate rapid apoptosis induced by cytotoxic T lymphocytes and Fas. J. Biol. Chem. **275:**9725–9733.
45. **Suwa, H., G. Ohshio, T. Imamura, G. Watanabe, S. Arii, M. Imamura, S. Narumiya, H. Hiai, and M. Fukumoto.** 1998. Overexpression of RhoC gene correlates with progression of ductal adenocarcinoma of the pancreas. Br. J. Cancer **77:**147–152.
46. **Van Aelst, L., and C. D'Souza-Schorey.** 1997. Rho GTPases and signaling networks. Genes Dev. **11:**2295–2322.
47. **Vidal, A., S. S. Millard, J. P. Miller, and A. Koff.** 2002. Rho activity can alter the translation of p27 mRNA and is important for Ras^{V12}-induced transformation in a manner dependent on p27 status. J. Biol. Chem. **277:**16433–16440.
48. **Webster, G. A., and N. D. Perkins.** 1999. Transcriptional cross talk between NF-κB and p53. Mol. Cell. Biol. **19:**3485–3495.
49. **Welsh, C. F., et. al.** 2001. Timing of cyclin D1 expression within G1 phase is controlled by Rho. Nat. Cell Biol. **3:**950–957.
50. **Westwick, J. K., R. J. Lee, Q. T. Lambert, M. Symons, R. G. Pestell, C. J. Der, and I. P. Whitehead.** 1998. Transforming potential of Dbl family proteins correlates with transcription from the cyclin D1 promoter but not with activation of Jun NH2-terminal kinase, p38/Mpk2, serum response factor, or c-Jun. J. Biol. Chem. **273:**16739–16747.
51. **Westwick, J. K., Q. T. Lambert, G. J. Clark, M. Symons, L. Van Aelst, R. G. Pestell, and C. J. Der.** 1997. Rac regulation of transformation, gene expression, and actin organization by multiple, PAK-independent pathways. Mol. Cell. Biol. **17:**1324–1335.
52. **Whitehead, I. P., Q. T. Lambert, J. A. Glaven, K. Abe, K. L. Rossman, G. M. Mahon, J. M. Trzaskos, R. Kay, S. L. Campbell, and C. J. Der.** 1999. Dependence of Dbl and Dbs transformation on MEK and NF-κB activation. Mol. Cell. Biol. **19:**7759–7770.
53. **Wu, W. J., S. Tu, and R. A. Cerione.** 2003. Activated Cdc42 sequesters c-Cbl and prevents EGF receptor degradation. Cell **114:** 715–725.
54. **Yoshioka, K., F. Matsumura, H. Akedo, and K. Itoh.** 1998. Small GTP-binding protein Rho stimulates the actomyosin system, leading to invasion of tumor cells. J. Biol. Chem. **273:**5146–5154.
55. **Zhao, R., K. Gish, M. Murphy, Y. Yin, D. Notterman, W. H. Hoffman, E. Tom, D. H. Mack, and A. J. Levine.** 2000. Analysis of p53-regulated gene expression patterns using oligonucleotide arrays. Genes Dev. **14:**981–993.
56. **Zheng, Y.** 2001. Dbl family guanine nucleotide exchange factors. Trends Biochem. Sci. **26:**724–732.
57. **Zindy, F., C. M. Eischen, D. H. Randle, T. Kamijo, J. L. Cleveland, C. J. Sherr, and M. F. Roussel.** 1998. Myc signaling via the ARF tumor suppressor regulates p53-dependent apoptosis and immortalization. Genes Dev. **12:**2424–2433.
58. **Zohn, I. M., S. L. Campbell, R. Khosravi-Far, K. L. Rossman, and C. J. Der.** 1998. Rho family proteins and Ras transformation: the RHOad less traveled gets congested. Oncogene **17:**1415–1438.

Molecular Biology of the Cell
Vol. 12, 3717–3732, December 2001

Na,K-ATPase Activity Is Required for Formation of Tight Junctions, Desmosomes, and Induction of Polarity in Epithelial Cells

Sigrid A. Rajasekaran,[*†] Lawrence G. Palmer,[*] Sun Y. Moon,[‡] Alejandro Peralta Soler,[§] Gerard L. Apodaca,[‖] Jeffrey F. Harper,[¶] Yi Zheng,[‡] and Ayyappan K. Rajasekaran[†#]

[†]Department of Pathology and Laboratory Medicine, University of California, Los Angeles, Los Angeles, California 90095; [*]Department of Physiology, Weill Medical College of Cornell University, New York, New York 10021; [‡]Department of Biochemistry, University of Tennessee, Memphis, Tennessee 38163; [§]Lankenau Medical Research Center, Wynnewood, Pennsylvania 19096; [¶]Department of Cell Biology, The Scripps Research Institute, La Jolla, California 92037; and [‖]Department of Cell Biology and Physiology, University of Pittsburgh, Pittsburgh, Pennsylvania 15261

Submitted July 9, 2001; Revised September 7, 2001; Accepted September 24, 2001
Monitoring Editor: Guido Guidotti

Na,K-ATPase is a key enzyme that regulates a variety of transport functions in epithelial cells. In this study, we demonstrate a role for Na,K-ATPase in the formation of tight junctions, desmosomes, and epithelial polarity with the use of the calcium switch model in Madin-Darby canine kidney cells. Inhibition of Na,K-ATPase either by ouabain or potassium depletion prevented the formation of tight junctions and desmosomes and the cells remained nonpolarized. The formation of bundled stress fibers that appeared transiently in control cells was largely inhibited in ouabain-treated or potassium-depleted cells. Failure to form stress fibers correlated with a large reduction of RhoA GTPase activity in Na,K-ATPase-inhibited cells. In cells overexpressing wild-type RhoA GTPase, Na,K-ATPase inhibition did not affect the formation of stress fibers, tight junctions, or desmosomes, and epithelial polarity developed normally, suggesting that RhoA GTPase is an essential component downstream of Na,K-ATPase-mediated regulation of these junctions. The effects of Na,K-ATPase inhibition were mimicked by treatment with the sodium ionophore gramicidin and were correlated with the increased intracellular sodium levels. Furthermore, ouabain treatment under sodium-free condition did not affect the formation of junctions and epithelial polarity, suggesting that the intracellular Na^+ homeostasis plays a crucial role in generation of the polarized phenotype of epithelial cells. These results thus demonstrate that the Na,K-ATPase activity plays an important role in regulating both the structure and function of polarized epithelial cells.

INTRODUCTION

Junctional complexes such as tight junctions, adherens junctions, and desmosomes play a fundamental role in maintaining the polarized phenotype and vectorial transport functions of epithelial cells. The tight junction (zonula occludens) forms a continuous belt at the boundary between the apical and lateral plasma membrane domains of neighboring epithelial cells (Farquhar and Palade, 1963). Structurally characterized by the fusion of the exoplasmic leaflets of contiguous plasma membranes, tight junctions selectively regulate the passage of molecules across the paracellular pathway (gate function) and passively separate molecules into the apical and basolateral plasma membrane domains (fence function). A functional tight junction is crucial to maintain the polarized phenotype of epithelial cells (Rodriguez-Boulan and Nelson, 1989; Mitic and Anderson, 1998; Stevenson and Keon, 1998). The adherens junction (zonula adherens) is localized below the tight junction and consists of cell adhesion and signaling molecules and may regulate events that mediate adhesion between epithelial cells (Yap *et al.*, 1997). Desmosomes are focal points of intercellular contact at which neighboring cells are tightly bound to one another and provide resilience and tensile strength to the epithelial monolayer (Garrod *et al.*, 1996). The mechanisms that regu-

[#] Corresponding author. E-mail address: arajasekaran@mednet.ucla.edu.

© 2001 by The American Society for Cell Biology

late the formation and maintenance of these junctions in epithelial cells are not well understood.

The Na,K-ATPase is an oligomeric transmembrane protein consisting of two noncovalently linked α- and β-subunits. It catalyzes an ATP-dependent transport of three sodium ions out and two potassium ions into the cell per pump cycle, thereby generating a transmembrane sodium gradient across the plasma membrane. The sodium gradient generated by the enzyme provides the primary energy for uptake and extrusion of a variety of solutes by epithelial cells and is crucial for efficient functioning of other Na^+-coupled transport systems (Katz, 1988; Lingrel *et al.*, 1994). The Na,K-ATPase is localized to the basolateral plasma membrane in most epithelial cells and has been widely used as a marker for epithelial polarity (McNeil *et al.*, 1990). However, a role for the Na,K-ATPase itself in the induction of epithelial polarity has not been shown.

Previous studies have implicated E-cadherin function in the formation and maintenance of junctional complexes and the polarized phenotype of epithelial cells (Imhof *et al.*, 1983; Gumbiner *et al.*, 1988; Watabe *et al.*, 1994). E-Cadherin is a basolateral transmembrane protein that mediates cell-cell contact between epithelial cells by homophilic interaction (Nose *et al.*, 1988). However, expression of a dominant negative mutant of E-cadherin in Madin-Darby canine kidney (MDCK) cells did not affect tight junctions or desmosomes (Troxell *et al.*, 2000), indicating that other factors are involved in the maintenance of these junctions in MDCK cells. Recently, we have shown that in Moloney-sarcoma virus transformed MDCK (MSV-MDCK) cells expression of E-cadherin alone was not sufficient to induce tight junctions and desmosomes. Coexpression of Na,K-ATPase β-subunit and E-cadherin was required to induce these junctions and a polarized phenotype in MSV-MDCK cells (Rajasekaran *et al.*, 2001). We also found that MSV-MDCK cells contain about threefold higher intracellular sodium levels ($[Na^+]_i$) compared with wild-type MDCK cells. Forced expression of both the Na,K-ATPase β-subunit and E-cadherin but not E-cadherin alone significantly reduced the $[Na^+]_i$ (Rajasekaran *et al.*, 2001). These studies suggested that $[Na^+]_i$ regulated by the Na,K-ATPase may play a role in the formation of epithelial tight junctions and desmosomes and the induction of a polarized phenotype of epithelial cells.

RhoA GTPase, a Ras-related small GTP-binding protein, is involved in the formation of stress fibers in Swiss 3T3 cells (Ridley and Hall, 1992; Van Aelst and D'Souza-Schorey, 1997; Mackay and Hall, 1998). Recent studies have indicated a role for RhoA GTPase in the assembly and function of tight junctions in epithelial cells (Nusrat *et al.*, 1995; Takaishi *et al.*, 1997; Jou *et al.*, 1998). However, mechanisms that regulate RhoA function in polarized epithelial cells are not known. In this study, we demonstrate that inhibition of Na,K-ATPase during epithelial polarization prevents the formation of tight junctions and desmosomes and suppresses the endogenous RhoA activity in MDCK cells. Na,K-ATPase inhibition in cells overexpressing wild-type RhoA GTPase does not affect the formation of tight junctions and desmosomes, indicating that RhoA GTPase is a downstream effector of Na,K-ATPase and is crucial for the formation of tight junctions and desmosomes in MDCK cells. Gramicidin, a sodium ionophore that specifically increases the intracellular sodium levels, mimicked the effects of Na,K-ATPase inhibition, suggesting that increased intracellular sodium levels may play a role in the inhibition of the formation of tight junctions, desmosomes, and polarized epithelia. Our results for the first time provide evidence that the Na,K-ATPase plays an important role in regulating both the structure and function of polarized epithelial cells.

MATERIALS AND METHODS

Ca^{2+}-Switch Assay

Confluent MDCK monolayers (clone II, passage 4; kindly provided by Dr. Enrique Rodriguez-Boulan, Weill Medical College of Cornell, New York, NY) were subjected to calcium switch assay as described previously (Rajasekaran *et al.*, 1996). Briefly, the cells were trypsinized until single cell suspensions were obtained and plated onto Costar Transwells with 0.4-μm pore size (Corning, Corning, NY) (3×10^6 cells/24 mm) or glass coverslips in a 12-well tissue culture plate (4×10^5 cells/well). The cells were allowed to attach in normal Ca^{2+}-containing DMEM (1.8 mM Ca^{2+}). Thereafter, the cells were rinsed gently in SMEM (minimum essential medium for suspension culture) (Invitrogen, Carlsbad, CA) containing <5 μM Ca^{2+} (low Ca^{2+} medium) and 5% dialyzed fetal bovine serum (FBS) and incubated for ~16 h at 37°C. Before transfer of the cells to medium containing normal Ca^{2+} levels (1.8 mM), the MDCK monolayers were pretreated with either ouabain (50 μM; Sigma Chemical, St. Louis, MO), gramicidin (1 μM; Molecular Probes, Eugene, OR), or valinomycin (50 μM; Molecular Probes) for 1 h in low Ca^{2+} medium at 37°C. Dimethyl sulfoxide (DMSO), used as a solvent for these drugs, was added to control cells. For the switch, the low Ca^{2+} medium was replaced by normal culture medium containing the corresponding drugs and the cells were incubated at 37°C for indicated times. Sodium-free conditions were obtained as described in Fernandez and Malnic (1998). For this purpose single cell suspensions of MDCK cells were plated onto Transwells, allowed to attach, and incubated in low Ca^{2+} medium as described above. The switch was performed with the use of *N*-methyl-D-glucamine (NMDG) buffer in which NaCl was substituted with NMDG (Sigma Chemical) (5 mM KCl, 1.8 mM $CaCl_2$, 1 mM $MgCl_2$, 30 mM HEPES, 147 mM *N*-methyl-D-glucamine, 10 mM glucose, pH 7.4). Before the experiment the cells were rinsed twice with Ca^{2+}-free NMDG buffer (NMDG buffer lacking $CaCl_2$ and FBS) and then incubated in Ca^{2+}-free NMDG buffer containing 5% dialyzed FBS and either DMSO or ouabain as described above. For the switch the Ca^{2+}-free NMDG buffer was replaced with NMDG buffer containing DMSO or ouabain, respectively, and the cells were incubated at 37°C for up to 4 h. Potassium-free conditions were obtained as described in Le *et al.* (1999). For this purpose, the Ca^{2+}-switch was performed with the use of a K^+-free buffer (140 mM NaCl, 1.8 mM $CaCl_2$, 1 mM $MgCl_2$, 20 mM HEPES, 10 mM glucose, pH 7.4), which contained 5% FBS dialyzed against the K^+-free buffer. Before the experiment the cells were rinsed twice with Ca^{2+}- and K^+-free buffer (K^+-free buffer lacking $CaCl_2$) and preincubated in Ca^{2+}/K^+-free buffer/5% FBS for 1 h. For the K^+ repletion the cells were incubated in normal medium at 37°C for 3–5 h. The Ca^{2+}-switch assays for MDCK-$RhoA_{wt}$ cells were performed as described previously (Leung *et al.*, 1999).

Immunofluorescence and Confocal Microscopy

Immunofluorescence was performed on cells fixed with methanol as described previously (Rajasekaran *et al.*, 1996). Antibodies against ZO-1 and occludin (Zymed Laboratories, South San Francisco, CA), desmocollin (DC7G6; gift from Dr. Margaret Wheelock, University of Toledo, Toledo, Ohio), desmoplakin (gift from Dr. Manijeh Pasdar, University of Alberta, Alberta, Canada), and E-cadherin (DECMA; Sigma Chemical) were used. To detect filamentous actin the cells were fixed in paraformaldehyde and labeled with fluorescein isothiocyanate (FITC)-phalloidin (Sigma Chemical). Epifluores-

cence analysis was performed with the use of an Olympus AX 70 microscope. Confocal microscopy to monitor polarized distribution of domain-specific markers was performed with the use of a Fluoview laser scanning confocal microscope (Olympus America, Melville, NY). To detect FITC-labeled antigens, samples were excited at 488 nm with an Argon laser and the light emitted between 525 and 540 nm was recorded. Images were generated and analyzed with the use of the Fluoview image analysis software (version 2.1.39; Olympus America, Melville, NY).

Immunoblot Analysis

For immunoblot analysis, monolayers were lysed in a lysis buffer (95 mM NaCl, 25 mM Tris pH 7.4, 0.5 mM EDTA, 2% SDS, 1 mM phenylmethylsulfonyl fluoride, and 5 μg/ml each of antipain, leupeptin, and pepstatin). The lysates were briefly sonicated and centrifuged at 14,000 rpm in a Microfuge for 10 min. The supernatants were used for further analysis. Protein concentrations of the cell lysates were determined with the use of the Bio-Rad DC reagent (Bio-Rad Laboratories, Hercules, CA) according to manufacturer's instructions. Equal amounts of protein (100 μg) were separated by SDS-PAGE and transferred to nitrocellulose membrane (Schleicher & Schuell, Keene, NH). The blots were blocked with 10% nonfat dry milk in phosphate-buffered saline (PBS) and then incubated for 2 h at room temperature with primary antibody diluted in 10% milk/PBS. After incubation the blots were washed three times with PBS/0.3% Tween 20 and then incubated for 1 h at room temperature with horseradish peroxidase-conjugated secondary antibody (1:4000 in 10% milk). Bound antibody was detected by peroxidase-catalyzed enhanced chemiluminescence (PerkinElmer Life Sciences, Boston, MA). Densitometric analysis and quantification of the intensity of the individual bands was carried out with an ImageQuant software package (Molecular Dynamics, Sunnyvale, CA).

Transepithelial Electrical Resistance (TER) Measurements

To measure the transepithelial electrical resistance, the cells on Transwell filters were subjected to the Ca^{2+}-switch assay as described above, and at the indicated time points the resistance of the monolayers was determined with the use of an EVOM epithelial voltohmeter (World Precision Instruments, Sarasota, FL). The values were normalized for the area of the filter after subtracting the background resistance of a filter without cells.

Electron Microscopy

Confluent monolayers grown on Transwells (see above) were fixed in 2.5% glutaraldehyde in 0.1 M sodium cacodylate buffer, pH 7.4, for 2–4 h at room temperature and processed for transmission electron microscopy as described previously (Rajasekaran *et al.*, 1996). Ultrathin sections were contrasted with uranyl acetate and lead citrate and examined with a Joel (1200EX) electron microscope. The presence of tight junctions and desmosomes was quantified in ~50 randomly selected cell-cell contact sites in each experiment. In MDCK cells adherens junctions were not easily discernible when tight junctions were present and therefore they were not quantified. However, when tight junctions were absent, like in ouabain-treated cells, adherens junctions were clearly observed and quantified. Representative results are shown.

Endogenous RhoA/Rac1 Activity Assay

The glutathione agarose-immobilized GST-PAK1, which contains the Rac1 interactive domain of human PAK1 (residues 51–135), and GST-Rhotekin, which contains the Rho binding domain of Rhotekin (residues 1–89), were expressed and purified in *Escherichia coli* by with the use of the pGEX-2T vector as described previously (Ren *et al.*, 1999; Zhu *et al.*, 2000). The cells were washed with ice-cold PBS buffer once before lysis in a buffer containing 50 mM Tris-HCl, pH 7.4, 100 mM NaCl, 10 mM $MgCl_2$, 1% Triton X-100, 1 mM dithiothreitol, 10 μg/ml each of leupeptin and aprotinin, and 1 mM phenylmethylsulfonyl fluoride at 4°C. Cell lysates were clarified by centrifugation at 13,000 $\times$ *g* at 4°C for 10 min. To load the endogenous small G proteins with GDP or guanosine-5′-*O*-(3-thio)triphosphate (GTPγS), aliquots of lysates were incubated for 10 min at ambient temperature in the presence of 10 mM EDTA and 0.5 mM GDP or GTPγS. The loading reactions were stopped by the addition of 20 mM $MgCl_2$ and switching the temperature to 4°C. Equal volumes of lysates were incubated with GST-PAK1 or GST-Rhotekin (10 μg/lysate sample) immediately for 40 min at 4°C under constant agitation. The lysate-incubated beads were washed three times with the lysis buffer, and the bound RhoA and Rac1 were detected by anti-RhoA and anti-Rac1 antibodies (Santa Cruz Biotechnology, Santa Cruz, CA; Upstate Biotechnology, Lake Placid, NY) and visualized by enhanced chemiluminescence (PerkinElmer Life Sciences). Quantification of the immunoblots was performed with the use of AlphaImager system (Alpha Innotech, San Leandro, CA). For comparison of the level of the active RhoA and Rac1, the amount of GST-Rhotekin or PAK-bound small GTP-binding protein was normalized to the total amount of RhoA and Rac1 in cell lysates in each sample.

Atomic Emission Spectrometry

Subconfluent monolayers of MDCK cells treated without or with 50 μM ouabain, 1 μM gramicidin, or 50 μM valinomycin for 2 h or cells incubated in K^+-free buffer for 2 h were rinsed three times with 10 ml each of 0.25 M sucrose. The cells of five 100-mm dishes each were pooled in 0.25 M sucrose, digested with HNO_3 (Ultrex II; J.T. Baker, Phillipsburg, NJ) at a final concentration of 40% at 65°C for 15 h and diluted 1:2 with Millipore (Bedford, MA) Milli-Q UF plus filtered water. The ion concentrations were measured with the use of an inductively coupled plasma atomic emission spectrometer (Vista Axial 730; Varian, Walnut Creek, CA). The concentrations for Na^+ (588.995 nm), K^+ (766.941 nm), and Mg^{2+} (285.213 nm) were determined and the Na^+ and K^+ concentrations were normalized to the total Mg^{2+} content (internal control).

RESULTS

Na,K-ATPase Inhibition by Ouabain Prevents Formation of Functional Tight Junctions, Desmosomes, and Establishment of Epithelial Polarity

To understand the role of Na,K-ATPase in the formation of tight junctions and desmosomes we used a Ca^{2+}-switch assay which is commonly used to monitor the development of junctional complexes in MDCK cells (Gonzalez-Mariscal *et al.*, 1985). In the Ca^{2+}-switch assay, MDCK monolayers formed in the presence of low calcium (<5 μM) medium, are transferred to medium containing normal calcium levels (1.8 mM), which increases cell-cell contact and initiates assembly of junctional complexes. To test whether Na,K-ATPase enzymatic activity is necessary for development of junctions, we pretreated MDCK monolayers maintained in low calcium medium with ouabain to specifically inhibit Na,K-ATPase for 1 h before transfer to normal calcium-containing medium. At selected times, cells were fixed and the presence of tight junctions was monitored by immunofluorescence localization of tight junction proteins, transmission electron microscopy (TEM), and by measuring the TER. Desmosomes were visualized by immunofluorescence of desmosomal proteins and TEM.

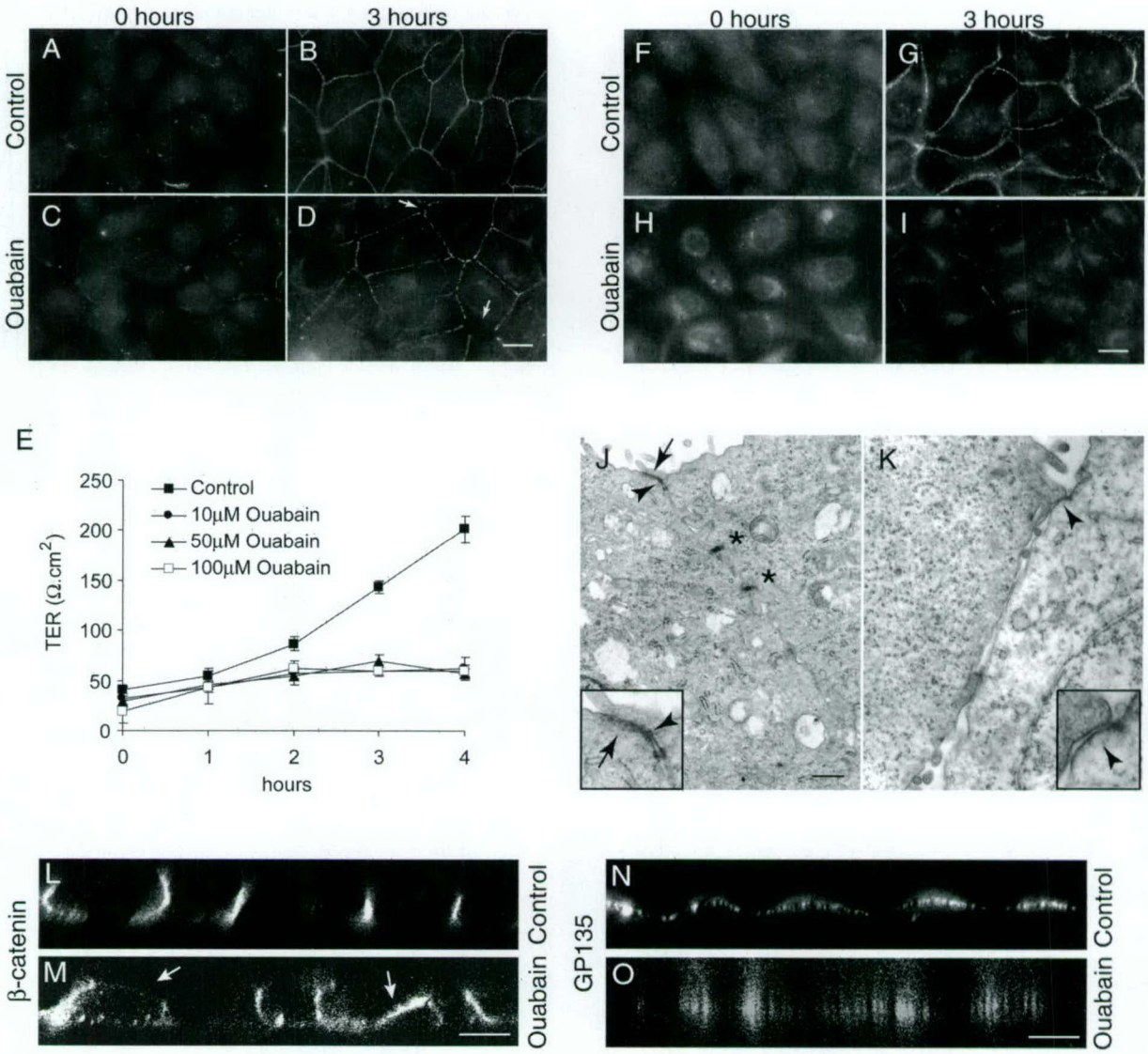

Figure 1. Inhibition of Na,K-ATPase activity prevents the formation of tight junctions and desmosomes and the induction of polarity in MDCK cells. (A–D) Immunofluorescence localization of ZO-1. At 0 h in both control (A) and ouabain-treated cells (C), the ZO-1 staining is intracellular. At 3 h ouabain-treated cells show incomplete ZO-1 rings (arrows in D) compared with the complete ring-like staining revealed by control cells (B). (E) Transepithelial electrical resistance measurement. Ouabain-treated cells did not show an increase in the TER over time. (F–I) Immunofluorescence localization of desmocollin. Note that in ouabain-treated cells the desmocollin staining is predominantly intracellular (I) compared with control cells (G). At 0 h in both control (F) and ouabain-treated cells (H) the desmocollin staining is intracellular. (J and K) Transmission electron microscopy. Tight junctions (arrows), adherens junctions (arrowheads), and desmosomes (asterisks) were formed in control cells (J), whereas ouabain-treated cells (K) had no tight junctions and desmosomes. Inserts are the higher magnification of the tight junction regions in J and K. (L–O). Confocal microscope X-Z sections. Note the polarized localization of β-catenin (L) and GP135 (N) in control cells and nonpolarized distribution of these markers in ouabain-treated cells (M and O). Bars in A–D and F–I, 10 μm; J and K, 500 nm; and L–O, 5 μm.

Before the Ca^{2+}-switch (0 h), the tight junction protein ZO-1 showed cytoplasmic staining in both control and ouabain-treated cells (Figure 1, A and C). At 1 and 2 h after the Ca^{2+}-switch, ZO-1 was localized to the plasma membrane with a discontinuous staining pattern. A visible difference in the ZO-1 staining pattern between control and ouabain-treated cells was not detected at these time points (our unpublished results). At 3 h, the ZO-1 staining in control cells showed a continuous staining pattern (Figure 1B), indicating that the tight junctions were established. In contrast, in ouabain-treated cells, the ZO-1 staining remained discontinuous with a beaded appearance and with regions clearly lacking ZO-1 (Figure 1D, arrows). Prolonged incubation did not change the discontinuous staining pattern of ZO-1. Instead, ZO-1 became even more intracellular. Other tight junction proteins such as occludin showed a similar

staining pattern (our unpublished results). Ouabain treatment did not affect the protein levels of ZO-1 as revealed by immunoblot analysis (our unpublished results). These results showed that in the presence of ouabain tight junction proteins translocate to the plasma membrane but fail to form a complete ring-like pattern like in control cells.

A functional tight junction is required to maintain the polarized distribution of distinct apical and basolateral markers. In MDCK cells the TER measurement during the Ca^{2+}-switch assay has been used to monitor formation of functional tight junctions (Gonzalez-Mariscal *et al.*, 1985; Jou *et al.*, 1998). Cells grown on Transwell filters were subjected to a Ca^{2+}-switch assay and the development of TER was measured. The TER in control cells gradually increased after the Ca^{2+}-switch and within 3 h reached ~200 $\Omega \cdot cm^2$, a value reported for MDCK clone II (Gonzalez-Mariscal *et al.*, 1985; Jou *et al.*, 1998) (Figure 1E). In contrast, the TER in ouabain-treated cells reached only ~50 $\Omega \cdot cm^2$, and this value did not increase over 4 h of ouabain treatment. Moreover, confocal microscope vertical (X-Z) sections revealed a polarized distribution of β-catenin (a basolateral marker) (Rajasekaran *et al.*, 1996) (Figure 1L) and GP135 (an apical marker) (Ojakian and Schwimmer, 1988) (Figure 1N) in control cells, whereas in ouabain-treated cells these markers were distributed in a nonpolarized manner (Figure 1, M and O). These results indicate that ouabain-mediated inhibition of Na,K-ATPase activity prevents formation of functional tight junctions and the establishment of polarization in MDCK cells.

To monitor the assembly of desmosomes we used antibodies against desmoplakin, a peripheral membrane protein and desmocollin, a transmembrane protein localized to desmosomes (Garrod *et al.*, 1996). Both markers showed identical patterns. The results obtained from the anti-desmocollin antibody staining are shown (Figure 1, F–I). In both control and ouabain-treated cells, at 0 h of the Ca^{2+}-switch, desmocollin was distinctly localized intracellular with barely detectable levels on the plasma membrane (Figure 1, F and H). Desmocollin and desmoplakin were predominantly cytoplasmic at 1 and 2 h after the Ca^{2+}-switch (our unpublished results). After 3 h of Ca^{2+}-switch the desmocollin staining in control cells revealed a distinct dot-like pattern circumscribing the cells, typical of the desmosome staining pattern in MDCK cells (Figure 1G). In contrast, in ouabain-treated cells, after 3 h of Ca^{2+}-switch, desmocollin was predominantly intracellular with barely detectable staining at the cell-cell contacts (Figure 1I). This pattern was maintained after prolonged incubation with ouabain. Immunoblot analysis of desmoglein (a membrane component of the desmosome) and desmoplakin did not show significant changes in the levels of these proteins in ouabain-treated cells (our unpublished results). These results demonstrate that inhibition of Na,K-ATPase activity largely affects translocation of desmosomal proteins to the plasma membrane, whereas it does not affect translocation of tight junction proteins to the plasma membrane.

To further confirm the effect of ouabain on the assembly of tight junctions and desmosomes we performed TEM of control and ouabain-treated cells after 3 h of Ca^{2+}-switch. TEM revealed the presence of typical tight junctions, adherens junctions, and desmosomes in cell-cell contact sites in control cells (Figure 1J). In contrast, in ouabain-treated cells tight junctions and desmosomes were rarely detected, although adherens junction-like structures were clearly seen (Figure 1K). Quantitative analysis of the TEM data was performed by scoring the number of tight junctions and desmosomes in ~50 cell-cell contact sites. Control cells revealed tight junctions and desmosomes in 96 and 100% of cell-cell contacts, respectively. In contrast, ouabain-treated cells showed putative tight junctions in only 14% and desmosome-like structures in 15% of the cell-cell contacts. Ouabain-treated cells showed typical adherens junctions in 54% of the cell-cell contacts. Taken together, these results demonstrate that inhibition of Na,K-ATPase by ouabain prevents formation of functional tight junctions and desmosomes and the polarized phenotype in MDCK cells.

Effect of Na,K-ATPase Inhibition on Formation of Tight Junctions, Desmosomes, and Establishment of Polarity Is Reversible

As an independent means to test the role of Na,K-ATPase in the formation of tight junctions and desmosomes we used K^+ depletion to inhibit Na,K-ATPase (Pollack *et al.*, 1981; Pressley 1988; Buffin-Meyer *et al.*, 1996). In this assay, the pump function can be restored by the addition of K^+ and thus the reversibility of the effect of Na,K-ATPase inhibition can be tested. MDCK cells maintained in low calcium medium were preincubated in K^+- and Ca^{2+}-free buffer for 1 h to inactivate the Na,K-ATPase and the Ca^{2+}-switch assay was performed in K^+-free medium. Immunofluorescence staining of ZO-1 after 3 h of switch to K^+-free medium containing Ca^{2+} showed ZO-1 localized to the plasma membrane although without forming a continuous ring-like structure (Figure 2A). This pattern was similar to that of ouabain-treated cells (Figure 1D). Subsequent incubation of these cells for 5 h in K^+-containing medium resulted in a complete ZO-1 ring circumscribing the cells (Figure 2B). The TER of MDCK cells in K^+-free buffer did not increase up to 3 h after the Ca^{2+}-switch (Figure 2E). However, upon transfer of the cells from K^+-free to K^+-containing culture medium, the TER increased dramatically and reached a value of ~400 $\Omega \cdot cm^2$ (Figure 2E) within 2 h, indicating formation of functional tight junctions. Confocal microscope vertical (X-Z) sections of cells maintained in K^+-free medium revealed a nonpolarized distribution of β-catenin (Figure 2H) and GP135 (Figure 2J). Subsequent transfer of these cells to K^+-containing culture medium resulted in the polarized distribution of these markers (Figure 2, I and K). The assembly of desmosomes in K^+-free buffer was similar to ouabain-treated cells. In K^+-free buffer the translocation of desmocollin to the plasma membrane was inhibited and the staining was predominantly intracellular (Figure 2C). Subsequent incubation of these cells in K^+-containing culture medium for 5 h resulted in a dot-like desmocollin staining at the sites of cell-cell contact (Figure 2D), indicating formation of desmosomes. Electron microscopy studies confirmed the absence of tight junctions and desmosomes in MDCK cells maintained in K^+-free buffer (Figure 2F), whereas a subsequent transfer to K^+-containing culture medium resulted in the formation of tight junctions and desmosomes (Figure 2G). Quantitative TEM analysis of cells maintained in K^+-free buffer showed the presence of tight junctions and desmosomes in only 2 and 3% of cell-cell contacts, respectively. After K^+ restoration tight junctions were detected in 90%

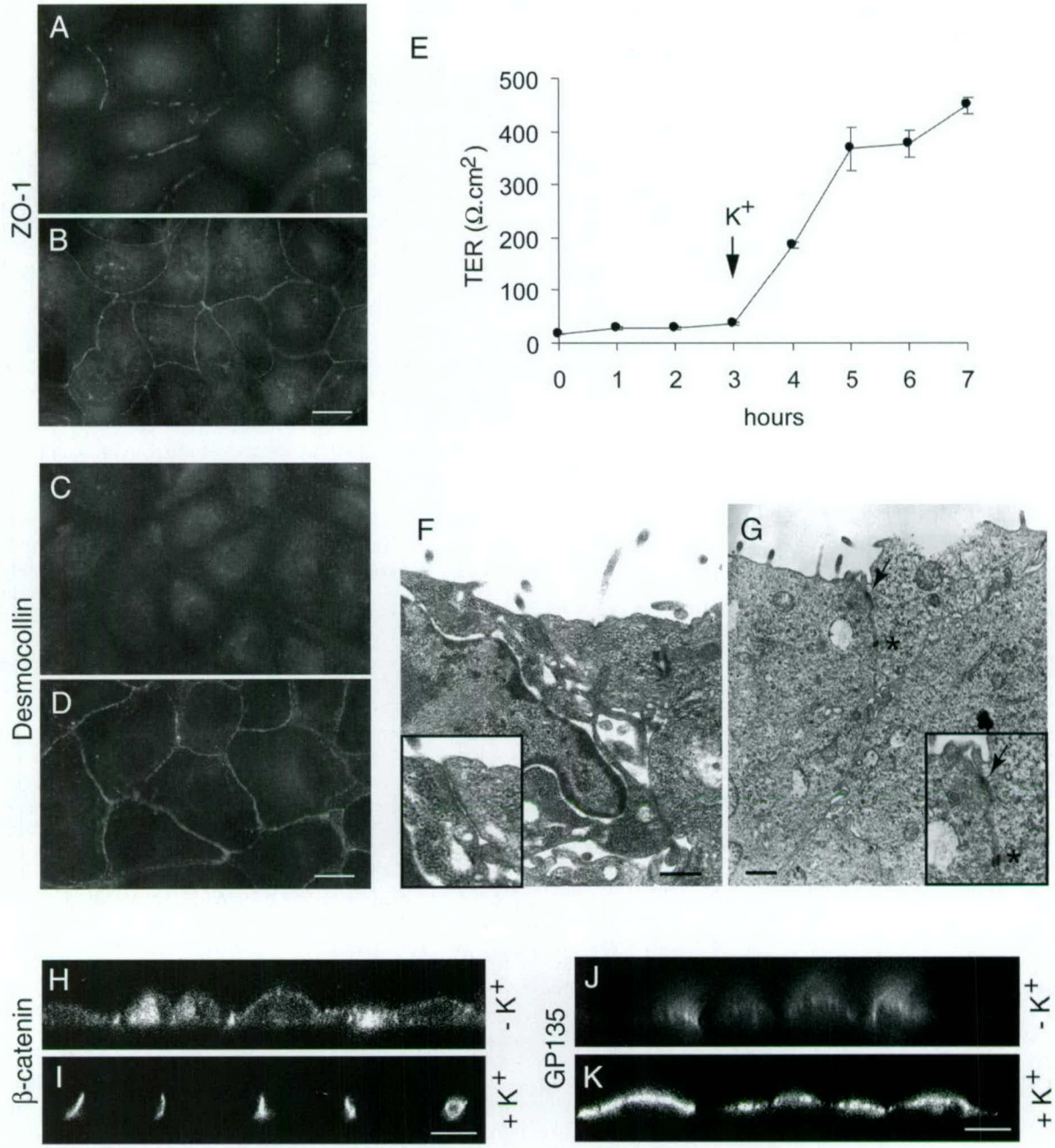

Figure 2. Na,K-ATPase-mediated inhibition of formation of tight junctions and desmosomes is reversible. Immunofluorescence localization of ZO-1 (A and B) and desmocollin (C and D). Cells incubated in K^+-free medium show an incomplete ZO-1 ring at the plasma membrane region (A) and intracellular localization of desmocollin (C). Replenishment of K^+ results in a complete ZO-1 ring (B) and plasma membrane localization of desmocollin (D). (E) Measurement of TER. Note an increase in the TER as soon as the cells are shifted to K^+-containing medium. (F and G) Transmission electron microscopy. Note the absence of tight junctions (arrow) and desmosomes (asterisk) in K^+-free medium (F) and their presence in K^+-containing medium (G). Insets in F and G are the higher magnifications of tight junction regions. (H–K) Confocal microscope X-Z sections. Note the nonpolarized distribution of β-catenin (H) and GP135 (J) under K^+-depleted condition and the polarized distribution of β-catenin (I) and GP135 (K) after K^+ repletion. Bars in A–D, 10 μm; F and G, 500 nm; and H–K, 5 μm.

and desmosomes in 85% of cell-cell contacts. These results further demonstrate that Na,K-ATPase enzymatic activity is necessary for formation of tight junctions and desmosomes in MDCK cells.

Inhibition of Na,K-ATPase in Na^+-free Medium Does not Affect Formation of Tight Junctions, Desmosomes, and Epithelial Polarity

Inhibition of Na,K-ATPase results in an increased intracellular sodium concentration (Pollack *et al.*, 1981; Rayson 1989; Yamamoto *et al.*, 1993; Rajasekaran *et al.*, 2001) and sodium measurements with the use of atomic emission spectrometry revealed that the intracellular sodium levels $[Na^+]_i$ of MDCK cells (~12 mM) (Rajasekaran *et al.*, 2001) increased >10-fold upon ouabain treatment or sevenfold by K^+ depletion. The intracellular K^+ level of MDCK cells was 148 mM. Inhibition of sodium pump by ouabain or K^+ depletion decreased the intracellular potassium concentration to 12 and 50% of the control, respectively. To test whether increased $[Na^+]_i$ is involved in the inhibition of tight junction and desmosome formation we first treated MDCK cells with ouabain in Na^+-free medium to prevent the increase of $[Na^+]_i$ after ouabain treatment. Cells maintained in low calcium medium were subjected to a Ca^{2+}-switch in a Na^+-free medium with or without ouabain as described in MATERIALS AND METHODS. After 3 h of Ca^{2+}-switch, the cells were fixed and stained for tight junction and desmosomal proteins. As shown in Figure 3, both control (Figure 3A) and ouabain-treated cells (Figure 3B) clearly showed a complete ZO-1 ring on the plasma membrane, indicating that tight junctions are formed in these cells. Immunofluorescence of desmocollin (Figure 3, C and D) and desmoplakin (our unpublished data) revealed a distinct dot-like staining pattern circumventing the cells in both control (Figure 3C) and ouabain-treated cells (Figure 3D). Control and ouabain-treated cells showed high TER values within 4 h of Ca^{2+}-switch in Na^+-free medium (Figure 3E). Under Na^+-free conditions the control cells had a higher TER resistance compared with cells maintained in normal medium (compare Figures 1E and 3E), possibly due to decreased tight junction permeability. Confocal microscope vertical (X-Z) sections confirmed the polarized distribution of β-catenin and GP135 in both control and ouabain-treated cells (Figure 3, H–K). In contrast to the effect of ouabain on junction formation in Na^+-containing medium ouabain treatment in Na^+-free medium did not decrease the number of tight junctions or desmosomes in both control (Figure 3F) and ouabain-treated cells (Figure 3G). Cell-cell contacts of cells in Na^+-free medium showed tight junctions and desmosomes similar to control cells in Na^+-containing medium. Because in Na^+-free medium ouabain treatment did not affect the formation of tight junctions, desmosomes and establishment of polarity these results are consistent with the idea that increased $[Na^+]_i$ after inhibition of Na,K-ATPase may be involved in the inhibition of the formation of tight junctions and desmosomes in MDCK cells. Furthermore, these results also establish that the observed effect of ouabain is not due to a toxic side effect.

Sodium Ionophore Gramicidin Treatment Affects Formation of Tight Junctions, Desmosomes, and Establishment of Polarity

To further test whether increased $[Na^+]_i$ affects formation of tight junctions and desmosomes we treated MDCK cells with the sodium ionophore gramicidin and a potassium ionophore, valinomycin. Sodium ionophores have been used widely to test the involvement of intracellular sodium on cell functions (Harber *et al.*, 1987; Yamamoto *et al.*, 1993; Liu *et al.*, 2000). Gramicidin A is an ion channel-forming antibiotic that greatly facilitates Na^+ entry into cells (Rothstein and Mack, 1990), and specifically increases the intracellular Na^+ concentration. Valinomycin is a cyclic dodecadepeptide that transports K^+ through the plasma membrane, inducing a potassium leak (Vaaraniemi *et al.*, 1997). Intracellular sodium measurements revealed a >12-fold increase in $[Na^+]_i$ in gramicidin-treated cells, whereas valinomycin-treated cells did not reveal a significant change in the intracellular sodium levels compared with untreated MDCK cells. Treatment of MDCK cells with gramicidin during the Ca^{2+}-switch showed an effect similar to that of ouabain. Three hours after the Ca^{2+}-switch, ZO-1 was clearly localized on the plasma membrane, although without a continuous ring pattern (Figure 4A). The immunofluorescence staining of occludin showed identical results (our unpublished results). In the presence of gramicidin, 3 h after the Ca^{2+}-switch, immunofluorescence of desmocollin (Figure 4B) and desmoplakin (our unpublished results) showed a predominantly cytoplasmic staining pattern similar to ouabain-treated cells (compare Figures 4B and 1I). In contrast to gramicidin-treated cells, valinomycin-treated cells resembled control cells. Three hours after the Ca^{2+}-switch ZO-1 formed a continuous ring at the plasma membrane (Figure 4C). Occludin showed a similar staining pattern (our unpublished results). Both desmocollin (Figure 4D) and desmoplakin (our unpublished results) showed a punctate staining pattern at cell-cell contact sites. Consistent with the localization of tight junction proteins, valinomycin-treated cells had TER values of ~250$\Omega \cdot cm^2$ within 4 hours. In contrast, gramicidin-treated cells did not develop TER with time (Figure 4E). Confocal microscope vertical (X-Z) sections of gramicidin-treated cells revealed nonpolarized distribution of β-catenin (Figure 4F) and GP135 (Figure 4H), whereas in valinomycin-treated cells these markers were distributed in a polarized manner (Figure 4, G and I). Furthermore, TEM revealed tight junctions and desmosomes in valinomycin-treated cells but showed a significant decrease in junctions in gramicidin-treated cells (our unpublished results). Tight junctions and desmosomes were present in 100% of the cell-cell contacts in valinomycin-treated cells, whereas gramicidin-treated cells showed putative tight junctions in only 23% and desmosome-like structures in 14% of the cell-cell contacts. Taken together, these results demonstrate that the intracellular Na^+ homeostasis regulated by Na,K-ATPase is involved in the assembly of functional tight junctions, desmosomes, and the induction of polarity in MDCK cells.

Inhibition of Na,K-ATPase Prevents Formation of Bundled Stress Fibers

Recent studies have implicated a role for filamentous actin in regulation of tight junctions (Nusrat *et al.*, 1995; Jou *et al.*,

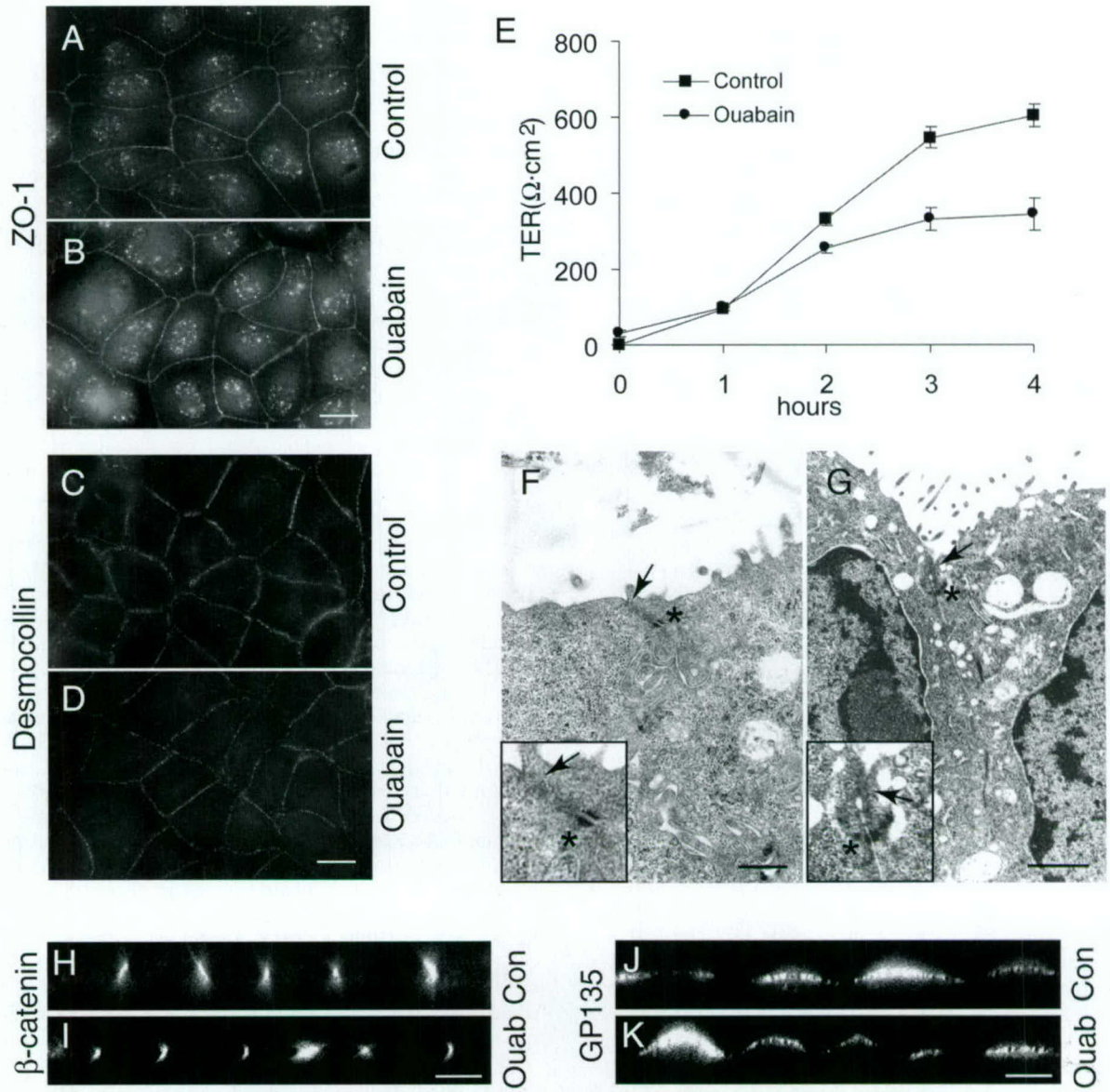

Figure 3. Ouabain treatment under sodium-free conditions does not affect the formation of tight junctions and desmosomes. A and B and C and D are the immunofluorescence localization of ZO-1 and desmocollin, respectively. Note the comparable staining pattern in control (A and C) and ouabain-treated (B and D) cells. (E) Measurement of TER. (F and G) Transmission electron micrographs of control (F) and ouabain-treated (G) cells show tight junctions (arrow) and desmosomes (asterisk). Insets are the higher magnification of the tight junction region in F and G. (H–K) Confocal microscope X-Z sections. Note the polarized distribution of β-catenin and GP135 in control and ouabain-treated cells. Bars in A–D, 10 μm; F and G, 500 nm and 1 μm, respectively; and H–K, 5 μm.

1998) and desmosomes (Vasioukhin *et al.*, 2000). Therefore, we tested whether Na,K-ATPase plays a role in the organization of the actin cytoskeleton during the formation of tight junctions and desmosomes in MDCK cells. Organization of the actin cytoskeleton was monitored by FITC-phalloidin labeling and epifluorescence microscopy. In control cells, at 0 h stress fibers were not detected at the bottom of the cells (Figure 5A). After 1 h of Ca^{2+}-switch stress fibers began to appear at the bottom of the cells (our unpublished results) and after 3 h bundles of stress fibers were apparent (Figure 5B). These bundles of stress fibers gradually disappeared and were not detected after 48 h of Ca^{2+}-switch (our unpublished results). In contrast, in ouabain-treated cells the bundled stress fibers did not form (Figure 5, C and D). However, these cells showed a distinct cortical actin cytoskeleton more close to the bottom of the cells (Figure 5D). Like in ouabain-treated cells, K^+ depletion also inhibited the formation of bundles of stress fibers and induced a distinct cortical actin closer to the base of the cells (Figure 5E). Adding K^+ to the cells maintained in low K^+ resulted in bundles of

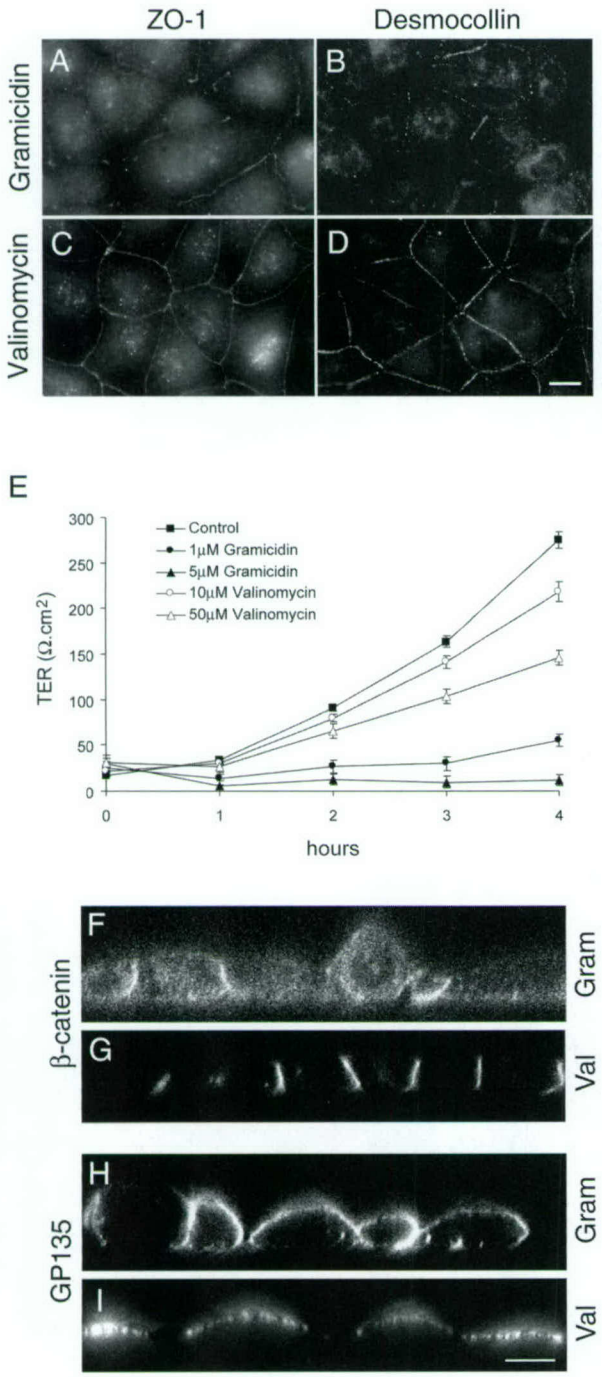

Figure 4. Treatment of MDCK cells with the sodium ionophore gramicidin inhibits the formation of tight junctions. (A and C) Immunofluorescence localization of ZO-1 and desmocollin (B and D), respectively, of gramicidin- (A and B) and valinomycin (C and D)-treated cells. (E). TER measurement of gramicidin- and valinomycin-treated cells. (F–I) Confocal microscope X-Z sections. Bars in A–D, = 10 μm; F–I, 5 μm.

stress fibers as seen in control cells (compare Figure 5, B and F). Formation of bundled stress fibers was markedly inhibited by gramicidin but not by valinomycin (our unpublished results). These results indicate that the transient formation of bundled stress fibers correlates with the assembly of tight junctions and desmosomes and that inhibition of Na,K-ATPase prevents the formation of bundled stress fibers.

Endogenous RhoA Activity Is Highly Reduced in Na,K-ATPase Inhibited or Gramicidin-treated Cells

The RhoA GTPase has been implicated in regulation of actin stress fiber formation in fibroblasts and in epithelial cells (Ridley and Hall, 1992; Mackay and Hall 1998; Jou and Nelson, 1998; Jou *et al.*, 1998). Moreover, both RhoA and Rac1, a closely related family member, are essential for the assembly and function of tight junctions in MDCK cells (Jou *et al.*, 1998). Therefore, we tested the possible involvement of these GTPases in the Na,K-ATPase-mediated formation of junctional complexes. For this purpose, we determined the endogenous levels of active RhoA in control cells and ouabain-treated cells with the use of an in vitro biochemical assay (Ren *et al.*, 1999; Zhu *et al.*, 2000). In this assay, GST-Rhotekin, a GST-fusion protein containing the Rho binding domain (which binds active RhoA bound to GTP) is incubated with cell lysate and the bound, active RhoA is detected by immunoblot analysis. The specificity of this assay is demonstrated by loading the cell lysate with a nonhydrolyzable analog of GTP, GTPγS (total RhoA), and by replacing GTPγS with GDP that inactivates Rho and therefore does not bind to GST-Rhotekin (Figure 5G, compare lanes 9 and 10). Consistent with the formation of stress fibers, control cells showed high levels of active RhoA (Figure 5G, lanes 5–8, and G′) compared with ouabain-treated cells in which the level of active RhoA gradually decreased and became undetectable after 2 h of treatment (Figure 5G, lanes 1–4, and G′). The protein levels of RhoA remained unchanged in both control and ouabain-treated cells (Figure 5G, labeled as total, lanes 1–10). Like in ouabain-treated cells, depletion of K^+ resulted in the inhibition of RhoA activity (Figure 5H, lanes 1–3, and H′) and addition of K^+ resulted in the reactivation of RhoA activity (Figure 5H, lanes 4 and 5, and H′). These results indicate that the Na,K-ATPase activity has a direct impact on the activation state of RhoA. Gramicidin-treated cells showed reduced RhoA activity compared with valinomycin-treated cells (Figure 5I, compare lanes 2–4 and 5–7, and I′), indicating that increased intracellular sodium may either directly or indirectly inhibit the activity of RhoA. We also measured the endogenous Rac1 activity in response to modulation of Na,K-ATPase activity and found that neither the expression level nor the activation state of Rac1 was affected by ouabain or K^+ depletion (our unpublished results). Thus, Na,K-ATPase appears to be a specific upstream regulator of RhoA GTPase.

Overexpression of Wild-Type RhoA GTPase Abolishes Effects of Na,K-ATPase Inhibition on Junction Formation and Epithelial Polarity

Both the dominant negative and active forms of RhoA GTPase have profound effects on tight junctions in MDCK cells (Jou *et al.*, 1998). Therefore, to further validate the specific

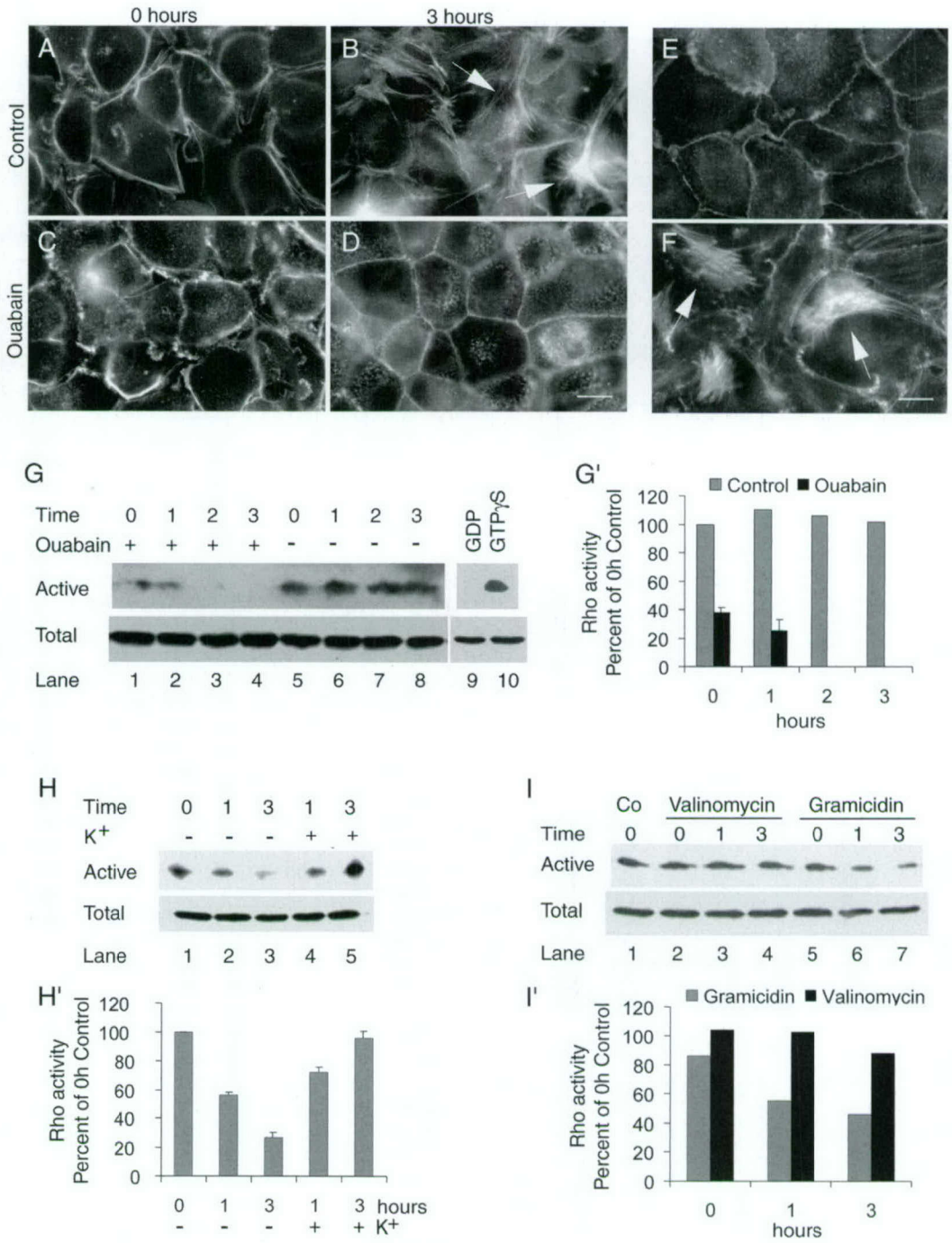

Figure 5. Inhibition of Na,K-ATPase prevents the formation of bundled stress fibers and inhibits RhoA GTPase activity. (A–F) FITC-phalloidin staining of filamentous actin. At 0 h no stress fibers were detected in control cells (A) and cells treated with ouabain (C). Bundled stress fibers were present at 3 h in control cells (B, arrows) but were not detected in ouabain-treated cells (D). Phalloidin labeling of cells maintained under K^+-free condition (E) and cells transferred to K^+-containing medium (F) are shown. Note the presence of bundled stress fibers (arrows) after transfer to K^+-containing medium. Bars in A–F, 10 μm. (G and G′) Effect of ouabain treatment on RhoA activity. (G) Immunoblot showing active and total RhoA in ouabain-treated and control cells. The results shown are the representative data obtained from three independent experiments. (G′) Quantification of the immunoblot data represents the average of three independent determinations done in duplicate. Bars indicate the SE. For control the error bars are so small that they are not seen in the figure. (H and H′) Effect of K^+ depletion and repletion on the RhoA activity. Immunoblot of active and total RhoA (H) and quantification of the immunoblot data (H′) representing the mean of two independent determinations done in duplicate. (I and I′) Effect of gramicidin and valinomycin on RhoA activity. Immunoblot of total and active RhoA (I) and quantification of the immunoblot data done in duplicate (I′).

role of RhoA in formation of tight junctions and desmosomes we used MDCK cells expressing wild-type RhoA GTPase (MDCK-$RhoA_{wt}$) under control of the tetracycline repressible transactivator. In MDCK-$RhoA_{wt}$ cells, the levels of RhoA increased severalfold after withdrawal of the transcription repressor doxycycline (DC) (Figure 6A) (Leung *et al.*, 1999). In induced cells (−DC) the level of active RhoA was 2.7-fold more than that of control cells maintained in the presence of doxycycline (+DC). Three hours after ouabain treatment, induced cells showed 2.1-fold more active RhoA GTPase than uninduced cells (Figure 6B). Consistent with the presence of active RhoA in induced cells, bundled stress fibers were distinctly seen after 3 h of ouabain treatment, whereas these fibers were scarcely present in uninduced cells (Figure 6, C and D). On ouabain treatment RhoA-induced cells revealed an uninterrupted ZO-1 staining pattern, whereas uninduced cells showed a disrupted staining pattern (Figure 6, E and F). The TER of ouabain-treated induced cells was significantly higher than that of uninduced cells ($p < 0.01$) (Figure 6I). Furthermore, confocal microscope vertical sections revealed a polarized distribution of β-catenin and GP135 in induced ouabain-treated cells (Figure 6, J and L). In contrast, in uninduced cells these markers were distributed in a nonpolarized manner (Figure 6, K and M). These results demonstrate that functional tight junctions are formed even in the presence of ouabain in RhoA-overexpressing cells. Desmocollin revealed a distinct plasma membrane localization in induced, ouabain-treated cells (Figure 6G), whereas uninduced cells showed an intracellular staining pattern (Figure 6H). TEM revealed tight junctions and desmosomes in 88% of the cell-cell contacts in induced, ouabain-treated cells, whereas uninduced cells showed putative tight junctions in only 12% and desmosome-like structures in 18% of the cell-cell contacts (Figure 6, N and O). These results are consistent with the idea that Na,K-ATPase mediates its action through RhoA and that RhoA function is essential for the formation of tight junctions and desmosomes and to maintain the polarized phenotype of MDCK cells.

Levels and Localization of E-Cadherin and Its Associated α-,β-, and γ-Catenins Are not Affected in Na,K-ATPase-inhibited Cells

The cell adhesion molecule E-cadherin has been implicated in formation and maintenance of tight junctions and desmosomes (Gumbiner *et al.*, 1988; Watabe *et al.*, 1994). Therefore, we tested whether ouabain treatment of MDCK cells affects expression or localization of E-cadherin in these cells. In control cells, at 0 h E-cadherin showed a predominant intracellular staining. At this time point the plasma membrane localization of E-cadherin was barely detectable (Figure 7A). After 3 h of Ca^{2+}-switch the intracellular staining of E-cadherin decreased dramatically, whereas the plasma membrane staining increased (Figure 7B). In ouabain-treated cells at 0 h E-cadherin was localized intracellularly similar to that of control cells (Figure 7C). At 3 h after Ca^{2+}-switch, like in control cells, the intracellular E-cadherin staining decreased and the plasma membrane staining increased at cell-cell contact sites (Figure 7D). Immunoblot analysis of total cell lysates of control and ouabain-treated cells showed no differences in the levels of E-cadherin, α-, β-, and γ-catenin (Figure 7E). Coimmunoprecipitation showed no detectable differences in the levels of α-, β-, and γ-catenin associated with E-cadherin in control and ouabain-treated cells (our unpublished results). In addition, ouabain-treated cells revealed adherens junctions (Figure 1K), the formation of which requires functional E-cadherin (Gumbiner *et al.*, 1988; Watabe *et al.*, 1994; Yap *et al.*, 1997). These results indicate that E-cadherin is functional in ouabain-treated cells and that inhibition of Na,K-ATPase function does not affect expression or localization to the plasma membrane of E-cadherin and catenins in MDCK cells.

DISCUSSION

Distinct Signaling Mechanisms May Regulate Formation of Tight Junctions and Desmosomes

We used two independent methods, ouabain treatment or K^+ depletion, to show that inhibition of Na,K-ATPase prevents the formation of functional tight junctions and desmosomes and the induction of polarity in MDCK cells. Rapid restoration of tight junctions, desmosomes, and epithelial polarity upon K^+ repletion demonstrated that the effects of Na,K-ATPase inhibition were reversible and that Na,K-ATPase function is involved in the formation of these junctions in MDCK cells. In a previous report we suggested that the tight junction formation may involve two independent events i.e., E-cadherin-dependent initial translocation of tight junction proteins to the plasma membrane and an E-cadherin-independent assembly of functional tight junctions (Rajasekaran *et al.*, 2001). Na,K-ATPase function appears to be involved in the latter event because tight junction proteins were clearly seen on the plasma membrane in Na,K-ATPase inhibited cells yet these cells did not develop TER and had a highly reduced number of tight junctions compared with control cells. E-cadherin-dependent signaling events have been suggested to mediate the translocation of tight junction proteins from the cytoplasm to the plasma membrane (Balda *et al.*, 1996; Rajasekaran *et al.*, 1996). Because ouabain-treated MDCK cells express functional E-cadherin, the localization of tight junction proteins at the plasma membrane suggests that E-cadherin-mediated signaling was not affected in these cells. Therefore, functional E-cadherin might be essential for initial events that trigger the translocation of ZO-1 to the plasma membrane, whereas Na,K-ATPase function is crucial for events that regulate the formation of an undisrupted ZO-1 ring, functional tight junctions, and consequently, the polarized epithelial phenotype.

It has been suggested that tight junctions and desmosomes are formed in a coordinate manner after E-cadherin-mediated cell-cell contact in epithelial cells (Gumbiner *et al.*, 1988). We found a distinct difference in the staining pattern of tight junction and desmosomal proteins in Na,K-ATPase inhibited cells. In contrast to tight junction proteins the localization of desmosomal proteins to the plasma membrane was substantially reduced and desmosomes were poorly assembled in the presence of ouabain and during K^+ repletion. These results suggest that signaling events that mediate the translocation of desmosomal proteins to the plasma membrane and the formation of desmosomes require the function of Na,K-ATPase and might be regulated in part by E-cadherin-independent mechanisms.

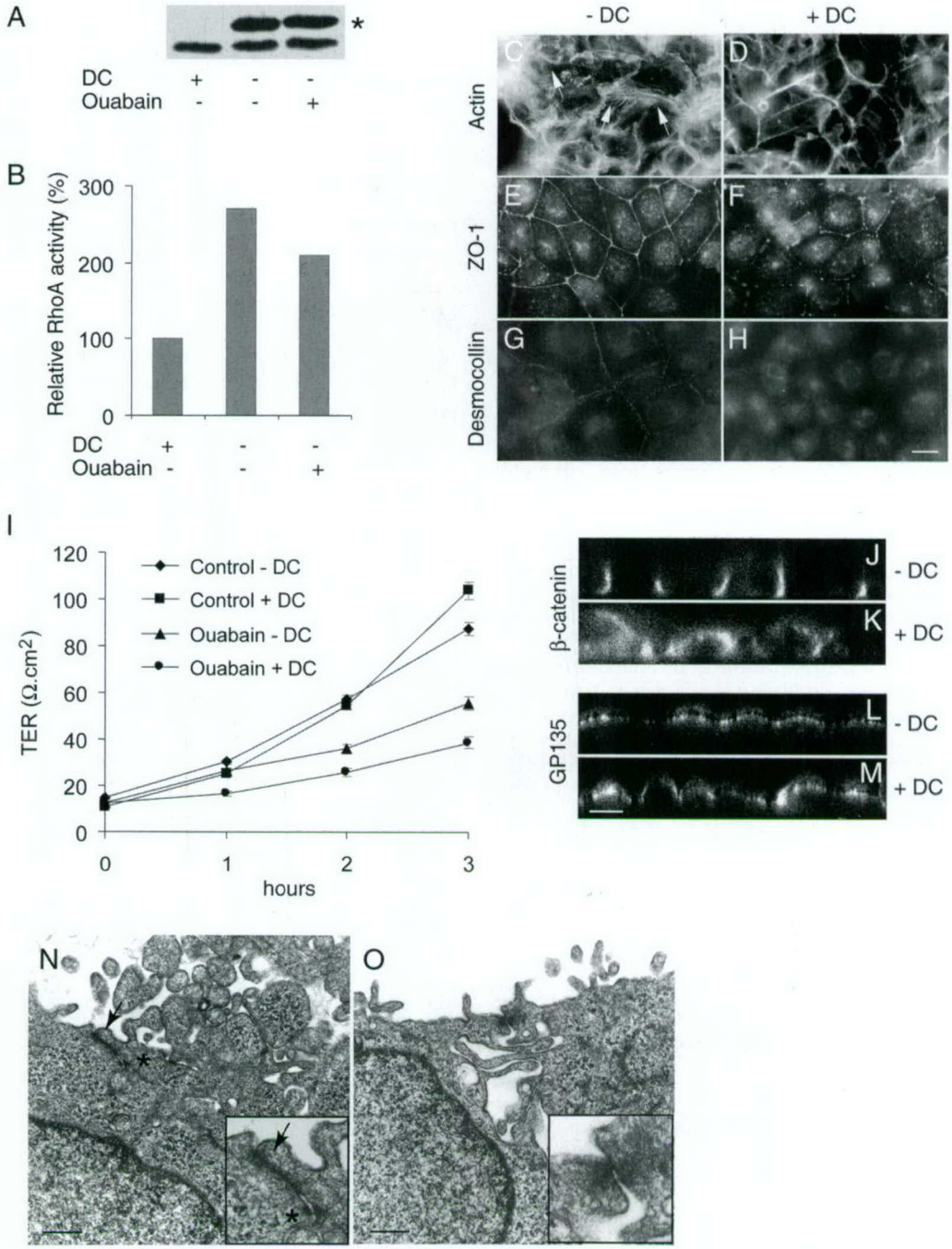

Figure 6. Formation of tight junctions, desmosomes and the induction of polarity in ouabain-treated MDCK-RhoA$_{wt}$ cells overexpressing RhoA. −DC and +DC represent ouabain-treated induced and noninduced MDCK-RhoA$_{wt}$ cells, respectively. (A) RhoA immunoblot showing induced high molecular mass Myc-tagged (*) and endogenous RhoA after the withdrawal of DC. (B) Relative levels of active RhoA GTPase. The results shown are the representative data obtained from two independent experiments. (C and D) FITC-phalloidin staining of filamentous actin. Note the presence of bundled stress fibers in C and their absence in D. (E and F) Immunofluorescence of ZO-1. Ouabain-treated induced cells show a complete ring-like staining compared with the incomplete ZO-1 ring in noninduced cells. (G and H) Immunofluorescence of desmocollin. In ouabain-treated induced cells desmocollin is localized to the plasma membrane compared with the intracellular staining in noninduced cells (I). Measurement of TER (J–M). Confocal microscope X-Z sections. Note the polarized distribution of β-catenin and GP135 in ouabain-treated induced cells. (N and O) Transmission electron microscopy. Tight junctions (arrow) and desmosomes (asterisk) are present in ouabain-treated induced cells. Inserts are the higher magnification of the tight junction region in N and O. Bars in C–H, 10 μm; J–M, 5 μm; and N and O, 500 nm.

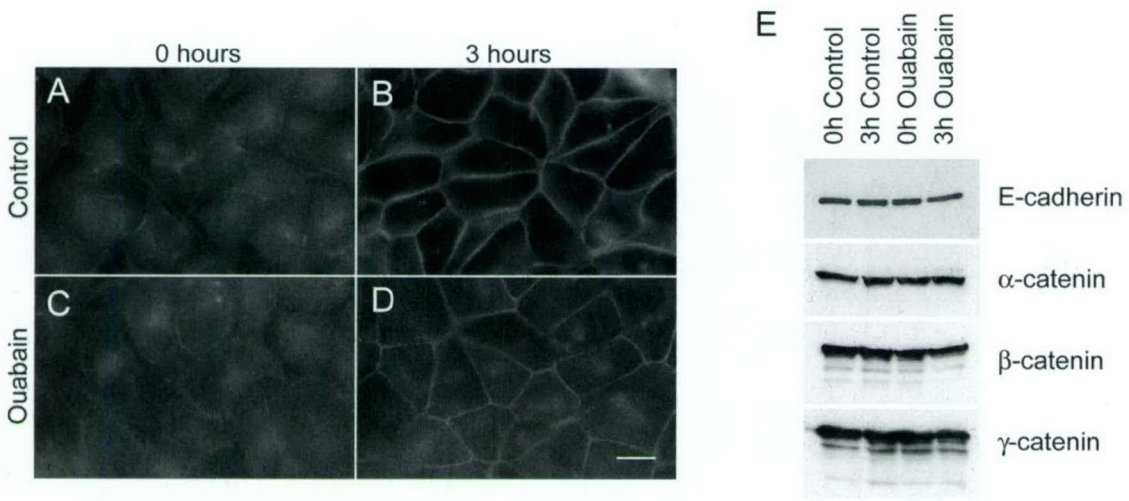

Figure 7. E-Cadherin and catenin expression in ouabain-treated MDCK cells. (A–D) Immunofluorescence of E-cadherin. At 0 h E-cadherin was localized intracellular in both control (A) and ouabain-treated (C) cells. At 3 h E-cadherin was localized on the plasma membrane in control cells (B) and in ouabain-treated cells (D). (E) Immunoblot analysis of E-cadherin, α-catenin, β-catenin, and γ-catenin. Ouabain treatment of MDCK cells during Ca^{2+}-switch did not significantly alter the expression levels of E-cadherin, α-catenin, β-catenin, or γ-catenin. Bar, 10 μm.

Despite functional E-cadherin expression in ouabain-treated cells, the absence of functional tight junctions and desmosomes indicates that E-cadherin function is not sufficient for formation of these junctions in MDCK cells. Potempa and Ridley (1998) have shown that hepatocyte growth factor treatment of MDCK cells did not affect tight junctions and desmosomes but specifically affected adherens junctions the formation of which requires functional E-cadherin. Furthermore, we have shown that tight junction and desmosome formation is not stimulated by ectopic expression of E-cadherin alone in MSV-MDCK cells, but requires coexpression of the β-subunit of Na,K-ATPase (Rajasekaran *et al.*, 2001). In view of these recent results, we suggest that E-cadherin-mediated cell-cell contacts have a role in the signaling events that mediate translocation of tight junction proteins to the plasma membrane, an essential early event required for the assembly of tight junctions in epithelial cells. Thus, E-cadherin function is necessary but may not be sufficient for formation of functional tight junctions and the induction of polarity in MDCK cells. Formation of functional tight junctions and desmosomes additionally requires E-cadherin-independent mechanisms that depend on normal functioning of Na,K-ATPase. Once these junctions are formed and polarity is established, epithelial cells should maintain these junctions to perpetuate their polarized phenotype. Expression of a dominant negative mutant of E-cadherin in polarized MDCK cells did not affect tight junctions or desmosomes, indicating that E-cadherin function may not be necessary to maintain tight junctions and desmosomes in polarized epithelial cells (Troxell *et al.*, 2000). Contreras *et al.* (1999) suggested that prolonged treatment of MDCK monolayers with ouabain resulted in the loss of viability of ~60% of cells and reduced cell-cell and cell-substratum contact and suggested the existence of a link between the pump and attachment. Recent studies in cardiac myocytes have implicated Na,K-ATPase as a signal transducer through protein–protein interactions (Liu *et al.*, 2000). We conclude that signaling mechanisms mediated by both E-cadherin and Na,K-ATPase are likely involved in the formation of functional tight junctions and desmosomes in epithelial cells.

Regulation of RhoA GTPase Activity by Na,K-ATPase and Its Role in Tight Junction and Desmosome Formation

The large reduction of stress fibers in Na,K-ATPase-inhibited cells prompted us to test whether RhoA GTPase, which has been implicated in the formation of stress fibers (Ridley and Hall, 1992; Mackay and Hall, 1998), is affected by Na,K-ATPase inhibition. Ouabain treatment and K^+ depletion consistently reduced levels of endogenous active RhoA in wild-type MDCK cells and of exogenously expressed RhoA in the MDCK T23 clone, indicating that inhibition of Na,K-ATPase specifically inhibits RhoA activity. Reactivation of the Na,K-ATPase by K^+ repletion resulted in an increase in the levels of endogenous active RhoA GTPase and concomitant formation of bundled stress fibers, suggesting that Na,K-ATPase function reversibly regulates the activity of RhoA GTPase and formation of stress fibers. The levels of active Rac 1 remained the same in control and ouabain-treated cells (our unpublished results), indicating that Na,K-ATPase might mediate its action specifically through RhoA GTPase. Reduced RhoA activity correlated with highly reduced number of tight junctions, desmosomes, and lack of polarity in Na,K-ATPase-inhibited cells. Moreover, cells overexpressing wild-type RhoA GTPase can bypass the inhibitory effect of Na,K-ATPase on the formation of tight junctions, desmosomes, and induction of epithelial polarity, indicating that RhoA GTPase is an essential component downstream of Na,K-ATPase function linking Na,K-ATPase to the formation of functional tight junctions, desmosomes,

and induction of polarity in MDCK cells. Whether the modulation of RhoA activity by Na,K-ATPase is through a direct or indirect effect on RhoA GTPase activity remains to be clarified.

Previous studies with the use of inhibitors and mutant forms of RhoA GTPase have implicated RhoA GTPase in the assembly and function of tight junctions. Nusrat *et al.* (1995) have shown that inhibition of Rho in T84 cells causes dispersion of ZO-1 to the cytoplasm and concomitant decrease in the TER. In MDCK cells expressing a dominant negative mutant of RhoA, ZO-1 was localized to the plasma membrane and the tight junction structure was preserved yet TER was low in these cells, indicating that altering RhoA activity affects the function of tight junctions (Jou *et al.*, 1998). Na,K-ATPase inhibited cells did not develop TER, showed discontinuous ZO-1 staining on the plasma membrane, and revealed highly reduced numbers of tight junctions, indicating that Na,K-ATPase-mediated RhoA GTPase inhibition affects both the assembly and function of tight junctions in MDCK cells. However, inhibition of the Na,K-ATPase reduced TER even in cells overexpressing RhoA (Figure 6), suggesting that other factors are also important in the alteration in tight junctional permeability when intracellular Na^+ is increased. Although the TER was consistently affected in all these reports (Nusrat *et al.*, 1995; Jou *et al.*, 1998; this study), the difference between our results and others regarding the localization of ZO-1 to the plasma membrane and tight junction assembly is not clear. We suggest that actin polymerization mediated by RhoA GTPase might be necessary for the molecular reorganization and association of tight junction proteins to the actin cytoskeleton to assemble tight junctions and to regulate their permeability function.

Plasma membrane localization of desmosomal proteins and the formation of desmosomes in ouabain-treated cells overexpressing wild-type RhoA demonstrated that Na,K-ATPase-regulated RhoA function is essential for both the translocation of desmosomal proteins to the plasma membrane and the formation of desmosomes in MDCK cells. These events may require active actin polymerization mediated by active RhoA GTPase. In fact, a recent study demonstrated a role for stress fibers in the assembly of desmosomes in keratinocytes (Vasioukhin *et al.*, 2000).

The polarity of apical and basolateral markers was consistently altered in Na,K-ATPase-inhibited cells. Furthermore, polarized distribution of domain-specific markers in ouabain-treated wild-type RhoA overexpressing MDCK cells indicates that Na,K-ATPase-regulated RhoA GTPase function is essential to maintain the polarity in MDCK cells. Although the loss of polarity in Na,K-ATPase-inhibited cells largely appears to be due to the lack of tight junctions, we cannot rule out that Na,K-ATPase inhibition might also affect mechanisms involved in the polarized sorting of proteins in epithelial cells (Yeaman *et al.*, 1999).

How Na,K-ATPase inhibition affects the formation of tight junctions, desmosomes, induction of polarity, and negatively regulates RhoA GTPase function is currently not known. The effect does not appear to be a simple degeneration of cellular function because it is readily reversible. Moreover, translocation of tight junction proteins to the plasma membrane under Na,K-ATPase-inhibited conditions suggests that other aspects of epithelial polarization are not impaired in these cells. The phenomena are better correlated

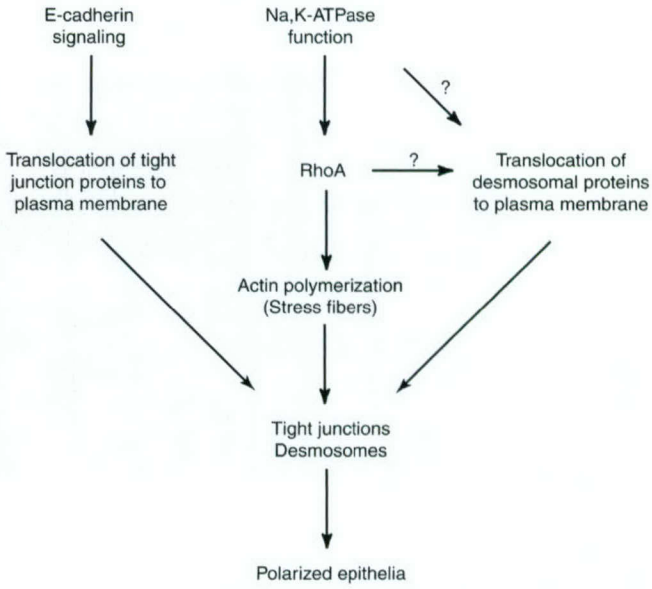

Figure 8. Schematic model of the formation of tight junctions and desmosomes in epithelial cells (see text for details).

with the absolute concentration of Na^+ in the cell than with the Na^+ gradient across the plasma membrane. Removal of extracellular Na^+ will also collapse the gradient but did not prevent formation of tight junctions or induction of polarity. Thus, aspects of cell function such as cytoplasmic pH or Ca^{+2} concentration, which depend on the transmembrane Na^+ gradient, are probably not involved. The simplest interpretation of the results is that the normal intracellular Na^+ homeostasis primarily regulated by Na,K-ATPase is involved in the modulation of RhoA activity. It is also possible that the effects might be mediated by a decrease in cell K^+ or depolarization of the plasma membrane potential rather than by Na^+ itself. Finally, although there were no obvious differences in cell size between control and Na,K-ATPase-inhibited cells, we cannot rule out small cell volume changes that might have led to the observed phenotype. We recognize that alteration of the intracellular sodium homeostasis by the inhibition of Na,K-ATPase may induce multiple biochemical changes in cells. However, rapid reversibility of effects induced by Na,K-ATPase inhibition such as formation of tight junctions, desmosomes, bundled actin stress fibers, restoration of RhoA activity, and induction of polarity by K^+ repletion strongly suggests that Na,K-ATPase function plays an important role in the assembly of junctions and induction of polarity in epithelial cells through a RhoA-mediated pathway.

Model for Formation of Tight Junctions and Desmosomes in Polarized Epithelial Cells

Based on our results, we propose a model for formation of tight junctions and desmosomes in epithelial cells. According to this model tight junctions and desmosomes are formed in parallel by two independent pathways (Figure 8) yet linked by RhoA GTPase. E-Cadherin-mediated signaling events translocate tight junction proteins from the cytoplasm

to the plasma membrane. Formation of functional tight junctions then requires active polymerization of actin mediated by RhoA. The desmosomal assembly is mediated by signaling events regulated by Na,K-ATPase. These signaling events might be directly involved in the translocation of desmosomal proteins to the plasma membrane. Alternatively, RhoA-mediated actin polymerization could be involved in the translocation of desmosomal proteins to the plasma membrane and the final assembly of desmosomes. Thus, we propose that Na,K-ATPase function, mediated at least in part by RhoA, plays an important role in formation of tight junctions and desmosomes and thus in the biogenesis of polarized epithelia.

ACKNOWLEDGMENTS

We thank Drs. Ernest Wright and Gregory Payne for critical reading of the manuscript. We thank Dr. Joel Pardee for encouragement and support. We thank Dr. Elliot Landaw for statistical analysis of the TER data. This work is primarily supported by a Grant-in-Aid award 1162-Gl1 from the American Heart Association (Western States Affiliate) (to A.K.R) and in part by Department of Defense grants PC-991140 and PC-970546 (to A.K.R), a Department of Defense Breast Cancer Program grant BC990290 (to Y.Z), and National Institutes of Health CA-67113 grant (to A.P.S). Metal analysis was supported by a National Science Foundation grant DBI-0077378 to J.F.H. S.A.R is supported by a Fellowship from Toohey Foundation. A.K.R is a member of the Jonsson Comprehensive Cancer Center.

REFERENCES

Balda, M.S., Whitney, J.A., Flores, C., Gonzalez, S., Cereijido, M., and Matter, K. (1996). Functional dissociation of paracellular permeability and transepithelial electrical resistance and disruption of the apical-basolateral intramembrane diffusion barrier by expression of a mutant tight junction membrane protein. J. Cell Biol. *134*, 1031–1049.

Buffin-Meyer, B., Marsy, S., Barlet-Bas, C., Cheval, L., Younes-Ibrahim, M., Rajerison, R., and Doucet, A. (1996). Regulation of renal Na^+,K^+-ATPase in rat thick ascending limb during K^+-depletion: evidence for modulation of Na^+ affinity. J. Physiol. *490*, 623–632.

Contreras, R.G., Shoshani, L., Flores-Maldonado, C., Lazaro, A., and Cereijido, M. (1999). Relationship between Na^+,K^+-ATPase and cell attachment. J. Cell Sci. *112*, 4223–4232.

Farquhar, M.G., and Palade, G.E. (1963). Junctional complexes in various epithelia. J. Cell Biol. *17*, 375–412.

Fernandez, R., and Malnic, G. (1998). H^+ ATPase and Cl^- interaction in regulation of MDCK cell pH. J. Membr. Biol. *163*, 137–145.

Garrod, D., Chidgey, M., and North, A. (1996). Desmosomes: differentiation, development, dynamics, and disease. Curr. Opin. Cell Biol. *5*, 670–678.

Gonzalez-Mariscal, L., Chavez de Ramirez, B., and Cereijido, M. (1985). Tight junction formation in cultured epithelial cells (MDCK). J. Membr. Biol. *86*, 113–125.

Gumbiner, B., Stevenson, B., and Grimaldi, A. (1988). The role of the cell adhesion molecule uvomorulin in the formation and maintenance of the epithelial junctional complex. J. Cell Biol. *107*, 1575–1587.

Harber, R.S., Pressley, T.A., Loeb, J.N., and Ismail-Beigi, F. (1987). Ionic dependence of active Na-K transport: "clamping of cellular Na^+ with monensin. Am. J. Physiol. *253*, F26–F33.

Imhof, B.A., Vollmers, H.P., Goodman, S.L., and Birchmeier, W. (1983). Cell-cell interaction and polarity of epithelial cells: specific perturbation using a monoclonal antibody. Cell *35*, 667–675.

Jou, T.-S., and Nelson, W.J. (1998). Effects of regulated expression of mutant RhoA and Rac1 small GTPases on the development of epithelial (MDCK) cell polarity. J. Cell Biol. *142*, 85–100.

Jou, T.-S., Schneeberger, E.E., and Nelson, W.J. (1998). Structural and functional regulation of tight junctions by RhoA and Rac1 small GTPases. J. Cell Biol. *142*, 101–115.

Katz, A.I. (1988). Role of Na-K-ATPase in kidney function. In: The Na^+,K^+ Pump. Part B. Cellular Aspects, ed. J.C. Skou, J.G. Norby, A.B. Maunsbach, and M. Esmann, New York: Alan R. Liss, 207–232.

Le, T.L., Yap, A.S., and Stow, J.L. (1999). Recycling of E-cadherin: a potential mechanism for regulating cadherin dynamics. J. Cell Biol. *146*, 219–232.

Leung, S.-M., Rojas, R., Maples, C., Flynn, C., Ruiz, W.G., Jou, T.-S., and Apodaca, G. (1999). Modulation of endocytic traffic in polarized Madin-Darby canine kidney cells by the small GTPase RhoA. Mol. Biol. Cell *10*, 4369–4384.

Lingrel, J.B., Van Huysse, J., O'Brien, W., Jewell-Motz, E., Askew, R., and Schultheis, P. (1994). Structure-function studies of the Na,K-ATPase. Kidney Int. *45* (suppl 44), S32–S39.

Liu, J., Tian, J., Haas, M., Shapiro, J.I., Askari, A., and, Xie, Z. (2000) Ouabain interaction with cardiac Na,K-A.T.Pase initiates signal cascades independent of changes in intracellular Na^+ and Ca^{2+} concentrations. J. Biol. Chem. *275*, 27838–27844.

Mackay, D.J.G., and Hall, A. (1998). Rho GTPases. J. Biol. Chem. *273*, 20685–20688.

McNeil, H., Ozawa, M., Kemler, R., and Nelson, W.J. (1990). Novel function of the cell adhesion molecule uvomurulin as an inducer of cell surface polarity. Cell *62*, 309–316.

Mitic, L.L., and Anderson, J.M. (1998). Molecular architecture of tight junctions. Annu. Rev. Physiol. *60*, 121–142.

Nose, A., Nagafuchi, A., and Takeichi, M. (1988). Expressed recombinant cadherins mediate cell sorting in model systems. Cell *54*, 993–1001.

Nusrat, A. Giry, M., Turner, J.R., Colgan, S.P., Parkos, C.A., Carnes, D., Lemichez, E., Boquet, P., and Madara, J.L. (1995). Rho protein regulates tight junctions and perijunctional actin organization in polarized epithelia. Proc. Natl. Acad. Sci. USA *92*, 10629–10633.

Ojakian, G.K., and Schwimmer, R. (1988). The polarized distribution of an apical cell surface glycoprotein is maintained by interactions with the cytoskeleton of Madin-Darby canine kidney cells. J. Cell Biol. *107*, 2377–2387.

Pollack, L.R., Tate, E.H., and Cook, J.S. (1981). Na^+,K^+-ATPase in HeLa cells after prolonged growth in low K^+ or ouabain. J. Cell Physiol. *106*, 85–97.

Potempa, S., and Ridley, J.A. (1998). Activation of both MAP kinase and phosphatidylinositide 3-kinase by Ras is required for hepatocyte growth factor/scatter factor-induced adherens junction disassembly. Mol. Biol. Cell *9*, 2185–2200.

Pressley, T.A. (1988). Ion concentration-dependent regulation of Na,K-pump abundance. J. Membr. Biol. *105*, 187–195.

Rajasekaran, A.K., Hojo, M., Huima, T., and Rodriguez-Boulan, E. (1996). Catenins and Zonula Occludens-1 form a complex during early stages in the assembly of tight junctions. J. Cell Biol. *132*, 451–463.

Rajasekaran, S.A., Palmer, L.G., Quan, K., Harper, J.F., Ball, W.J. Jr., Bander, N.H., Peralta Soler, A., and Rajasekaran, A.K. (2001). Na,K-ATPase β-subunit is required for epithelial polarization, suppression of invasion, and cell motility. Mol. Biol. Cell. *12*, 279–295.

Rayson, B.M. (1989). Rates of synthesis and degradation of Na^+,K^+-ATPase during chronic ouabain treatment. Am. J. Physiol. *256*, C75–C80.

Ren, X., Kiosses, W., and Schwartz, M.A. (1999). Regulation of the small GTP-binding protein Rho by cell adhesion and the cytoskeleton. EMBO J. *18*, 578–585.

Ridley, A.J., and Hall, A. (1992). The small GTP-binding protein rho regulates the assembly of focal adhesions and actin stress fibers in response to growth factors. Cell *70*, 389–399.

Rodriguez-Boulan, E., and Nelson, W.J. (1989). Morphogenesis of the polarized epithelial cell phenotype. Science *245*, 718–725.

Rothstein, A., and Mack, E. (1990). Volume-activated K^+ and Cl^- pathways of dissociated epithelial cells (MDCK): role of Ca^{2+}. Am. J. Physiol. *258*, C827–C834.

Stevenson, B.R., and Keon, B.H. (1998). The tight junction: morphology to molecules. Annu. Rev. Cell Dev. Biol. *14*, 89–109.

Takaishi, K., Sasaki, T., Kotani, H., Nishioka, H., and Takai, Y. (1997). Regulation of cell-cell adhesion by Rac and Rho small G proteins in MDCK cells. J. Cell Biol. *139*, 1047–1059.

Troxell, M.L., Gopalakrishnan, S., McCormack, J., Poteat, B.A., Pennington, J., Garringer, S.M., Schneeberger, E.E., Nelson, W.J., and Marrs, J.A. (2000). Inhibiting cadherin function by dominant mutant E-cadherin expression increases the extent of tight junction assembly. J. Cell Sci. *113*, 985–996.

Vaaraniemi, J., Huotari, V., Lehto, V.P., and Eskelinen, S. (1997). Effect of PMA on the integrity of the membrane skeleton and morphology of epithelial MDCK cells is dependent on the activity of amiloride-sensitive ion transporters and membrane potential. Eur. J. Cell Biol. *74*, 262–272.

Van Aelst, L., and D'Souza-Schorey, C. (1997). Rho GTPases and signaling networks. Genes Dev. *11*, 2295–2322.

Vasioukhin, V., Bauer, C., Yin, M., and Fuchs, E. (2000). Directed actin polymerization is the driving force for epithelial cell-cell adhesion. Cell *100*, 209–219.

Watabe, M., Nagafuchi, A., Tsukita, S., and Takeichi, M. (1994). Induction of polarized cell-cell association and retardation of growth by activation of the E-cadherin-catenin adhesion system in a dispersed carcinoma cell line. J. Cell Biol. *127*, 247–256.

Yamamoto, K., *et al.* (1993). Regulation of Na,K-adenosine triphosphatase gene expression by sodium ions in cultured neonatal rat cardiocytes. J. Clin. Invest. *92*, 1889–1895.

Yeaman, C., Grindstaff, K.K., and Nelson, W.J. (1999). New perspectives on mechanisms involved in generating epithelial cell polarity. Physiol. Rev. *79*, 73–98.

Yap, A.S., Brieher, W.M., and Gumbiner, B.M. (1997). Molecular and functional analysis of cadherin-based adherens junctions. Annu. Rev. Cell Dev. Biol. *13*, 119–146.

Zhu, K., Debrecini, B., Li, R., and Zheng, Y. (2000). Identification of Rho GTPase-dependent sites in the DH domain of oncogenic Dbl that are required for transformation. J. Biol. Chem. *275*, 25993–26001.

Genetic deletion of the *Pten* tumor suppressor gene promotes cell motility by activation of Rac1 and Cdc42 GTPases

Joanna Liliental*†, Sun Young Moon‡, Ralf Lesche*§, Ramanaiah Mamillapalli¶, Daming Li¶, Yi Zheng‡, Hong Sun¶ and Hong Wu*§

***Pten* (Phosphatase and tensin homolog deleted on chromosome 10) is a recently identified tumor suppressor gene which is deleted or mutated in a variety of primary human cancers and in three cancer predisposition syndromes [1]. Pten regulates apoptosis and cell cycle progression through its phosphatase activity on phosphatidylinositol (PI) 3,4,5-trisphosphate (PI(3,4,5)P_3), a product of PI 3-kinase [2–5]. Pten has also been implicated in controlling cell migration [6], but the exact mechanism is not very clear. Using the isogenic *Pten*$^{+/+}$ and *Pten*$^{-/-}$ mouse fibroblast lines, here we show that Pten deficiency led to increased cell motility. Reintroducing the wild-type *Pten*, but not the catalytically inactive *Pten* C124S or lipid-phosphatase-deficient *Pten* G129E mutant, reduced the enhanced cell motility of Pten-deficient cells. Moreover, phosphorylation of the focal adhesion kinase p125^{FAK} was not changed in *Pten*$^{-/-}$ cells. Instead, significant increases in the endogenous activities of Rac1 and Cdc42, two small GTPases involved in regulating the actin cytoskeleton [7], were observed in *Pten*$^{-/-}$ cells. Overexpression of dominant-negative mutant forms of Rac1 and Cdc42 reversed the cell migration phenotype of *Pten*$^{-/-}$ cells. Thus, our studies suggest that Pten negatively controls cell motility through its lipid phosphatase activity by down-regulating Rac1 and Cdc42.**

Addresses: *Howard Hughes Medical Institute, †Department of Microbiology and Molecular Immunology, and §Department of Molecular and Medical Pharmacology, University of California at Los Angeles School of Medicine, 650 Circle Drive South, Los Angeles, California 90095-1735, USA. ‡Department of Biochemistry, University of Tennessee, Memphis, Tennessee 38163, USA. ¶Department of Genetics, Yale University School of Medicine, 333 Cedar Street, New Haven, Connecticut 06520, USA.

Correspondence: Hong Wu
E-mail: hwu@mednet.ucla.edu

Received: **23 November 1999**
Revised: **4 January 2000**
Accepted: **21 January 2000**

Published: **24 March 2000**

Current Biology 2000, 10:401–404

0960-9822/00/$ – see front matter
© 2000 Elsevier Science Ltd. All rights reserved.

Results and discussion

To test the role of Pten in cell migration, we established independent immortalized fibroblast lines from wild-type and *Pten* deficient (*Pten*$^{-/-}$) mice, using the 3T9 protocol [8]. Similar to primary mouse embryonic fibroblasts [4], the immortalized *Pten*$^{-/-}$ cell lines showed increased levels of phosphorylation of protein kinase B/Akt compared to their wild-type counterparts and were resistant to serum-deprivation induced apoptosis. In contrast to our observation with wild-type and *Pten*$^{-/-}$ embryonic stem cells [4], however, no significant differences in the rates of cell proliferation and the levels of the cyclin-dependent kinase inhibitor p27^{KIP1} could be detected between log-phase growing wild-type and *Pten*$^{-/-}$ fibroblast cells (data not shown).

Pten$^{-/-}$ fibroblasts have an increased cell motility, as shown by a classic 'wound healing' assay (Figure 1a, left panels) [9]. They were able to completely close the wound within 15 hours, whereas wild-type cells took almost 30 hours. To demonstrate that the increase in cell migration is an individual cell based and cell division-independent event, we employed a colloidal-gold based motility assay [10]. This assay revealed that *Pten*$^{-/-}$ fibroblasts could produce longer 'trails' than wild-type cells in a defined time period, indicating that *Pten*$^{-/-}$ cells indeed migrate faster than the wild-type cells (Figure 1a, middle panels). In order to obtain more quantitative measurements of the migration distance, we employed a modified 'wound healing' assay. In this assay, cells are first seeded on coverslips, and then transferred to a new plate coated with fibronectin. Upon transfer, cells migrate from the rim of the coverslip outwards onto the new plate. As shown in Figure 1a (right panels) and quantified in Figure 1b with independent cell lines, *Pten*$^{-/-}$ cells migrate almost twice as fast as wild-type cells. Moreover, careful observation of cell morphology revealed that *Pten*$^{-/-}$ fibroblasts appeared rounded and had intense cortical F-actin staining (Figure 1c). Together, these results suggest that Pten negatively regulates signaling pathways controlling cell migration.

In order to determine whether increased cell migration in *Pten*$^{-/-}$ cells is due to lack of the Pten phosphatase activity or if other structural motifs may play a role, we re-introduced either wild-type *Pten* or *Pten* C124S, a catalytically inactive mutant, into the *Pten*$^{-/-}$ cells by retrovirus infection [11]. We used a retroviral vector that expresses the gene of interest and the green fluorescent protein (GFP) as a bicistronic mRNA. GFP-positive, thus *Pten*-expressing, cells were sorted by fluorescence activated cell sorting (FACS) following retroviral infection. Wild-type *Pten* and the C124S mutant were expressed in comparable levels in the sorted populations (Figure 2c). As shown in Figure 2a

Figure 1

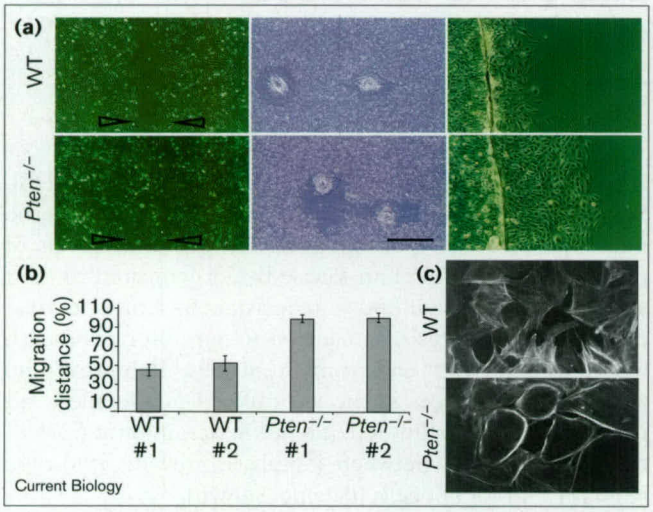

Pten-deficient fibroblasts migrate faster than wild type. **(a)** An equal number of wild-type (WT) or *Pten*$^{-/-}$ fibroblasts were seeded on a fibronectin-coated plate and cultured for 24 h. Migration into the wound is shown 15 h after the wound was introduced (left panels; open arrowheads point to the boundaries of the wound at time = 0). In the middle panel, 2×10^3 cells per well were seeded on colloidal gold-coated 6-well dishes in duplicates. Migration of wild-type or *Pten*$^{-/-}$ fibroblasts is shown at 24 h. The scale bar represents 10 μm. In the right panels, wild-type or *Pten*$^{-/-}$ fibroblasts grown on glass coverslips were placed onto 5 μg/ml fibronectin-coated dishes and cultured for 15 h. **(b)** Cell motility was assessed and compared using independent cell lines. Migration distances were determined by taking seven independent measurements from each coverslip. Each experiment was conducted in triplicate, and mean ± SD was calculated. The migration distance is normalized so that 100% represents migration distance of *Pten*$^{-/-}$ cells. **(c)** *Pten*$^{-/-}$ cells exhibited increased cortical actin polymerization as compared to the wild-type cells. Briefly, log-phase growing fibroblasts were cultured without serum for 20 h. After fixation in 4% paraformaldehyde, cells were permeabilized with 0.2% Triton X-100 and stained for F-actin using rhodamine–phalloidin (Molecular Probes).

Figure 2

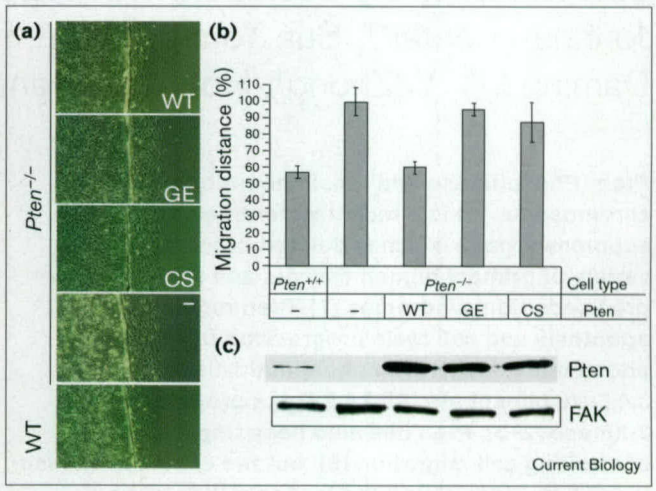

Increased cell motility in *Pten*$^{-/-}$ cells is due to the lack of lipid phosphatase activity of *Pten*. **(a)** *Pten*$^{-/-}$ cells were infected with retroviral GFP vectors containing wild-type *Pten* (WT), G129E (GE), or C124S (CS) *Pten* mutants. Control wild-type or *Pten*$^{-/-}$ cells were infected with viruses containing GFP only. 48 h later, GFP positive cells were sorted by fluorescence-activated cell sorting (FACS), seeded onto glass coverslips in triplicate, and grown for an additional 5 h. Cells on coverslips were then replaced onto a fibronectin-coated surface and incubated for 15 h. **(b)** Quantitative representation of (a). Cell migration is normalized so that 100% represents the migration distance of *Pten*$^{-/-}$ cells infected by empty vector. **(c)** Pten protein levels in uninfected and infected cells after FACS sorting. Western blots of total protein extracts were probed with an affinity-purified anti-Pten antibody. Blots were reprobed with anti-FAK antibody (Santa Cruz Biotechnology) to confirm equal loading.

and quantified in Figure 2b, wild-type *Pten*, but not the C124S mutant, could fully reverse the migration phenotype of *Pten*$^{-/-}$ cells, confirming that the enhanced motility is directly due to the lack of Pten phosphatase activity.

Recent studies suggested that $PI(3,4,5)P_3$ is a major substrate for Pten both *in vitro* [2] and *in vivo* [3,4]. Interestingly, *Pten* G129E is deficient for the phosphatase activity towards $PI(3,4,5)P_3$, while its activity towards synthetic protein substrates is unaffected [12]. Using the *Pten* G129E mutant, we further tested whether Pten controls cell migration through its lipid phosphatase activity or its protein phosphatase activities. *Pten* G129E behaved similarly to the C124S mutant as they were both unable to rescue the migration phenotype in this assay. This experiment suggests that the enhanced motility of *Pten*$^{-/-}$ cells is a result of the loss of Pten phosphatase activity, in particular, its lipid-phosphatase activity.

It has been suggested that Pten negatively regulates cell migration by directly dephosphorylating p125^{FAK} and changing mitogen-activated protein (MAP) kinase activity [6,13]. In order to test whether p125^{FAK} phosphorylation and MAP kinase activation are also affected by the loss of *Pten*, we examined the tyrosine phosphorylation status of these proteins. Whole cell lysates from log-phase growing wild-type or *Pten*$^{-/-}$ fibroblasts were immunoprecipitated with 4G10 anti-phosphotyrosine antibody and western blotted with anti-FAK antibody (Figure 3a, upper panel), or were immunoprecipitated with anti-FAK antibody and western blotted with 4G10 (Figure 3b, lower panel). In contrast to what would be predicted if Pten could directly dephosphorylate p125^{FAK}, no difference in tyrosine phosphorylation of p125^{FAK} could be detected in *Pten*$^{-/-}$ fibroblast lines compared to wild-type cells. The activation status of MAP kinases was not affected by the *Pten* deletion either, but the level of Akt phosphorylation was significantly increased in *Pten*$^{-/-}$ fibroblast cell lines (data not shown), similar to what we have observed previously in *Pten*$^{-/-}$ embryonic stem cells [4]. These results suggest that the enhanced cell motility caused by *Pten* deficiency may be mediated by effectors other than p125^{FAK} and MAP kinases.

Figure 3

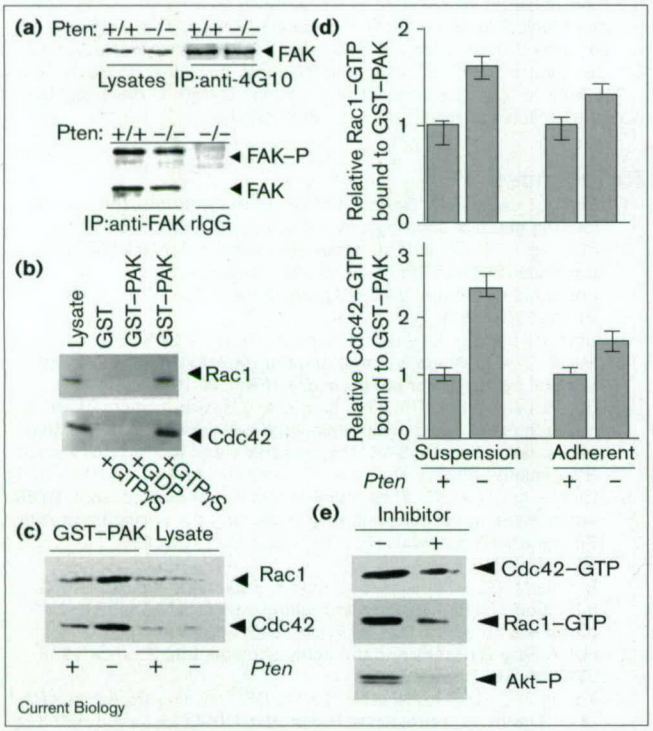

Pten deletion results in activation of Rac1 and Cdc42, but not FAK. **(a)** FAK phosphorylation is not affected by *Pten* deletion. Upper panel, equal amounts of proteins were immunoprecipitated with anti-phosphotyrosine antibody (4G10, Upstate Biotechnology). Western blots were probed with anti-FAK antibody. Bottom panel, anti-FAK immunoprecipitates were western blotted with 4G10 (for phosphorylated FAK, FAK–P) or an anti-FAK antibody. rIgG indicates immunoprecipitation with a rabbit isotype control antibody. **(b)** GST–PAK binding is specific for GTP. *Pten*$^{-/-}$ fibroblast lysates were loaded with GTPγS or GDP prior to affinity precipitation with GST or GST–PAK immobilized on 10 μg glutathione–agarose beads. The precipitated proteins were analyzed by western blot with anti-Rac1 (Upstate Biotechnology) or anti-Cdc42 (Santa Cruz Biotechnology) antibody, respectively. Results are representative of three independent experiments. **(c)** The GST–PAK precipitates from wild-type (+) and *Pten*$^{-/-}$ (−) fibroblasts under log phase growing conditions, along with total cell lysates, were analyzed by western blot with anti-Rac1 or anti-Cdc42 antibodies. **(d)** Wild-type or *Pten*$^{-/-}$ cells, either in suspension or adherent, were lysed and subjected to GST–PAK affinity precipitation analysis. The Rac1–GTP (upper graph) or Cdc42–GTP (lower graph) activities detected by western blot were normalized to the amount of Rac1 or Cdc42 in whole cell lysates. Results are means ± SD from three experiments. **(e)** *Pten*$^{-/-}$ cells were treated with 20 μM LY294002 (shown here, +), or 50 nM wortmannin (not shown), or DMSO vehicle control (−) for 6 h before harvesting. Cell lysates were precipitated with GST–PAK and blotted with anti-Rac1 or anti-Cdc42 antibodies, respectively. In parallel, aliquots of cell lysates were analyzed with anti-phospho-Akt antibody (New England Biolabs).

As increased cell motility is associated with a deficiency in Pten lipid-phosphatase activity, and cells in which *Pten* is genetically deleted contain elevated levels of $PI(3,4,5)P_3$ [3,4], we next examined whether activation of known

Figure 4

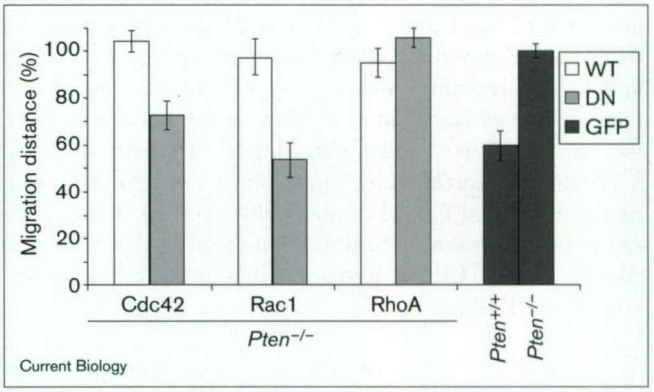

Increased motility of *Pten*$^{-/-}$ cells can be reversed by expression of dominant-negative (DN) Rac1 and Cdc42, but not RhoA. Cell motility was assessed by directly measuring the migration distance 15 h after plating, and presented as an average of three independent experiments. WT, wild-type constructs were expressed; GFP, a GFP-expressing vector only was expressed.

downstream $PI(3,4,5)P_3$ effectors might be responsible for the increased cell migration phenotype in *Pten*$^{-/-}$ cells. Activation of Cdc42 and Rac1 has been implicated in promoting cell migration [7] and their GDP/GTP exchange factors (GEFs) can be activated in a $PI(3,4,5)P_3$-dependent manner [14,15]. We therefore examined whether Pten deficiency leads to changes in the Rac1 and Cdc42 activities. In this assay, the p21-binding domain of PAK1 was expressed as a GST-fusion protein. GST–PAK1 can specifically recognize Rac1–GTP or Cdc42–GTP forms, but not GDP-bound forms, suggesting that the affinity precipitation assay is specific and effective in assessing the activation states of Rac1 and Cdc42 (Figure 3b). We then examined the level of endogenous GTP-bound forms of Rac1 or Cdc42 in *Pten*$^{-/-}$ cells and wild-type cells. As shown in Figure 3c, there are marked increases of the GTP-bound forms of Rac1 and Cdc42 in logarithmically growing *Pten*$^{-/-}$ cells compared to wild-type cells, although the total protein levels are not affected by the *Pten* status. As $PI(3,4,5)P_3$ levels were highly sensitive to growth conditions [4], we also examined the Rac1 and Cdc42 activities in unfavorable confluent culture conditions. There is a notable ~30% increase in Rac1–GTP content and a ~50% increase in Cdc42–GTP content compared to the wild-type cells (Figure 3d). When similar assays were performed using suspended cell cultures which lack the adherent stimuli, ~60% and ~130% increases of Rac1–GTP and Cdc42–GTP forms, respectively, were observed (Figure 3d, suspension). The extent of elevation in the endogenous Cdc42 and Rac1 activities in *Pten*$^{-/-}$ cells were consistent when independent cell lines were used, and reintroducing wild-type *Pten* into *Pten*$^{-/-}$ cells led to a decrease in the GTP-bound forms of Rac1 and Cdc42 (data not shown).

Recent experiments demonstrated that a correlation exists between activation of the activity of PI 3-kinase and the activities of Rac1 and Cdc42 [14–17]. However, whether PI 3-kinase functions downstream or upstream of Rac1 and Cdc42 remains unclear. To test whether Rac1 and Cdc42 were activated in a PI 3-kinase dependent manner, we treated *Pten*$^{-/-}$ cells with the PI 3-kinase inhibitor LY294002 or wortmannin. Figure 3e shows that the activities of Rac1 and Cdc42 dramatically decrease upon treatment with PI 3-kinase inhibitors, indicating that similar to Akt, Rac1 and Cdc42 activation in *Pten*$^{-/-}$ cells is downstream of PI 3-kinase.

To formally prove that the elevated endogenous activities of Rac1 and Cdc42 in *Pten*$^{-/-}$ cells are responsible for the increased cell migration phenotype, we introduced either wild-type or dominant negative forms of Rac1 (N17Rac1) and Cdc42 (N17Cdc42) into *Pten*$^{-/-}$ cells by retroviral infection. These mutants are thought to act by sequestering specific GEFs necessary for activation of Rac1 and Cdc42, preventing their functions. Figure 4 shows that expression of N17Rac1 and N17Cdc42 in *Pten*$^{-/-}$ cells could reverse the cell migration phenotype by 100% and 50%, respectively. The less efficient reversion by N17Cdc42 is not due to the lower expression level (data not shown), but could reflect the suggested hierarchical relationship between Rac1 and Cdc42, where Cdc42 is thought to function upstream of Rac1 [7]. As a control for the specificity of these GTPases, we also expressed the dominant negative form of RhoA (N19RhoA), a GTPase involved in focal adhesion and stress fiber formation [18,19]. No effect on the migration of *Pten*$^{-/-}$ fibroblasts was observed with N19RhoA, or with the wild-type Rho GTPases (Figure 4). These results indicate that Rac1 and Cdc42 serve as downstream effectors of Pten in the regulation of cell migration.

In summary, we show that inactivation of the *Pten* tumor suppressor gene promotes cell motility in fibroblasts. In contrast to previous reports that Pten negatively regulates cell migration by directly dephosphorylating p125^{FAK} and changing MAP kinase activities, we demonstrate genetically that the tumor suppressor Pten controls cell motility by down regulating Rac1 and Cdc42 GTPases, and this negative regulation is dependent on the lipid phosphatase activity of Pten. In combination with our previous work and other studies, we suggest that Pten exerts its tumor suppressor function not only at the stage of tumor initiation, but also in tumor progression and metastasis.

Supplementary material

Supplementary material including additional methodological details is available at http://current-biology.com/supmat/supmatin.htm.

Acknowledgements

We thank H. Herschman, O. Witte, C. Sawyers, K. Shuai, X. Liu for critical reading of the manuscript. We thank X.L. Liu and H.L. Lodish of MIT for kindly providing pMX-IRES-GFP vector, and Jing Gao and Nadia Gavrilova for technical assistance. R.L. is supported by the Deutsche Forschungsgemeinschaft and a Carolan Seed grant (to H.W.). H.S. is a Pew Scholar in the Biomedical Sciences. H.W. is an Assistant Investigator of the Howard Hughes Medical Institute and V Foundation Scholar. This work was supported by the V foundation and a Carolan Seed grant (to H.W.); American Cancer Society (RPG-97-146) and National Institutes of Health grant (GM53943 to Y.Z.); Department of the Army (DAMD 17-98-1-8271) and National Institutes of Health grant (CA77695 to H.S.).

References

1. Eng C, Peacocke M: **Genetics of Cowden syndrome: through the looking glass of oncology.** *Int J Oncology* 1998, **12:**701-710.
2. Maehama T, Dixon JE: **The tumor suppressor, PTEN/MMAC1, dephosphorylates the lipid second messenger, phosphatidylinositol 3,4,5-trisphosphate.** *J Biol Chem* 1998, **273:**13375-13378.
3. Stambolic V, Suzuki A, de la Pompa JL, Brothers GM, Mirtsos C, Sasaki T, *et al.*: **Negative regulation of PKB/Akt-dependent cell survival by the tumor suppressor PTEN.** *Cell* 1998, **95:**29-39.
4. Sun H, Lesche R, Li DM, Liliental J, Zhang H, Gao J, *et al.*: **PTEN modulates cell cycle progression and cell survival by regulating phosphatidylinositol 3,4,5,-trisphosphate and Akt/protein kinase B signaling pathway.** *Proc Natl Acad Sci USA* 1999, **96:**6199-6204.
5. Cantley LC, Neel BG: **New insights into tumor suppression: PTEN suppresses tumor formation by restraining the phosphoinositide 3-kinase/AKT pathway.** *Proc Natl Acad Sci USA* 1999, **96:**4240-4245.
6. Tamura M, Gu J, Matsumoto K, Aota S, Parsons R, Yamada KM: **Inhibition of cell migration, spreading, and focal adhesions by tumor suppressor PTEN.** *Science* 1998, **280:**1614-1617.
7. Hall A: **Rho GTPases and the actin cytoskeleton.** *Science* 1998, **279:**509-514.
8. Kamijo T, Zindy F, Roussel MF, Quelle DE, Downing JR, Ashmun RA, *et al.*: **Tumor suppression at the mouse INK4a locus mediated by the alternative reading frame product p19ARF.** *Cell* 1997, **91:**649-659.
9. Xu W, Baribault H, Adamson ED: **Vinculin knockout results in heart and brain defects during embryonic development.** *Development* 1998, **125:**327-337.
10. Takaishi K, Sasaki T, Takai Y: **Cell motility assay and inhibition by Rho-GDP dissociation inhibitor.** *Methods Enzymol* 1995, **256:**336-347.
11. Grignani F, Kinsella T, Mencarelli A, Valtieri M, Riganelli D, Lanfrancone L, *et al.*: **High-efficiency gene transfer and selection of human hematopoietic progenitor cells with a hybrid EBV/retroviral vector expressing the green fluorescence protein.** *Cancer Res* 1998, **58:**14-19.
12. Myers MP, Pass I, Batty IH, Van der Kaay J, Stolarov JP, Hemmings BA, *et al.*: **The lipid phosphatase activity of PTEN is critical for its tumor suppressor function.** *Proc Natl Acad Sci USA* 1998, **95:**13513-13518.
13. Gu J, Tamura M, Yamada KM: **Tumor suppressor PTEN inhibits integrin- and growth factor-mediated mitogen-activated protein (MAP) kinase signaling pathways.** *J Cell Biol* 1998, **143:**1375-1383.
14. Van Aelst L, D'Souza-Schorey C: **Rho GTPases and signaling networks.** *Genes Dev* 1997, **11:**2295-2322.
15. Han J, Luby-Phelps K, Das B, Shu X, Xia Y, Mosteller RD, *et al.*: **Role of substrates and products of PI 3-kinase in regulating activation of Rac-related guanosine triphosphatases by Vav.** *Science* 1998, **279:**558-560.
16. Tolias KF, Cantley LC, Carpenter CL: **Rho family GTPases bind to phosphoinositide kinases.** *J Biol Chem* 1995, **270:**17656-17659.
17. Keely PJ, Westwick JK, Whitehead IP, Der CJ, Parise LV: **Cdc42 and Rac1 induce integrin-mediated cell motility and invasiveness through PI(3)K.** *Nature* 1997, **390:**632-636.
18. Nobes CD, Hall A: **Rho, rac, and cdc42 GTPases regulate the assembly of multimolecular focal complexes associated with actin stress fibers, lamellipodia, and filopodia.** *Cell* 1995, **81:**53-62.
19. Ridley AJ, Paterson HF, Johnston CL, Diekmann D, Hall A: **The small GTP-binding protein rac regulates growth factor-induced membrane ruffling.** *Cell* 1992, **70:**401-410.

THE JOURNAL OF BIOLOGICAL CHEMISTRY
Vol. 278, No. 45, Issue of November 7, pp. 44617–44625, 2003
Printed in U.S.A.
© 2003 by The American Society for Biochemistry and Molecular Biology, Inc.

A Novel Strategy for Specifically Down-regulating Individual Rho GTPase Activity in Tumor Cells*

Received for publication, August 13, 2003
Published, JBC Papers in Press, August 25, 2003, DOI 10.1074/jbc.M308929200

Lei Wang, Linda Yang, Yongneng Luo, and Yi Zheng‡

From the Division of Experimental Hematology and Molecular Developmental Biology Program, Children's Hospital Research Foundation, University of Cincinnati, Cincinnati, Ohio 45229

The Rho family GTPases RhoA, RhoB, and RhoC regulate the actin cytoskeleton, cell movement, and cell growth. Unlike Ras, up-regulation or overexpression of these GDP/GTP binding molecular switches, but not activating point mutations, has been associated with human cancer. Although they share over 85% sequence identity, RhoA, RhoB, and RhoC appear to play distinct roles in cell transformation and metastasis. In NIH 3T3 cells, RhoA or RhoB overexpression causes transformation whereas RhoC increases the cell migration rate. To specifically target RhoA, RhoB, or RhoC function, we have generated a set of chimeric molecules by fusing the RhoGAP domain of p190, a GTPase-activating protein that accelerates the intrinsic GTPase activity of all three Rho GTPases, with the C-terminal hypervariable sequences of RhoA, RhoB, or RhoC. The p190-Rho chimeras were active as GTPase-activating proteins toward RhoA *in vitro*, co-localized with the respective active Rho proteins, and specifically down-regulated Rho protein activities in cells depending on which Rho GTPase sequences were included in the chimeras. In particular, the p190-RhoA-C chimera specifically inhibited RhoA-induced transformation whereas p190-RhoC-C specifically reversed the migration phenotype induced by the active RhoC. In human mammary epithelial-RhoC breast cancer cells, p190-RhoC-C, but not p190-RhoA-C or p190-RhoB-C, reversed the anchorage-independent growth and invasion phenotypes caused by RhoC overexpression. In the highly metastatic A375-M human melanoma cells, p190-RhoC-C specifically reversed migration, and invasion phenotypes attributed to RhoC up-regulation. Thus, we have developed a novel strategy utilizing RhoGAP-Rho chimeras to specifically down-regulate individual Rho activity and demonstrate that this approach may be applied to multiple human tumor cells to reverse the growth and/or invasion phenotypes associated with disregulation of a distinct subtype of Rho GTPase.

The Ras-related Rho family of small GTPases regulates the actin cytoskeletal organization, cell to cell or cell to extracellular matrix adhesion, intracellular membrane trafficking, gene transcription, apoptosis, and cell cycle progression (1–3). Like Ras, they exist in an inactive, GDP-bound and an active, GTP-bound conformations. Rho GTPases are activated by a class of positive regulators, the Dbl family guanine nucleotide exchange factors (GEFs)[1] that catalyze the release of bound GDP and facilitate the binding of GTP (4), whereas deactivation of Rho proteins is achieved through their intrinsic GTP-hydrolytic activities that are further stimulated by a class of negative regulators, the GTPase-activating proteins (GAPs) (5). A third class of regulators of Rho GTPases, the Rho GDP-dissociation inhibitors, can negatively impact Rho protein activities by sequestering them in the GDP-bound state and preventing effective cycling between the two conformational states (6). Upon binding to GTP, Rho GTPases may further interact with an array of potential effector molecules to elicit cellular responses (7).

It has become increasingly clear that Rho proteins play important roles in many aspects of cancer development, and each member of the Rho family may be involved to a different extent at different tumor progression stages (8–10). For example, it was shown that constitutively active RhoA has oncogenic potential (11), and RhoA acts as a critical signaling component in Ras-induced transformation (12). Furthermore, RhoA promotes the invasiveness of rat hepatoma cells (13) and induces metastasis of NIH 3T3 fibroblasts (14), whereas RhoC was revealed as a key regulator of migration and metastasis in a human melanoma cell line (15). Upon introduction into normal mammalian epithelial cells, RhoC readily caused transformation and invasion, leading to an inflammatory breast cancer cell phenotype (16). On the other hand, RhoB is required for the apoptotic responses induced by farnesyltransferase inhibitors or DNA damaging agents and may have a suppressor or negative modifier function in cancer progression (17). Unlike Ras, there are no reports of mutation-caused constitutive activation of Rho proteins in tumors. Recent studies of primary human tumors (18–21) revealed that many Rho GTPases, including RhoA and RhoC, are highly expressed in a variety of cancer types such as colon, lung, testicular germ cell, head and neck squamous cell carcinoma, pancreatic ductal adenocarcinoma, and inflammatory breast cancer, and in some cases, the Rho protein up-regulation and/or overexpression correlates with poor prognosis (22). These observations help put Rho proteins in a lineup of potential molecular targets for anti-cancer therapy (8).

Currently available molecular tools to target Rho GTPase pathways at the small G-protein level include the dominant negative mutants of Rho proteins (23), the p21-binding domain of effectors (24) and a class of bacterial toxins that can modify

* This work was supported by National Institutes of Health Grants GM 60523 and GM 53948. The costs of publication of this article were defrayed in part by the payment of page charges. This article must therefore be hereby marked "*advertisement*" in accordance with 18 U.S.C. Section 1734 solely to indicate this fact.

‡ To whom correspondence should be addressed: Tel.: 513-636-0595; Fax: 513-636-3768; E-mail: yi.zheng@chmcc.org.

[1] The abbreviations used are: GEF, guanine nucleotide exchange factor; CS, calf serum; FBS, fetal bovine serum; GAP, GTPase-activating protein; GST, glutathione *S*-transferase; HME, human mammary epithelial; GFP, green fluorescent protein; EGFP, enhanced GFP; DMEM, Dulbecco's modified Eagle's medium; Ni-NTA, nickel-nitrilotriacetic acid; HA, hemagglutinin.

Rho GTPase functions (25). Although they have been widely used in cell biological studies, each of these reagents has its own drawbacks. The dominant negative forms of Rho proteins act by sequestering the upstream GEF activators of endogenous Rho GTPases and tend to be nonspecific among closely related Rho family members (23). Further, because of their non-catalytic nature, a 3–5-fold overexpression *versus* the endogenous Rho protein level is typically needed for effective blockage of the endogenous activity, and this may not be desirable in many *in vivo* situations. Similarly, the limited specificity of effector p21-binding domains and bacterial toxins such as *Clostridium botulinum* C3-transferase is worrisome in terms of differentiating the roles of highly homologous isoforms such as RhoA, RhoB, and RhoC. Furthermore, very little is known about the anti-cancer potential of these Rho GTPases inhibitors.

Because RhoGAPs have been established as the major class of negative regulators of Rho GTPase signaling (5), and some of them are actually known for their tumor suppressor function (26, 27), another possible approach for inhibiting Rho GTPase activities in tumor cells is to employ RhoGAPs as antagonists for Rho activities. The conserved GAP domain in RhoGAPs contains the necessary and sufficient structural determinants for Rho protein recognition and GTPase catalysis but displays limited substrate specificity (5). For example, the RhoGAP domain of p190 RhoGAP can catalyze GTP hydrolysis of RhoA, RhoB, and RhoC equally well but works weakly on Rac or Cdc42 (28, 29). It depends on other regulatory domains in the RhoGAP to direct and regulate substrate selection and catalysis *in vivo* (30, 31). Conversely, although Rho proteins may share up to 90% sequence identity, each Rho subtype appears to play distinct roles in cellular transformation and metastasis. The differences in Rho GTPase functions may come in part from their distinct subcellular localization patterns that are mostly determined by the unique C-terminal hypervariable sequences in each case (32, 33).

In the present study, we have developed a novel strategy combining the RhoGAP domain of p190 RhoGAP with the C-terminal hypervariable sequences of Rho proteins to specifically target RhoA, RhoB, or RhoC activity in human tumor cells. We show that although RhoA, RhoB, and RhoC are equally effective in stimulating actin stress fiber formation and focal complex assembly in NIH 3T3 cells, RhoA and RhoB are capable of transforming cells whereas RhoC induces cell migration. The chimera made of p190 and the C terminus of RhoA specifically inhibited RhoA-induced cell transformation whereas the p190-RhoC chimera specifically reversed RhoC-mediated migration phenotype by down-regulating RhoC activity. Moreover, when applied to the HME-RhoC human inflammatory breast cancer cells or to the A375-M human melanoma cells, the p190-RhoC chimera was effective in reversing the anchorage-independent growth and/or the invasion phenotypes that were attributed to RhoC up-regulation. Our results suggest that such a RhoGAP-based approach targeting specific Rho GTPase activity could be useful in reversing tumor cell phenotypes associated with disregulation of a distinct subtype of Rho GTPase.

EXPERIMENTAL PROCEDURES

Site-directed Mutagenesis—Site-directed mutants of human RhoA, RhoB, and RhoC were generated by polymerase chain reactions using the *Pfu* polymerase, with primers that contained the desired mutations following the published protocols (34). The mutant cDNAs were subcloned into the BamHI and EcoRI sites of mammalian expression vector pCEFL-GST, and the mutants were expressed as glutathione *S*-transferase (GST) fusions (35). The sequences of mutagenized DNA inserts were confirmed by automated sequencing. All point mutants used are described by single-letter amino acid denominations.

Construction of p190-Rho Chimeras—p190-Rho chimeric cDNAs were generated by fusing the cDNAs encoding the RhoGAP domain of rat p190 and the cDNAs encoding the C terminus of human RhoA, RhoB, or RhoC after PCR amplification of the respective sequences. The primer sequences are as follows: for RhoA C terminus, 5′ GCGAATTCTCACAAGACAAGGCAACCAGATTTTTTCTTCCCACGTCTAGCTTGCAGAGAAGACAACTGATTTTCCTGC 3′; for RhoB C terminus, 5′ GCGAATTCTCATAGCACCTTGCAGCAGTTGATGCAGCCGTTCTGGGAGCCGTAGCTTCTGCAGAGAAGACAACTGATTTTCCTGC 3′; and for RhoC C terminus, 5′ GCGAATTCTCAGAGAATGGGACAGCCCCTCCGACGCTTGTTCTTGCGGACCTGGAGAGAAGACAACTGATTTTCCTGC 3′. The ligation products of cDNAs encoding p190RhoGAP domain, and the respective Rho sequences were cloned into the MIEG-3-$(HA)_3$ and SF91-EMCV-IRES-GFP retroviral vectors that express the chimeras as $(HA)_3$- or FLAG-tagged fusions, together with the enhanced green fluorescent protein (EGFP) bicistronically (36, 57, 58), as well as the pCEFL-GST vector for transient expression in mammalian cells.

Cell Culture and Transfection—NIH 3T3 cells were cultured in DMEM supplemented with 10% calf serum (CS) in a 5% CO_2 incubator at 37 °C. COS-7 cells, and the retroviral packaging Phoenix cells were cultured in DMEM with 10% fetal bovine serum (FBS). The A375 and HME tumor cell lines were maintained as described (15, 16). To generate stable transfectants, NIH 3T3 cells were seeded in 6-well plate at a density of 1.5×10^5 cells in DMEM medium supplemented with 10% CS. These cells were transfected with the pCEFL-GST-Rho constructs in the next day using LipofectAMINE Plus (Invitrogen) following the manufacturer's instructions. Selection of stable transfectants was carried out by adding 0.35 mg/ml of G418 to the culture medium 48 h after transfection. After ~2 weeks culturing in the selection medium, the surviving cells including over 100 colonies were examined for the expression of GST fusion proteins by anti-GST immunoblotting.

GTPase Activity Assay—The intrinsic and p190GAP-stimulated GTPase activities of RhoA were measured as described (34) by the nitrocellulose filter-binding method. Briefly, recombinant RhoA were preloaded with [γ-^{32}P]GTP (10 μCi, 6000Ci/mmol; PerkinElmer Life Sciences) in a 100-μl buffer containing 50 mM HEPES, pH 7.6, 0.2 mg/ml bovine serum albumin, and 0.5 mM EDTA for 10 min at ambient temperature before the addition of $MgCl_2$ to a final concentration of 5 mM. An aliquot of the [γ-^{32}P]GTP-loaded RhoA was mixed with GAP assay buffer containing 50 mM HEPES, pH 7.6, 100 mM NaCl, 0.2 mg/ml bovine serum albumin, and 5 mM $MgCl_2$ in the presence or absence of various GAPs. At different time points the reaction was terminated by filtering the reaction mixture through nitrocellulose filters. The radioactivity retained on the filters were then subjected to quantitation by scintillation counting.

Retroviral Gene Transfer—Various p190-Rho chimeras were expressed in NIH 3T3 cells or tumor cells by the retroviral infection method. Production of recombinant retrovirus in the retroviral packaging Phoenix cells and subsequent host cell infection were carried out according to the described protocols (36, 37). The infected cells were harvested 72 h post-infection. EGFP-positive cells (typically 10–50%) were isolated by fluorescence-activated cell sorting and were used for further analysis.

Rho Effector Pull-down Assay—To determine the RhoA, RhoB, or RhoC activity in cells, the effector pull-down assay (38) was carried out in the respective cells that have been serum-starved for 20 h. The effector probe for Rho-GTP, recombinant $(His)_6$-Rhotekin, was expressed and purified from *Escherichia coli* and immobilized on the Ni-NTA-agarose beads. The bead-associated $(His)_6$-Rhotekin (about 1 μg/sample) was incubated with the respective cell lysates expressing various GST-Rho proteins for 45 min at 4 °C, and the co-precipitates were analyzed by Western blotting with anti-GST or anti-Rho monoclonal antibody.

Transformation Assay—Measurements of the anchorage-independent growth of mutant Rho protein expressing cells or tumor cells were carried out as described (38, 39). Briefly, 2×10^4 cells were suspended in the 10% FBS-supplemented Ham's F-12 complete medium with growth factors and 0.3% agarose and were plated on top of a solidified, 0.6% agarose. The cells were fed weekly by the addition of 1 ml of medium. Three weeks after plating, the colonies grown larger than 50 μm in diameter were scored under a microscope. To measure cell transforming activity, 5×10^3 cells transfected with various Rho constructs were mixed with 5×10^4 wild type NIH 3T3 cells and were plated in 100-mm dishes in a medium containing DMEM supplemented with 10% CS. The cells were fed every other day, and the visible foci were scored 14 days post-plating.

Wound Healing and Migration Assays—For wound healing assays,

cells were plated at 2×10^6/dish density in 60-mm diameter dishes. A plastic pipette tip was drawn across the center of the plate to produce a clean 1-mm-wide wound area after the cells have reached confluency. After a 12-h culturing in DMEM supplemented with 0.5% CS, cell movement into the wound area was examined at different time points using a phase-contrast microscope. The distances between the leading edge of the migrating cells and the edge of the wound were compared (40).

Cell migration was also measured by using a Transwell plate inserted with a 6.5-mm polycarbonate membrane (8.0-μm pore size; Costar Corp.). Briefly, 5×10^4 cells were suspended in 0.2 ml of culture medium and were added to the upper chamber. 10% FBS in culture medium was used as chemoattractant in the lower chamber. The cells were incubated for 16 h in a humidified CO_2 incubator at 37 °C. The cells that traversed the 8.0-μm membrane pores and spread to the lower surface of the membrane were stained with 5% Giemsa solution, and the cells retained in the membrane were counted in at least six different fields. Each experiment was carried out in triplicate, and the error bars represent the mean standard error.

Invasion Assay—Cell invasion assays were performed using the 6.4-mm Biocoat Matrigel invasion chambers equipped with the 8.0-μm pore sized PET membrane filters (BD Biosciences) according to the manufacturer's instructions. Briefly, 2.5×10^4 cells were suspended in 0.5 ml of culture medium and were added to the upper chamber. 10% FBS in the culture medium was plated in the lower chamber as chemoattractant. Cells in the invasion chambers were incubated in a humidified incubator. The cells that traversed the Matrigel matrix and the 8-μm membrane pores and spread to the lower surface of the filters were stained with 5% Giemsa solution for visualization. Each data point of the invasion test was derived from triplicate chambers, and error bars represent the mean standard error.

Immunofluorescence—Cells grown on coverglasses were fixed with 3.7% formaldehyde in phosphate-buffered saline for 15 min and washed with phosphate-buffered saline once followed by permeabilization with 0.1% Triton X-100 for 20 min. The cells were then blocked with 2% bovine serum albumin for 20 min. For actin staining, the cells were incubated with rhodamine-phalloidin. For vinculin staining, the cells were labeled with anti-vinculin monoclonal antibody (Sigma) followed by incubation with a rhodamine-conjugated goat anti-mouse secondary antibody. To determine the intracellular localization of various Rho proteins and p190-Rho chimeras, the fluorescence-activated cell sorting-isolated, EGFP-positive cells were labeled with anti-HA monoclonal antibody or with anti-GST polyclonal antibody followed by rhodamine- or cy5-conjugated secondary antibody staining. The stained cells were mounted onto slides in Aqua-mount and viewed with a Zeiss LSM510 confocal microscopy or a Leica fluorescence microscopy equipped with the deconvolution software (Improvision, Inc.).

RESULTS

Distinct Roles of RhoA, RhoB, and RhoC in Cell Transformation and Migration—Among the three closely related Rho proteins, RhoA, RhoB, and RhoC, RhoA is the best characterized one and has been shown to regulate actin stress fiber and focal complex formation (41), to promote cell growth (39) and to transform NIH 3T3 fibroblasts (42). By contrast, the function of RhoB or RhoC in fibroblasts has not been examined in detail and has not been directly compared with that of RhoA. To make comparisons of the cellular roles of RhoA, RhoB, and RhoC, we have generated two sets of activating mutants for each of the Rho proteins: the fast-cycling Rho-F30L and the GTPase-defective Rho-Q63L. Both types of the mutants result in the net enhancement of the active Rho-GTP species in cells but involve distinct mechanisms; Rho-F30L proteins contain significantly increased intrinsic GDP/GTP exchange activity and remain responsive to RhoGAP stimulation to cycle between the GDP- and GTP-bound states (39), whereas the Rho-Q63L mutants cannot hydrolyze bound GTP and are locked into the GTP-bound active conformation (42). We introduced these mutants into NIH 3T3 cells and generated the mutant expressing stable clones. Western blots show that the two mutant forms of all three Rho GTPases were expressed in the cells but at a lesser level than the endogenous Rho (Fig. 1*A*).

Staining of the cells with fluorescently labeled phalloidin or anti-vinculin antibody revealed that under the serum-free conditions, both active forms of RhoB and RhoC stimulated the actin stress fiber and focal adhesion plaque formation, effects similar to that induced by the active RhoA mutants or by 10% CS stimulation (Fig. 1, *B* and *C*). Because the amino acid sequences of the three Rho proteins are over 85% identical overall and are almost 100% identical in the switch I effector domain, it is likely that they utilize the same set of effector targets to mediate actin structural changes and focal adhesion assembly.

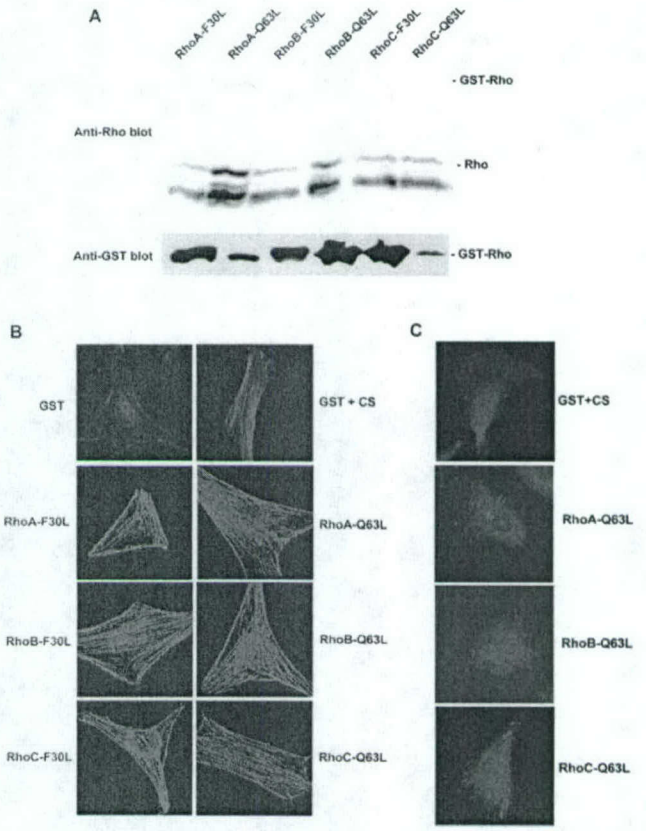

FIG. 1. **The expression of two active mutant forms of RhoA, RhoB, and RhoC and their effects on the actin structure and focal adhesion complex in NIH 3T3 cells.** *A*, the two active forms (F30L and Q63L) of RhoA, RhoB, and RhoC proteins were expressed as GST fusions in NIH 3T3 cells by using the pCEFL-GST vector. The expression level of the GST fusions in the stably transfected clones was determined by Western blotting using anti-Rho (*top panel*, whole cell lysates) and anti-GST (*lower panel*, glutathione-beads enriched) antibodies. *B*, the effects of these two active forms of RhoA, RhoB, and RhoC on cell actin structures were visualized by staining cells with rhodamine-conjugated phalloidin after a 24-h period of serum starvation. *C*, the focal adhesion plaques of the cells were visualized by anti-vinculin staining and fluorescence microscopy under similar conditions as in *B*. *CS*, 10% of calf serum was present.

Although RhoB has been suggested to be involved in Ras-mediated oncogenic transformation (43), RhoA is the only one among the three that has been shown to possess transforming activity (42). When the transformation ability of the RhoA, RhoB, and RhoC mutants were directly compared in a foci-forming assay, we found that RhoB displayed a potent transforming activity similar to RhoA in both RhoB-F30L and RhoB-Q63L forms. In contrast, neither active forms of RhoC were able to transform cells (Fig. 2*A*). RhoA was shown previously (44) to be involved in fibroblast cell movement by mediating cell body contraction. When the migration rates of the cells expressing the active mutants of RhoA, RhoB, or RhoC were compared in a wound healing assay, we found that RhoC, but not RhoA or RhoB, was able to significantly increase migration of the cells

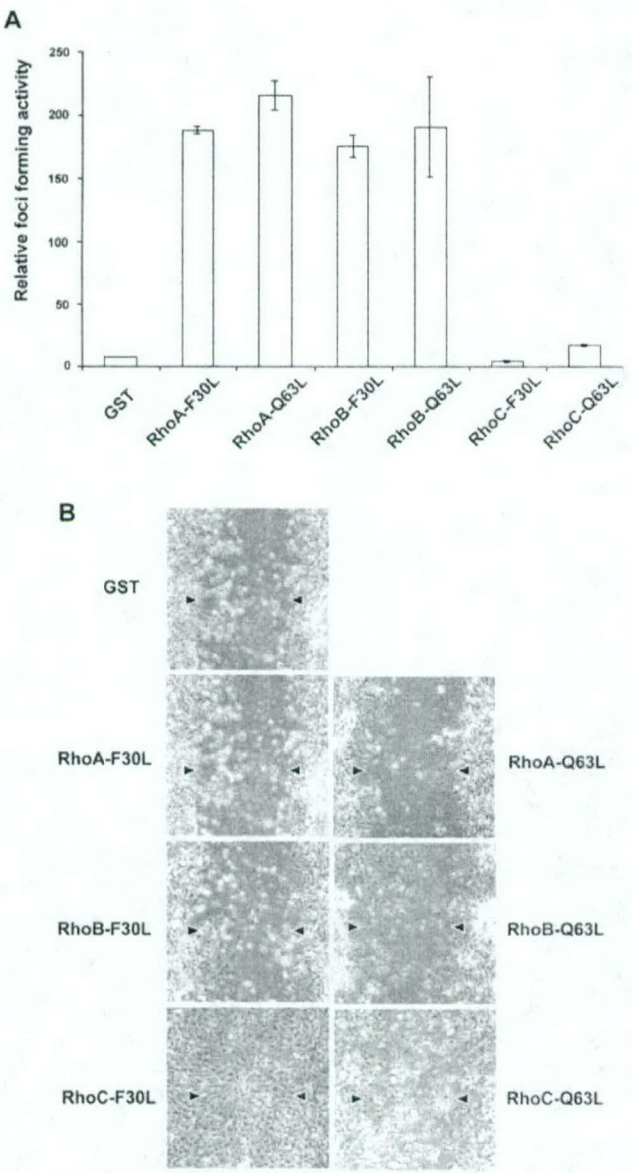

FIG. 2. **Direct comparison of the transformation and migration activities of the two active mutant forms of RhoA, RhoB, and RhoC.** *A*, 5,000 mutant RhoA, RhoB, RhoC, or GST expressing NIH 3T3 cells were combined with 50,000 wild type cells and were grown for 2 weeks. The resulting foci were quantified by Giemsa staining. *B*, cell migration was measured by the wound healing assay. Cells were seeded on the 60-mm-diameter dishes and grown in the presence of 10% CS to confluence. A wound was introduced by scraping with a 1–20-μl pipette tip across the center of the dish. The serum concentration in the medium was reduced to 0.5% after cell wounding, and the cells were incubated for 12 h before the photos were taken. The *arrowheads* indicate the cell edges immediately after wounding.

from the edge of the wound to the open space in the middle of the wound (Fig. 2*B*). These results indicate that individual Rho proteins have unique functions in the two aspects related to tumorigenesis, transformation and migration. RhoA, in particular, is important for cell growth control and transformation, whereas RhoC might be a key player in mediating cell movement. Although RhoB is capable of transforming cells under the overexpression conditions, it may serve as a sensor for DNA damage signals and mediate apoptotic responses of the cells based on the genetic evidence (17). The functional differences of these Rho proteins might be attributed to the sequence divergence in their C-terminal hypervariable region, an area that is

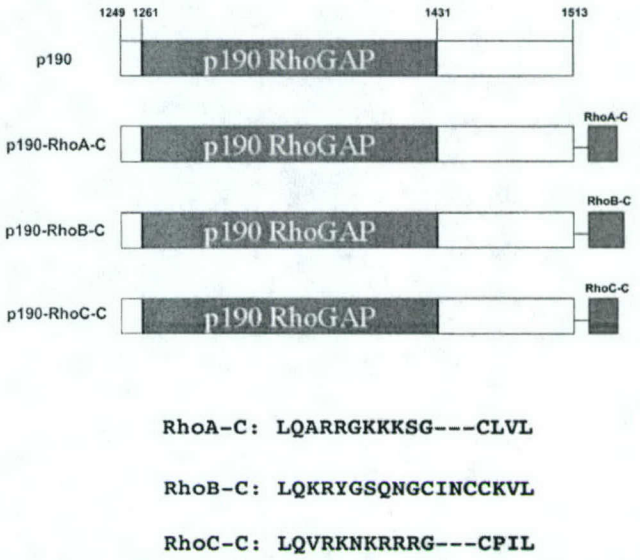

FIG. 3. **A schematic diagram of the Rho targeting constructs of p190GAP fused with the C-terminal sequences of RhoA, RhoB, or RhoC.** The amino acid sequence numbers of p190GAP and the sequences of the respective Rho proteins in the chimeras are indicated.

known to be critical for their distinct intracellular distribution (32, 33).

Targeting Individual Rho GTPase Activities by p190-Rho Chimeras—The commonly used biochemical tools to implicate the involvement of a Rho protein in a particular signaling pathway include the dominant negative mutant of the Rho protein and certain bacterial toxins that can modify the Rho protein function. These reagents are limited by their nonspecific nature in interfering with Rho GTPase functions (23, 25) and may have limited therapeutic value in targeting specific Rho proteins. To specifically inhibit individual Rho protein function, we hypothesize that the negative regulatory role of RhoGAPs, the RhoGAP domain in particular, could be exploited to down-regulate Rho protein activity if it is directed to where the active Rho GTPase substrates reside in cells. The RhoGAP domain of p190 has been demonstrated previously (28, 29) as a catalyst to specifically stimulate GTP-hydrolysis of Rho, not Rac or Cdc42, but it cannot distinguish among the RhoA, RhoB, and RhoC subtypes. When introduced into cells by microinjection, it is mostly cytosolic and readily disassembled the actin stress fiber structure (45). In cells the RhoGAP domain is likely to be tightly regulated by other structural motifs in full-length p190, and both of its catalytic activity and intracellular location may be altered by phosphorylation and protein-protein interaction in response to extracellular stimuli (30, 31). On the other hand, the C-terminal polybasic hypervariable region of Rho proteins, including the CAA*X* isoprenylation motif, appears to determine the subcellular distribution of respective Rho GTPases (32, 33). It seemed therefore logical that by fusing the RhoGAP domain with the C-terminal region of individual Rho protein we would provide the catalytic, GTP-hydrolyzing domain with a specific Rho targeting signal. When expressed at a low level in a controlled manner, such a GAP-Rho chimera might constitute an effective and specific inhibitor of individual Rho activity. Thus, we have generated a set of p190 GAP domain and the C terminus of RhoA, RhoB, or RhoC chimeric constructs to test this hypothesis (Fig. 3).

To ensure that the C-terminal sequences of various Rho proteins fused to the GAP domain of p190 do not interfere with the GAP function of p190, we expressed the GST-tagged p190 and p190-Rho chimeras in COS-7 cells, purified them by glu-

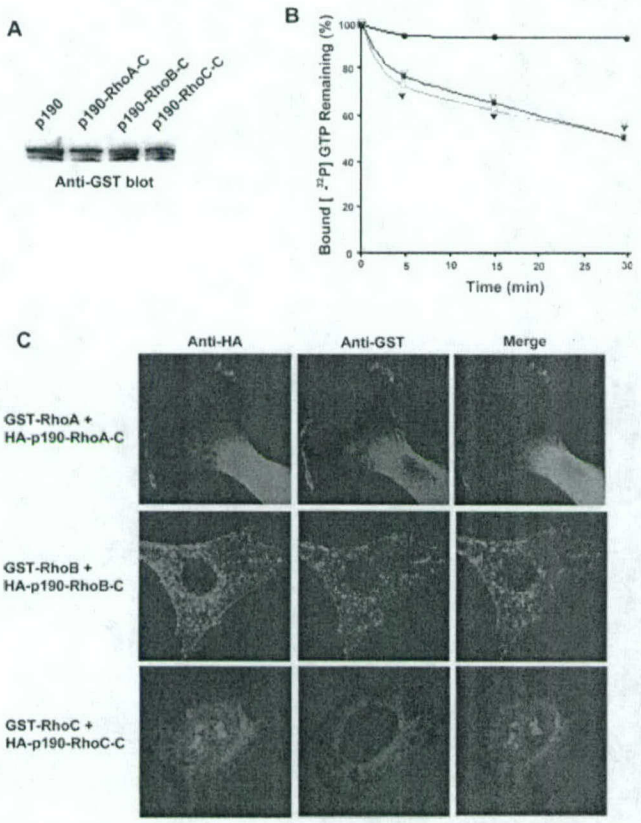

FIG. 4. **The p190-Rho chimeras are active GAPs *in vitro* and target to the intracellular compartments where respective active Rho proteins reside.** *A*, various p190GAP and p190-Rho chimeras were expressed in COS-7 cells by using the pCEFL-GST vector and were purified from the transfected cells by glutathione-agarose affinity chromatography. The GST-p190 and chimera proteins were detected by anti-GST Western blotting. *B*, the GAP activities of the respective proteins were assayed on recombinant RhoA-[γ-^{32}P]GTP by a filter binding assay. *Closed circles*, GST; *open squares*, p190 GAP domain; *open triangles*, p190-RhoA-C; *closed triangles*, p190-RhoB-C; *closed squares*, p190-RhoC-C. *C*, co-localization of the p190-Rho chimeras with that of the F30L mutant form of RhoA, RhoB, or RhoC. The GST-Rho-F30L expressing cells were infected with the respective retrovirus expressing HA-tagged p190-Rho chimeras, and the EGFP-positive cells were isolated and imaged after anti-GST and anti-HA immunofluorescence staining. The anti-GST and anti-HA staining patterns, as well as the overlay of the images, are shown.

tathione-agarose affinity beads, and compared their GAP activities *in vitro* (Fig. 4*A*). Under similar doses, p190-RhoA-C, p190-RhoB-C, and p190-RhoC-C displayed comparable GAP activities as p190 GAP domain alone on the RhoA substrate to stimulate [γ-^{32}P]GTP hydrolysis in a time-dependent manner (Fig. 4*B*), indicating that all four p190 and p190-Rho chimera proteins are functional. To further determine whether the C-terminal sequences of Rho proteins in the chimeras could indeed dictate intracellular localization of the fused p190 GAP domain, we next examined the localization patterns of p190-RhoA-C, p190-RhoB-C, and p190-RhoC-C by immunofluorescence and made comparisons with those of the respective Rho-F30L proteins expressed in these cells. As shown in Fig. 4*C*, p190-RhoA-C was found mostly in the cytosol with a small proportion localized at the plasma membrane. This was similar to that of the GST-RhoA-F30L distribution pattern revealed by anti-GST immunostaining and appeared to co-localize with the anti-GST immunofluorescence (Fig. 4*C*). p190-RhoB-C was found in the intracellular vesicles reminiscent of endosomes, similar to the RhoB-F30L locations (see Fig. 4*C* and Ref. 33). Likewise, p190-RhoC-C displayed a similar localization pattern to RhoC-F30L and co-localized with anti-GST signals with a uniquely diffused but punctuated pattern around the perinuclear region (Fig. 4*C*). These results suggest that the different C-terminal sequences of the Rho proteins can direct the p190-Rho chimeras to distinct locations similar to the Rho GTPases themselves.

To evaluate the efficacy and specificity of the chimeric constructs in cells, we employed the above described fast-cycling mutant Rho-F30L and GTPase-defective mutant Rho-Q63L expressing cells as testing systems, taking advantage of the facts that the F30L mutant form of the Rho GTPases is fully responsive to GAP stimulation whereas the GTPase-defective Rho-Q61L mutants would not be affected by the RhoGAP treatment, but both mutant forms behave similarly in eliciting cellular effects such as induction of transformation or migration. We chose two retroviral expression vectors, SF91-EMCV-IRES-GFP and MIEG3, for delivery of the constructs, because the former one allows high copy number insertion of the chimeras into the host cell genome whereas the latter typically introduces a single or low copy number of gene of interests, and both contain a bicistronically expressed EGFP as a marker that permits quick and semi-quantitative isolation of the p190 expressing cells base on the EGFP fluorescence (36, 37, 57, 58). When the fluorescence-activated cell sorting-purified EGFP-positive cells were examined for the expression of Flag (by SF91-EMCV-IRES-GFP)- or HA (by MIEG3)-tagged p190-Rho chimeras by Western blotting, all constructs were found to be expressed at a similar level (data not shown).

To examine whether the p190-Rho chimeras can be used to specifically target individual Rho GTPase activities, the GTP-bound form of RhoA-F30L or RhoC-F30L in cells co-expressing RhoA-F30L or RhoC-F30L, together with p190, p190-RhoA-C, p190-RhoB-C or p190-RhoC-C, were probed by affinity precipitation with immobilized His-Rhotekin. As shown in Fig. 5*A* and Fig. 6*A*, p190-RhoA-C and p190-RhoC-C specifically down-regulated the RhoA-F30L and RhoC-F30L activity by ~50 and ~60%, respectively. Moreover, in cells expressing the GTPase-defective form of RhoA or RhoC, *i.e.* RhoA-Q63L or RhoC-Q63L, p190-RhoA-C and p190-RhoC-C did not affect the amount of RhoA-Q63L-GTP and RhoC-Q63L-GTP precipitated from the cell lysates by Rhotekin (data not shown). Thus, the p190-Rho chimeras, p190-RhoA-C and p190-RhoC-C in particular, can specifically down-regulate individual Rho protein activity depending on the C-terminal sequences of the Rho protein fused to the RhoGAP domain.

To demonstrate the functional outcome of p190-Rho chimera application, the transformation and migration phenotypes caused by expression of RhoA-F30L or RhoC-F30L (Fig. 2) were examined in cells co-expressing RhoA-F30L or RhoC-F30L and various chimeras. Fig. 5*B* and Fig. 6*B* show that the RhoA-F30L-induced transformation can be specifically inhibited by expression of p190-RhoA-C using the high copy number retroviral vector, SF91-EMCV-IRES-GFP, whereas the RhoC-F30L-stimulated cell migration can be specifically reverted by p190-RhoC-C but not by p190, p190-RhoA-C, or p190-RhoB-C, by using the low copy number vector, MIEG3. Moreover, the p190-Rho chimeras had no effect on the RhoA-Q63L- or RhoC-Q63L-induced cell transformation or migration (data not shown). These results further suggest that the p190-Rho chimeras are useful tools to functionally revert cellular phenotypes caused by elevation of individual Rho activity.

Reversal of Tumor Cell Transformation and/or Invasion by p190-RhoC-C Chimera—We next asked whether the p190-Rho chimeras could be applied to human cancer cells that show characteristics of transformation and/or invasion because of overexpression or up-regulation of specific Rho GTPase. It has

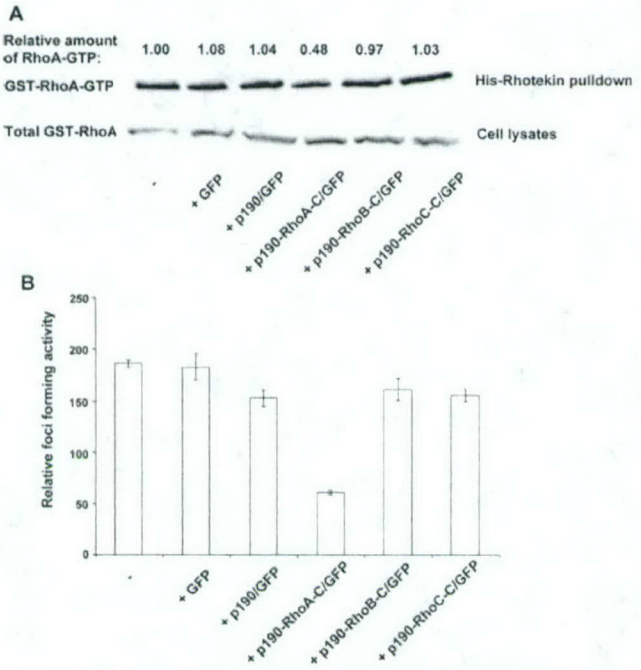

FIG. 5. **The p190-RhoA-C construct specifically down-regulates RhoA biochemical activity and RhoA-induced transformation in cells.** *A*, determination of the cellular activity of RhoA after treatment with various p190-Rho chimeras by the Rho-effector pull-down assay. The GST-RhoA-F30L expressing cells infected with retroviruses containing various p190-Rho chimeric constructs expressed by SF91-EMCV-IRES-GFP vector were lysed, and the cell lysates were incubated with His-tagged Rhotekin immobilized on Ni-NTA beads. The co-precipitated RhoA-F30L-GTP were analyzed by Western blotting with anti-GST monoclonal antibodies (*upper panel*). The total amount of GST-RhoA-F30L in each sample were shown in the *lower panel*. *B*, inhibition of the RhoA-induced cell transformation by p190-RhoA-C. The foci formation induced by F30LRhoA expression in NIH 3T3 cells were quantified as in Fig. 2 after transduction with retrovirus containing the SF91-EMCV-IRES-GFP vector alone, p190, or various p190-Rho chimeras.

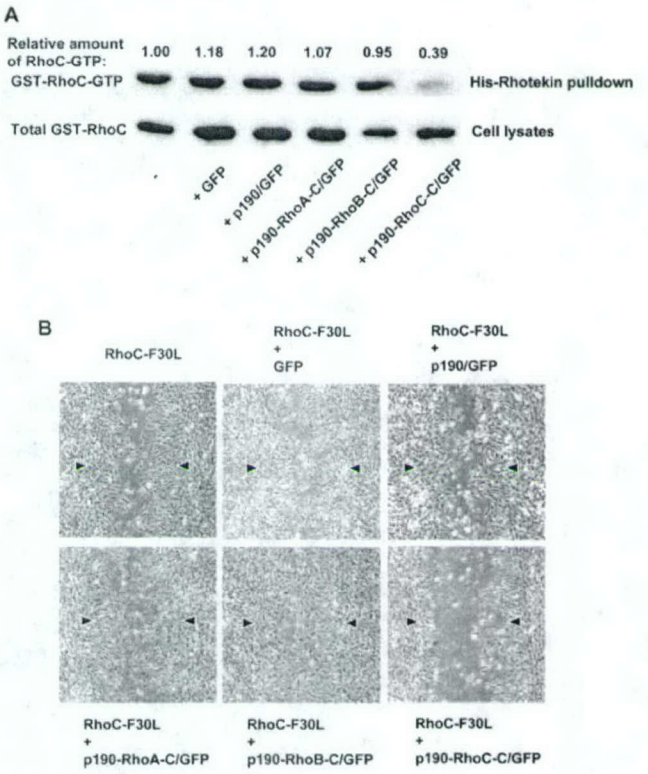

FIG. 6. **The p190-RhoC-C construct specifically down-regulates RhoC biochemical activity and RhoC-induced cell migration.** *A*, determination of the cellular activity of RhoC after treatment with various p190-Rho chimeras by the Rho-effector pull-down assay. The GST-RhoC-F30L expressing cells infected with retroviruses containing various p190-Rho chimeric constructs expressed by MIEG3 vector were lysed, and the cell lysates were incubated with His-tagged Rhotekin immobilized on Ni-NTA beads. The co-precipitated RhoC-F30L-GTP and total amount of RhoC-F30L in the lysates were analyzed by Western blotting with anti-GST monoclonal antibodies. *B*, reversal of the RhoC-induced cell migration by p190-RhoC-C. The motile RhoC-F30L expressing NIH 3T3 cells were transduced with retrovirus containing the MIEG3 vector alone, p190GAP, or various p190-Rho chimeras. The effects on the cell migration over a 12-h period were examined by wound healing assay. *Arrowheads* indicate the cell edges immediately after the wounds were introduced.

been demonstrated previously (16) that the HME acquire the transformation and invasion activities by overexpression of RhoC, resulting in phenotypes similar to that of inflammatory breast cancer cells. In the soft agar-based growth assay, very few colonies were seen grown in the control retrovirus-treated HME cells (Fig. 7*A*). Upon introduction of RhoC, the colony-forming activity of the cells (HME-RhoC) increased dramatically. As shown in Fig. 7*A*, the colony-forming activity of HME-RhoC cells was inhibited by ~5-fold upon treatment with the retrovirus expressing p190-RhoC-C whereas it was not affected by the control EGFP expressing virus or virus expressing p190, p190-RhoA-C, or p190-RhoB-C. Moreover, the invasive activity of HME-RhoC was also specifically inhibited by p190-RhoC-C but not by EGFP alone or by p190, p190-RhoA-C, or p190-RhoB-C (Fig. 7*B*).

In a previous gene array screening, the mRNA level of RhoC was found to be significantly elevated in the highly metastatic human melanoma A375-M cells compared with the non-invasive parental A375 cells (15). The invasive and metastatic properties of A375-M were attributed in part to the increased RhoC activity (15). When the set of p190-Rho chimeras were applied to the A375-M tumor cells, the p190-RhoC-C chimera was found to reduce both the migration and the invasion activities of A375-M significantly (Fig. 8, *A* and *B*), similar to the extent caused by forced expression of excess amount of dominant negative RhoA (15). Again, p190, p190-RhoA-C, or p190-RhoB-C, as well as the retrovirus-expressed EGFP, had no detectable effect on the migration or invasion property of the tumor cells (Fig. 8, *A* and *B*). Thus, it appears that the p190-Rho chimeras can be applied to human tumor cells to specifically down-regulate individual Rho GTPase activities and to reverse the growth and/or invasion phenotypes associated with overexpression of a distinct subtype of Rho GTPase.

DISCUSSION

The genes encoding H-, N- and K-Ras GTPases were among the first human oncogenes identified and have been found to be mutated in about 30% of human cancers (46). These mutations typically result in constitutively active Ras proteins that are GTPase-defective and unresponsive to Ras GAP stimulation. To target oncogenic Ras in cancer, several strategies have been developed. Farnesyltransferase inhibitors inhibit Ras function by preventing its post-translational modification by farnesyl isoprenoid (47), and the intracellular antibody capture technology was effective in generating intrabodies that bind to the oncogenic Ras protein (48). Another approach was the generation of a set of peptides derived from mutated Ras to act as antigens for cytotoxic and helper T-cell recognition for immunotherapy (49). Antisense technology has also been applied to specifically inhibit the expression of pathogenic Ras to reverse Ras-induced tumor proliferation (50). Recent progress in small

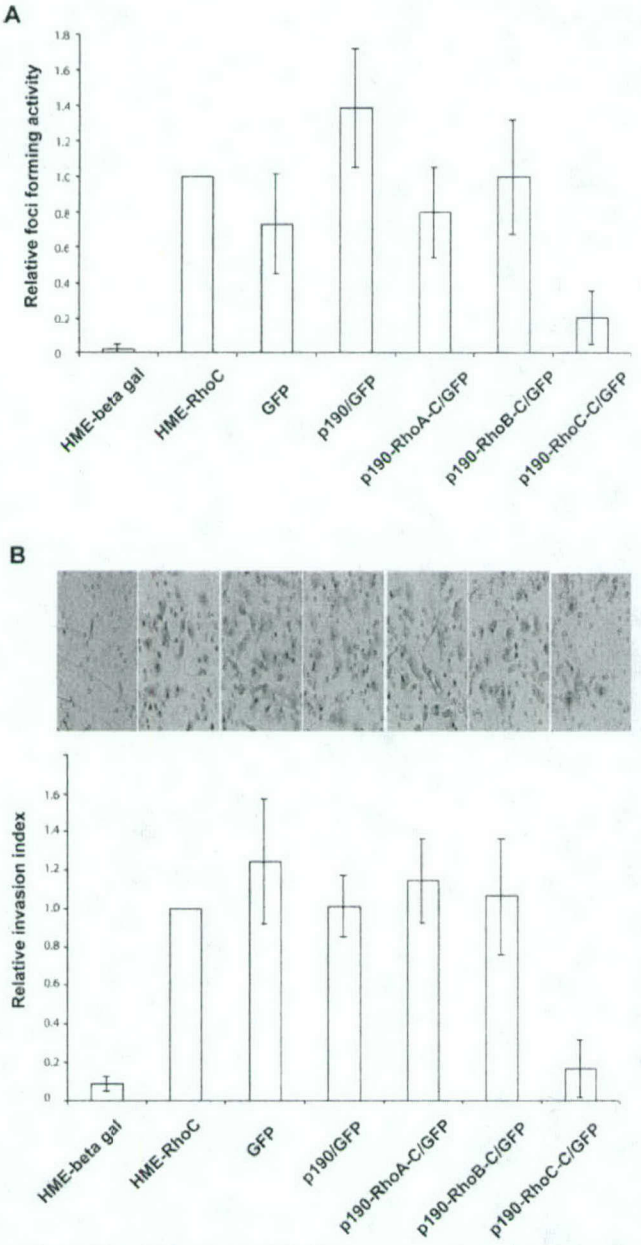

FIG. 7. **The effect of p190-RhoC-C on the anchorage-independent growth and invasion properties of the human breast cancer cells HME-RhoC.** *A*, the abilities of HME, HME-RhoC, and HME-RhoC transduced with various p190-Rho chimeras with MIEG3 vector to grow on soft agar were compared 3 weeks after plating the cells on 0.3% of soft agar. *B*, the invasive activity of the HME-RhoC cells and those transduced with various p190-Rho chimeras were assayed in a Matrigel-coated transwell. The cells that succeeded in invasion into the Matrigel were quantified 16 h after plating.

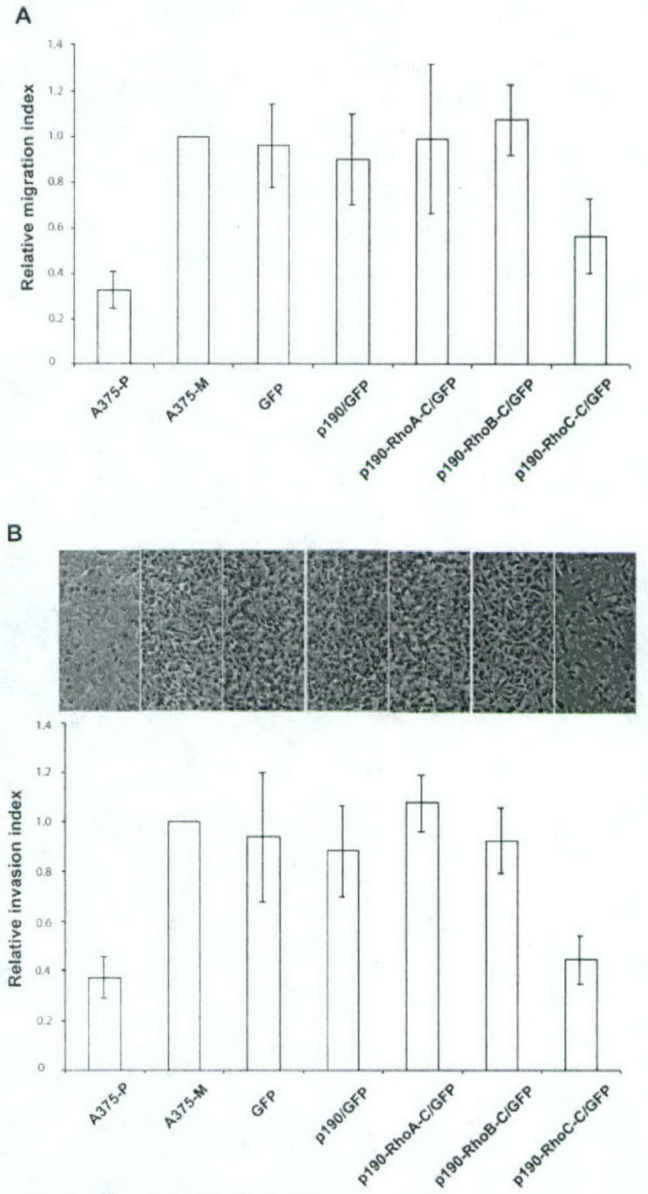

FIG. 8. **The p190-RhoC-C chimera was effective in reversing the migration and invasion phenotypes of the metastatic human melanoma A375-M cells.** *A*, the migration ability of the A375 parental cells and the metastatic A375-M cells transduced with the retrovirus encoding the MIEG3 vector alone, p190GAP, or various p190-Rho chimeras was assayed in a transwell. The cells that moved into the pore of the transwell membranes after a 16-h incubation were quantified. *B*, the cells were induced to invade the matrigel-coated membranes by 10% FBS in a transwell for 48 h. The number of cells invaded into the matrigel was counted. The quantitative results were derived from experiments carried out in triplicate.

interference RNA technology may present additional means to specifically target signaling molecules whose overexpression or elevated activity is associated with cancer development (59, 60). However, some of these strategies are still at an infant stage of development or have encountered difficulties at the cell biology stage or when applied to clinical cases, and it remains a challenge to develop novel approaches that may effectively alter the Ras-associated tumorigenic properties by interfering with Ras or Ras-pathway related signaling molecules.

Rho GTPases are key regulators of multiple cell functions related to cancer development (8). They affect cell-to-cell or cell-to-extracellular matrix adhesion, cell movement and morphological transformation, gene induction, apoptosis, and cell cycle progression (1–3). Moreover, RhoA, Rac1, and Cdc42 have been implicated as essential components for Ras-induced transformation (11). Accumulating evidence points to specific roles of individual members of Rho family in different aspects of the tumor development, such as increased proliferation, loss of contact inhibition, transformation, invasion into the adjacent tissues, and metastasis to the distant organs (8–10). Similar to Ras, Rho GTPases and the signaling pathways controlled by them may therefore make attractive targets for therapeutic intervention in cancer.

Unlike Ras, no constitutively activating mutations of Rho

proteins have been found in human tumors so far. Extensive screening has revealed that up-regulation or overexpression, rather than mutation, of specific Rho GTPases often associates with tumorigenesis and sometimes correlates with poor prognosis (18–22). Currently proposed methods of interfering with Rho GTPase function include designing geranylgeranyltransferase inhibitors for Rho proteins similar to the farnesyltransferase inhibitors for Ras, inhibiting the GEF activity or Rho-GEF interaction to suppress endogenous Rho activity, blocking the interaction between a Rho GTPase and its specific downstream effectors, and inactivating effector functions (8). Although these approaches are reasonable and may yield useful reagents for blocking Rho GTPase pathways (*e.g.* compound Y35674 specifically inhibits Rho kinase activity; see Ref. 51), most have not evolved to a stage where a specific inhibition of selected Rho functions can be achieved. At the Rho activity level, dominant negative mutants of Rho GTPases and Rho GTPase-modifying bacterial toxins remain the predominant reagents of choice for the cell biological studies of Rho protein function (23, 25). However, concern over their specificity and efficacy in many situations limits their value, and whether they can be applied to the study of human diseases or be used for therapeutic purposes remains to be tested.

The RhoGAP family regulatory proteins of Rho GTPases include over 70 mammalian members (5). The GAP activities of RhoGAPs are tightly controlled in cells via complex protein-protein or protein-lipid interactions so that the Rho GTPases would not be in the off-state all the time. Many RhoGAP domains, however, appear to represent a constitutively active structural module and display limited specificity toward the Rho GTPase substrates. Under overexpression or microinjection conditions, RhoGAP domain alone could cause Rho GTPase down-regulation and disruption of certain Rho-mediated cellular functions (45, 52, 53). This likely is because of partial saturation of intracellular compartments by the introduced RhoGAP domain and may not be desirable in studies to extract more specific function of individual members of Rho GTPases. In this context, the concern for specificity when utilizing RhoGAP domain alone for down-regulation of Rho proteins is similar to the use of dominant negative Rho GTPases or bacterial toxins.

In the present studies, we hypothesize that the negative regulatory role of the RhoGAP domain could be exploited to specifically down-regulate individual Rho protein activity, provided that it could be expressed at a level in a controlled manner and could be directed to sites where active Rho GTPase substrates are localized by means of the C-terminal intracellular targeting sequences of the Rho protein. In particular, p190GAP fused with the RhoA, RhoB, or RhoC C-terminal sequences might be useful for specific down-regulation of the respective cellular Rho GTPase activities. This is an attractive model system, because as we demonstrated in NIH 3T3 cells, RhoA, RhoB, and RhoC play different roles in mediating cell transformation and migration (Fig. 2). Previous gene targeting studies of RhoB function have shown that distinct from the positive influence on tumor growth or metastasis by RhoA or RhoC (11, 15), RhoB may act as a negative modifier or suppressor in cancer development, mediating cellular responses to DNA damage or farnesyltransferase inhibitors (17). Thus, achieving specific targeting of different subtypes of Rho proteins would be highly desirable in the treatment of tumor cells to reverse the growth and/or invasion phenotypes caused by overexpression of RhoA or RhoC while preserving the tumor suppressor function of RhoB.

As a demonstration of principle, we showed that the p190-Rho chimeras were biochemically active as GAPs for RhoA *in vitro* and indeed co-localized to the distinct intracellular locations specified by the Rho C-terminal sequences. This differential localization may also partly explain the differential functions displayed by different Rho subtypes. Further cellular assays revealed that p190-Rho chimeras specifically down-regulated Rho protein activities in cells depending on the C-terminal sequences in the chimeras when expressed in a controlled manner by retroviral induction. Moreover, p190-RhoA-C and p190-RhoC-C specifically inhibited the RhoA- or RhoC-stimulated cell transformation or migration. Although it was effective in specifically down-regulating RhoA or RhoC activity and in reversing the transformation or migration phenotype induced by the respective fast-cycling mutant, p190-RhoA-C and p190-RhoC-C had no effect on the activity of or phenotype induced by the GTPase-defective mutant RhoA-Q63L or RhoC-Q63L. These results validate the RhoGAP-based approach to specifically down-regulate the biochemical and biological activity of individual Rho subtypes in cells.

To examine the efficacy of this approach in tumor cells, we applied the p190-Rho chimera constructs to two different human tumor cells of which the oncogenic and invasive properties have previously been attributed to elevated RhoC expression (15, 16). In both the breast cancer HME-RhoC cells and the melanoma A375-M cells, p190-RhoC-C, but not other p190-Rho constructs, had a potent inhibitory effect on the anchorage-independent growth and/or migration and invasion. Thus, the p190-Rho-based method appears to work exceptionally well at the tumor cell level in specifically down-regulating the activity of an individual Rho subtype and in reversing the tumor cell phenotypes. It remains to be seen whether this approach can be used in other cancer cell types and whether the reversal of phenotypes of the cancer cells will hold in an animal model.

Like other cases of retrovirus-based gene transfer approach, the copy number of the introduced p190-Rho chimeras in the host cells will likely to be critical for the efficacy of their application. Although p190-RhoC-C was effective in down-regulating the biochemical activity and migration phenotype of RhoC when expressed with the low copy number vector MIEG3 (Fig. 6), we have found that expression of p190-RhoA-C or p190-RhoB-C with MIEG3 is insufficient for down-regulating the biochemical activity or transforming activity of RhoA-F30L or RhoB-F30L (data not shown). However, expression of p190-RhoA-C with the high copy number retroviral vector, SF91-EMCV-IRES-GFP, which has been in use for human gene therapy trials (57, 58), can specifically decrease both the biochemical activity of F30LRhoA and the RhoA-F30L-induced transformation under conditions in which p190-RhoB-C, p190-RhoC-C, or p190 alone expressed by using the same vector did not affect RhoA-F30L activity or the RhoA-F30L-induced transformation (Fig. 5). These results highlight the importance of dose dependence in effectiveness and specificity when applying this method to future animal and human trials.

In addition to p190, which is active GAP toward RhoA, RhoB, and RhoC, the GAP domain of Bcr has been shown to be specific for Rac but cannot distinguish among Rac1, Rac2, and Rac3 subtypes (54), whereas Cdc42GAP favors catalyzing the GTP hydrolysis of Cdc42 but remains quite active toward other Rho proteins (55). Like that of RhoA, RhoB, and RhoC, the C-terminal sequences of Rac1, 2, and 3 and Cdc42, including the lipid modification CAA*X* motif, have been known to direct their distinct intracellular localization patterns (33). Given the strong evidence of a role of various Rac subtypes and Cdc42 in tumorigenesis and other human diseases (8, 56), it will be of interest to test whether the BcrGAP fused with the respective Rac C-terminal sequences and the Cdc42GAP fused with the corresponding Cdc42 sequences would work as nicely to specif-

ically down-regulate their respective Rho GTPase substrates when expressed in cells in a controlled manner as the p190-RhoA-C and p190-RhoC-C chimera toward RhoA or RhoC shown in the current studies. These RhoGAP-based constructs may also provide valuable tools for the cell biological studies of individual Rho protein functions that might not have been appreciated previously by the dominant negative mutant approach or the toxin treatment.

Acknowledgments—We thank Drs. R. O. Hynes (MIT) and S. D. Merajver (University of Michigan) for the kind gifts of melanoma A375-M cells and breast cancer HME-RhoC cells. We are grateful to Chris Baum and Elke Will for providing the SF91-EMCV-IRES-GFP vector.

REFERENCES

1. Van Aelst, L., and D'Souza-Schorey, C. (1997) *Genes Dev.* **11,** 2295–2322
2. Hall, A. (1998) *Science* **279,** 509–514
3. Etienne-Manneville, S., and Hall, A. (2002) *Nature* **420,** 629–635
4. Zheng, Y. (2001) *Trends Biochem. Sci.* **26,** 724–732
5. Moon, S. Y., and Zheng, Y. (2003) *Trends Cell Biol.* **13,** 13–22
6. Olofsson, B. (1999) *Cell Signal.* **11,** 545–554
7. Bishop, A. L., and Hall, A. (2000) *Biochem. J.* **348,** 241–255
8. Sahai, E., and Marshall, C. J. (2002) *Nat. Rev. Cancer* **2,** 133–142
9. Keely, P. J. (2001) *Lancet* **358,** 1744–1745
10. Jaffe, A. B., and Hall, A. (2002) *Adv. Cancer Res.* **84,** 57–80
11. Zohn, I. M., Campbell, S. L., Khosravi-Far, R., Rossman, K. L., and Der, C. J. (1998) *Oncogene* **17,** 1415–1438
12. Qiu, R., Chen, J., McCormick, F., and Symons, M. (1995) Proc. *Natl. Acad. Sci. U. S. A.* **92,** 11781–11785
13. Yoshioka, K., Matsumura, F., Akedo, H., and Itoh, K. (1998) J. *Biol. Chem.,* **273,** 5146–5154
14. del Peso, L., Hernández-Alcoceba, R., Embade, N., Carnero, A., Esteve, P., Paje, C., and Lacal, J. C. (1997) *Oncogene* **15,** 3047–3057
15. Clark, E. A., Golub, T. R., Lander, E. S., and Hynes, R. O. (2000) *Nature* **406,** 532–535
16. van Golen, K. L., Wu, Z. F., Qiao, X. T., Bao, L. W., and Merajver, S. D. (2000) *Cancer Res.* **60,** 5832–5838
17. Prendergast, G. C. (2001) *Nat. Rev. Cancer* **1,** 162–168
18. Kamai, T., Arai, K., Tsujii, T., Honda, M., and Yoshida, K. (2001) *BJU Int.* **87,** 227–231
19. Fritz, G., Just, I., and Kaina, B. (1999) *Int. J. Cancer* **81,** 682–687
20. Schnelzer, A., Prechtel, D., Knaus, U., Dehne, K., Gerhard, M., Graeff, H., Harbeck, N., Schmitt, M., and Lengyel, E. (2000) *Oncogene* **19,** 3013–3020
21. Jordan, P., Brazao, R., Boavida, M. G., Gespach, C., and Chastre, E. (1999) *Oncogene* **18,** 6835–6839
22. Suwa, H., Ohshio, G., Imamura, T., Watanabe, G., Arii, S., Imamura, M., Narumiya, S., Hiai, H., and Fukumoto, M. (1998) *Br. J. Cancer* **77,** 147–152
23. Feig, L. A. (1999) *Nat. Cell Biol.* **1,** E25–E27
24. Nur-E-Kamal, M. S. A., Kamal, J. M., Qureshi, M. M., and Maruta, H. (1999) *Oncogene* **18,** 7787–7793
25. Lerm, M., Schmidt, G., and Aktories, K. (2000) *FEMS Microbiol. Lett.* **188,** 1–6
26. Yuan, B. Z., Miller, M. J., Keck, C. L., Zimonjic, D. B., Thorgeirsson, S. S., and Popescu, N. C. (1998) *Cancer Res.* **58,** 2196–2199
27. Wang, D. Z., Nur-E-Kamal, M. S., Tikoo, A., Montague, W., and Maruta, H. (1997) *Cancer Res.* **57,** 2478–2484
28. Zhang, B., and Zheng, Y. (1998) *Biochemistry* **37,** 5249–5257
29. Settleman, J., Narasimhan, V., Foster, L. C., and Weinberg, R. A. (1992) *Cell* **69,** 539–549
30. Brouns, M. R., Matheson, S. F., Hu, K. Q., Delalle, I., Caviness, V. S., Silver, J., Bronson, R. T., and Settleman, J. (2000) *Development* **127,** 4891–4903
31. Brouns, M. R., Matheson, S. F., and Settleman, J. (2001) *Nat. Cell Biol.* **3,** 361–367
32. Adamson, P., Paterson, H. F., and Hall, A. (1992) *J. Cell Biol.* **119,** 617–627
33. Michaelson, D., Silletti, J., Murphy, G., D'Eustachio, P., Rush, M., and Philips, M. R. (2001) *J. Cell Biol.* **152,** 111–126
34. Li, R., Zhang, B., and Zheng, Y. (1997) *J. Biol. Chem.* **272,** 32830–32835
35. Vanni, C., Mancini, P., Gao, Y., Ottaviano, C., Guo, F., Salani, B., Torrisi, M. R., Zheng, Y., and Eva, A. (2002) *J. Biol. Chem.* **277,** 19745–19753
36. Gu, Y., Jia, B., Yang, F. C., D'Souza, M., Harris, C. E., Derrow, C., Zheng, Y., and Williams, D. A. (2001) *J. Biol. Chem.* **276,** 15929–15938
37. Yang, F.-C., Atkinson, S. J., Gu, Y., Borneo, J. B., Roberts, A. W., Zheng, Y., Pennington, J., and Williams, D. A. (2001) *Proc. Natl. Acad. Sci. U. S. A.* **98,** 5614–5618
38. Zhu, K., Debrecini, B., Li, R., and Zheng, Y. (2000) *J. Biol. Chem.* **275,** 25993–26001
39. Lin, R., Cerione, R. A., and Manor, D. (1999) *J. Biol. Chem.* **274,** 23633–23641
40. Guo, F., Gao, Y., Wang, L., and Zheng, Y. (2003) *J. Biol. Chem.*, **278,** 14414–14419
41. Ridley, A. J., and Hall, A. (1992) *Cell* **70,** 389–399
42. Khosravi-Far, R., Solski, P. A., Clark, G., K., Kinch, M. S., and Der, C. J. (1995) *Mol. Cell. Biol.* **15,** 6443–6453
43. Prendergast, G. C., Khosravi-Far, R., Solski, P. A., Kurzawa, H., Lebowitz, P. F., and Der, C. J. (1995) *Oncogene* **10,** 2289–2296
44. Nobes, C. D., and Hall, A (1999) *J. Cell Biol.* **144,** 1235–1244
45. Ridley, A. J., Self, A. J., Kasmi, F., Paterson, H. F., Hall, A., Marshall, C. J., and Ellis, C. (1993) *EMBO J.* **12,** 5151–5160
46. Bos, J. L. (1989) *Cancer Res.* **49,** 4682–4689
47. Crooke, S. T. (1996) *Antisense Nucleic Acid Drug Dev.* **6,**145–147
48. Tanaka, T., and Rabbitts, T. H. (2003) *EMBO J.* **22,** 1025–1035
49. Gjertsen, M. K., Bakka, A., Breivik, J., Saeterdal, I., Solheim, B. G., Soreide, O., Thorsby, E., and Gaudernack, G. (1995) *Lancet* **346,** 1399–1400
50. Midgley, R. S., and Kerr, D. J. (2002) *Antisense Nucleic Acid Drug Dev.* **44,**109–120
51. Uehata, M, Ishizaki, I., Satoh, H., Ono, T., Kawahara, T., Morishita, T., Tamakawa, H., Yamagami, K., Inui, J., Maekawa, M., and Narumiya, S. (1997) *Nature* **389,** 990–994
52. Cicchetti, P., Ridley, A., Zheng, Y., Cerione, R. A., and Baltimore, D. (1995) *The EMBO J.* **14,** 3127–3135
53. Lamarche-Vane, N., and Hall, A (1998) J. *Biol. Chem.* **273,** 29172–29177
54. Zhang, B., Chernoff, J., and Zheng, Y. (1998) J. *Biol. Chem.* **273,** 8776–8782
55. Barfod, E., Zheng, Y., Kuang, W., Hart, M., Evans, T., Cerione, R. A., and Ashkenazi, A. (1993) *J. Biol. Chem.* **268,** 26059–26062
56. Boettner, B., and Van Aelst, L. (2002) *Gene* **286,** 155–174
57. Schwieger, M., Löhler, J., Friel, J., Scheller, M., Horak, I., and Stocking, C. (2002) *J. Exp. Med.* **196,** 1227–1240
58. Schambach, A., Wodrich, H., Hildinger, M., Bohne, J., Krausslich, H. G., and Baum, C. (2000) *Mol. Ther.* **2,** 435–445
59. Devroe, E., and Silver, P. A. (2002) *BMC Biotechnology* http://www.biomedcentral.com/1472–6750/2/15
60. McManus, M. T., and Sharp, P. A. (2002) *Nat. Rev. Genet.* **3,** 737–747

Multiple functions of NaK-ATPase: Role in PI3-kinase signaling and suppression of cell motility

Sonali P. Barwe[1], Gopalakrishnapillai Anilkumar[1], Sun Y. Moon[2], Yi Zheng[2], Julian Whitelegge[3], Sigrid A. Rajasekaran[1], and Ayyappan K. Rajasekaran[1†]

[1]Department of Pathology and Laboratory Medicine, David Geffen School of Medicine, University of California, Los Angeles, CA 90095, USA.
[2]Division of Experimental Hematology and Molecular Developmental Biology Program, Children's Hospital Research Foundation, University of Cincinnati, Cincinnati, OH 45229, USA.
[3]Psychiatry & Biobehavioral Sciences, David Geffen School of Medicine, University of California, Los Angeles, CA 90095, USA.

[†]Correspondence should be addressed to
Ayyappan K. Rajasekaran
Department of Pathology and Laboratory Medicine
Room 13-344 CHS
University of California, Los Angeles
Los Angeles, California 90095
Phone (310) 825-1199
Fax (310) 267-2410
Email: arajasekaran@mednet.ucla.edu

One sentence summary: The Na,K-ATPase α- and β-subunits suppress cell motility in a PI3-kinase and Rac1 dependent manner via protein-protein interactions.

Abstract

Cell motility is an important event during normal development and cancer metastasis. The mechanisms controlling cell motility are poorly understood. In this study, we demonstrate a novel mechanism involving cross talk between α_1- and β_1 -subunits of Na,K-ATPase in PI3-kinase signaling and suppression of cell motility. The α_1- associates with the regulatory subunit of PI3-kinase and the β_1- binds to annexin II and locally activates PI3-kinase and Rac1 at the lamellipodia. Pharmacological inhibition of Na,K-ATPase neither affected α_1- association to PI3-kinase nor annexin II binding to β_1- indicating that Na,K-ATPase ion transport function and suppression of cell motility are independent events.

The Na,K-ATPase, consisting of α_1 and β_1 subunits regulates the intracellular ion homeostasis. Na,K-ATPase function is important for the regulation of epithelial cell structure and transport functions (*1-4*). Dysfunction of Na,K-ATPase has been implicated in various epithelial cell diseases such as polycystic kidney disease (*5*) hypertension (*6*), hypomagnesaemia (*7*) ischemia (*8*) and cancer (*1, 9-11*). While both the subunits are required for the function of Na,K-ATPase, the specific role of β_1-subunit remains unclear. However, recent studies indicate that the β_1-subunit might have additional functions in epithelial cells. The levels of β_1-subunit protein were low in tumor tissues of an aggressive form of kidney cancer (*9*) and in highly motile Moloney Sarcoma Virus transformed Madin-Darby canine kidney (MSV-MDCK) cells (*1*). Repletion of β_1-subunit in MSV-MDCK cells suppressed their motility (*1*). The transcription factor Snail reduces the expression of proteins involved in suppression of cell motility in epithelial cells, both during normal development as well as the progression of carcinoma (*12*). The β_1-subunit expression was transcriptionally suppressed by Snail indicating that normal β_1-subunit expression is involved in the suppression of cell motility in epithelial cells (*11*).

To study the mechanism by which the β_1-subunit of Na,K-ATPase controls cell motility, we used MSV-MDCK cells ectopically expressing the β_1-subunit. Expression of untagged (MSV-Na,K-β_1) or GFP-tagged β_1-subunit (MSV-Na,K-β_1 -GFP) decreased the motility (*13*) by 50 ± 1.7 % and 45 ± 4.5 %, respectively compared to MSV-MDCK vector cells. Cells expressing a cytoplasmic tail deletion mutant of β_1-subunit (MSV-

Na,K-β_1ΔCD-GFP) did not show a reduction in the motility (Fig.1A), suggesting that the cytoplasmic tail of β_1-subunit is essential for the suppression of cell motility.

Immunofluorescence analysis revealed that in MSV-Na,K-β_1 cells, the β_1-subunit was concentrated at the actin rich lamellipodia whereas in MSV-Na,K-β_1ΔCD-GFP cells, lamellipodia were sparsely present and showed abundant stress fibers like in parental MSV-MDCK cells (Fig. 1B). The α_1-subunit co-localized with the β_1-subunit at the lamellipodia (Fig.S1). These results indicated that the ectopic expression of full length β_1-subunit induced lamellipodia by the reorganization of the actin cytoskeleton.

The formation of lamellipodia requires remodeling of the cortical actin cytoskeleton, which is governed by the activity of Rac1 in fibroblasts and epithelial cells (*14, 15*). To test whether Rac1 is involved in the β_1-subunit mediated lamellipodia formation, we used an *in vitro* biochemical assay to determine the endogenous levels of active Rac1. MSV-MDCK cells expressing full length β_1-subunit showed 7-8-fold increase in the levels of active Rac1 compared to MSV-MDCK vector and MSV-Na,K-β_1ΔCD-GFP cells (Fig.1C). The total Rac1 levels were similar in all these cell lines. To further substantiate the role of Rac1 in the suppression of motility, we generated MSV-MDCK cells expressing constitutively active L61 Rac1, a mutant that is defective in GTPase activity and is thought to exist constitutively in the GTP-bound form (MSV-L61Rac1) (*14*). If Rac1 is involved in the suppression of cell motility, then over expression of constitutively active Rac1 in MSV-MDCK cells should induce lamellipodia and reduce their motility. As expected, a 45% reduction in the motility was observed in MSV-L61Rac1 cells compared to the vector transfected MSV-MDCK cells (MSV-MIEG3) (Fig. 1D). MSV-L61 Rac1 cells displayed large lamellipodia with Rac1

localized to the lamellipodia and revealed highly reduced stress fibers (Fig. S2). These results demonstrated that increased Rac1 activity is associated with the suppression of motility in MSV-MDCK cells expressing the β_1-subunit.

Although the precise mechanism is still not known, previous studies have demonstrated that PI3-kinase is involved in the activation of Rac1 (*16, 17*). To test whether the activation of Rac1 is mediated by PI3-kinase, we treated MSV-Na,K-β_1 cells with specific pharmacological inhibitors of PI3-kinase such as Wortmannin and LY294002. Treatment with these PI3-kinase inhibitors drastically reduced the lamellipodia and increased stress fibers in MSV-Na,K-β_1 cells compared to the untreated cells (Fig. 2A). Removal of Wortmannin reinduced the lamellipodia indicating that the effect of PI3-kinase on the induction of lamellipodia is reversible (data not shown). Reduced amount of lamellipodia correlated with diminished levels of active Rac1 whereas the levels of total Rac1 remained unchanged in these cells (Fig. 2B). Furthermore, inhibition of PI3-kinase activity resulted in an increased motility of MSV-Na,K-β_1 cells (Fig. 2C). We then designed experiments to test whether PI3-kinase is activated in MSV-Na,K-β_1 cells. The Class I PI3-kinase is composed of two subunits, a 110 kDa catalytic subunit, and a 85 kDa regulatory subunit. The tyrosine phosphorylation of the p85 subunit is coupled to the activation of this subunit, which in turn activates the catalytic subunit (*18*). Although the total levels of p85 remained similar, the MSV-Na,K-β_1 cells showed 1.8-fold higher levels of tyrosine phosphorylated p85 subunit as compared to the MSV-MDCK cells (Fig. S3). Furthermore, PH-Akt-GFP a probe that can indicate local activation of PI3-kinase (*19, 20*) co-localized with the β_1-subunit at the lamellipodia in MSV-Na,K-β_1 cells, whereas in MSV-MDCK cells it was present mostly

in the cytoplasm (Fig.2D). Taken together, these results demonstrated that PI3-kinase is involved in the activation of Rac1 and suppression of cell motility in MSV-MDCK cells expressing β_1-subunit. Furthermore, the colocalization of PH-Akt-GFP with the β_1-subunit at the lamellipodia indicated the presence of products of PI3-kinase activation at the lamellipodia together with the β_1-subunit.

The requirement of the cytoplasmic domain of the β_1-subunit to suppress cell motility suggested that this domain might interact with protein/s involved in the suppression of motility in MSV-MDCK cells. To test this possibility we used the cytoplasmic domain of the β_1-subunit fused with glutatione S-transferase (Na,K-β_1CD-GST) to identify associated proteins by MALDI-Toff (*13*). A candidate binding protein identified by MALDI-Toff was annexin II. Annexin II binds anionic phospholipids such as PIP_3, a product of PI3-kinase activation, is found in the preparations of lamellipodia and is known to suppress cell motility (*21-24*). The Na,K-β_1CD-GST pulled down annexin II in a concentration dependent manner from MSV-Na,K-β_1 cell lysates (Fig. 3A). To further characterize the association of annexin II with the β_1-subunit, canine annexin II was cloned (*25*) and expressed as a GST-fusion protein in *E. coli*. The GST-annexin pulled down β_1-subunit from MSV-Na,K-β_1 cell lysates (Fig.3B). To test whether β_1-subunit association with annexin II occurs *in vivo*, we used co-immunoprecipitation analysis (*13*). Considerable amounts of annexin II co-immunoprecipitated with anti-β_1-subunit antibody but not with the anti-α_1-subunit antibody (Fig.3C). In addition, anti-β_1-subunit antibody did not coimmunoprecipitate annexin II from MSV-Na,K-$\beta_1\Delta$CD-GFP cells (Fig. 3C) demonstrating that the cytoplasmic domain of the β_1-subunit mediates the association with annexin II *in vivo*.

We then tested whether the β_1-subunit association with annexin II is dependent on the activation of PI3-kinase. In order to examine this possibility, MSV-Na,K-β_1 cells were treated with LY294002 and the amount of annexin II coimmunoprecipitated with the β_1-subunit was quantified. While the LY294002 treatment did not affect the total levels of annexin II, there was a 80% reduction in the amount of annexin II coimmunoprecipitated with the β_1-subunit in LY294002 treated cells compared to the control cells (Fig. 3D). These results demonstrate that annexin II binding to the β_1-subunit is markedly dependent on the activation of PI3-kinase.

Previous studies have shown that the p85 subunit of PI3-kinase associates with the α_1-subunit of Na,K-ATPase and activates PI3-kinase (*26*). Immunoprecipitates of p85 in MSV-Na,K-β_1 cells contained 3-fold more α_1-subunit compared to parental MSV-MDCK vector and MSV-Na,K-$\beta_1\Delta$CD-GFP cells (Fig.4A). Immunoprecipitation with anti-α_1-subunit antibody followed by immunoblotting with anti-phosphotyrosine antibody revealed increased amounts of tyrosine phosphorylated p85 associated with the α_1-subunit in MSV-Na,K-β_1 cells compared to MSV-MDCK vector and MSV-Na,K-$\beta_1\Delta$CD-GFP cells (Fig. 4B). This result indicated that increased association of p85 with the α_1-subunit is involved in the activation of PI3-kinase signaling (*26*). MSV-Na,K-β_1 cells contain 2-fold more α_1-subunit than MSV-MDCK vector and MSV-Na,K-$\beta_1\Delta$CD-GFP cells (*27*) indicating that increased levels of α_1-subunit is involved in the activation of PI3 kinase. To further confirm this notion, we ectopically expressed α_1-subunit in Na,K-$\beta_1\Delta$CD-GFP cells. These cells showed increased tyrosine phosphorylation of p85 associated with α_1- subunit (Fig.4C) but did not reveal lamellipodia or reduced motility

indicating that PI3-kinase activation by α-subunit alone is not sufficient to suppress motility in MSV-MDCK cells (Fig.S4) and that the downstream signaling involving the β_1-subunit is essential.

While PI3-kinase inhibition increased the amount of stress fibers, abolished lamellipodial localization of the β_1-subunit and reduced the Rac1 activity in MSV-Na,K-β_1 cells, inhibition of the enzyme activity of Na,K-ATPase by ouabain neither altered lamellipodial localization of the β_1-subunit nor increased the stress fiber content (Fig. 4D) or levels of active Rac1 (Fig. 4E). Also, ouabain treatment did not affect annexin II binding to the β_1-subunit (Fig. 4F) and α_1-subunit binding to the p85 subunit of PI3-kinase (Fig. 4G). Furthermore, the motility of control and ouabain treated cells in a wound assay was similar (data not shown). These results demonstrate that suppression of cell motility by Na,K-ATPase is independent of its pump function.

Association of the α_1-subunit with the p85 subunit of PI3-kinase and the β_1-subunit with annexin II, which binds to PIP_3, a product of PI3-kinase, suggest that PI3-kinase signaling, Rac1 activation and suppression of cell motility in MSV-Na,K-β_1 cells involves a cross talk between the two subunits of Na,K-ATPase. How might Na,K-ATPase be involved in the suppression of cell motility? We suggest that the increased expression of the α_1-subunit leads to the activation of the p85 regulatory subunit resulting in the activation of PI3-kinase (*26*). Activation of PI3-kinase leads to increased binding of annexin II to the β_1-subunit, and results in the localization of these proteins at the plasma membrane. Sequestration of Rac1 into this complex by annexin II (*28*) then leads to the formation of lamellipodia eventually leading to the suppression of cell motility. Since pharmacological inhibition of Na,K-ATPase does not prevent lamellipodia

formation or Rac1 activation, we suggest that the suppression of motility by Na,K-ATPase is primarily mediated by protein-protein interaction of the Na,K-ATPase α_1- and β_1- subunits rather than its ion transporting function.

PI3-kinase dependent Rac1 activation is also involved in E-cadherin mediated cell-cell adhesion (*29-33*). However, MSV-Na,K-β_1 cells lack E-cadherin (*1*) and therefore, Rac1 activation in MSV-Na,K-β_1 cells is independent of cadherin mediated adhesion and is dependent on the expression of the β_1-subunit in these cells. Reexpression of either E-cadherin or the β_1-subunit reduced the motility of these cells whereas coexpression of both these proteins suppressed the motility even further indicating that the functions of both these proteins synergistically suppress the motility of carcinoma cells (*1*). Therefore, the loss of either E-cadherin or the β_1-subunit in carcinoma cells might be associated with their increased motility and invasive behavior and ability to increase the expression of both these proteins in carcinoma cells should have significant therapeutic value to impede cancer cell invasion and metastasis.

References and Notes

1. S. A. Rajasekaran *et al.*, *Mol Biol Cell* **12**, 279-95 (Feb, 2001).
2. J. L. Genova, R. G. Fehon, *J Cell Biol* **161**, 979-89 (Jun 9, 2003).
3. S. M. Paul, M. Ternet, P. M. Salvaterra, G. J. Beitel, *Development* **130**, 4963-74 (Oct, 2003).
4. S. A. Rajasekaran *et al.*, *Am J Physiol Cell Physiol* **284**, C1497-507 (Jun, 2003).
5. P. D. Wilson *et al.*, *Am J Physiol* **260**, F420-30 (Mar, 1991).
6. V. L. Herrera, H. X. Xie, L. V. Lopez, N. J. Schork, N. Ruiz-Opazo, *J Clin Invest* **102**, 1102-11 (Sep 15, 1998).
7. I. C. Meij *et al.*, *Nat Genet* **26**, 265-6 (Nov, 2000).
8. T. Matsuda, I. Shimizu, Y. Murata, A. Baba, *Brain Res* **576**, 263-70 (Apr 3, 1992).
9. S. A. Rajasekaran *et al.*, *J Urol* **162**, 574-80 (Aug, 1999).
10. C. Espineda *et al.*, *Cancer* **97**, 1859-68 (Apr 15, 2003).
11. C. E. Espineda, J. Chang, J. Twiss, S. A. Rajasekaran, A. K. Rajasekaran, *Mol Biol Cell* (Dec 29, 2003).
12. M. A. Nieto, *Nat Rev Mol Cell Biol* **3**, 155-66 (Mar, 2002).
13. (Materials and methods are available as supporting material on *Science* Online.).
14. A. J. Ridley, H. F. Paterson, C. L. Johnston, D. Diekmann, A. Hall, *Cell* **70**, 401-10 (Aug 7, 1992).
15. A. J. Ridley, P. M. Comoglio, A. Hall, *Mol Cell Biol* **15**, 1110-22 (Feb, 1995).
16. H. C. Welch, W. J. Coadwell, L. R. Stephens, P. T. Hawkins, *FEBS Lett* **546**, 93-7 (Jul 3, 2003).
17. P. T. Hawkins *et al.*, *Curr Biol* **5**, 393-403 (Apr 1, 1995).
18. C. Gentili, S. Morelli, A. Russo De Boland, *J Cell Biochem* **86**, 773-83 (2002).
19. S. J. Watton, J. Downward, *Curr Biol* **9**, 433-6 (Apr 22, 1999).
20. A. Gray, J. Van Der Kaay, C. P. Downes, *Biochem J* **344 Pt 3**, 929-36 (Dec 15, 1999).
21. D. M. Waisman, *Mol Cell Biochem* **149-150**, 301-22 (Aug-Sep, 1995).
22. L. D. Ghitescu, A. Gugliucci, F. Dumas, *Diabetes* **50**, 1666-74 (Jul, 2001).
23. C. Balch, J. R. Dedman, *Exp Cell Res* **237**, 259-63 (Dec 15, 1997).
24. J. W. Liu *et al.*, *Oncogene* **22**, 1475-85 (Mar 13, 2003).
25. S. P. Barwe, Rajasekaran, A.K., *AY422991* (2003).
26. G. A. Yudowski *et al.*, *Proc Natl Acad Sci U S A* **97**, 6556-61 (Jun 6, 2000).
27. S. A. Rajasekaran, *unpublished results* (2001).
28. M. D. Hansen, J. S. Ehrlich, W. J. Nelson, *J Biol Chem* **277**, 45371-6 (Nov 22, 2002).
29. P. L. Hordijk *et al.*, *Science* **278**, 1464-6 (Nov 21, 1997).
30. E. E. Sander, J. P. ten Klooster, S. van Delft, R. A. van der Kammen, J. G. Collard, *J Cell Biol* **147**, 1009-22 (Nov 29, 1999).
31. V. M. Braga, L. M. Machesky, A. Hall, N. A. Hotchin, *J Cell Biol* **137**, 1421-31 (Jun 16, 1997).
32. K. Takaishi, T. Sasaki, H. Kotani, H. Nishioka, Y. Takai, *J Cell Biol* **139**, 1047-59 (Nov 17, 1997).
33. A. S. Yap, E. M. Kovacs, *J Cell Biol* **160**, 11-6 (Jan 6, 2003).

34. Supported by NIH DK56216 and Department of Defense DAMD-17 –02-0661 and DAMD-17-00-1-0454 grants. We thank Drs. Tamas Balla for PH-Akt-GFP, Robert Farley, for canine Na,K-ATPase β-subunit cDNA and William James Ball Jr. for Na,K-ATPase antibodies.

Figure Legends

Fig. 1. Na,K-ATPase β_1-subunit expression suppresses cell motility by reorganization of the actin cytoskeleton in a Rac1-dependent manner. (**A**) Migration of MSV-MDCK cells expressing either GFP (1), Na,K-ATPase β_1-subunit (2), GFP tagged Na,K-ATPase β_1-subunit (3) or GFP tagged Na,K-ATPase β_1-subunit ΔCD (4) across trans-well filters. (**B**) Confocal three-dimensional (3D)-reconstructions showing actin organization (red) of MSV-MDCK-GFP (a), MSV-Na,K-β_1-GFP (b), MSV-Na,K-$\beta_1\Delta$CD-GFP (c) and colocalization of Na,K-β_1-GFP with filamentous actin (yellow) at the lamellipodia (d). The GFP fluorescence in a and c is not shown to reveal stress fibers clearly. (**C**) Immunoblot showing active and total endogenous Rac1 in MSV-MDCK-GFP (1), MSV-Na,K-β_1 (2), MSV-Na,K-β_1-GFP (3) and MSV-Na,K-$\beta_1\Delta$CD-GFP (4) cells. The graph shows quantification of the immunoblot data. (**D**) Migration of MSV-MDCK cells transfected with MIEG3 vector (■) or L61Rac1 (□). Bar, 25 μm

Fig. 2. PI3-kinase is required for the Na,K-ATPase β_1-subunit mediated suppression of cell motility and enhancement of Rac1 activity. (**A**) Phalloidin staining showing actin organization of MSV-Na,K-β_1 cells treated with DMSO, wortmannin or LY294002. (**B**) Immunoblot showing active and total levels of endogenous Rac1 in DMSO or LY294002 treated MSV-MDCK and MSV-Na,K-β_1 cells. (**C**) Migration of MSV-Na,K-β_1 cells treated with DMSO or wortmannin across trans-well filters. (**D**) Immunolocalization of Na,K-ATPase β_1-subunit and PH-Akt-GFP in MSV-MDCK and MSV-Na,K-β_1 cells. Bar, 25 μm.

Fig. 3. Na,K-ATPase β_1-subunit cytoplasmic tail interacts with annexin II in a PI3-kinase dependent manner. (A) 10 or 20 μg of GST-Na,K-β_1CD was incubated with 1 mg of MSV-Na,K-β_1 cell lysate and the annexin II pulled down by GST-Na,K-β_1CD was determined by immunoblotting. (B) GST-annexin II pull down MSV-Na,K-β_1 cell lysate showing Na,K-ATPase β_1-subunit interaction with annexin (C) Na,K-ATPase α_1-subunit or β_1-subunit from MSV-Na,K-β_1 and MSV-Na,K-$\beta_1\Delta$CD-GFP cell lysates was immunoprecipitated (IP) using corresponding antibodies and analyzed by immunoblotting (IB) for the presence of annexin II. (D) MSV-Na,K-β_1 cells were treated with DMSO or LY294002 and lysed. 1 mg of total protein was used for immunoprecipitating Na,K-ATPase β_1-subunit. The amount of annexin II bound to Na,K-ATPase β_1-subunit was detected by immunoblotting. The graph shows the quantification of the immunoblot data.

Fig. 4. Analysis of the role of Na,K-ATPase α_1-subunit and enzyme activity in PI3-kinase signaling and Rac1 activation. (A) After immunoprecipitation (IP) of p85 subunit from 1mg of MSV-MDCK, MSV-Na,K-β_1 and MSV-Na,K-$\beta_1\Delta$CD-GFP cell lysates co-precipitating α_1-subunit was detected by immunoblotting (IB). (B) MSV-MDCK, MSV-Na,K-β_1 and MSV-Na,K-$\beta_1\Delta$CD-GFP cells were lysed and Na,K-ATPase α_1-subunit was immunoprecipitated. The precipitate was analyzed by immunoblotting for tyrosine phosphorylated p85 subunit by using anti-phosphotyrosine antibodies. The blots were stripped and reprobed for p85 subunit to confirm the presence of p85 (data not shown). (C) MSV-Na,K-$\beta_1\Delta$CD-GFP cells expressing α1-subunit showing increased levels of

tyrosine phosphorylated p85. The amount of tyrosine phosphorylated p85 subunit in the parental and the transfected cells was determined by immunoprecipitating p85 subunit from 1mg of cell lysates, followed by blotting with anti-phosphotyrosine antibodies. (D) MSV-MDCK and MSV-Na,Kβ_1 cells showing actin organization after treatment with ouabain. For E, F and G, MSV-Na,K-β_1 cells treated with DMSO or ouabain were used. (E) Immunoblot showing the active and total levels of endogenous Rac1, (F) annexin II bound to Na,K-ATPase β_1-subunit and (G) p85 subunit bound to α_1-subunit. Bar, 25 μm

Supporting Online Material
www.sciencemag.org
Materials and Methods
Figs. S1, S2, S3, S4, S5
References

Fig. 1

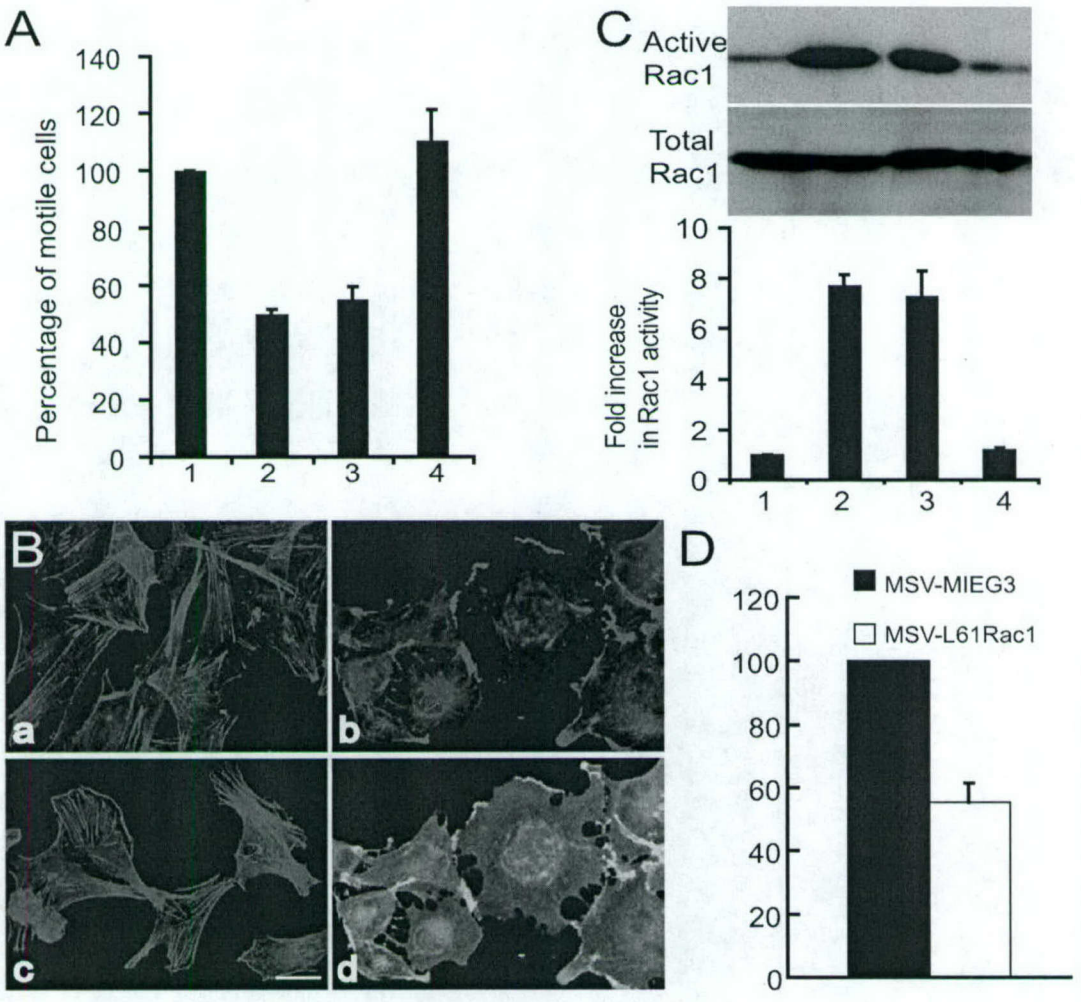
A
Percentage of motile cells
140
120
100
80
60
40
20
0
1
2
3
4
C
Active Rac1
Total Rac1
Fold increase in Rac1 activity
10
8
6
4
2
0
1
2
3
4
B
a
b
c
d
D
MSV-MIEG3
MSV-L61Rac1
120
100
80
60
40
20
0

Fig. 2

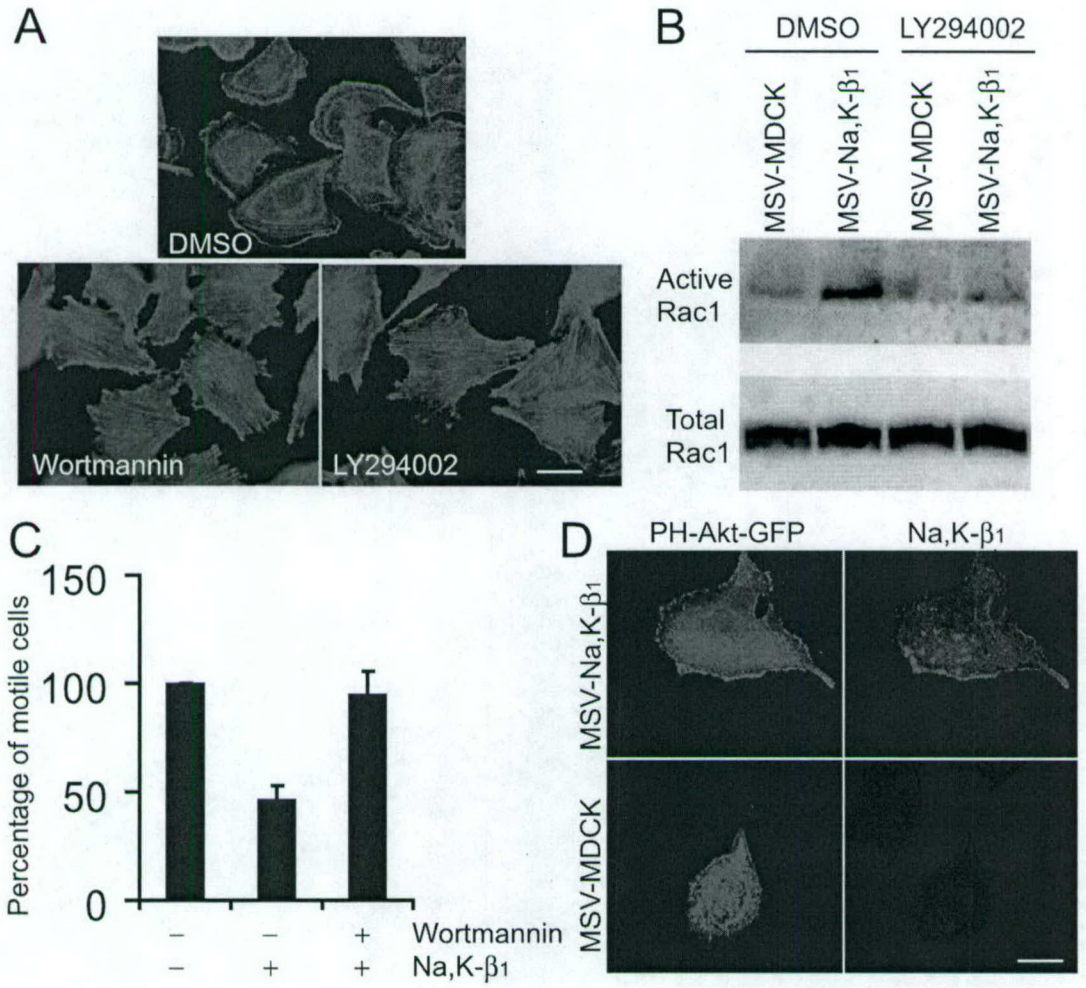
A
DMSO
Wortmannin
LY294002
B
DMSO
LY294002
MSV-MDCK
MSV-Na,K-β1
MSV-MDCK
MSV-Na,K-β1
Active Rac1
Total Rac1
C
Percentage of motile cells
150
100
50
0
– – +
– + +
Wortmannin
Na,K-β1
D
PH-Akt-GFP
Na,K-β1
MSV-Na,K-β1
MSV-MDCK

Fig. 3

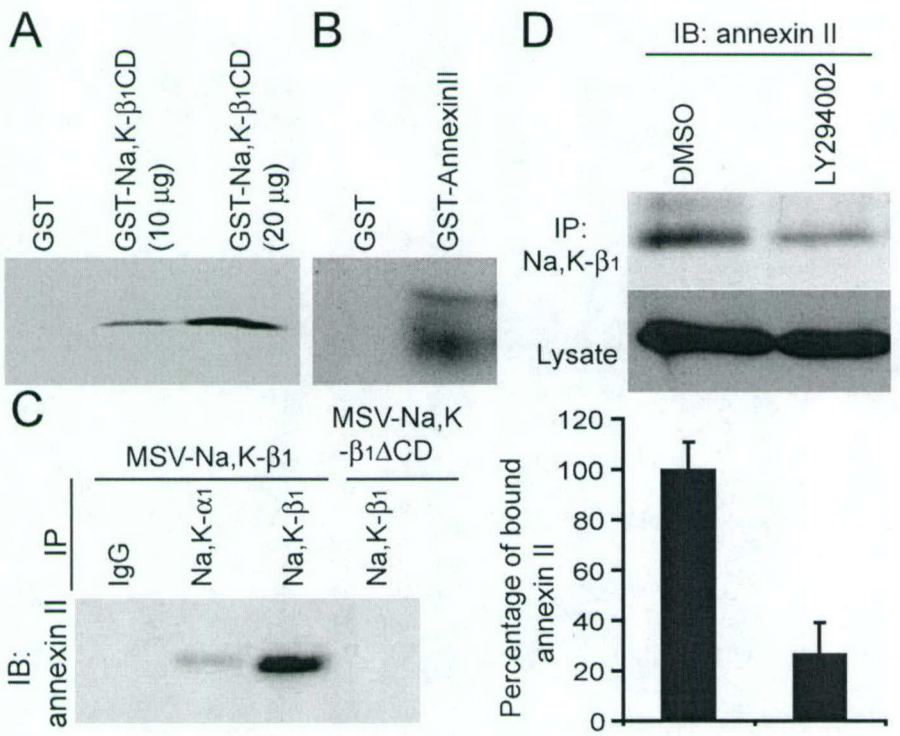
A
GST
GST-Na,K-β1CD (10 μg)
GST-Na,K-β1CD (20 μg)
B
GST
GST-AnnexinII
C
MSV-Na,K-β1
MSV-Na,K -β1ΔCD
IP
IgG
Na,K-α1
Na,K-β1
Na,K-β1
IB: annexin II
D
IB: annexin II
DMSO
LY294002
IP: Na,K-β1
Lysate
Percentage of bound annexin II
120
100
80
60
40
20
0

Fig. 4

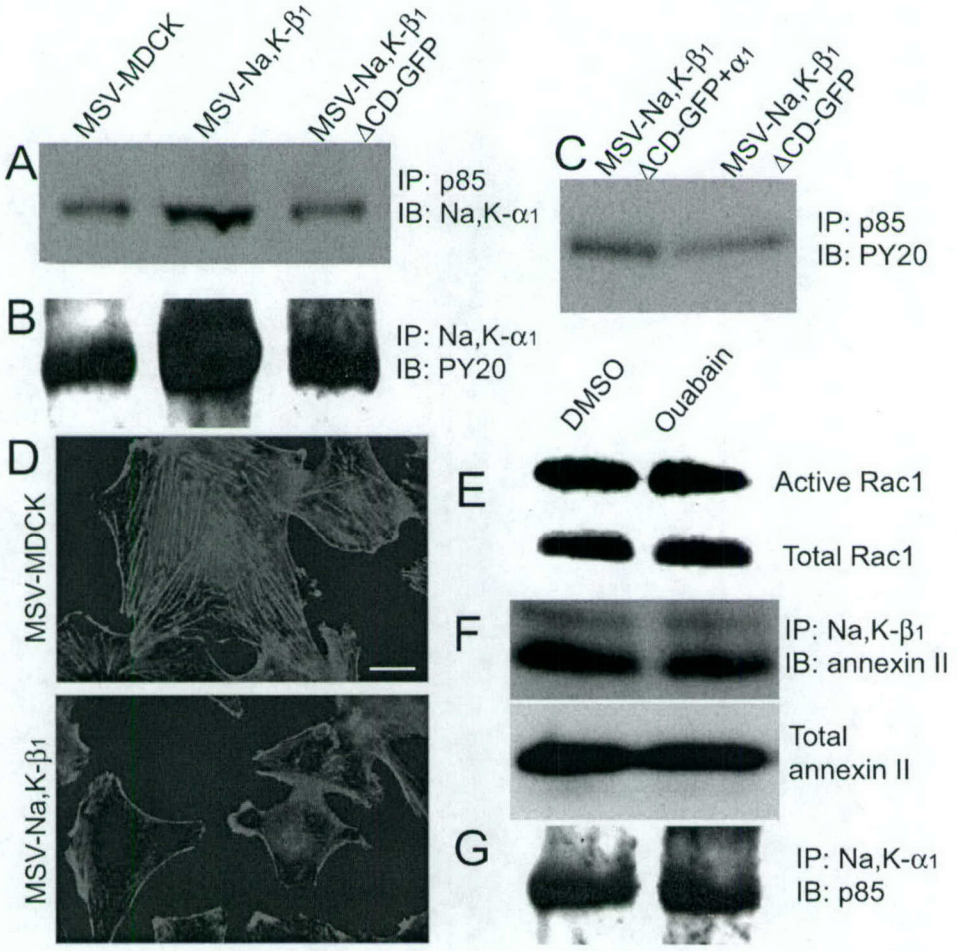
MSV-MDCK
MSV-Na,K-β1
MSV-Na,K-β1 ΔCD-GFP
A
IP: p85
IB: Na,K-α1
B
IP: Na,K-α1
IB: PY20
C
MSV-Na,K-β1 ΔCD-GFP+α1
MSV-Na,K-β1 ΔCD-GFP
IP: p85
IB: PY20
D
MSV-MDCK
MSV-Na,K-β1
DMSO
Ouabain
E
Active Rac1
Total Rac1
F
IP: Na,K-β1
IB: annexin II
Total annexin II
G
IP: Na,K-α1
IB: p85

S1

A
B
C

S2

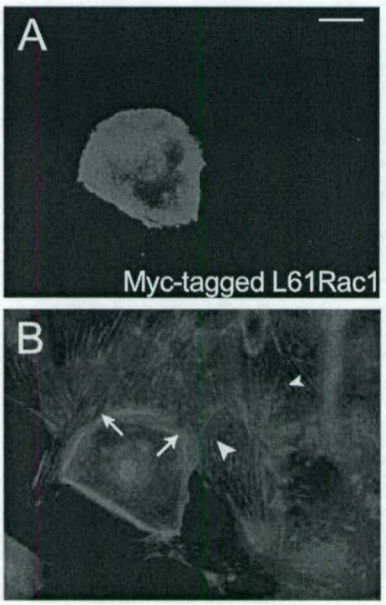
A
Myc-tagged L61Rac1
B

S3

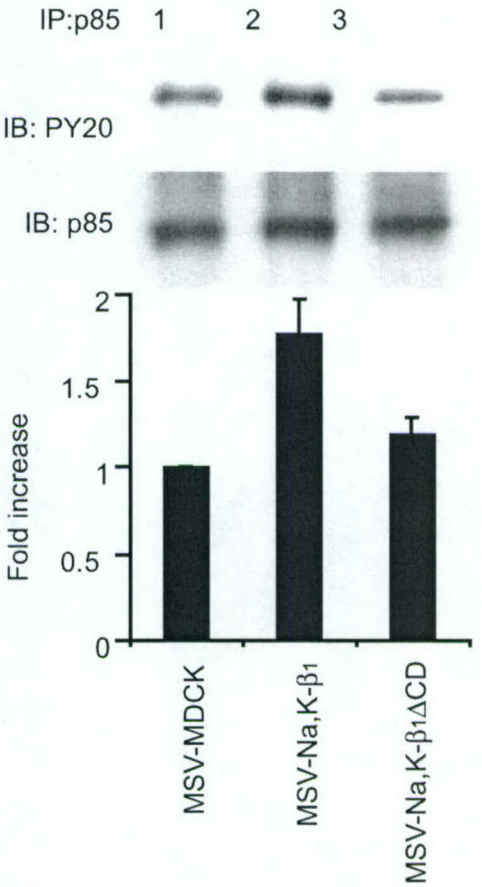
IP:p85 1 2 3
IB: PY20
IB: p85
Fold increase
2
1.5
1
0.5
0
MSV-MDCK
MSV-Na,K-β1
MSV-Na,K-β1ΔCD

S4

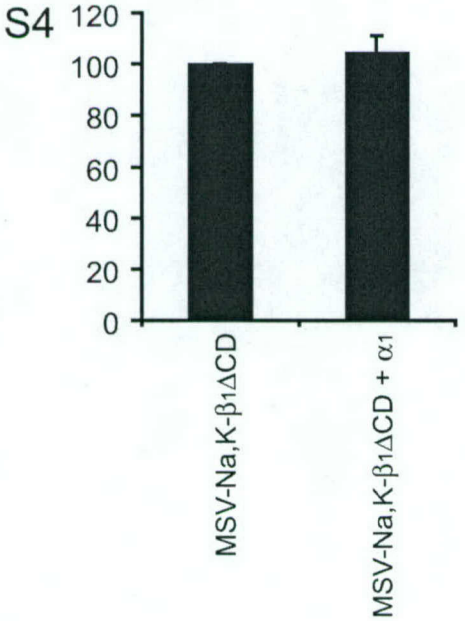
120
100
80
60
40
20
0
MSV-Na,K-β1ΔCD
MSV-Na,K-β1ΔCD + α1